AMRL-TR-71-88

LINK SYSTEM OF THE HUMAN TORSO

RICHARD G. SNYDER
DON B. CHAFFIN
RODNEY K. SCHUTZ

THE UNIVERSITY OF MICHIGAN

AUGUST 1972

AEROSPACE MEDICAL RESEARCH LABORATORY
AEROSPACE MEDICAL DIVISION
AIR FORCE SYSTEMS COMMAND
WRIGHT-PATTERSON AIR FORCE BASE, OHIO

NOTICES

When US Government drawings, specifications, or other data are used for any purpose other than a definitely related Government procurement operation, the Government thereby incurs no responsibility nor any obligation whatsoever, and the fact that the Government may have formulated, furnished, or in any way supplied the said drawings, specifications, or other data, is not to be regarded by implication or otherwise, as in any manner licensing the holder or any other person or corporation, or conveying any rights or permission to manufacture, use, or sell any patented invention that may in any way be related thereto.

Organizations and individuals receiving announcements or reports via the Aerospace Medical Research Laboratory automatic mailing lists should submit the addressograph plate stamp on the report envelope or refer to the code number when corresponding about change of address or cancellation.

Do not return this copy. Retain or destroy.

Please do not request copies of this report from Aerospace Medical Research Laboratory. Additional copies may be purchased from:

National Technical Information Service
5285 Port Royal Road
Springfield, Virginia 22151

AIR FORCE/56780/4 June 1973 — 200

Security Classification

DOCUMENT CONTROL DATA - R & D

(Security classification of title, body of abstract and indexing annotation must be entered when the overall report is classified)

1. ORIGINATING ACTIVITY (Corporate author) The University of Michigan, Biomedical Dept., Highway Safety Research Institute, and Dept. of Industrial Eng., College of Eng., Ann Arbor Mi 48105	2a. REPORT SECURITY CLASSIFICATION Unclassified 2b. GROUP N/A

3. REPORT TITLE

Link System of the Human Torso

4. DESCRIPTIVE NOTES (Type of report and inclusive dates)

Final Report, June 1970 - July 1971.

5. AUTHOR(S) (First name, middle initial, last name)

Richard G. Snyder; Don B. Chaffin; Rodney K. Schutz.

6. REPORT DATE	7a. TOTAL NO. OF PAGES	7b. NO. OF REFS

8a. CONTRACT OR GRANT NO.	9a. ORIGINATOR'S REPORT NUMBER(S)
F-33615-70-0-1777 b. PROJECT NO. 7184 c. Task No. 718408 d. Work Unit 007	HSRI-71-112 9b. OTHER REPORT NO(S) (Any other numbers that may be assigned this report) AMRL-TR-71-88

10. DISTRIBUTION STATEMENT

11. SUPPLEMENTARY NOTES	12. SPONSORING MILITARY ACTIVITY
	Aerospace Medical Research Lab., Aerospace Medical Division, Air Force Systems Command, Wright-Patterson AFB, Ohio

13. ABSTRACT

The objective of this study has been to develop a quantitative description of the mobility of the human torso. This has been accomplished by a systematic multi-disciplinary investigation involving techniques of cadaver dissection, anthropometry, radiography and cinefluoroscopy, photogrammetric, and computer analysis. Seventy-two anthropometric dimensions were obtained on 28 male volunteers, including bone lengths of the extremities and vertebral landmarks. These subjects were statistically matched for both stature and weight to a 1967 USAF anthropometric survey of 2385 adult males. Both radiographs and photographs from different viewing angles were then taken of the subjects while they performed specific reach motions. Statistical regressions were obtained which describe how specific surface markers and bone reference points move in relation to the elbow position for both seated and standing subjects. The major results of the study are, 1) prediction equations and graphs depicting both surface marker and bone reference point locations for a large range of body positions and specific anthropometric variables, 2) prediction equations and graphs describing how the base of the spine reference point (fifth lumbar spinal surface marker) moves in relation to defined seated and standing reference points for given reaches, and 3) a statistical tabulation with illustrations of 72 anthropometric dimensions. It was found that the surface landmarks selected could predict precise locations of the underlying anatomical landmarks. Both the prediction equations and graphical results allow the construction of alternative linkage systems of the human torso for design purposes.

DD FORM 1 NOV 68 1473

Security Classification

14. KEY WORDS	LINK A		LINK B		LINK C	
	ROLE	WT	ROLE	WT	ROLE	WT
Human Engineering						
Extremities Motion						
Torso Motion						
Neck Motion						
Spinal Motion						
Anthropometry						
Workspace						
Human Model						
Anatomy						
Body Links						
Range of Motion						
Photogrammetric						
X-Ray						
Somatotypes						

SUMMARY

A cadaver study was initially performed to define precise bone and surface landmarks, and to determine orthogonal radiographic procedures. Reference points on the radiographs of the cadaver in various torso configurations were marked to provide a standard reference system for later interpretation of living subject radiographs. A special radiographic facility was constructed for obtaining dimensionally accurate radiographs from widely varying angles, and, a four-camera photogrammetric facility was constructed. Special computer programs were written to reduce the radiographic and photographic data to the three-space coordinates of each reference point.

Seventy-two anthropometric dimensions were obtained on each of twenty-eight healthy male subjects. The subjects were selected to match the 1967 USAF Anthropometric Survey on height distribution. The mean weight of the subjects also closely matched the USAF survey. Nineteen subjects provided the final radiographic data, and 15 provided the final photographic data. These data consisted of bone and surface marker coordinates obtained while each subject positioned his torso in various torso configurations. To obtain different torso configurations, the subjects reached with their right elbow to various target locations while in either a seated or standing position.

Statistical analysis of the radiographic data provided prediction equations depicting the movements of the ten surface markers relative to adjacent bone structures. In addition, normal torso skeletal dimensions with specific anthropometry were developed for a limited set of torso configurations. Graphs of these results have also been presented for future design reference.

The photogrammetric data depicted the surface marker coordinates for a wide range of torso configurations. In addition, they provided a means of determining the whole torso mobility. This was deemed necessary since the torso is a group of relatively small bone links that function as a geometric unit. Statistical analysis of the photogrammetric data (over 4500 marker coordinates were included) resulted in prediction equations that depict the coordinates of each surface marker as a function of the elbow position. These prediction equations were developed for the "general" male population (averaged over all the subjects' anthropometric variability), and for specific anthropometric variables. Graphs of the movement of each surface marker as a function of elbow positions have been constructed for both general and selected anthropometric conditions. From inspection of these graphs a designer can readily determine with known dimensional accuracy the torso configuration of a

seated or standing person whose right arm is required to be in various positions. The inspection of the anthropometric prediction model graphs also clearly describe the effects of major anthropometric variables on torso mobility.

A statistical analysis of the sagittal plane mobility of the cervical neck was also available from the radiographic data. This provided quantification of the degree of mobility at the various cervical levels for various head orientations, as well as developing the surface-to-bone vectors. A clear indication of the nasion motion path has been also provided.

This project has provided means of developing new techniques for the study of human torso mobility. These techniques have been applied to the quantification of torso mobility during one-arm reaches without a back support. The resulting data analysis has provided many specific concepts regarding torso geometry, and the effects of specific anthropometric variables. The use of prediction equations to describe torso mobility appears to be justified. The accuracy seems to be comparable to other "hard-link" biokinematic models of the seated operator , while the speed of predicting a specific configuration could possibly reduce computer modeling time to less than 1/100th of its present value. It now remains to develop the torso mobility prediction models so that they will reflect such practical considerations as (1) varying seat configurations; (2) different restraint systems; (3) tasks involving two hands; (4) various hand force requirements; and (5) different forearm and hand orientations.

FOREWORD

The work presented in this report was accomplished under the provisions of contract F-33615-70-C-1777 issued 15 June, 1970 by the Aerospace Medical Research Laboratory (AMRL), (AFSC), Wright Patterson Air Force Base, Ohio. This investigation was conducted in direct support of the Joint Army-Navy Aircraft Instrument Research (JANAIR) program to obtain basic data critical to cockpit geometry evaluation. The 13-1/2 month study was completed 31 July, 1971. Technical monitor was Kenneth W. Kennedy, Anthropology Branch, AMRL.

This investigation was conducted by joint multidisciplinary effort of the Biomedical Department, Highway Safety Research Institute, and by the Department of Industrial Engineering, College of Engineering, in consultation with the Departments of Anatomy and Radiology of The University of Michigan Medical School.

Major authors and investigators are Professor Richard G. Snyder, Head, Biomedical Department, the Highway Safety Research Institute and Department of Anthropology, Professor Don B. Chaffin and Rodney K. Schutz of the Department of Industrial Engineering. Professor F. Gaynor Evans of the Department of Anatomy, and Joseph W. Young, Chief, Anatomy Laboratory, Civil Aeromedical Research Institute, Federal Aviation Administration, Oklahoma City, were instrumental in the development of the concepts and the experimental design.

The authors gratefully acknowledge the assistance of a number of specialists who provided invaluable support in the conduct of this study. Dr. Walter M. Whitehouse, Professor of Radiology and Chairman of the Department of Radiology provided advice and expert assistance in establishing the radiographic protocols. William Price, HSRI Supervisory Radiologic Technician, gave unstintingly of his time and experience in the initial portion of the experimental radiographic studies, and Wayne L. Harris, conducted much of the radiographic analysis. Dr. Kerry Kilpatrick, now of the University of Florida, was instrumental in setting up the experimental modeling, and throughout the study Professor James Foulke, also of the Department of Industrial Engineering, provided knowledgeable assistance. Peter M. Fuller, presently at the Department of Physiology, University of Virginia, assisted with the initial cadaver work. Pamela Bradley of the Kresge Research Institute, assisted with cineradiographic fluoroscopy and with the photogrammetry. Doctoral student K. Park, assisted by Terry Cavanaugh, was responsible for much of the computer programming. Graduate students J. Sinnamon and M. Becker were responsible for the final data analysis. We also wish to acknowledge M. Bolton's editing of the data analysis and final

editing. Stephen Vanek analyzed the radiographic measurements, managed the subject pool, and assisted with the data reduction. Peter Van Eck contributed immensely to the subject data reduction and analysis of the final data. Many illustrations were prepared by Steven Fischer and manuscript preparation assistance was greatly aided by the efforts of Menthele G. Waller. And finally, we wish to acknowledge the competent and cheerful secretarial assistance of Mrs. Gayle Kirma, Biomedical secretary, Mrs. Sharon Marr and Mrs. Susan Kamon, Industrial Engineering Department secretaries.

This technical report has been reviewed and is approved.

Clinton L. Holt, Colonel, USAF, MC
Commander
Aerospace Medical Research
Laboratory

TABLE OF CONTENTS

Part III. Surface Marker Movement and Radiographic Results of Skeletal Mobility

LIST OF ILLUSTRATIONS

LIST OF TABLES

P A R T I

LINK SYSTEM OF THE HUMAN TORSO

SECTION I

INTRODUCTION

Statement of the Problem

The objective of this study has been to determine dimensional data on the link systems of the living human male torso. Three specific tasks have been conducted in this investigation, consisting of

(1) The development of accurate dimensional and positional information regarding the segment links of the human male torso, including the neck, shoulder girdle, thoracic and lumbar regions, and the pelvic girdle, and the normal excursions of these links in the living.

(2) The correlation of the torso and limb end-positions (center of joint rotation), lengths of functional torso links and link excursions to palpable body landmarks and linear dimensions of the body obtainable through conventional anthropometric techniques.

(3) The development of techniques by which the lengths and excursions of torso and limb links may be estimated and located using anthropometric dimensions and landmarks as measured on the USAF population in 1967.

The basic data obtained in these tasks from the cadaver and living human subjects also lends itself to the development of kinematic models to provide the user with easily retrievable design information regarding functional torso configurations.

Scope

This study has been approached from a systems engineering viewpoint. Data were developed through the initial dissection and anatomical, anthropometric, and radiographic measurement of an adult male cadaver. This required an experimental approach to establish reliable and meaningful techniques, which served as a basis for the measurement and subsequent description of human torso mobility.

Early in this study it became apparent that the cadaver data were of more limited value than previous studies had led us to believe, and as a result greater emphasis was placed upon radiographic techniques in the living. Radiographic data from the initial cadaver revealed poor contrast between tissues which made many contemplated measurements impossible. Similarly, initial radiographic data from preliminary test subjects revealed density problems technically impossible to overcome when the subject's arm was rotated in certain positions (longitudinal to axis of the humerus), which necessitated omitting certain planned arm movements. In addition, restrictions in the safe x-ray exposures for the living subjects limited the amount of available data from each subject. These preliminary findings suggested the addition of photogrammetry to the experimental design.

Specifically, the radiographic study had a two-fold objective: (1) to confirm that the placement of surface markers on the torso was in accordance with specific anthropometric marker definitions; and (2) to quantitatively define the movement of the surface markers in relation to specific bone reference points over a limited range of torso configurations. The photogrammetric study had as its objective to develop a quantitative description of the coordinates of the torso surface markers (placed on an anthropometrically well described group of people) for a large range of torso configurations.

To accomplish these objectives a radiographic facility was designed by which x-rays of specific dimensional characteristics were obtained. These were analyzed with the assistance of computer programs to produce three-space coordinates of the skeletal and surface reference points. Likewise, a special four camera photogrammetry system was constructed. This allowed each surface marker to be estimated in three-space coordinates (via other computer programs) as the subjects positioned their torsos in various configurations.

These radiographic and photographic data were analyzed by developing regressions of these data onto both the anthropometric data and the elbow positions for both seated and standing persons. For design purposes, the output of these regressions were plotted for various design situations. Figure 1 depicts these developments.

Since traditional anthropometry has some functional limitations in certain workspace applications, these measurements were supplemented by additional measures at other selected torso landmarks. (Descriptions of these and data formats may be referred to in Appendix A of this report.) Further measurements, believed to be unique to an anthropometric study, were taken directly on the living subjects relative to extremity bone lengths. These latter data would enable a user to correlate our torso linkage findings with previous studies by the late Professor Dempster (1955,1956,1964) for the extremities since comparable basic measurements were obtained. Finally, using the dimensions and

landmarks measured on the 1967 USAF population, as provided by the Anthropology Branch, Aerospace Medical Research Laboratory, Wright-Patterson Air Force Base, graphs depicting the torso mobility of two extreme percentiles of this population were developed for design reference.

Background

Traditionally, anthropometry has been limited to stereotyped dimensions describing the body surface and has been reproducible through palpable and precisely defined landmarks. While such studies have contributed greatly to many areas of application, such measurements are often inadequate when dynamic or functional descriptions are necessary. Design of aircraft cockpit or aerospace crew capsules, for example, require both kinematic and geometric (ergospheric) information. The ability of the operator to reach controls with maximum efficiency and minimum fatigue, as well as his ability to move them, perform tasks, apply pressure torgues, and make required motions are determined by his range of motion at joints of the body. For any population a range of individual capabilities will be found. For an individual, range of joint motion is determined by the skeletal configuration, by the muscle, tendon and ligamental attachments, the amount of tissue, and the articulation.

Some data are presently known for kinematic characteristics of the extremities; however, no knowledge of the link systems of the torso are available. Such basic information of the human body is of major importance to design engineers, and can form a basis for a major advance in the construction of anthropomorphic dummies, can provide a basic input for seat ejection vertebral protection and can establish techniques for subsequent and more detailed investigations. As in any area where a major need for data has long been recognized, the reasons why such information has remained unknown relates to technical problems, availability of support for the necessary effort, ability to form a multidisciplinary team of competent investigators, adequate facilities and resources to accomplish the objective, and creative ability to establish necessary techniques.

During movements, dimensional changes occur linearly over body joints, causing linear distance increase over the convex surface of a joint when it is bent, and a linear decrease on the concave surface of the joint as tissue is bunched up. This has been an important consideration in the design of pressure suits (Emanuel and Barter, 1957). Mobility of the joint has been found to decrease only slightly between ages 20 and 60, declining about 10% by age 70 (West, 1945). No significant differences in mobility have been described between young and middle-aged subjects (Salter and Darcus, 1953; Hewitt, 1928). Beyond age 45 arthritis increases, markedly resulting in a decreased joint mobility in an older population (Smyth, 1959). While no studies have compared racial differences, Sinelnikoff and Grigorowitsch

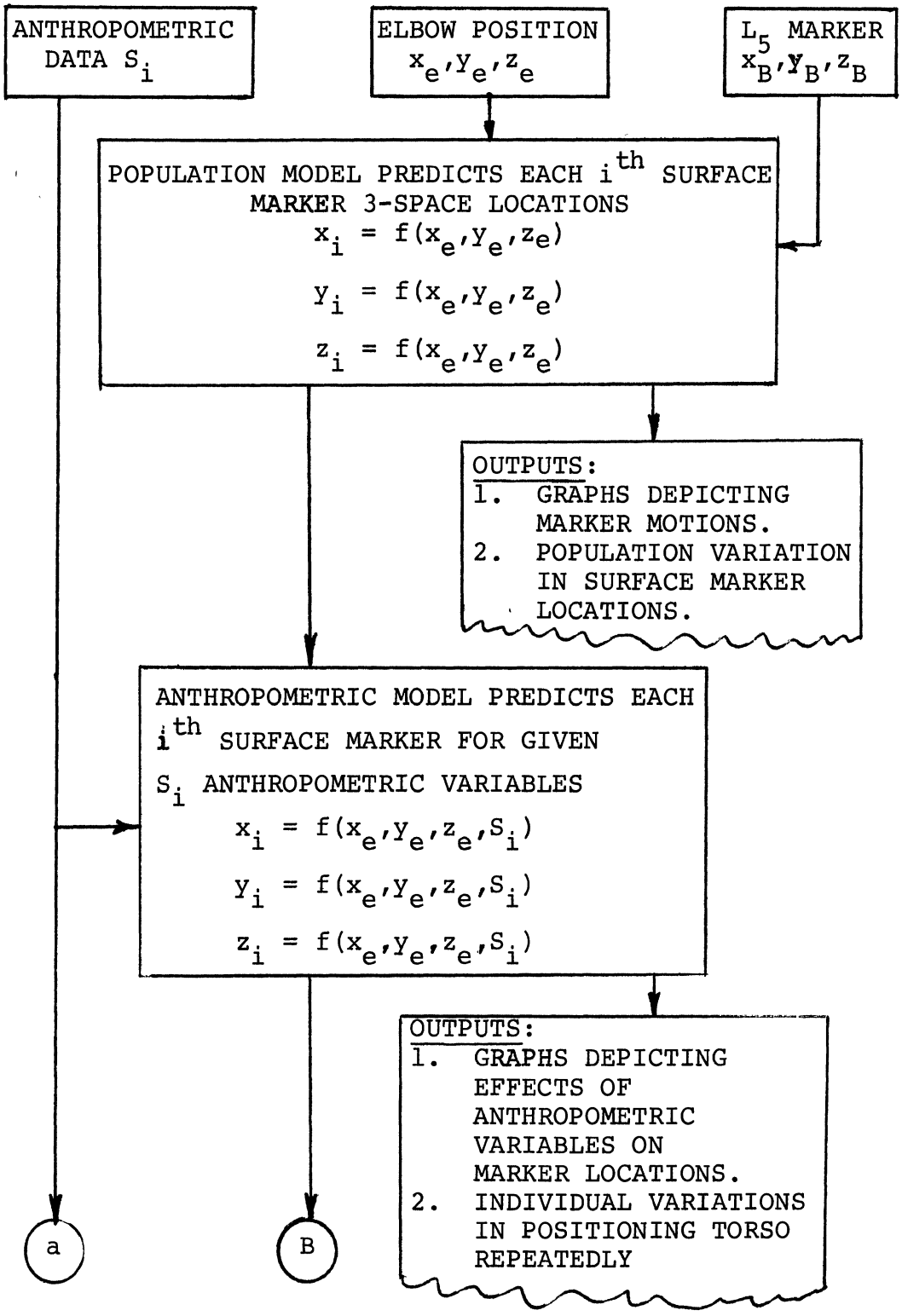

FIGURE 1

TORSO MOBILITY PREDICTION MODEL

Figure 1 continued

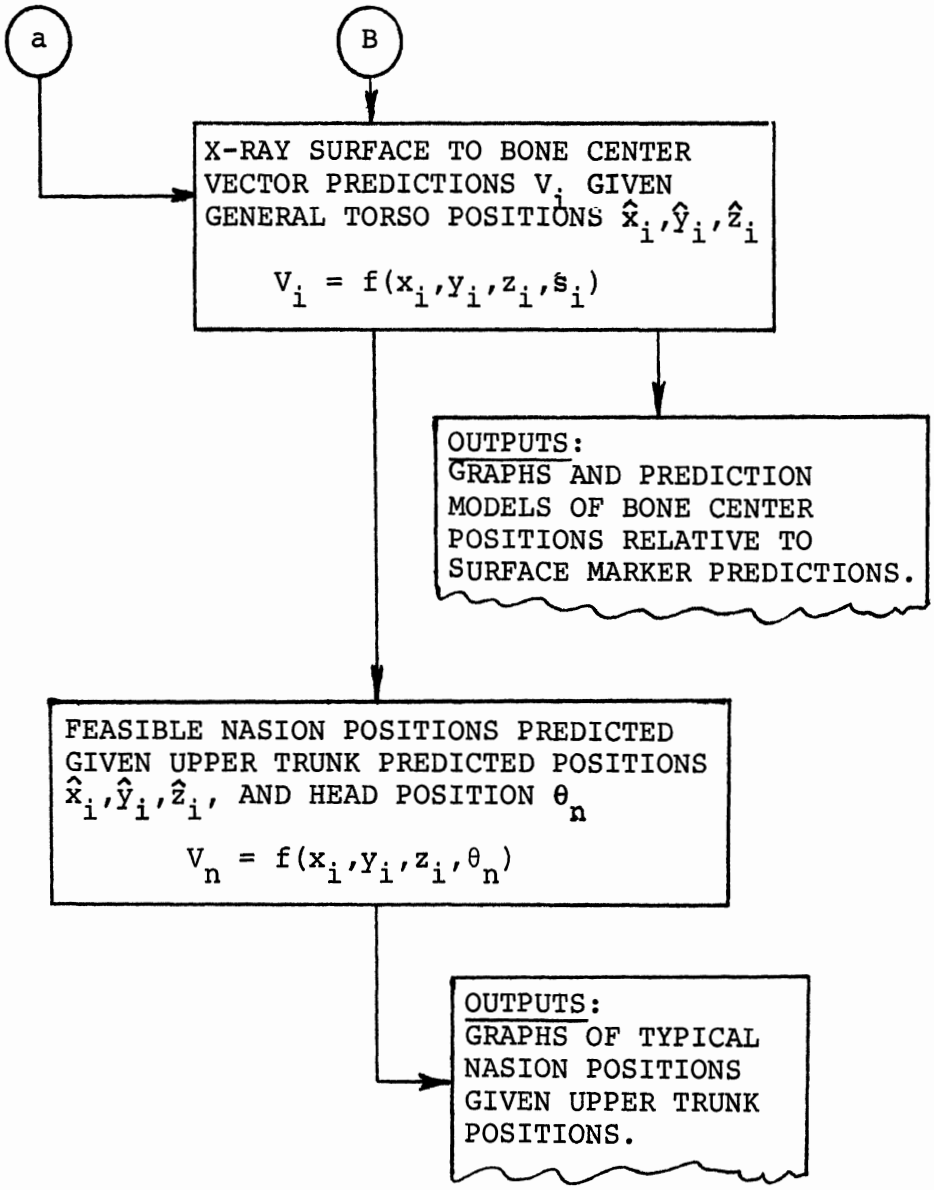

(1931) found that females may exceed males in range of motion of all joints except the knee, and female wrist motion may exceed that of the male by as much as 14 degrees. Similarly, thin individuals appear to have greater range of motion than more obese individuals, with average and muscular body builds being intermediate (Barter, Emanuel and Truett, 1957). Sinelnikoff and Grigorowitsch (1931) found such variations could exceed 10 degrees. Physical exercise, if not excessive, may also contribute to increasing joint range of motion (Keegan, 1962). There appears to be little more than 4 degrees bilateral difference between left and right limb motion (Salter and Darcus, 1953; Gilliland, 1921). Body position or movement in one body part influences range of motion of another part, resulting in greater wrist flexion with the hand pronated than supinated, or in greater hand rotation if shoulder girdle movements are added to those at the elbow. For flight crews, flight clothing may restrict unimpedded motions (Saul and Jaffe, 1955; Nicoloff, 1957), decreasing them by as much as 20 degrees (Dusek, 1958). More recently consideration of motions under zero-gravity have become of interest relative to manned space flight (Dzendolet and Rievley, 1959).

In a major study conducted at The University of Michigan for the Aero Medical Laboratory and published in 1955, Dempster studied the structure of limb joints and the range and type of motions utilizing materials from eight cadavers ranging from 52 to 83 years of age (averaging nearly 69 years). Previous work by Braune and Fischer (1889), and Harless (1860) had provided only limited information from cadaver studies. Thirty-nine living subject representatives of the 1950 Air Force population were studied, resulting in maximum dimensions of workspace for the seated individual, and of kinematic motions (Dempster, 1955, 1956).

In later work supported by the Public Health Service, Dempster developed a means of estimating limb bone and link dimensions from over-body measurements (1964). Range of motion of the neck is still poorly defined.

In our review of 203 clinical papers concerning cervical hyper-extension-hyperflexion injury none of the authors claimed to have measured the actual degree of dorsal or ventral flexion of the neck; thus the limits of motion beyond which trauma occurs is not known. In animal subjects anesthesia produces an artifact and has been shown to impair the stretch reflex (Reichel, 1966). Cervical joint motion has been studied by multiple-exposure films (Dempster, 1955), and cyclograms (Drillis, 1959). Other photographic techniques were devised by Taylor and Blaschke (1951), and Eberhart and Inman (1951). The normal range of neck flexion has been the subject of several studies, but reproducibility, range of variation in individuals, and lack of adequate landmark standards have been difficulties encountered in voluntary human tests. Glanville and Kreezer (1937) demonstrated range of normal voluntary motion of males (ages 20-40) to be 59.8 degrees

(S.D. 11.7 degrees) ventral flexion, and 61.2 degrees dorsal flexion. Defebaugh (1964) found a mean flexion of 57.9 degrees (S.D. 7.9 degrees) and 79.2 degrees extension. The lower limit for both studies was found to be 41 degrees.

Sensors attached to the skin have been found to inaccurately reflect motion of vertebrae in relation to each other during movements of the torso. Experimental work at Berkeley has involved insertion of 3/32-inch diameter threaded steel pins through the skin and anchoring them to the spinous processes at various levels of the thoracolumbar spine under local anesthetic, and using sensing devices to analyze the motion (Sabanas and Porter, 1967).

Other studies have involved range of motion of the wrist on 79 male subjects (Daniels and Hertzberg, 1952). While numerous investigators have treated the mechanics of joint motion, generally of the extremities, a comprehensive coverage is found in Steindler (1964). Kinematic characteristics of the limbs are known to a limited extent; however, similar information concerning joint range of motion of the torso is currently unavailable.

This study represents a first major attempt to obtain torso mobility data using a systems approach. The human torso is not a few long solid links with simple articulations, but rather is a complex group of short links that move as a functional group. Thus only through a systems approach can the total functional mobility of the torso be described. It is believed that this study contributes major insights into torso mobility modeling.

The first part of this study provides the text description of the experimental techniques and results. Part II tabulates appendices A through G and provides data relative to anthropometric procedures and data and a description of the photogrammetric techniques. In particular, this part illustrates in considerable detail the specific techniques utilized and described in Part I. The third part describes surface marker movement and radiographic results of the skeletal mobility. Thus, the reader should refer to the appendices provided in Parts II and III to obtain specific detailed data upon which the text description in Part I is based.

SECTION II

ANTHROPOMETRY

Cadaver Dissection

An initial basic task in this study was to define and establish the relationship of surface anthropometry and landmarks to anatomical landmarks and spatial points related to joint centers of rotation. Cadaver dissection was believed to be essential to define and establish the anatomical reference system, not only as related to the surface anthropometry, but also to make precise and direct measurements as a check on radiographic methods. The cadaver also proved to be of particular value in establishing the radiographic techniques since it could be subjected to multiple radiation exposures and provided necessary baseline information prior to use of living human subjects.

The cadaver used was a caucasoid male, approximately 55 years old, weighing 197 pounds, and 171.2 cm stature. To assist in realistic positioning and joint motion of the cadaver, it was prepared by manually exercising the primary joints of the cervical (neck), shoulder girdle (gleno-humeral joint), pelvic girdle (hip joint), elbows and knees. Radiographs were taken of the entire torso and adjacent structures to determine that there were no anomalies, and to provide a complete set of x-ray films for use as a basic measurement tool.

Several experimental techniques for precise spatial measurement during cadaver dissection were used. In order to measure the cadaver center of joint rotation in space and precisely orient surface and anatomical landmarks dissected and exposed, a device was designed and built as illustrated in Figure 2. This consisted of a 6 X 3 foot box fitted with a plexiglass top and leveled with the autopsy table upon which it was positioned. The specimen was placed upon this device in the supine position. One quarter inch holes placed every 1/4 inch along the plexiglass portion adjacent to the specimen's torso allowed either a probe to be inserted from beneath or a beam of light to be concentrated on a point from below. An exact distance along this posterior-anterior (X) axis could be determined and correlated to a longitudinal (Z) and lateral (Y) axis readout from the surface of the plexiglass. A micrometer equipped with a dial gage allowed readings to 1/10 millimeter. This initial measurement technique was finally eliminated because of too many disadvantages. A primary problem was that points not directly along the lateral border of the specimen could not be determined without major repositioning of the specimen, which also changed the basic reference points.

A technique was subsequently devised which allowed

relatively accurate 3-dimensional direct measurements of anatomical landmark reference points to be made without moving the specimen. This apparatus, illustrated in Figures 2 and 3, consisted of a metal framework which was leveled with the surface of the autopsy table auxillary table top. Moveable scales, with plumb bobs attached, allowed three coordinate X, Y, Z axis measurements relative to the zero point, which was arbitrarily selected at the vertex. A plumb bob was used to obtain a precise measurement in the X (vertical) axis. While this technique is slow, it proved to be simple and accurate.

The subject was measured in accordance with the selected USAF criteria and conventional anatomical landmarks were located and marked. Marking of landmarks was accomplished in several different ways. Round lead pellet markers were affixed with Kadon to various selected surface landmarks. The lead markers were located on the cadaver specimen at the following landmarks: vertex, right and left tragion, nasal root depression, opisthocranion, cervicale, right and left sterno-clavicular joints, right and left acromion, right and left lateral epicondyles, right and left medial epicondyles, right and left anterior superior iliac spines, right and left trochanter, and the center of the spinous processes of each vertebra. These marks showed up clearly on x-ray film and provided accurate reference points.

Landmarks were also located in depth through the use of long pins. These were positioned at the surface landmark and dissection of underlying soft tissues proceeded until the anatomical landmark of the hard tissue was located. In each case the surface landmark was found to have been located almost identically (within 1-3 millimeters) with the underlying anatomical landmark.

In these initial measurements the surface sites were jointly cross-checked by three investigators. Surface anthropometry, however, could not be taken accurately on the cadaver specimen because of tissue differences and compressibility in comparison to the living, and landmarks were thus selected based upon critical relationship to the major torso hinge points and ability to obtain them. Since definitions of landmarks are at variance in the literature, and many may be imprecise in practice, an initial problem concerned agreement on anatomical surface landmark definitions, and subsequently precise definition of the internal skeletal landmarks as identified and measured on the radiographic film of the living subjects. Description of these landmarks for the purpose of this study are provided in Appendixes A and B.

Dissection of major joints was meticulously performed leaving the surface pins in place to determine precision with which the surface landmark would coincide with anatomical landmark. Results were surprisingly accurate, as previously noted. Once the joint (sterno-clavicular, head of the humerus, trochanter, and all dorsal vertebra) was exposed and overlying

muscle removed additional markers were implanted. Centers of movement in the X, Y, Z axis for the head of the right humerus and right trochanter of the femur were determined and marked by insertion of 3/4 inch steel nails (Figures 4 and 5). Nails were also inserted for x-ray reference planes at the sterno-clavicular, acromial, lateral articular aspect of the clavicle, and lateral and medial epicondyles. Subsequent x-ray evaluation of the location of these reference points demonstrated the difficulty in precisely orienting the axis (angle) of the nail, although the skeletal surface entrance point as marked by the nail was found to be quite accurate for calculation of intersecting planes upon the x-ray. It is not felt that the nails could be placed any more accurately by this technique.

The cadaver was next moved to an x-ray table and the left shoulder (gleno-humeral) and hip joints were then pinned as above while under constant fluoroscopic observation. In addition, a 16 mm cinefluoroscopic motion picture film was taken and reviewed to ensure that the pins were accurately centered while the joint was moved in all three axes.

Despite the accuracy obtained in the above techniques, it soon became apparent that use of further cadavers, as originally planned, would not provide sufficient additional useful data to be worthwhile. Our experience with the initial cadaver indicated that it was not nearly as critical for reference purposes to the living subject study as had been believed. Secondly, although considerable efforts were made to obtain the clearest possible x-rays of the cadaver, it was found that poor definition of tissue contrast rendered many measurements anticipated to be useful and necessary to this study impossible to obtain. These factors, coupled with problems in obtaining usable x-rays of living subjects in certain arm positions, led to an early decision to change the initial experimental design to place greater reliance upon the living study and to add photogrammetry as a necessary adjunct technique.

Living Subject Selection and Measurement

Selection of the experimental subjects was conducted in two stages. An initial survey to establish a subject screening pool was conducted in September and October and consisted of 75 male students of The University of Michigan. This pool was subsequently added to during the next few months until about 100 subjects were available for selection. The subjects were for the most part engineering undergraduates obtained with the permission of the instructor during regular class meeting. At this time only measurements of stature and sitting height were made, and weight was estimated by the subject to avoid having to completely unclothe each individual.

The objective of this preliminary survey was to provide a provisional pool of subjects from which final test subjects could

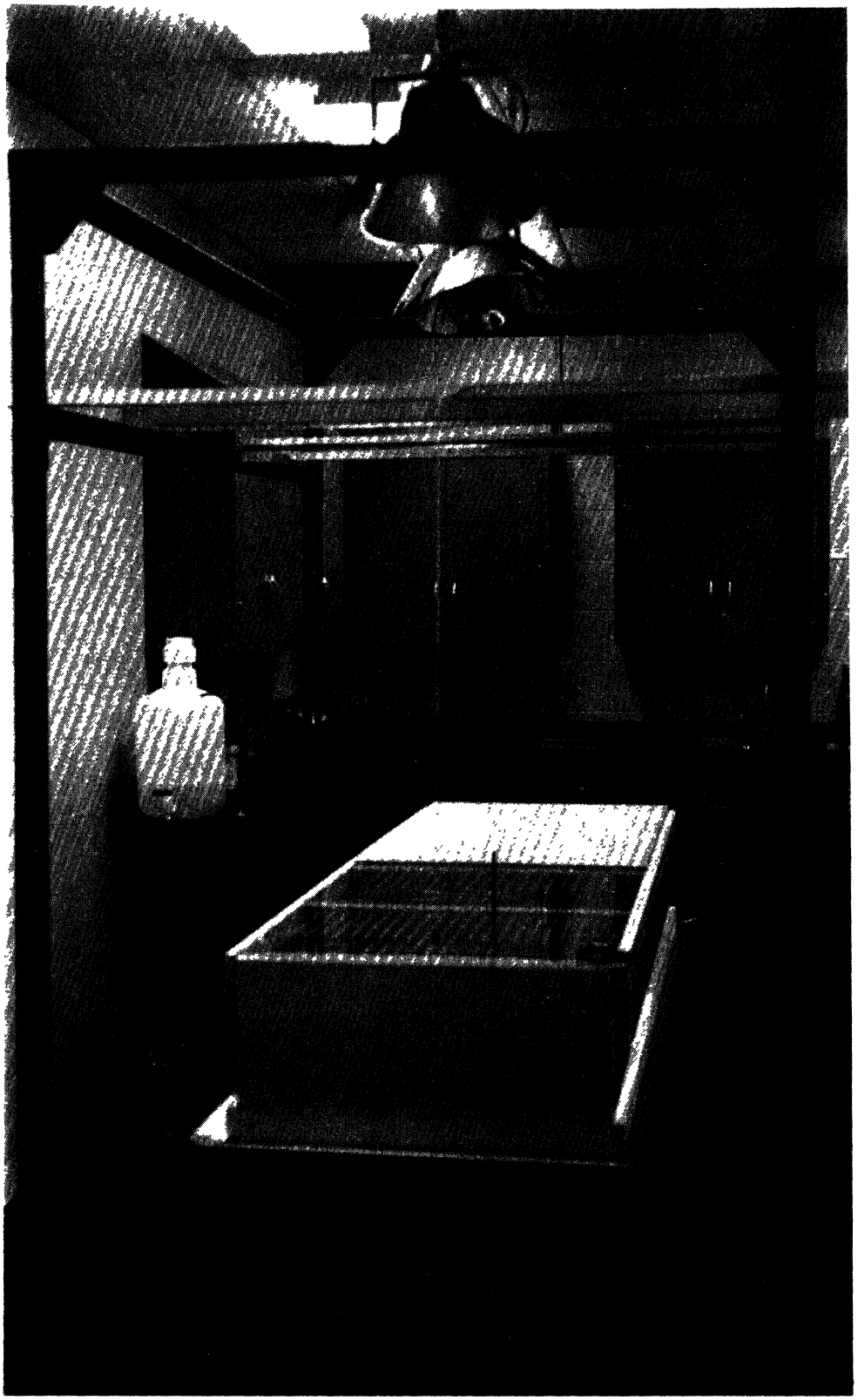

Figure 2. Dissection measurement apparatus used to determine spatial relationships. Overhead scales allow three axis plots of anatomical landmarks.

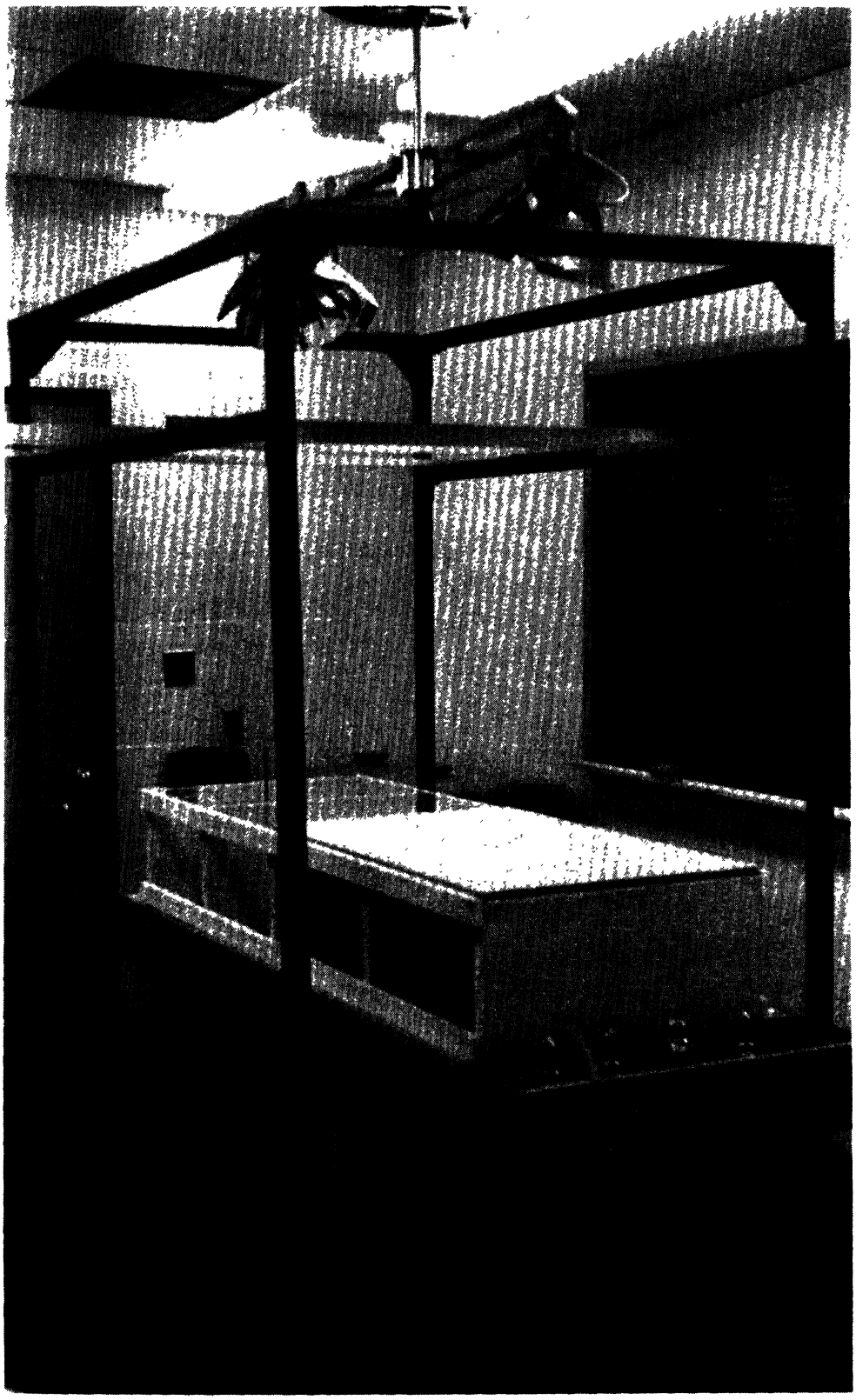

Figure 3. View of autopsy table with dissection apparatus in place. Specimen is positioned supine with head and torso over plexiglass portion.

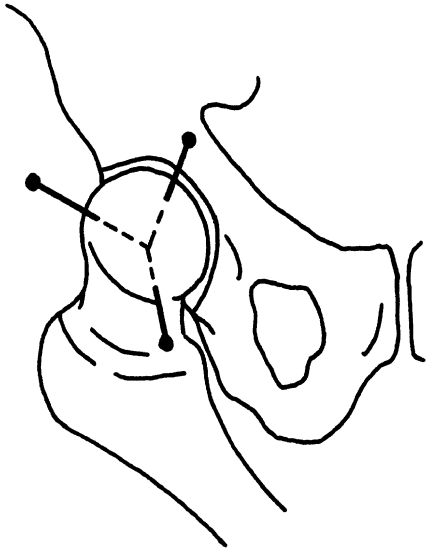

Figure 4. Sites of 3-axis pinning of the head of the femur (hip joint) to locate the center of joint rotation.

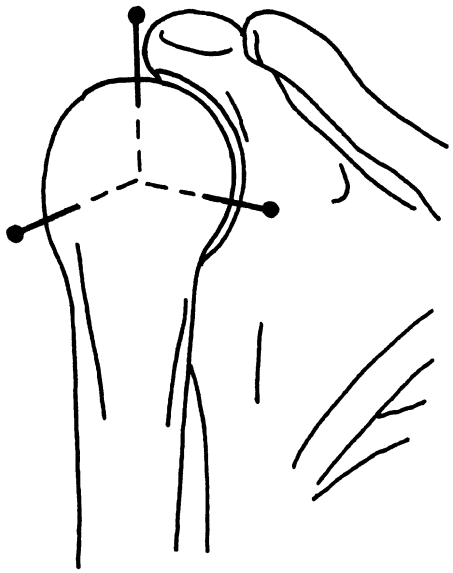

Figure 5. Location of steel pins placed in the head of the humerus to locate the center of rotation of the shoulder (gleno-humeral) joint.

be drawn, primarily upon a basis of stature with sitting height and weight secondary considerations. This also allowed a preliminary screening.

Initial arrangements for test subjects had been made through local military units, including the Navy and Army Reserve and National Guard. In practice, however, it was found that it would be very difficult to schedule these personnel due to conflicts with jobs which often would not allow then the time necessary to act as a subject. An additional consideration was that too small a military pool was available in the Ann Arbor area, and, further, that the majority of these were 18 or 19 year olds. We also found that the subject fee was not sufficient to interest the military reserve enlisted man, many of whom would have had to travel some distance to participate. The result was that it did not appear useful to pursue this source of subjects, and we turned to the student pool, which potentially provided veterans or those holding military reserve status.

Since the primary requirement of the subject selection is that they must be representative of the Air Force population as surveyed in 1967, two problems evolved. One involved the statistical basis to validly select a sample representative of a known group with respect to one or more variables. The second problem, which is perhaps more difficult, was concerned with the determination of which anthropometrics to consider, and further, precise agreement upon their definition.

The three measures utilized for sample selection were stature, sitting height, and weight. We found, however, that in many cases there was little relationship between the three measures within individual subjects (e.g., an individual who corresponded to the 50th percentile in stature might only be 14th percentile in sitting height, but 80th percentile in weight). Enormous variability was found in this respect. Thus, we primarily selected on the single variable of stature. Percentiles for stature, sitting height, and weight for the 1967 Air Force population are shown in Appendix E.

The statistical basis for selection (matching on one variable) is after Churchill.* Our subjects were primarily selected from the preliminary pool according to the required sample for each interval of stature shown in Table 1, for a total sample of 28 subjects. Although our stratified sample lacked two individuals in the 168.75 to 174.4 cm class intervals, it gained two over the required sample in the 183.75 to 186.74 cm class interval, providing a very slight bias toward greater stature than the 1967 USAF population. Mean stature was found to be 178.45 cm for the University of Michigan sample, compared to 177.34 cm for the USAF population. As predicted, the University of Michigan selected stature range was within the 1967 USAF stature range.

*Unpublished manuscript by E. Churchill, Selection of Experimental Sample Subjects. Antioch College, Yellow Springs, Ohio.

The University of Michigan sample compares very closely with the 1967 USAF population in the measures of weight and sitting height. The mean weight for the 28 subjects was 174.61 pounds, comparing closely to the USAF mean weight of 173.60 pounds. The University of Michigan sample had a mean sitting height of 93.11 cm, almost identical to the USAF mean sitting height of 93.18 cm. Our sample, as predicted, thus is comparable to the larger USAF population in these critical measurements.

TABLE 1

STATISTICAL BASIS FOR SUBJECT SELECTION BASED UPON SINGLE VARIABLE OF STATURE TO MATCH 1967 AIR FORCE POPULATION

Stature (cm)	USAF (1967)	%	X28	Sample Required	Sample Obtained
162.75 - 165.74	48	2.01	.56	1	1
165.75 - 168.74	132	5.53	1.55	1	1
168.75 - 171.74	237	9.93	2.78	3	2
171.75 - 174.74	401	16.81	4.71	5	4
174.75 - 177.74	443	18.57	5.20	5	5
177.75 - 180.74	459	19.24	5.39	5	5
180.75 - 183.74	309	12.95	3.63	4	4
183.75 - 186.74	198	8.3	2.32	2	4
186.75 - 189.74	117	4.9	1.37	1	1
189.75 - 192.74	41	1.71	.48	1	1
	2385*			28	28

The second category of problems requiring solution prior to commencement of subject anthropometry involved specific definition of landmarks, decision of required sites, and insurance that the measurements were actually taken in precisely the same way as was done in the 1967 survey. For this purpose agreement on these points was reached in a meeting held at Wright-Patterson Air Force Based on November 23. Measurements were demonstrated on a subject to standardize technique. At this time a number of additional measures were requested by monitor to be included, dealing primarily with skeletal linkages of the appendages, utilizing the definitions of Dempster, "Conversion Scales for Estimating Humeral and Femoral Lenghts and the Lengths of Functional Segments in the Limbs of American Caucasoid Males" (1964).

The anthropometry procedures and data forms developed for recording anthropometry on the subjects is shown in Appendix A. To facilitate measurement, 35 surface landmarks were initially palpated and marked. A total of 72 measurements were recorded, including several required for determining physique assessments. Following measurements, lead markers were placed at predetermined landmarks to be utilized as surface reference points in the

*Plus 19 men below 162.75 cm. and 16 men above 192.74 cm.

subsequent photogrammetric and radiographic analysis, as described in detail in Appendix B. Several measurements were rechecked directly from the radiographic films, and one measurement, clavicular length, was obtained solely from subject x-ray films. Although many measurements, particularly the bone lengths, could be most accurately measured from x-ray films, the restrictions on radiation dosage of our subjects severely limited the number and exposure allowable and prevented obtaining films of the extremities for this purpose.

Any anomalies or other comments pertinent to the subject were noted on the individuals' data form. For example, subject No. 29, on which a 43.3 cm right calf circumference was measured, upon inquiry noted that he had been a baseball catcher, which requires unusual leg muscular development. Similarly, one subject with unusual biceps development had been a champion discus thrower. Often bilateral variances may be explained by congenital or accidental trauma, and we attempted to eliminate from the sample any subjects with pertinent obvious abnormalities

Some comment should be made concerning the utility of different landmarks, since some may be made much more accurately than others. Tragion, when measured relative to the floor, for example, is particularly susceptible to change with subject head movement changes in sagittal plane. Vertebral spinous processes were best found by asking the subject to flex forward; however, care must be taken to relocate the landmark in the erect posture due to skin excursion. Trochanterion proved to be difficult to accurately locate in some subjects, due not only to tissue density at this site, but also to the individual architecture of the trochanteric lateral prominence, which sometimes is not a distinct palpable "point." Similarly, the accuracy with which bitrochanteric breadth may be measured may be variable due to overlying tissue. Lower arm skeletal measurements required assistance from an assistant in order to locate and measure radius and ulna length most accurately.

To reduce measurement error and ensure more accurate comparison with the 1967 USAF population, all measurements were made by the same investigator, utilizing the standardized techniques used by the Air Force Anthropology Branch where measurements were the same. Since anthropometrists may, and usually do, differ in technique somewhat, the initial training standardization session at Wright-Patterson AFB proved essential.

Intercorrelation coefficients for the 72 anthropometric variables were utilized in the surface marker predictive model developed during the final phase of this study. A detailed description of the procedure is discussed in Chapter III, Photogrammetric Procedures and Results. The 72 anthropometric measurements were categorized into 16 functional groupings. Each of these groups or subsets characterizes a different anthropometric attribute. The functional groupings were labeled:

stature, sitting height, trunk circumference, upper arm circumference, lower leg circumference, chest breadth, lower trunk breadth, upper arm breadth, lower leg breadth, upper arm length, upper extremity length, lower leg length, lower extremity length, skinfold thickness, weight, and seat back - to - trochanter length. A reduced correlation matrix was derived for the functional groups (see Section III). The diagonal elements specify the average correlation between elements within the same group. The off-diagonal elements of the matrix specify the correlation between groups. (see Section 3,1 p. 32). The intercorrelation between elements within a specific group proved to be large. This implies that only one measurement from each group is required to describe the anthropometric attributes defined by the groups. For example, the very high intercorrelation between the 18 measurements grouped in the 'stature' subset showed that stature, and weight was observed to be highly correlated with most of the other measurements. As a result, six anthropometric variables were determined.

Somatotypes

To provide another measure of the body physique, somatotype ratings were plotted for the 28 subjects. The system used was the Heath-Carter Technique, which requires measures of age, height, weight, skinfolds, bone diameters, and muscle girths, and results in an evaluation of "morphological components" (Heath and Carter, 1969). It is expressed as a three-number rating, each number representing evaluation of one of the three primary components of physique which describe individual variations in human body form and composition. This system differs from the classical technique of photographing the nude subject in three views and then subjectively assigning ratings (Heath and Carter, 1969), in that it is claimed to be entirely objective and based solely on objectively obtained measurements. A computer program designed by Dr. C. C. Snow at the Civil Aero Medical Research Institute, Oklahoma City, and presently in use in a somatotype study at the University of Oklahoma was used to reduce these somatotype data. We have previously utilized this technique in a study of Air Force test sled volunteers at Holloman Air Force Base (Robbins and Roberts, 1971).

The first number represents an evaluation of the subjects' relative fatness (endomorphy) or leanness, on a scale from 1/2 to 9, in intervals of 1/2 units. Low ratings for the first number signify physiques with little nonessential fat, while high ratings indicate high degrees of nonessential fat. The second number indicates the relative musculo-skeletal development (mesomorphy), or lean body mass consisting of the musculo-skeletal system, the soft organs, and total body fluids—or the whole body, less fat. Low-second-component ratings indicate light skeletal frames and little muscle relief, while high

ratings show marked musculo-skeletal development, as in many athletes. The third component refers to relative linearity of the individual physique (ectomorphy) and is largely based upon the height $/\sqrt[3]{\text{weight}}$ ratios. Low numbers here mean short extremities and low height $/\sqrt[3]{\text{weight}}$ ratios, while high ratings indicate linearity of body segments.

Ten measurements are required to compute the Heath-Carter somatotype (Heath and Carter, ref 29) weight, stature, humeral biepicondylar diameter, femoral biepicondylar diameter, flexed biceps circumference, calf circumference, and skinfold measures at the triceps, subscapular, suprailiac, and calf sites. Dimensions are uniformly taken on the right side of the body. The skinfolds were obtained with the Lange skinfold caliper,* which is adjusted to exert a constant pressure of 10 gm/mm^2 over an area of 20 to 40 mm^2. At each site, a double fold of skin is lifted by firmly grasping a fold between the thumb and forefinger about 1 centimeter from the point to which the caliper is to be applied. Readings are made within 3 seconds after application of the caliper, and the average is taken of several readings. Quite often the calf skin is "tight" and we have found an accurate reading difficult to take. These measurements were taken at the following sites: right triceps, right subscapular, right suprailiac, right posterior mid-calf; and results are tabulated in Appendix D, Section D.

In general, the subject data appeared to fall into the general mesomorphic-endomorphic area, normal for young U.S. males in better than average physical condition, and as representative of a military male population.

*Manufactured by Cambridge Instrument Company, Cambridge, Maryland.

SECTION III

PHOTOGRAMMETRY PROCEDURE AND RESULTS

The basis for the use of photogrammetry was to allow a single person to be studied in a greater number of body positions than was possible with the X-ray procedure described in the next section. In addition, the larger "viewing area" of a photograph provided the means to study whole torso configurations rather than simply the torso sectors permitted by the X-ray exposure limits.

Torso Configurations Studied

The positions each subject was asked to obtain were chosen to create various levels of torso strain. This was accomplished in the following manner. Each subject, either seated or standing, was asked to reach out (forearm vertical) and touch a dull stylus target with the medial/posterior aspect of his right elbow. To assure consistency with each subject, an inked dot was placed on each subject's elbow for reference. The target positions were selected to obtain a total of 70 different body configurations, as follows:

Sitting

45	Total points on elbow-reach envelope in Table 2
3	Vertical reaches (two up and one down)
48	Total sitting positions

Standing

5	Transverse planes (each 45° apart)
2	Horizontal planes (each 30° apart)
2	Distances from shoulder (normal and medium)
20	Total points on sphere
2	Vertical reaches
22	Total standing positions

Each of these positions was assigned a code for later reference, as presented in Table 3.

The total series of 70 tests was divided into 10 sets, each set containing 7 positions. The sets are defined in Table 4. There were 20 subjects assigned to this study, and each subject was required to perform 35 tests, with one replication on each of three sets and two replications on a fourth set. The assignment of sets to subjects is given in Table 5. This redundant method of assigning tests to subjects was necessary because it was not known at the outset how many of the 35 tests could be

TABLE 2

DIMENSIONS OF ELBOW ENVELOPES[1]

HORIZONTAL PLANE	HEIGHT OF ELBOW TARGET FROM FLOOR (Inches)	HORIZONTAL DISTANCE FROM CENTER LINE OF SHOULDER JOINT (RESTING) TO TARGET (Inches) FOR VARIOUS STRAIN CONDITIONS						
		COMFORTABLE NORMAL ENVELOPE	MEDIUM EXTENDED ENVELOPE	MAXIMUM EXTENDED ENVELOPE FOR TWO PERCENTILE MALE				
				Transversal Position from Sagittal Plane				
				-45°	0°	+45°	+90°	+135°
UPPER	Sitting 44. Standing 62.	11.	15.3	24.5	21.5	18.0	17.0	18.0
NORMAL	Sitting 37. Standing 55.	13.	18.0	24.5	24.5	21.0	20.0	21.0
LOWER	Sitting 30. Standing 48.	11.	15.3	24.5	24.5	21.0	20.0	21.0

[1]The envelopes were obtained by checking both 2 and 98 percentile (stature) individuals' elbow excursions for the five transversal planes and three horizontal planes with conditions of "comfortable," "medium extension," and "maximum possible for 2 percentile individual."

TABLE 3

POSITION CODES

ANGLE OF ARM MEASURED IN SAGITTAL PLANE		Transversal Plane Angle (degrees) Measured from Sagittal Plane Through Shoulder				
		-45° Left	0 Sagittal	45 Right	90 Frontal	135 (max) Behind
SITTING	135°	U1 U1e U1m	U2 U2e U2m	U3 U3e U3m	U4 U4e U4m	U5 U5e U5m
	90°	N1 N1e N1m	N2 N2e N2m	N3 N3e N3m	N4 N4e N4m	N5 N5e N5m
	45°	L1 L1e L1m	L2 L2e L2m	L3 L3e L3m	L4 L4e L4m	L5 L5e L5m
	Vertical	VU VUm	VL			
STANDING	135°	Us1e Us1m	Us2e Us2m	Us3e Us3m	Us4e Us4m	Us5e Us5m
	45°	Ls1e Ls1m	Ls2e Ls2m	Ls3e Ls3m	Ls4e Ls4m	Ls5e Ls5m
	Vertical	VsU VsUm				

N - Normal horizontal plane through shoulder
U - Upper plane (30° arm up at normal reach)
L - Lower plane (30° arm down at normal reach)
s - Standing
1 - 45° from shoulder sagittal plane (left)
2 - 0° shoulder (in sagittal plane)
3 - 45" from shoulder sagittal plane (right)
4 - 90° from shoulder sagittal plane (in frontal plane)
5 - 135° from shoulder sagittal plane (behind frontal plane)
e - Extended medium
m - Maximal extended

TABLE 4

DIVISION OF POSITIONS INTO SETS

SET NUMBER	TEST POSITIONS						
S1	VU	U1	U2m	Us3e	N3	L5	Ls4m
S2	U4e	Us5m	N1e	N5m	L3e	L1m	Ls2e
S3	VUm	U2	U3m	Us4e	N4	L1	Ls5m
S4	U5e	Us1m	N2e	N1m	L4e	L2m	Ls3e
S5	VL	U3	U4m	Us5e	N5	L2	Ls1m
S6	U1e	Us2m	N3e	N2m	L5e	L3m	L34e
S7	VsU	U4	U5m	Us1e	N1	L3	Ls2m
S8	U2e	Us3m	N4e	N3m	L1e	L4m	Ls5e
S9	VsUm	U5	U1m	Us2e	N2	L4	Ls3m
S10	U3e	Us4m	N5e	N4m	L2e	L5m	Ls1e

TABLE 5

TEST SETS FOR EACH SUBJECT

SUBJECT NUMBER	SEQUENCE OF SETS FOR EACH SUBJECT				
1 & 11	S1	S2	S3	S4	S1
2 & 12	S5	S6	S7	S8	S5
3 & 13	S9	S10	S1	S2	S9
4 & 14	S3	S4	S5	S6	S3
5 & 15	S7	S8	S9	S10	S7
6 & 16	S1	S2	S4	S3	S2
7 & 17	S5	S6	S8	S7	S6
8 & 18	S9	S10	S2	S1	S10
9 & 19	S3	S4	S6	S5	S4
10 & 20	S7	S8	S10	S9	S8

analyzed. The data reduction of the photographs is a very expensive, time-consuming process. Due to the availability of an "off-line" photo analysis system, the excessive "on-line" computer time was not needed to reduce the photographs to X-Y reference point locations. Thus all 35 frames of each subject were capable of economical analysis.

The capability of determing both the inter-subject and intra-subject variance was provided by the repetitions. Each subject was required to perform seven tests twice. The choice of test conditions in and between sets was statistically balanced thus; there was no risk of having the angles or distances confounded by the subject's height and weight. No subject performed more than two tests at one particular shoulder angle or at one particular reach distance.

The subjects were assigned to the test sequences in Table 5 according to their height and weight measurements. Although a one-dimensional ranking was not very precise, it was possible to contrast subjects at the top and bottom of the ranking scale, thus further reducing the chance that an intra-subject variance might change general inferences about the torso mobility.

Photographic Test Sequence

Each subject was brought to the photogrammetry laboratory after being X-rayed. Hence, the surface markers were in known locations, and his anthropometric dimensions had been established. He was instructed as to the procedure. The four orthogonal cameras were checked to assure that the first frame was positioned, and each camera was focused. The subject was then positioned as described above. With the subject in position, the photographer simultaneously triggered all four cameras by an electronic shutter release. The films were then automatically indexed while the subject was instructed as to the position for the next photograph. The frame identification numbers were changed, and the procedure was repeated until all 35 positions were recorded. The photographs in Figures 6-9 depict a subject from the three orthogonal views (front, side, above), and a rear view.

Subjects Used in Photogrammetry Study

As described in the preceding section, not all of the 28 measured subjects were included in the subsequent photogrammetric and X-ray studies. The design of the photogrammetric study required 20 persons at the onset. The design was such that subject size and position effects were balanced, thus greatly reducing the chance of a particular body position effect on mobility being biased due to the accidental loss of photographic data on one specifically sized individual.

Because all the surface points on the body had to be clearly

Figure 6. Frontal view of subject as seen by camera No. 1.

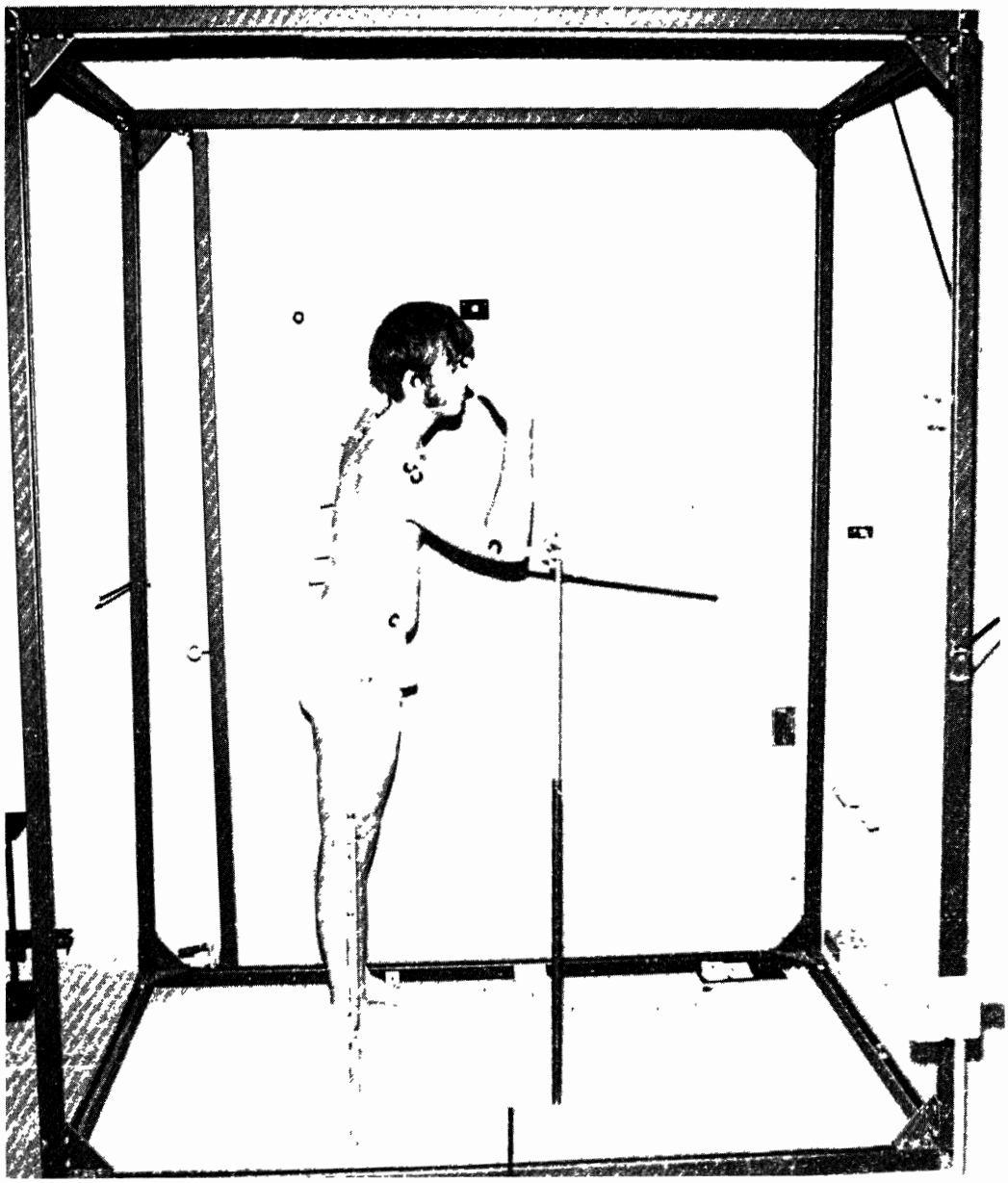

Figure 7. Side view of subject as seen by lateral camera No. 2, with subject in same positions as in preceding figure.

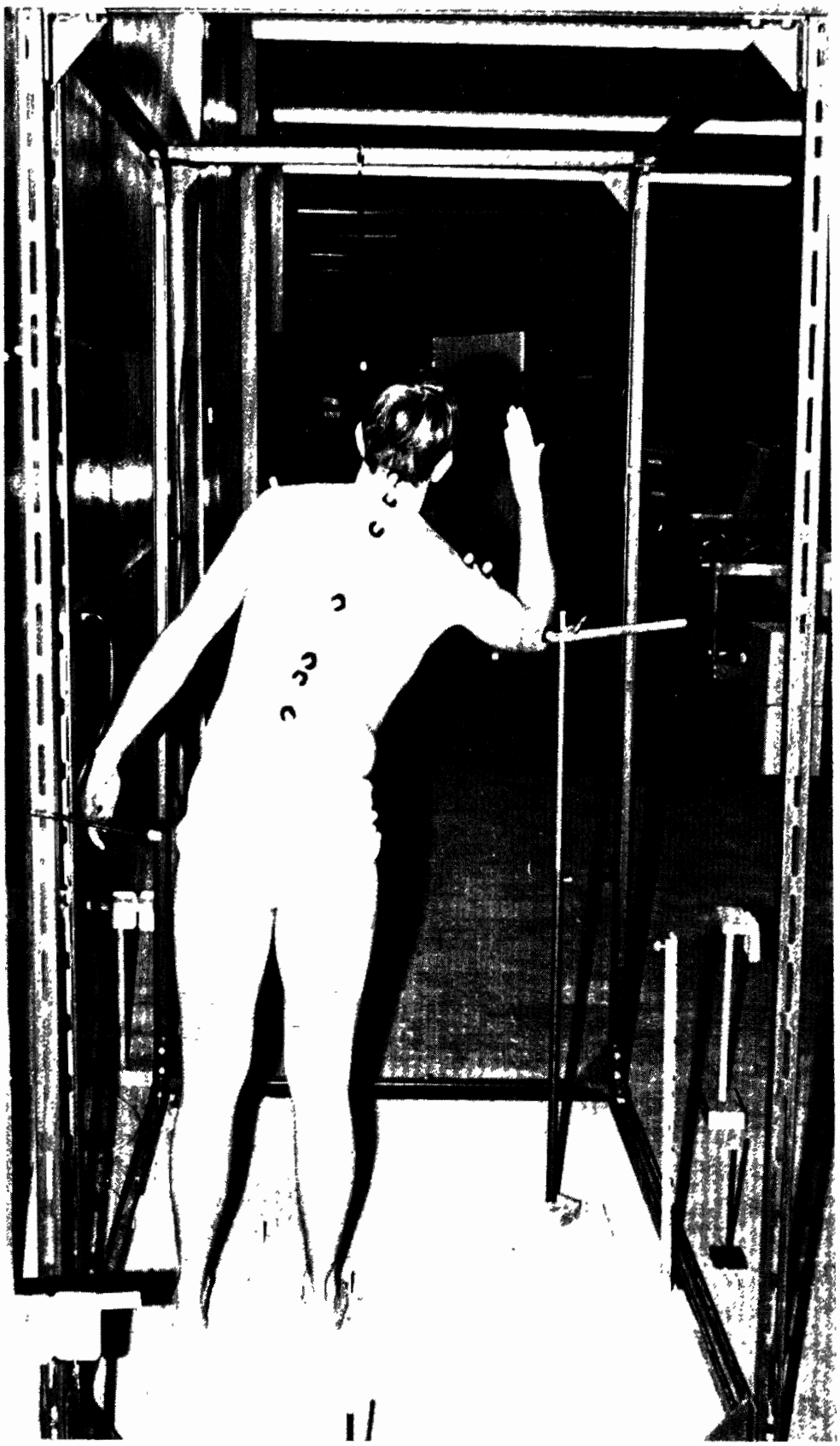

Figure 8. Rear view of subject as seen by rear camera No. 3, with subject in same position as in preceding figures.

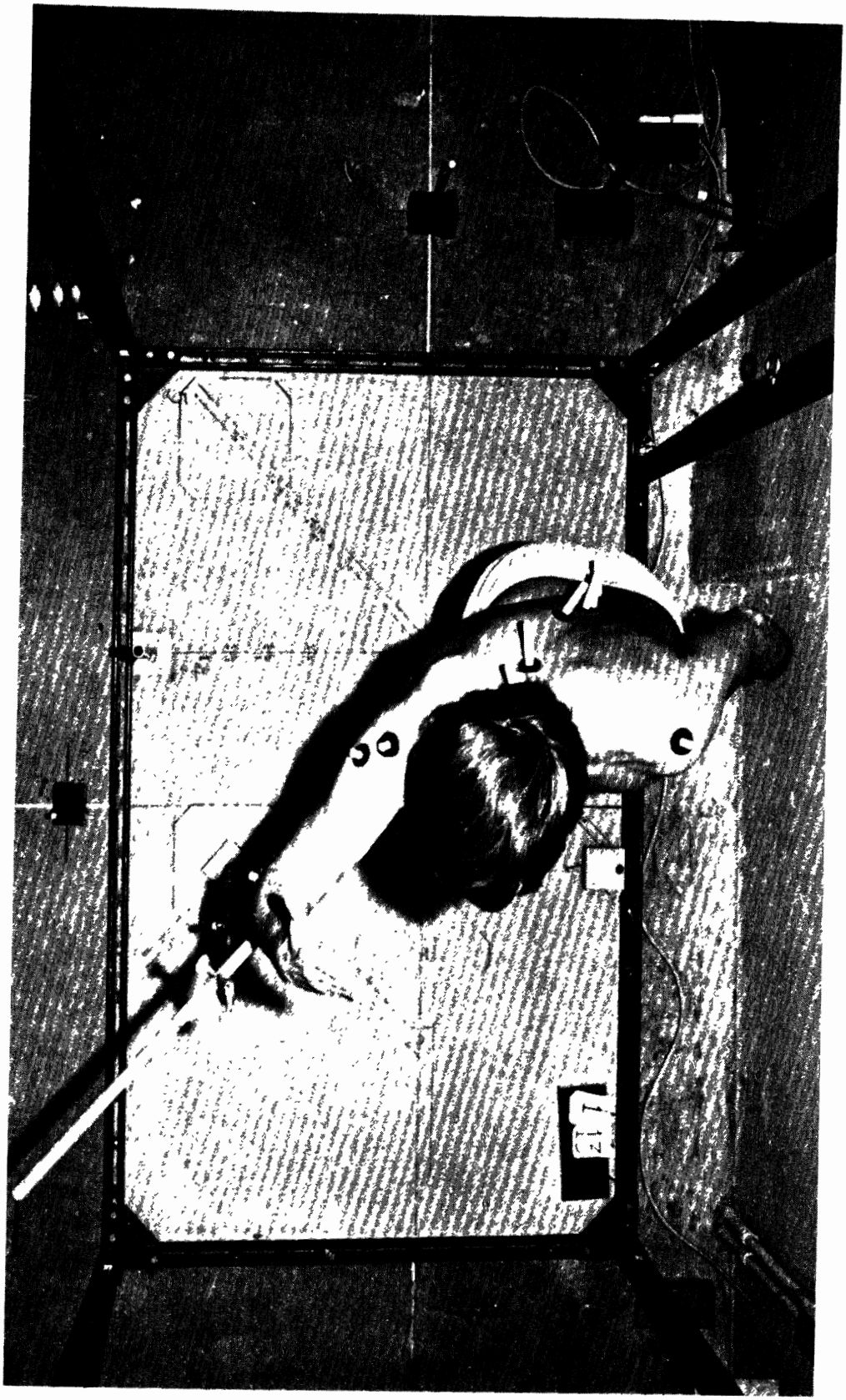

Figure 9. View from overhead camera No. 4 of subject in same position as in preceding figures.

visualized by at least two cameras for each position, there was a high probability of losing data. As it was, 15 of the original 20 subjects did supply adequate photographic data for the following analysis. Their stature and weight distributions are depicted in Figure 10. These subjects provided dimensional data on the locations of the following surface markers for all 35 torso positions (Appendix B describes each point in detail):

*Right acromion
*Left acromion
*Suprasternale
*C_7 surface spine marker-cervicale
*T_4 surface spine marker
*T_8 surface spine marker
*T_{12} surface spine marker
*L_2 surface spine marker
*L_5 surface spine marker
*Right anterior superior illiac spine

Photograph Data Reduction

The location of each of the surface markers in each photograph is obtained by rear projecting each photograph onto a Datacoder, produced by the BBN Company of Los Angeles, California. By moving a cursor over the point of interest and activating the system, a punched-paper tape of the coordinates is prepared. A photograph of this system is contained in Figure 11.

The punched-paper tapes from the Datacoder were then analyzed by a special computer algorithm.* This algorithm solves for the three space coordinates of each point by simultaneously considering the two-dimensional locations of each point viewed from two orthogonal directions. The mean repeatability of the procedure and equipment has been found to be 0.4 inch. A brief description of the algorithm is presented in Appendix F.

The output of the computer algorithm is a listing of the three-dimensional (3-space) coordinates of both the ten surface markers and the corresponding elbow target locations. Punched-card output was also provided for the development of prediction models, as described in the next section.

Prediction Model Development

The photogrammetric data of the surface markers previously listed for the trunk and shoulders were analyzed by developing linear and nonlinear least-squared error regressions of the

*The basis for this algorithm is described in a Ph.D. Dissertation by Kerry Kilpatrick, entitled "A Model for the Design of Manual Work Station," UNIVERSITY MICROFILMS, August, 1970.

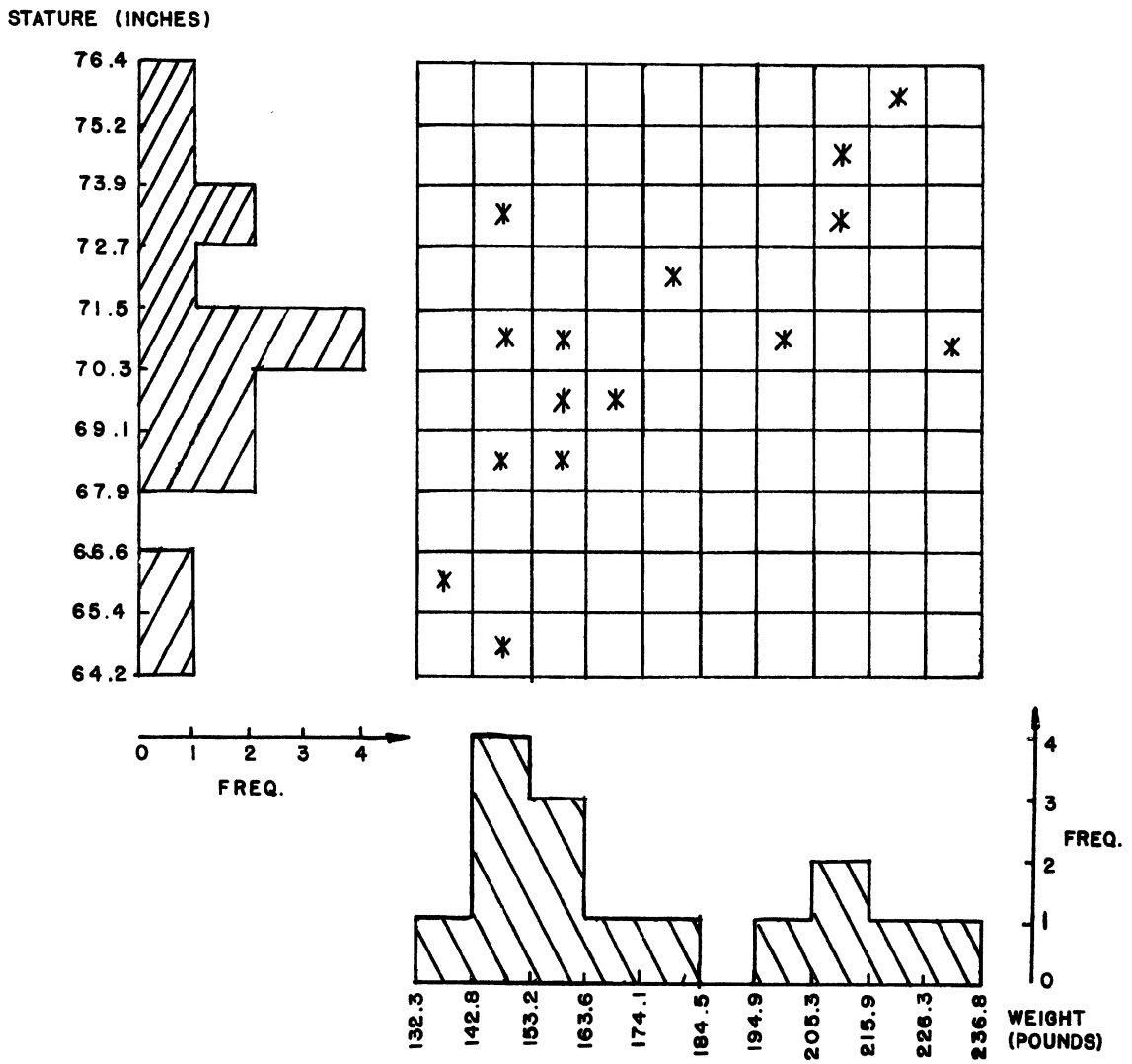

FIGURE 10

SUBJECT DIMENSIONS USED IN PHOTOGRAMMETRY STUDY

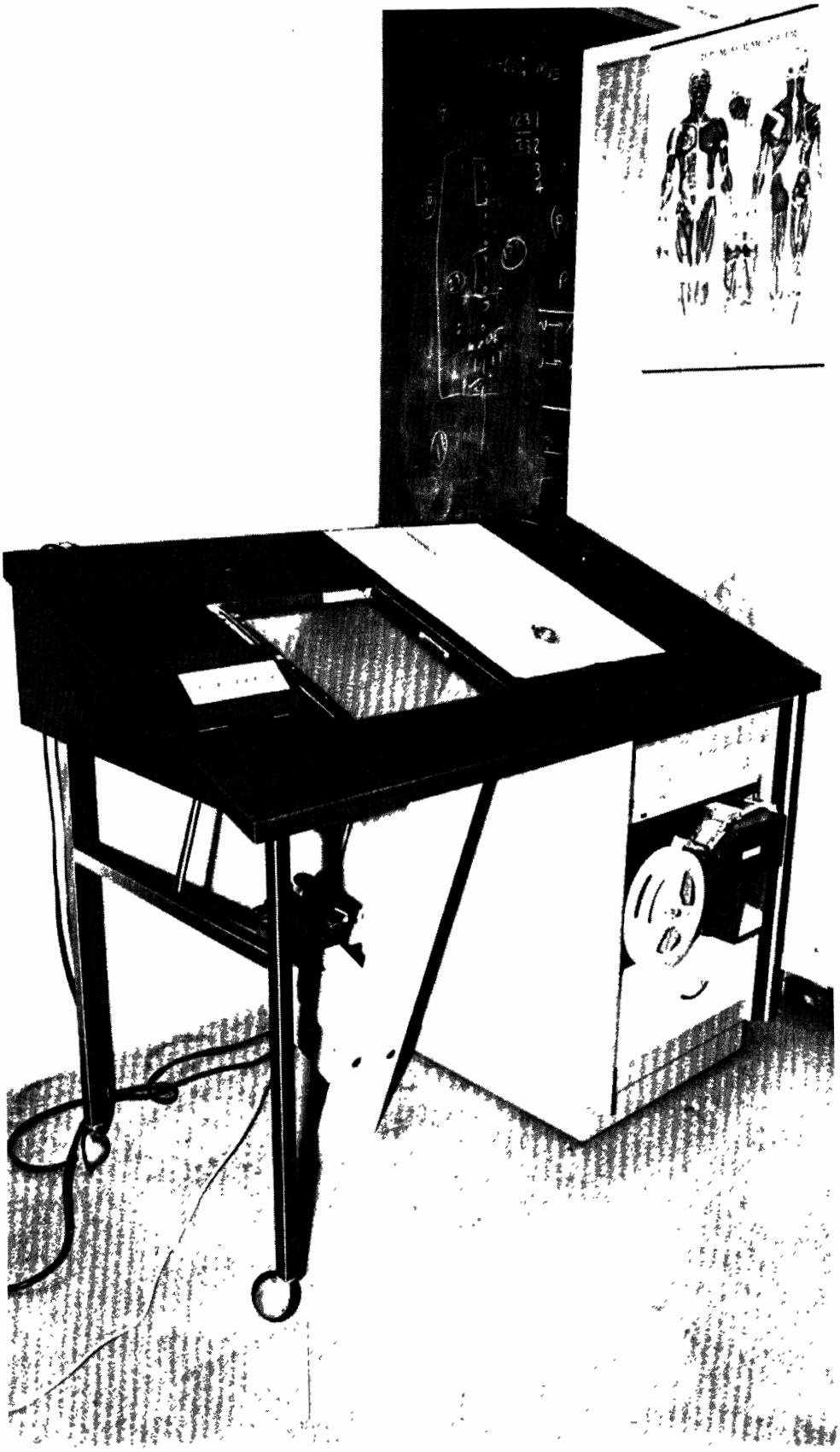

Figure 11. Off-line photographic data reduction system.

coordinates of each j^{th} surface marker (X_j, Y_j, Z_j) on each of the elbow coordinates (X_e, Y_e, Z_e), described in Table 2. This modeling does not include anthropometric variables, and hence it is referred to as a General Model of this form:

$$X_j = F_j(X_e, Y_e, Z_e)$$

$$Y_j = G_j(X_e, Y_e, Z_e)$$

$$Z_j = H_j(X_e, Y_e, Z_e)$$

The functions F_j were estimated by stepwise regressions. To perform these regressions, each surface marker was considered initially to be empirically related to the elbow coordinates, elbow coordinates squared, and elbow coordinates cubed. Admissible variables in the final functions were determined from consideration of both the coefficient of determination, R^2, and the standard error, S_e. When either S_e fell below 0.75 inch or the inclusion of an additional variable did not increase R^2 by more than 1 percent, the stepwise iteration was terminated.

Since the sample size exceeded 400 data points for each of the regressions, the resulting General Model of Torso Mobility has prediction capability in the widest sense. In most cases, only a limited number of variables were significant in the regressions; thus the degrees of freedom of the model remained quite high.

A second predictive model was developed to include anthropometric variables. This model is referred to as the Anthropometric Model. Its development involved the following:

1. Reviewing the inter-correlation matrix of each of the anthropometric variables described in Section II. This was done to define sets of variables directly appropriate to torso geometry, and variables which could predict the other variables with stated and acceptable accuracy. This procedure allowed identification of the following six different sets of variables which were both geometrically contrasting and had significant intercorrelations (average r > 0.4):

   *Standing Stature (var: #2,3,4,5,6,7,8,9,10, 13,14,17,18,19,20,21,23, and 24).
   *Sitting Height (var: #58,59,60, and 61).
   *Trunk Circumference (var: #47 and 48).
   *Upper Trunk Breadth (var: #12 and 15).
   *Upper Limb Length (var: #27 and 28).
   *Weight (var: #1).

Anthropometric variables not included in the above groups (e.g., those describing leg breadth, foot and hand widths, head circumference) were either highly correlated with other variables in the groups or were functionally unrelated to the present problem.

2. Selecting a set, S_j, of representative variables within each group. This was based on the variable which had a consistently high correlation with the other variables in the group. This resulted in the following variables being representative of each group:

    *Standing Stature (var: #2 - stature)
    *Sitting Height (var: #58 - sitting height)
    *Trunk Circumference (var: #47 - chest circumference)
    *Upper Trunk Breadth (var: #15 - biacromial breadth)
    *Upper Limb Length (var: #27 - humeral length)
    *Weight (var: #1 - body weight)

Further justification for these measures is based on their ease of measurement and apparent consistency, since they correlated (avg.r = .7) with other variables in each functional group.

The above six anthropometric variables were then included (as linear, squared and cubed transformations) in a second stepwise regression of each surface marker location. The result of these regressions was a torso mobility prediction model which included significant anthropometry. This is referred to as the Anthropometric Model and is of the form:

$$X_j = F_j(X_e, Y_e, Z_e, S_j)$$

$$Y_j = G_j(X_e, Y_e, Z_e, S_j)$$

$$Z_j = H_j(X_e, Y_e, Z_e, S_j)$$

The determination of whether a specific anthropometric variable (or its transformation) adds any significant contribution to the prediction of torso configurations was decided by again inspecting both the coefficient of determinations and the standard error estimation. If, in the process of the stepwise regression, the coefficient of determination became greater than 70 percent, an additional variable was not included if it only added one percent to the predicted variance in the surface point locations. Also, a variable was not included if the standard error of estimation became less than 1.5 inches, which is approaching the

average within-subject variability. If the standard error of estimation was greater than 1.5 inches, and the coefficient of determination was less than 70 percent, then variables were added until the increase in the coefficient of determination, averaged over the last three variables, was less than 0.5 percent.

Results of Prediction Models

General Model Results

The use of stepwise regressions with as many data points as were available from the photogrammetry study (at least 400 for each surface point) provided good estimates (as discussed in the next subsection) of how each surface point moves as a function of the elbow positions. The prediction equation coefficients are presented in Appendix G. For design purposes, a set of graphs depicting surface marker locations as a function of the elbow positions has been prepared. For the seated person, without considering specific anthropometry (i.e., general model) the graphic results are depicted in Appendix H. A similar set of graphic results for the standing person is presented in Appendix I.

Examination of these graphs discloses numerous spatial concepts regarding the functional mobility of the human torso when reaching out into the immediate environment with one arm. Some of these concepts have been listed with the set of graphs depicting each surface marker movement in the appropriate appendices. Thus a designer can refer to these comments to assist in the expected interpolation and extrapolation of the graphic results.

Anthropometric Model Results

The stepwise regression procedure developed good estimates of the combined effects of elbow locations and anthropometry (as discussed in the next subsection). The resulting prediction equation coefficients are presented in Appendix G.

To demonstrate the effects of specific anthropometric values, both 5- and 95-percentile values were chosen from the 1967 USAF anthropometric survey of USAF rated officers for the anthropometric variables to evaluate the Anthropometric Model. The data and the graphs depicting the predicted locations of the surface markers are summarized in Appendix J.

In general, the major anthropometric variables in torso mobility modeling are the sitting and/or standing heights. These particular variables have a directly proportional effect on the vertical height of the surface markers, and a secondary but

significant effect on the horizontal movements of the surface markers. The other anthropometric variables used in the stepwise regressions have lesser effects, as can be seen from their coefficients summarized in Appendix J.

Prediction Model Error Estimates

There are two major components to the analysis of how well a prediction model estimates the value of a dependent variable (i.e., the surface marker coordinates). The first component will be referred to as the inherent data variance; i.e., for the same set of independent conditions, there is some unpredictable variance in the dependent variable, due to a combination of such factors as motivation, coordination and basic measurement error. The second component for evaluation of a model is the variance in the data about the predicted values. This latter component combines the inherent data variance with variance owing to the model's not accounting for consistent variability in the data, i.e., model error.

Usually, data are presented in one dimensional form, thus its variability is easily evaluated. The surface marker data in three dimensions, however, and thus along a single vector, but in an infinite number of vectors radiating from its expected value. Figure 12 illustrates this concept.

An informative three-dimensional interpretation can be developed. Such an interpretation requires that the concepts of a "feasibility volume" and an average feasibility sphere be defined. If the same subject performs the same test twice, his torso configuration will not be exactly the same for the second test. If the same reach test was replicated several thousand times, the observed coordinates for a given surface marker would generate an egg shaped volume in space. This egg shaped volume can be called a feasibility volume. A different feasibility volume would be generated for each surface marker for each reach position. Each point in a given feasibility volume is not equally likely, but each is equally acceptable. The frequency of points is greater in the center than on the outer surface of the volume, but any of the delimited points could be realized by performing the reach test normally. A useful approximation for the feasibility volume is developed by defining an average feasibility sphere. An average feasibility sphere is a sphere inscribed within the feasible volume. This approximation has two advantages. First, the irregular volume is replaced by a more manageable entity, a perfect sphere. Second, since the sphere is inscribed within the volume, it concentrates attention on the high density segment of the total feasibility volume. The original irregular volume defines what could happen, while the sphere states what does happen in a majority of cases.

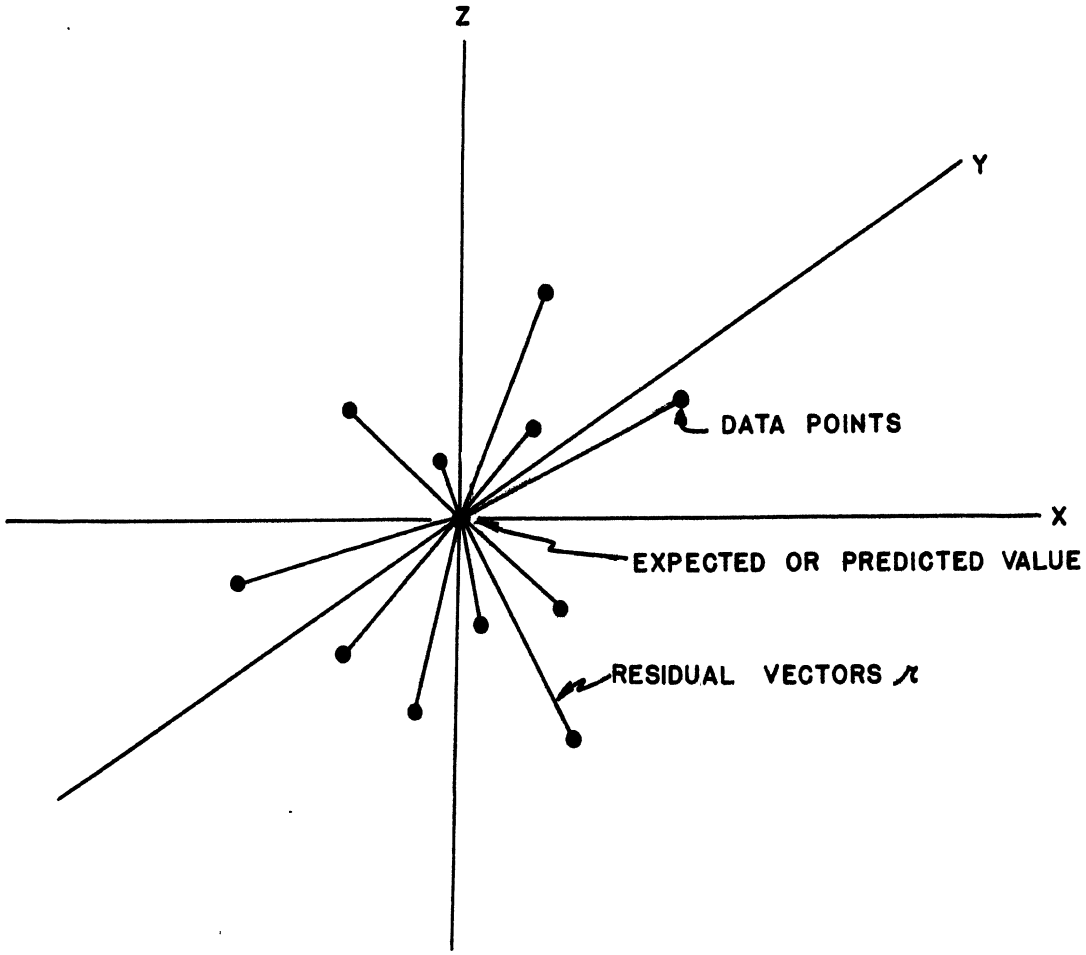

COMPARISON STATISTICS:

$$\overline{R} = \frac{1}{N} \sum_{i=1}^{N} r_i$$

$$\sigma_r = \sqrt{\sum_{i=1}^{N} (r_i - \overline{R})^2 / (N-1)}$$

FIGURE 12

ILLUSTRATION OF TECHNIQUE FOR EVALUATION OF MODEL PREDICTION ACCURACY

The size of the sphere used to represent the data depends upon the variance of the data and the proportion of the data to be encompassed within the sphere. Three different distributions were assumed—uniform, triangular, and exponential—to determine the proportion of the data in a volume encompassed by spheres of varying radii. The following displays the estimates of the effects of the three distributions.

1. Uniform distribution: $-r < x,y \;\&\; z < r$

$$f(x,y,z) = \frac{3}{4\pi r^3}\, dx\, dy\, dz$$

$$V_{\bar{R}} = .42 \qquad V_{\bar{R}+\sigma_r} = .84$$

2. Triangular distribution: $-r < x,y \;\&\; z < r$

$$f(x,y,z) = \frac{3}{\pi r^3} \cdot \frac{[\,1-(x^2+y^2+z^2)^{1/2}]}{r}$$

$$V_{\bar{R}} = .48 \qquad V_{\bar{R}+\sigma_r} = .80$$

3. Exponential distribution: $\infty < x,y \;\&\; z < \infty$

$$f(x,y,z) = \frac{1}{8\pi\theta}\, e^{\frac{-(x^2+y^2+z^2)}{\theta}}\, dx\, dy\, dz$$

$$V_{\bar{R}} = .58 \qquad V_{\bar{R}+\sigma_r} = .84$$

Because the volume of points encompassed by a sphere of a given radius is not sensitive to the distribution of points, as shown above, the inherent data variance and the prediction model accuracy can now be reported by two statistics which have a concise interpretation. These are:

$\bar{R}$ - The radius of a sphere encompassing approximately 50% of the observed data about an expected or predicted value.

$\bar{R}+\sigma_r$ - The radius of a sphere encompassing approximately 80% of the observed data about an expected or predicted value.

Both of these statistics were estimated for each surface marker to illustrate the inherent subject variance within the data, the General Model prediction error, and the Anthropometric

Model prediction error. Table 6 summarizes these values. By comparing the values of $\bar{R}$ in the table, it can be seen that the variability of the anthropometric model is two to three times larger than for the subjects alone. The variability of the general model is 2.5 to 3.5 times larger than the pure subject variability.

Numerical tests for goodness of fit of the models were not performed. These tests place severe restrictions on the form of the variance-covariance matrix and require the use of a non-central chi-square distribution. However, visual inspection of Table 6 implies that the null hypothesis that the variability of the model is the result of the subjects alone would be rejected.

The precision of the present model is probably better than is indicated in Table 6. In analyzing the data, it is very difficult to determine if outliers are correct or bogus. A vector residual of 3.00 inches could represent a drastic lack of fit or an error in the multiple stage data reduction process. The elimination of any of these questionable outliers could not be justified for the non-replicated data points. For the replicated points about 95% of the outliers greater than 3.00 inches were eliminated. An estimate of the true value of a data point can be achieved from the replicated data. Outliers can be questioned and rejected with confidence when necessary. The existence of relatively few bogus outliers in the data base for the models could easily account for the imperfect fit. One residual of 5 inches is equivalent to 20 normal residuals.

From the engineering design viewpoint, however, the prediction accuracy of the model is well within the state-of-the-art. Though it is difficult to compare these project results with other human geometry prediction model results, some analogies will be attempted. The largest single problem in this regard is that existing computerized man-models have slightly different end objectives than this project. Two of the best developed computerized man-models are the results of the Boeing Company's Cockpit Geometry Evaluation Project (for JANAIR under ONR contract N00014-68-0289 and NR213-065), and a University of Michigan Ph.D. thesis project completed by Kilpatrick (1969) (for the MTM Association and the Western Electric Company, Inc.). Both of these efforts assume a linkage representation of the body (two-link torso), which is then oriented in space by both empirical and logic-based algebraic functions of the hand positions relative to the seat (or pelvis). Tests of the prediction accuracies of these two models have been completed for specific tasks and subject groups (4 tasks with 25 subjects for Boeing Model, and 35 tasks with 5 subjects for Kilpatrick Model). In general, it appears that these models can predict the three-space coordinates of their defined shoulder and elbow joints to within a mean vector residual $\bar{R}$ of about 4 inches. In both of these validations a full back support was present, as opposed to only the

TABLE 6

VALUES OF $\bar{R}$ AND $R+\sigma_r$ (Inches) FOR VARIOUS SURFACE MARKERS

Surface Marker	Position	Within Subjects		General Model		Anthropometric Model	
		$\bar{R}$	$\bar{R}+\sigma_r$	$\bar{R}$	$\bar{R}+\sigma_r$	$\bar{R}$	$\bar{R}+\sigma_r$
Right Acromion	Seated	.71	1.11	2.19	3.13	1.79	2.69
	Standing	.85	1.51	2.00	2.95	1.76	2.57
Left Acromion	Seated	.91	1.28	2.46	3.45	2.03	2.91
	Standing	.83	1.27	2.66	3.85	2.05	2.93
Suprasternale	Seated	.73	1.00	2.09	2.98	1.79	2.59
	Standing	.77	.98	1.95	2.90	1.70	2.45
C_7	Seated	.78	1.39	2.36	3.45	2.17	3.20
	Standing	.70	1.32	1.97	2.88	1.77	2.57
T_4	Seated	.59	.92	1.98	2.85	1.62	2.42
	Standing	.84	1.36	1.82	2.76	1.50	2.13
T_8	Seated	.48	.77	1.58	2.32	1.29	1.94
	Standing	.52	.81	1.41	2.10	1.12	1.69
T_{12}	Seated	.38	.57	1.11	1.64	.90	1.36
	Standing	.38	.52	.95	1.45	.78	1.15
L_2	Seated	.35	.54	.95	1.35	.69	1.04
	Standing	.27	.36	.81	1.14	.49	.73
L_5	Seated	.53	.78	1.11	1.68	.99	1.51
	Standing	.64	1.08	1.68	2.59	1.37	2.06
Rt. Anter. Sup. Illiac	Seated	.75	1.36	1.82	2.97	1.47	2.53
	Standing	.44	.68	1.58	2.51	1.19	2.01

pelvic support used in the present project. In addition, the validations of these other models did not include the extreme reaches forward or the side and back reaches utilized in this project. However, the prediction models developed in this project are based on an elbow position rather than hand positions. The elimination of the forearm and hand links in this project certainly reduces the subjects' freedom of selection. Perhaps this is compensated for by the fact that the lack of a back support gave the subjects a greater degree of torso mobility than in the validations of the other two models by Boeing and Kilpatrick.

In summary, the torso prediction models developed in this project appear to give good representations of torso mobility over a large number of elbow positions, though a great deal of variability between subjects is not explained by the models. Thus the variance in torso mobility which is not explained by the Anthropometric Model is probably related to a combination of such subtle individual differences as muscular development, neurological coordination (learning) of muscle actions, joint/ligamentous structures, bone articulation geometries, and surface marker movements due to variable skin movements. This latter factor is discussed in the next section of the report. In general, though, subject anthropometry does not account for the noted differences in skeletal mobility. Thus skin movements and resulting marker movements are not believed to be major contributors to the residual errors of the prediction models.

Finally, two important practical aspects of the torso geometry prediction models should be noted. First, the models contain ten surface markers which describe the geometry of the torso, as opposed to the often-used two or three internal links. With a computer graphics capability, these prediction models could be used to depict a more human-like form on a CRT for design reference than the commonly used stick figures. To be capable of doing this, however, computer speed (i.e., program simplicity) is needed. The prediction model approach used in this project provides the fastest possible means to torso mobility determination. This technique could provide complete torso geometry predictions in two or three milliseconds, and with a minimum of computer memory. Thus a designer of a man-machine system could easily work "on-line" for the evaluation of various work place layouts and other manual task design variables.

Physical Environment Reference Point Determinations

The preceding torso surface marker coordinates have all been developed in reference to the location of the L_5 spine surface marker. Since the major orientation of the project was to model human torso geometry, this is justified. From the viewpoint of a person concerned with designing a work station, this means of

presenting the data restricts the immediate use of the data, and thus is not well justified. In an attempt to assist the designer, a prediction model has been developed which describes how the L_5 surface marker moved in relation to the seat reference point (SRP) for the seated operator, and the floor reference point (FRP) (the intersection of the mid-sagittal plane with the floor directly between the posterior aspects of the heels) for the standing operator.

It is obvious that any relationship between a body point and a reference point in the physical environment will be greatly dependent upon how the body is supported against gravity and restrained. For example, a softly padded seat will cause variations in the body-to-SRP distances due to body weight, whereas a hard bench can cause subjects to shift their pelvic positions to alleviate pressure points. Thus the following relationships must be understood to be dependent upon the specific physical environment used in the study.

A hard seat was used for the seated operator. It had a seat pan angle of 6° from the horizontal. The seat pan was 15 inches deep by 16 inches wide. The low back support used was at 13° from the vertical and rose only six inches above the seat pan, thus serving as a pelvis support only. No seat belt was used, but the subjects were instructed to keep their thighs in contact with the seat pan. The SRP was considered to be at the center of the intersection of the seat pan and seat back. When the subjects sat down in the chair they were positioned so the visualized mid-sagittal plane of the torso passed through the SRP. Direct measures of the SRP to L_5 surface marker distances of persons seated with their hands in their laps (i.e., a normal seated rest position) resulted in a value of 5.7 inches in the vertical axis being assumed as representative of the subject/seat condition. This value was then added to the prediction equations developed to describe how the L_5 surface marker for the seated person moved as a function of elbow positions. The results of this procedure are described in Appendix L.

For the standing operator studies, the subjects' feet were positioned as demonstrated earlier in Figures 6-9. They were instructed to keep both heels on the floor. The average FRP-to-L_5 surface marker distance was 41.4 inches in the vertical axis with the subjects in a relaxed standing position, arms at their sides. This value was added to the prediction equations developed to depict the L_5 surface marker movements for the standing operators as a function of right elbow positions. The results of this procedure are also described in Appendix K.

Inspection of the graphs of the L_5 surface marker motions in Appendix K reveals that as an unrestrained person reaches about his immediate environment, a significant movement of the lower torso takes place. This movement distance must be vectorally added to the coordinates of the other surface markers depicted in Appendices H through L if a reference point in the

physical environment is to be used for design purposes. However, because of the obvious interaction of the type of body support and restraint that exists in different physical environments, it is recommended that future designers estimate the position of the L_5 surface marker for their particular design situation. Then the previously presented data regarding the geometry of the other surface markers becomes of more direct benefit to the designer.

SECTION IV

RADIOGRAPHIC STUDIES

One of the most difficult problems in the construction of human linkage representations (e.g., computerized biokinematic models or anthropomorphic dummies) is the lack of data regarding how the joints move during various volitional elbow positions. This section describes how major articulations of the human torso are configured in relationship to the position of the body surface markers described in the preceding sections. Specifically, this section presents the procedure and results obtained from a systematic radiographic study of the skeletal forms of a group of persons maintaining various postures. The results are presented as both graphs and prediction equations which describe the vector distances between various bone articulations and surface markers. Some general conclusions regarding human skeletal torso mobility are drawn from these results.

Radiographic Procedure

The first step in developing the skeletal to surface relationships was to assure that a wide range of shoulder configurations would be obtained. This was accomplished by designing a fixture which would locate the right elbow in a set of predefined positions, much like that used for the photogrammetric studies. Figure 13 depicts the elbow positions chosen. It was later determined that the arm blocked the visualization of many torso bone reference points in several positions, so that the following specific positions were used:

1. A Plane (Upper), Positions 2,3,4,5
2. B Plane (Normal), Positions 3,4,5
3. C Plane (Lower), Positions 1,2,3,4
4. Arm vertical upward
5. Arm relaxed at side (vertical down)

For each of these arm positions, a pair of oblique X-rays were taken (anode offset from the mid-sagittal plane by ±30°), as illustrated in Figure 14. The bone position data analysis procedure is discussed in the next subsection.

To determine how the torso bone-to-surface distances could change with differing trunk configurations, a set of five lumbar and three thoracic configurations was obtained. These are:

1. Lumbar extension (in sagittal plane)
2. Lumbar normal seated rest
3. Lumbar flexion
4. Lumbar hyperflexion

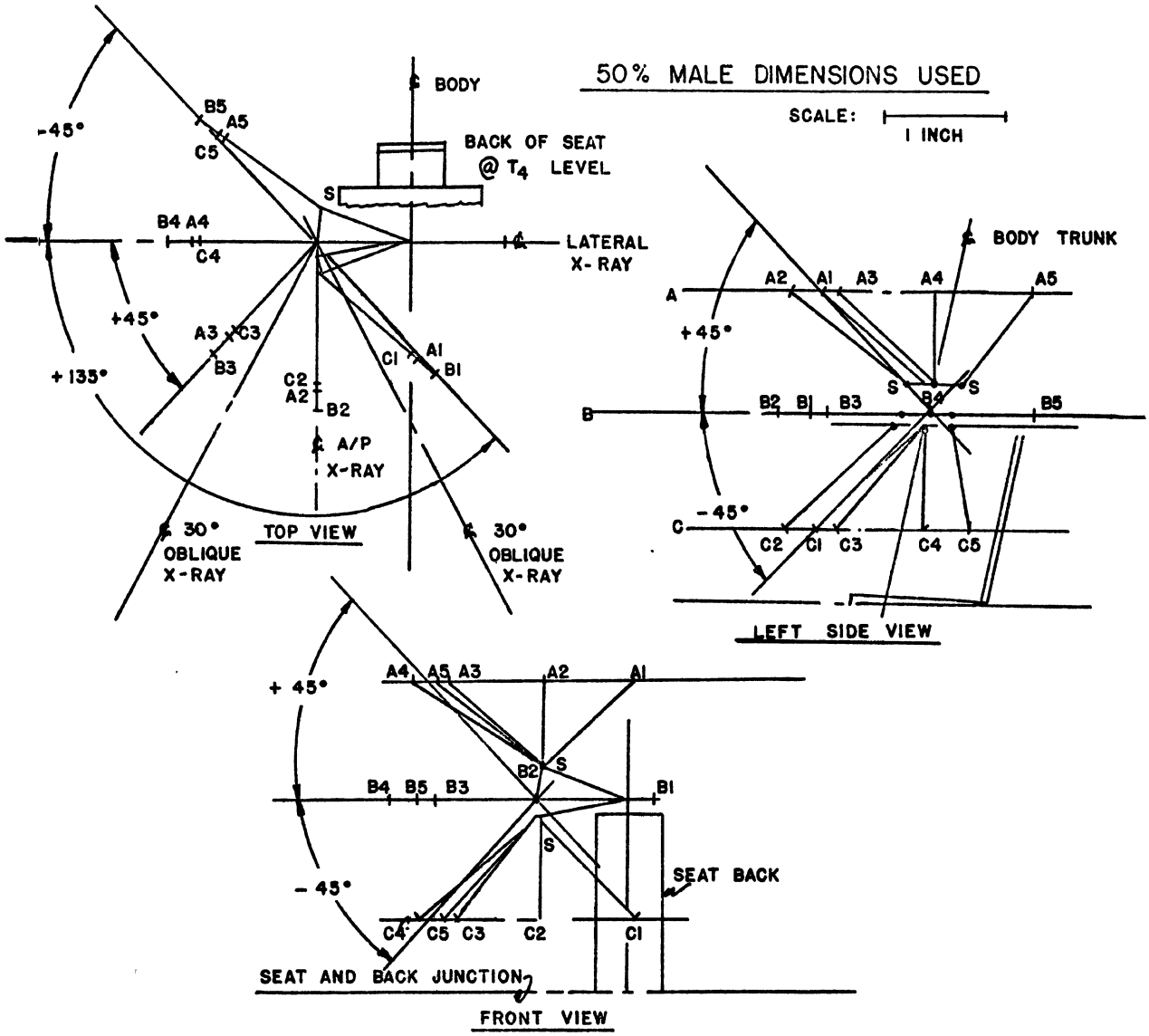

FIGURE 13

SHOULDER STUDY ELBOW POSITIONS

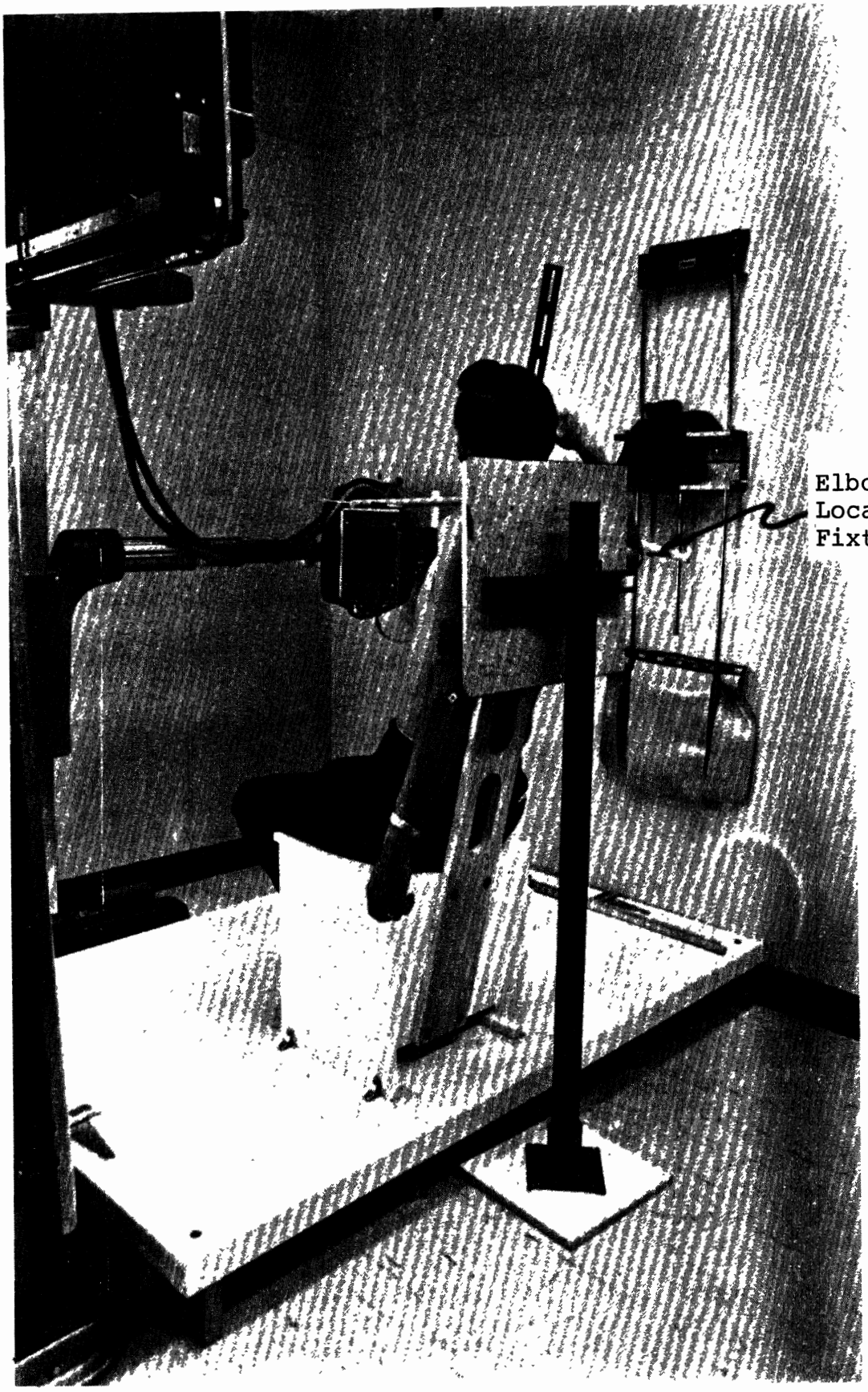

Figure 14. View of subject in seated position for 30° radiograph.

5. Lumbar lateral flexion
6. Thoracic hyperextension
7. Thoracic normal seated rest
8. Thoracic flexion

These positions were duplicated with an instruction for the person to rotate to the right "as far as possible" thus allowing the evaluation of trunk rotation per se. For each of these positions either lateral (sagittal plane) or A/P (frontal plane) or both views were X-rayed, depending upon which would produce the clearest depiction of the bone position. For example, if the movement was in the sagittal plane, a lateral X-ray was obtained. The rotated trunk positions required both views.

We believed that the configuration of the cervical neck would also affect the surface-to-bone distances as low as the C_7/T_1 level. In addition, we believed that it was possible to visualize the cervical spine on X-rays (at least in lateral views of sagittal movement) to the degree that its mobility could be quantified. This would assist in modeling the nasion position feasibility. To study the cervical spinal column, five positions of the neck were sought:

1. Cervical hyperextension
2. Cervical normal seated
3. Cervical flexion
4. Cervical hyperflexion
5. Cervical lateral flexion

Like the thoracic and lumbar studies, both lateral and A/P X-rays were obtained.

Subject Allocation

Because of a desire to maintain as low an X-ray exposure as possible, only nine 14" x 17" X-ray plates were obtained from each subject. This meant that the X-ray schedule would need to be constructed so as to assure that all of the desired body configurations were included in the total study by allocating different configurations to different subjects. A total of 22 subjects were included in the X-ray study, thus giving the potential for 198 X-rays. Because the shoulder X-rays had to be taken in pairs, as well as did some of the lumbar and thoracic exposures, a total of 84 body configurations could be studied. This allowed some repetition of certain positions believed to be more critical than others. For instance, the study of the effect of trunk rotation and lateral flexion was deemed of lesser importance than quantifying the effect of shoulder configuration on surface-to-bone distances. The schedule depicting the body positions for each subject is depicted in Table 7, page 47.

TABLE 7

X-RAY POSITIONS

(C-F.N-S.N; T-F.N-S.N and L-F.N-S.N)
Taken for all subjects (lateral)

Subject Number	First Position	Second Position	Third Position	Fourth Position
1	LI (L&R)	VU (L&R)	C-F.N-S.HE (Lat)	L-F.N-S.HF (Lat)
2	U3 "	Cr-F.N-S.N(AP&Lat)	Lr-F.N-S.F(AP&Lat)	
3	U2 "	VL(L&R)	C-F.N-S.F (Lat)	L-F.N-S.HE(Lat)
4	L2 "	Cr-F.N-S.HE(AP&Lat)	L-F.F-S.N (AP)	Ls-F.F-S.N (AP)
5	L2 "	U4 (L&R)	C-F.N-S.HF (Lat)	L-F.N-S.F (Lat)
6	U3 "	VL (L&R)	C-F.F-S.N (AP)	Ls-F.N-S.HE (Lat)
7	N3 "	Cr-F.N-S.F(AP&Lat)	Lr-F.N-S.N(AP&Lat)	
8	N3 "	U5 (L&R)	C-F.N-S.HE (Lat)	Ls-F.N-S.HF (Lat)
9	L3 "	VU (L&R)	C-F.N-S.F (Lat)	L-F.N-S.HE (Lat)
10	L3 "	Cr-F.N-S.HF(AP&Lat)	Lr-F.N-S.He(AP&Lat)	
11	U4 "	Ll (L&R)	C-F.N-S.HF (Lat)	L-F.N-S.F (Lat)
12	N4 "	L2 (L&R)	C-F.F-S.N (AP)	L-F.N-S.HF (Lat)
13	U4 "	Tr-F.N-S.N(AP&Lat)	Lr-F.N-S.F(AP&Lat)	
14	Ll "	N3 (L&R)	T-F.N-S.F (Lat)	Ls-F.F-S.N (AP)
15	U2 "	N4 (L&R)	T-F.N-S.HF (Lat)	L-F.F-S.N (AP)
16	N4 "	Cr-F.N-S.HE(AP&Lat)	Lr-F.N-S.N(AP&Lat)	
17	L4 "	U2 (L&R)	T-F.N-S.HE (Lat)	Ls-F.N-S.HF (Lat)
18	U5 "	L3 (L&R)	T-F.N-S.F (Lat)	Ls-F.N-S.HE (Lat)
19	L4 "	Cr-F.N-S.N(AP&Lat)	Lr-F.N-S.HE(AP&Lat)	
20	VU "	U3 (L&R)	T-F.N-S.HF (Lat)	L-F.F-S.N (AP)
21	VL "	L4 (L&R)	T-F.N-S.HE (Lat)	L-F.HG-S.N (AP)
22	U5 "	Cr-F.N-S.F(AP&Lat)	Tr-F.N-S.N(AP&Lat)	

Shoulder Studies (One Letter Component):
L - lower plane (30° below shoulder)
N - normal plane (through shoulder)
U - upper plane (30° above shoulder)
VU- vertical up
VL- vertical low (down)
The numbers designate the degree of rotation about the trunk axis--see photogrammetry.

Trunk Studies (Three Components):

Body Sector Moved	S-Sagittal Movement
C - Cervical	HE-Hyperextension
T - Thoracic	N -Norman erect
L - Lumbar	F -Flexion
s - Standing	HF-Hyperflexion
r - rotation	

F - Frontal Movement
F - Lateral Flexion
HF- Lateral Hyperflexion

Radiographic Data Reduction

The procedure for reducing the X-ray data to specific bone position data is described in this subsection. The first step in developing the procedure entailed placing a cadaver in the positions described in the preceding subsection. X-rays were then taken as outlined in Table 7 and carefully reviewed. Based on the partial dissection from which small lead shot markers were placed on the palpable bone points, and in reference to general anatomical bone geometry data, the cadaver X-rays were marked with a felt tip ink pen. Specifically, depending upon which sector of the body was being viewed (i.e., lumbar, thoracic, shoulder, or cervical), a small cross mark and reference number was placed over each bone or surface marker of interest. Table 8 describes the X-ray reference marks.

To provide both a consistent alignment of different X-rays and to scale the X-rays to the actual dimensions of the body, (i.e., parallax causes distortion magnification) a fixture was built which would display a set of reference points into each X-ray. By having the X-ray anode, film plane, and reference points at known distances from a reference point on the body (i.e., the right anterior superior illiac spine), it was possible to compute the actual bone distances of subjects. In actual practice, the measurements were established by "calibrating" the X-ray room. This was accomplished by placing markers on the walls and floor from which dowel pins could be projected to precisely position the X-ray anode with reference to the film and subject. Once these measurements were established for the different viewing angles, they were entered into a computer program which was written to compute the bone locations. The computer program flow chart is displayed in Figure 15. The general algorithm is similar to the photogrammetric procedure described in the preceding section.

After the X-rays were marked, a laboratory assistant read the X-Y coordinates of the marked locations, and with the following information punched it into the computer cards. The first two characters punched were digits identifying the subjects (numbers on Table 7). The third character was a letter displaying the body sector X-rayed as follows:

L - left side, 30° off mid-sagittal plane
R - right side, 30° off mid-sagittal plane
F - front view, A/P
S - side view, lateral

The fourth and fifth digits denoted the body positions studied, per Table 9. The next two digits specify which point was being read on the X-ray, and correspond to the code numbers in Table 8. The last digit indicates the "value" of a marker, thus providing a means to separate those data which are capable of being consistently located on the X-rays from those that are highly subjective. A rating of 1, 2, or 3 was given by the radiological

TABLE 8

X-RAY REFERENCE MARKS

CODE NUMBER	MARKER DESCRIPTIONS
1 & 2	Alignment and scaling points - common to all body sectors.
	Shoulder Sector
	Surface Markers (see Table
3	C5 spine marker
4	C7 " " - cervicale
5	T4 " "
6	T4 " "
7	Right acromion
8	Suprasternale
9	Humerus mark - 2 inches below right acromion
	Skeletal Points
10	C4/C5 interspace, intersection of disc center lines
11	C5/C6 " " " " " "
12	C6/C7 " " " " " "
13	C7/T1 " " " " " "
14	T1/T2 " " " " " "
15	T2/T3 " " " " " "
16	T3/T4 " " " " " "
17	T4/T5 " " " " " "
18	T5/T6 " " " " " "
19	T6/T7 " " " " " "
20	T7/T8 " " " " " "
21	T8/T9 " " " " " "
22	Sterno-clavicular junction
23	Acromion-clavicular junction
24	Projected center of humeral head-bisection of area of head
25	Proximal point on humeral center line-selected for shaft angle est.
26	Distal point on humeral center line-selected for shaft angle est.
27	C5 posterior aspect of spine
28	C7 posterior aspect of spine
29	T4 " " " "
30	T8 " " " "
31	Right acromion-most lateral and superior aspect

(continued on next page)

TABLE 8 (continued)

32	C5 surface marker corrected position-initial 3 x-rays
33	C7 " " " " " " "
34	T4 " " " " " " "
35	T8 " " " " " " "

Cervical Sector

Surface Markers

3	T4 spine marker
4	C7 spine marker - cervicale
5	C5 spine marker
6	Right tragion
7	Left tragion
8	Nasal root depression
19	Right acromion
27	C2 spine marker

Skeletal Points

9	C2/C3
10	C3/C4
11	C4/C5
12	C5/C6
13	C6/C7
14	C7/T1
15	T1/T2
16	T2/T3
17	T3/T4
18	T4/T5
20	T4 spine
21	C7 posterior aspect of spine
22	C5 " " " "
23	Right tragion
24	Left tragion
25	Nasal root depression
26	Right acromion-most lateral and superior aspect
28	C2 posterior aspect of spine
29	C2 surface marker corrected position-initial 3 x-rays
30	C5 " " " " " " "
31	C7 " " " " " " "
32	T4 " " " " " " "

Thoracic Sector

External Surface Markers

3	T12 spine marker
4	T4 spine marker
5	C7 spine marker (cervicale)
6	Right acromion
22	T8 spine marker

TABLE 8 (continued)

	Skeletal Points
7	T2/T3 interspace - intersection of disc centerlines
8	T3/T4 " " " " "
9	T4/T5 " " " " "
10	T5/T6 " " " " "
11	T6/T7 " " " " "
12	T7/T8 " " " " "
13	T8/T9 " " " " "
14	T9/T10 " " " " "
15	T10/T11 " " " " "
16	T11/T12 " " " " "
17	T12/L1 " " " " "
18	Right acromion-most lateral and superior surface
19	C7 posterior aspect of spine
20	T4 " " " "
21	T12 " " " "
27	T8 " " " "
23	C7 surface marker corrected position-initial 3 x-rays
24	T4 " " " " " " "
25	T8 " " " " " " "
26	T12 " " " " " " "

Lumbar Sector

	Surface Markers
3	L5 spine marker
4	L2 spine marker
5	Left anterior superior iliac spine
6	Right " " " "
7	Right trochanter
	Skeletal Points
8	L1/L2 interspace-intersection of disc centerline
9	L2/L3 " " " " "
10	L3/L4 " " " " "
11	L4/L5 " " " " "
12	L5/S1 " " " " "
13	Projected center of head of right femur-bisection of area of head
14	L5 posterior aspect of spine
15	L2 " " " "
16	Left anterior superior iliac spine
17	Right " " " "
18	L2 surface marker corrected location-initial 3 x-rays
19	L5 " " " " " " "

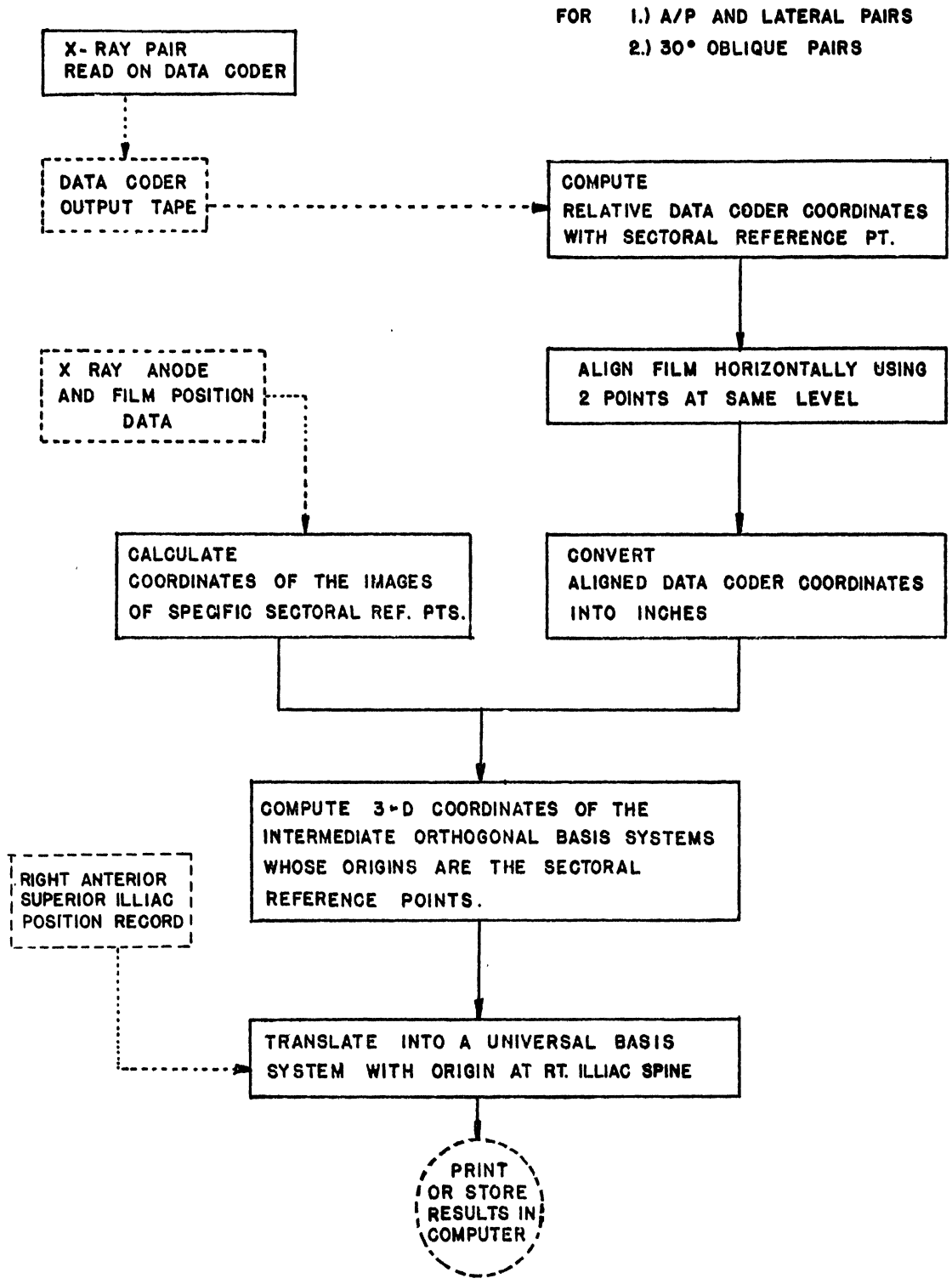

FIGURE 15

DATA REDUCTION PROGRAM STRUCTURE

TABLE 9

X-RAY AND POSITION CODES

X-RAY CODE	POSITION CODE	X-RAY ORIENTATION
1	C-F.N-S.HE	(Lat)
2	C-F.N-S.N	(Lat)
3	C-F.N-S.F	(Lat)
4	C-F.N-S.HF	(Lat)
5	C-F.F-S.N	(AP)
6	T-F.N-S.HE	(Lat)
7	T-F.N-S.N	(Lat)
8	T-F.N-S.F	(Lat)
9	T-F.N-S.HF	(Lat)
10	L-F.N-S.HE	(Lat)
11	L-F.N-S.N	(Lat)
12	L-F.N-S.F	(Lat)
13	L-F.N-S.HF	(Lat)
14	L-F.F-S.N	(AP)
15	L-F.HF-S.N	(AP)
16	Ls-F.N-S.HE	(Lat)
17	Ls-F.N-S.HF	(Lat)
18	Ls-F.F-S.N	(AP)
19	Cr-F.N-S.HE	(AP & Lat)
20	Cr-F.N-S.N	(AP & Lat)
21	Cr-F.N-S.F	(AP & Lat)
22	Cr-F.N-S.HF	(AP & Lat)
23	Tr-F.N-S.N	(AP & Lat)
24	Lr-F.N-S.HE	(AP & Lat)
25	Lr-F.N-S.N	(AP & Lat)
26	Lr-F.N-S.F	(AP & Lat)
27	L1	30/30 Obliques
28	U2	" "
29	L2	" "
30	U3	" "
31	N3	" "
32	L3	" "
33	U4	" "
34	N4	" "
35	L4	" "
36	U5	" "
37	VU	" "
38	VL	" "

technician for each mark on the X-ray, or he could note that a point was "missing."

The preceding X-ray data for each bone and surface point of interest was then reduced to a listing of 3-space coordinates relative to the right anterior superior iliac spine for each subject and position by the computer program. An example for one subject's data (plotted for visualizing) is presented in Figure 16.

The marker positions also were punched onto cards which were inputted to a second program. This program simply develops a listing of vector distances and directions between pairs of points. In essence, these vectors are the "links" depicted in Figure 16. This vector output has proved to be very useful in determining how the surface markers move relative to the skeletal points, and will be discussed in detail in the subsequent subsections.

Subjects Used in X-ray Study

As outlined above, 22 subjects were required in the total design. These subjects were the same as those used in the photogrammetric study. However, because of tissue density variations from one subject to another, some X-rays were not clear enough to provide good bone definitions, even though extreme care was taken in the taking and processing of the X-rays. The result was that 19 subjects provided the basic data. The stature and weight distributions of these subjects is presented in Figure 17. Even though data from three subjects were lost, a good population variability was still achieved.

A more specific problem was encountered when the X-rays of bone points were developed. On an average, 18 clear bone readings were obtained from each X-ray. This was about a 50% loss rate. In retrospect, it is not believed that this could be avoided by better procedures or equipment. The problem stems from a number of inherent limitations. First, X-rays of a subject could not be repeated due to the exposure limit. Hence, even when it is known that a loss of several points occurred, it could not be corrected. Second, to establish a vector distance, a pair of bone and surface points must be visualized. Many vectors were lost due to one point being covered by similarly dense tissue, or by the limited film size forcing its sacrifice to gain a few other points on the opposite side of the film. In general, the results are still believed to be quite adequate to infer how on an average the skeletal bones move relative to the surface markers when a person is executing various specific arm and torso positions. Some specific recommendations are proposed at the end of this report to assist those planning future studies of this type.

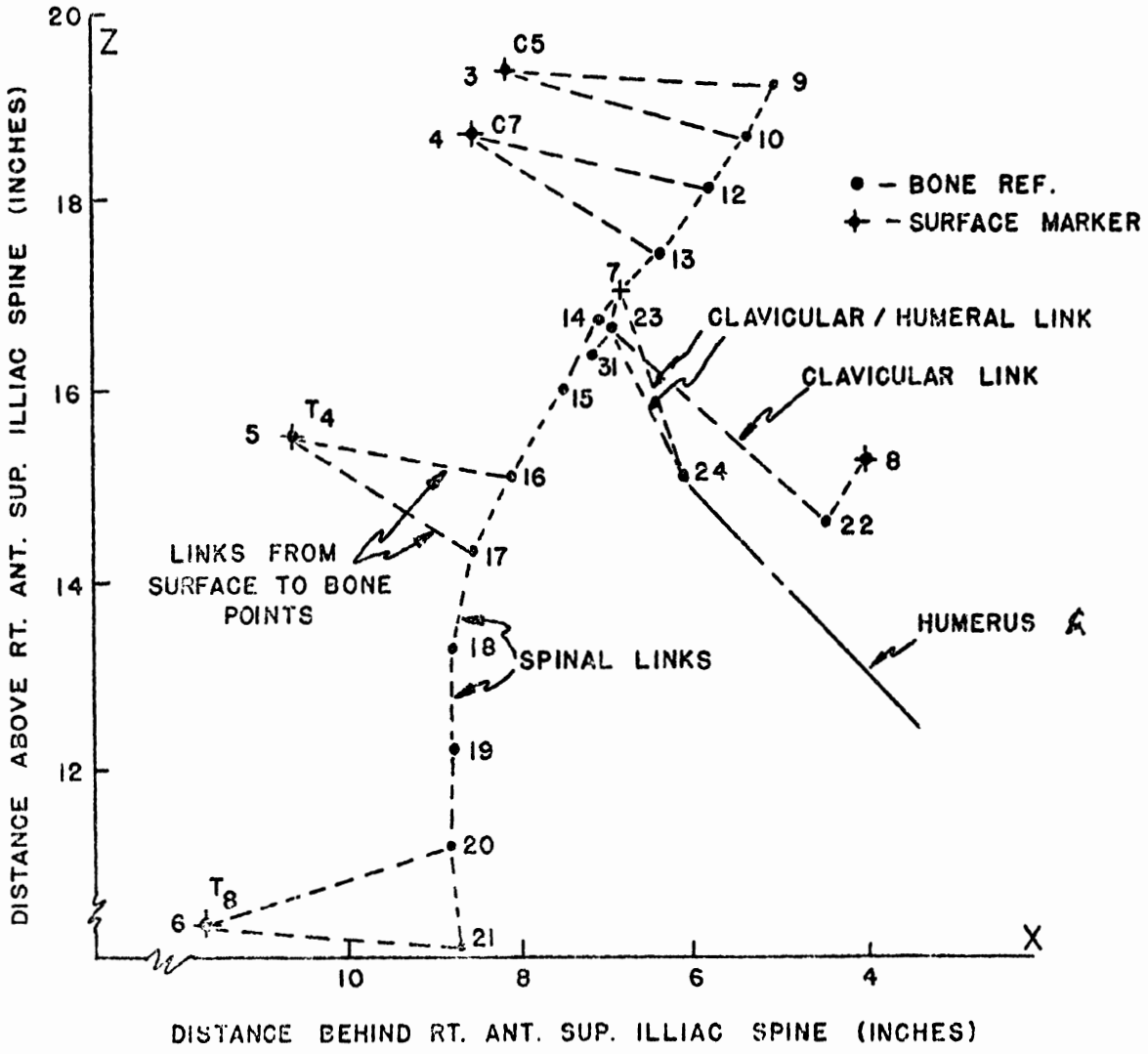

FIGURE 16

ILLUSTRATION OF X-RAY REFERENCE POINTS FROM LATERAL VIEW OF THORACIC AND LOWER CERVICAL AREAS FOR SUBJECT #28 IN POSITION #32

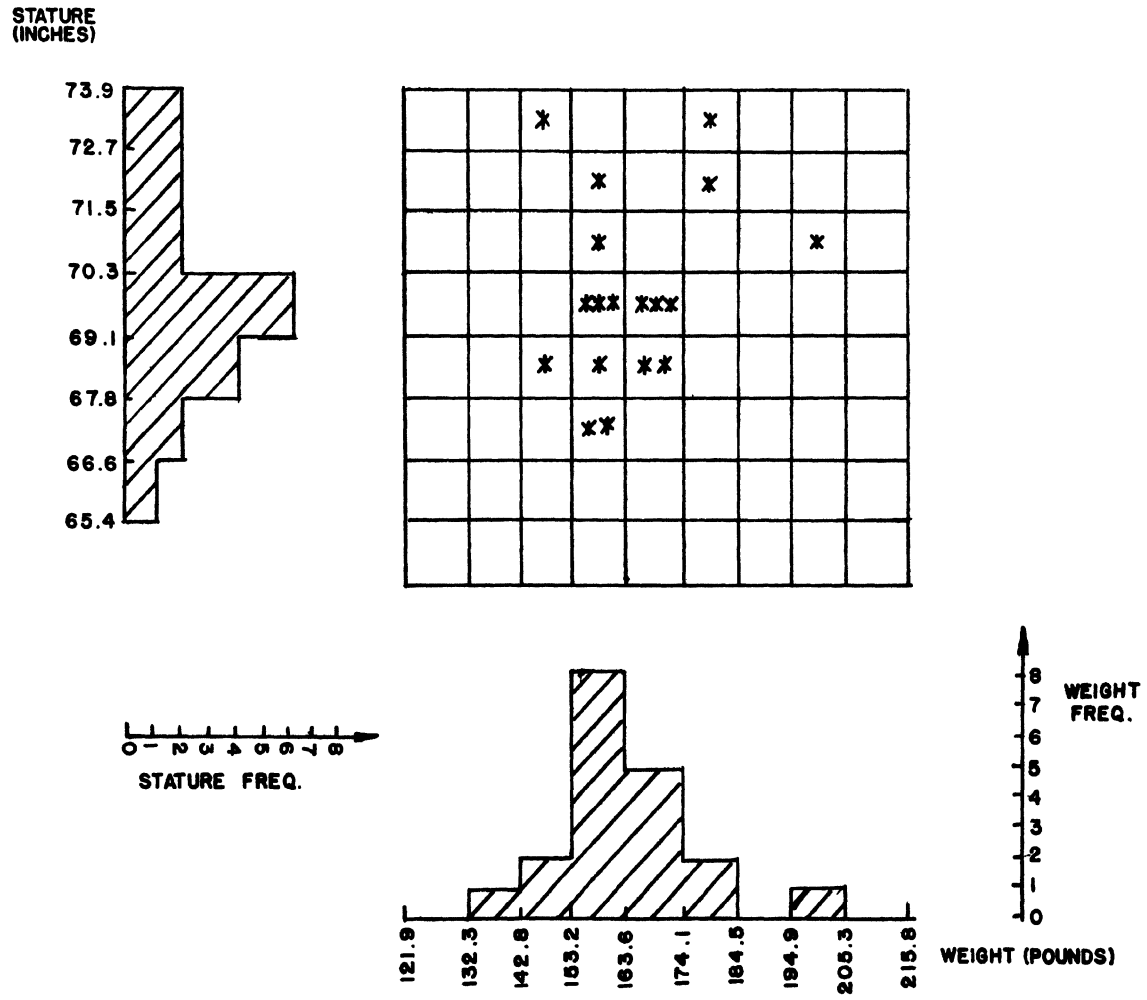

FIGURE 17

X-RAY SUBJECT STATURE AND WEIGHT DISTRIBUTIONS

Results of X-ray Studies

This subsection summarizes the results of the X-ray studies. It presents the results in both prediction equation and graphic form, thus allowing a person to most easily define how the surface to skeletal points of interest are positioned for given body configurations. Specifically, the results are reported in reference to the body sectors studied, i.e., the lumbar, thoracic, shoulder, and cervical areas. For each body sector, the vector distances between the major skeletal points and the surface points are described. Both means and standard deviations for these averaged over all positions are presented. An analysis of the effect of the specific body postures described at the beginning of this section is then reported.

Lumbar X-ray Study Results

The lumbar X-ray study data was sufficient to infer how the lumbar column is positioned relative to the two surface markers over the L_5 and L_2 spines. The mean and standard deviation of the vector distances and directions relating both the surface-to-disc centers (centers of vertebral interspaces) and the disc centers-to-centers are depicted in Table 10 averaged over all the seated positions analyzed: extension, normally seated, and slightly flexed.*

TABLE 10

LUMBAR X-RAY DATA SUMMARY
(Averaged over Positions)

Vector	Distance (Inches)		Vector Ang. From 12 o'clock (+ = Backwards)	
	Mean	S.D.	Mean	S.D.
L_5/S_1 Int. To L_5 Surf.	3.56	0.52	-84.01	15.02
L_2/L_3 Int. To L_2 Surf.	3.46	0.30	-92.42	14.18
L_5 Surf. To L_2 Surf.	3.70	0.97	-10.06	6.71
L_5/S_1 Int. To L_2/L_3 Int.	4.37	0.24	-8.55	7.08
L_5/S_1 Int. To L_4/L_5 Int.	1.44	0.09	-3.61	9.22
L_4/L_5 Int. To L_3/L_4 Int.	1.43	0.31	-10.82	9.03
L_3/L_4 Int. To L_2/L_3 Int.	1.52	0.32	-12.26	5.73
L_2/L_3 Int. To L_1/L_2 Int.	1.43	0.10	-11.91	7.42
L_5/S_1 Int. To L_1/L_2 Int.	5.78	0.33	-9.54	6.00

A full-scale drawing of the lumbar X-ray data is depicted in Figure 18.

*These body configurations are rigorously defined later in the subsection when the effect of lumbar movement is separated.

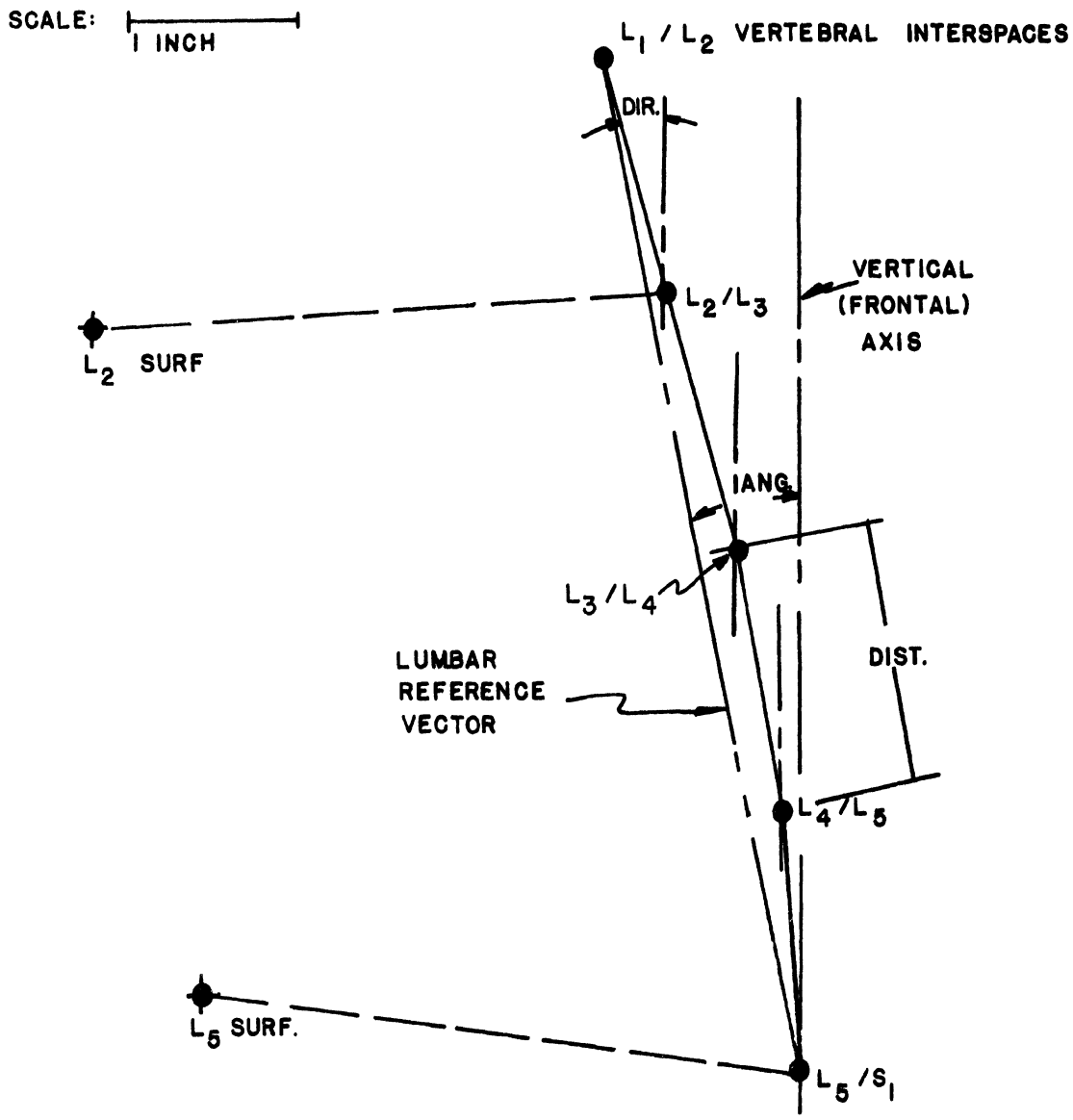

FIGURE 18

MEAN SEATED LUMBAR SPINE
(For orientation see Figure 23)
(Data in Table 10)

The analysis of the effect of flexion and extension of the lumbar spine on the surface-to-disc center vectors was accomplished by first defining a vector which would describe the degree of lumbar flexion and extension. This lumbar reference vector was chosen to be the vector from the L_5/S_1 vertebral interspace to the L_2/L_3 vertebral interspace. Thus, the sagittal plane angle between this vector and a vertical upward axis through the L_5/S_1 interspace would describe the degree of lumbar column flexion or extension that each subject displayed. This angle will be referred to as the lumbar reference angle (ANG). It is measured from the vertical axis, with positive being measured in the forward-facing direction.

To determine how the vectors connecting various bone and surface points change relative to the lumbar reference angle, both the vector distances and directions were regressed onto the lumbar reference axis. Plots of these data and the resulting regression lines are depicted in Appendix M. A summary of the resulting prediction equations is depicted in Table 11. After plotting the data, as in Appendix M, only linear regressions appeared to be justified. Both the simple correlation coefficient, r, and the F statistic (to determine whether the correlation coefficient is different than zero) are depicted. The significance level of the F statistic is set high, $\alpha = 0.05$ and $\alpha = 0.01$, based on the rationale that inclusion of an effect in a future torso mobility algorithm which is not valid could be costly, since it would be adding unnecessary complexity to an already complex synthesis. In other words, at this time, only major effects should be included to keep the development of torso mobility models as simple as possible.

Interpretation of Lumbar Mobility Results

Three general results are believed to be worthy of specific comment:

1. The vector distances (both from the surface-to-the-spinal interspaces and from vertebral interspace to interspace) did not significantly vary with the general inclination of the lumbar spine from the vertical.

2. The vertebral column and the surface markers move consistently with the general lumbar spine. The regression slopes show that approximately 20 percent more mobility is contributed by the lower segments (L_5/S_1 to L_3/L_4 levels) than by the upper segments (L_3/L_4 to L_1/L_2 levels).

3. The surface markers remained statistically constant in direction from the vertebral interspaces. This is particularly true for the L_5 surface marker. Apparently skin movement over the spines

TABLE 11

LUMBAR VECTOR PREDICTION EQUATIONS

Vector from Ref. Pt. 1 to Ref. Pt. 2	Vector Distance DIST.= (Inches)	N sample size	r corr.coef.	F[1] stat.	Vector Direction (see note) DIR=	N sample size	r corr.coef.	F[1] stat.
L_5/S_1 Interspace to L_5 Surface	3.35 - 0.021 (ANG)	18	-0.24	0.97	-73.31 + 1.06 (ANG)	18	0.43	3.63
L_2/L_3 Interspace to L_2 Surface	3.57 + 0.011 (ANG)	18	0.22	0.80	-80.31 + 1.26 (ANG)	18	0.53	6.29*
L_5 Surface to L_2 Surface	4.14 + 0.044 (ANG)	18	0.27	1.28	+ 2.77 + 0.72 (ANG)	18	0.66	12.1**
L_5/S_1 Interspace to L_2/L_3 Interspace	4.41 + .005 (ANG)	20	0.11	0.24	+ 2.20 + 1.13 (ANG)	20	0.95	185.4**
L_5/S_1 Interspace to L_4/L_5 Interspace	1.44 - 0.00006(ANG)	20	-0.004	0.0	+ 9.19 + 1.34 (ANG)	20	0.87	58.2**
L_4/L_5 Interspace to L_3/L_4 Interspace	1.50 + 0.007 (ANG)	20	0.14	0.35	+ 0.75 + 1.21 (ANG)	20	0.80	33.5**
L_3/L_4 Interspace to L_2/L_3 Interspace	1.50 - 0.002	20	-0.05	0.04	- 4.18 + 0.85 (ANG)	20	0.88	66.1**
L_2/L_3 Interspace to L_1/L_2 Interspace	1.46 + 0.003	20	0.18	0.64	- 5.54 + 0.67 (ANG)	20	0.54	7.43*
L_5/S_1 Interspace to L_1/L_2 Interspace	5.84 + 0.006 (ANG)	20	0.12	0.24	(See Below)			

note: Definition of Vector Directions:

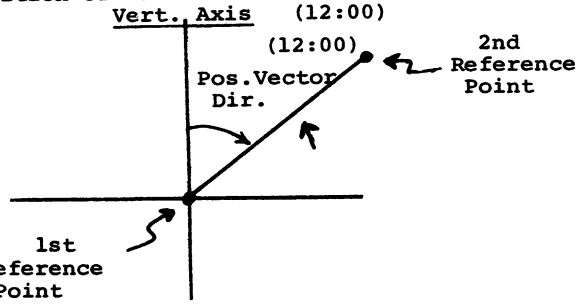

[1]The F statistic is a test of $H_0: r = 0$

during lumbar flexion compensates for the angular changes of the vertebrae.

The consistency of the vector distances with the angle of the lumbar spine suggests that in biokinematic models a single vector representing the lumbar spinal column is appropriate, and that its length and position is well predicted by the locations of L_2 and L_5 surface markers.

Thoracic X-ray Study Results

The data from the thoracic X-rays were sufficient to infer how the surface markers over the T_{12}, T_8, and T_4 spines move relative to the adjacent vertebral interspaces. The means and standard deviations of the major thoracic dimensions are presented in Table 12, averaged over the positions described later in the subsection. (The shoulder mobility study includes the upper part of the thoracic spine.)

TABLE 12

THORACIC X-RAY DATA SUMMARY
(Averaged over Positions)

Vector	Distance (Inches)		Vector Ang. From 12 o'clock (+ = Backwards)	
	Mean	S.D.	Mean	S.D.
T_{12}/L_1 Int. To T_{12} Surf.	3.06	0.33	+102.46	19.50
T_8/T_9 Int. To T_8 Surf.	3.16	0.29	+104.40	19.80
T_4/T_5 Int. To T_4 Surf.	2.98	0.27	-7.35	18.13
T_{12} Surf. To T_8 Surf.	4.33	0.81	-8.35	13.44
T_8 Surf. To T_4 Surf.	4.85	0.39	11.30	11.10
T_{12}/L_1 Int. To T_8/T_9 Int.	4.44	0.29	-2.88	6.96
T_8/T_9 Int. To T_4/T_5 Int.	3.73	0.27	16.22	10.11
T_{12}/L_1 Int. To T_4/T_5 Int.	8.04	0.54	6.14	8.12

A plot of the data is presented in Figure 19.

The analysis of the effect of flexion and extension of the torso on these dimensions was completed using the same procedure as outlined for the lumbar study. In essence, a reference vector was defined to provide a quantified measure of the degree of thoracic flexion or extension. This vector is from the T_{12}/L_1 vertebral interspace to the T_4/T_5 vertebral interspace. The reference angle (ANG) for the thoracic spine then is the angle measured from a vertical upwards axis (through the T_{12}/L_1 interspace) to this reference vector. A positive angle means that the second point to defining any vector (ex: T_4/T_5 interspace for the reference vector) lies forward of the first point (ex: T_{12}/L_1 interspace).

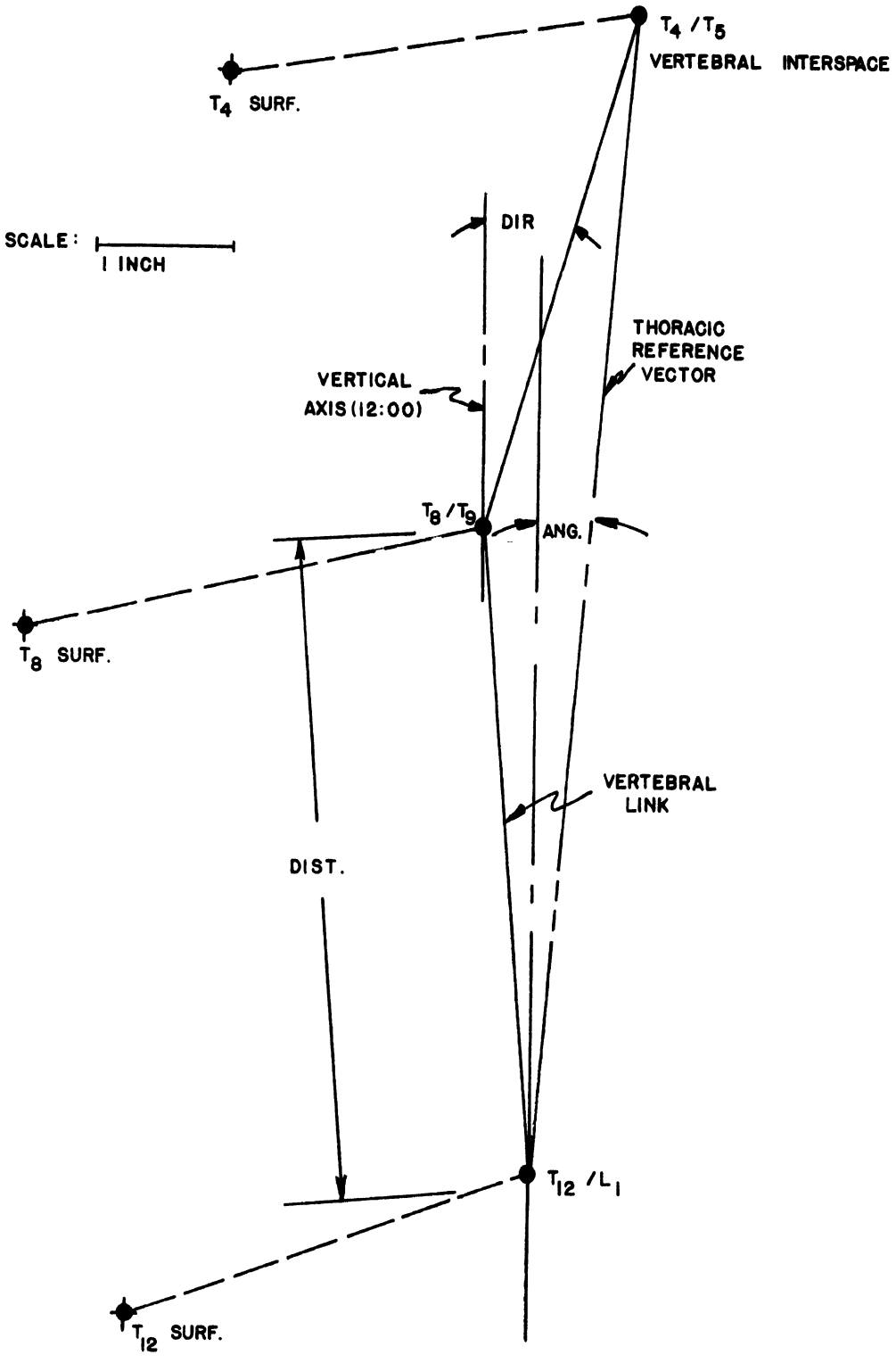

FIGURE 19

MEAN SEATED THORACIC SPINE LINKS
(For orientation see Figure 23)
(Data in Table 12)

Once again, the vector distances and directions between the various surface and bone points were regressed by a least squared error technique onto the degree of thoracic tilt (as measured by ANG for the thoracic spine). Plots of these data are presented in Appendix M Simple regressions were completed and are summarized in Table 13.

Interpretation of Thoracic Mobility Results

The X-ray study of thoracic movement has indicated the following general results:

1. The distances between both assumed large links of the column, and surface to column links, remain constant with various degrees of flexion and extension.

2. The distances of the surface-to-surface vectors vary with the degree of flexion and extension, thus displaying that there is a separate movement of the skin over the three spines of interest. The regression slopes for the direction of the vectors between the surface markers and vertebral interspaces indicate that there is more movement relative to the column at the T_8 level than at the T_{12} or T_4 levels. Thus, the T_{12} and T_4 markers would be better for determining the direction of the thoracic spine.

3. The highly consistent movement of the two vertebral links with the reference vector indicates that the thoracic spine moves as a unit.

In general, the thoracic spinal column can be considered to be a single link whose magnitude and direction can be determined from surface measurements, provided a correction is given for the orientation of the column when the measurements are taken.

Shoulder X-ray Study Results

The data from the shoulder X-rays provided the most challenging analysis problem due to the complex mobility of the shoulder. The data were obtained from pairs of oblique X-rays. Each person was positioned so that his right elbow was systematically located in widely varying angular deviations from a resting position. (Figure 13 at the beginning of this section describes these positions.) Thus the vector distances and directions between various surface and bone points were all dependent upon the placement of the elbow, i.e., the humeral reference angle. This reference angle was specified in a horizontal plane through the resting shoulder, i.e., two inches below the right acromion of a person at average height. It ranged from -45°

TABLE 13

THORACIC VECTOR PREDICTION EQUATIONS

Vector from Ref. Pt. 1 to Ref. Pt. 2	Vector Distance (Inches)	N sample size	r corr.coef.	F[1] stat.	Vector Direction (see note) DIR=	N sample size	r corr.coef.	F[1] stat.
T_{12}/L_1 Interspace to T_{12} Surface	2.98 + 0.014 (ANG)	16	0.34	1.74	+103.64 - 0.13(ANG)	16	-0.06	0.04
T_8/T_9 Interspace to T_8 Surface	3.11 + 0.007 (ANG)	13	0.32	1.41	-106.96 + 0.81(ANG)	13	0.47	3.46
T_4/T_5 Interspace to T_4 Surface	2.97 + 0.0029(ANG)	14	0.09	0.08	-88.93 + 1.27(ANG)	14	-0.57	5.4*
T_{12} Surface to T_8 Surface	4.19 + 0.042 (ANG)	14	0.60	6.82*	-11.71 + 1.07(ANG)	14	0.91	61.9**
T_8 Surface to T_4 Surface	4.73 + 0.029 (ANG)	11	0.69	8.03*	6.81 + 1.10(ANG)	11	0.90	40.4**
T_{12}/L_1 Interspace to T_8/T_9 Interspace	4.45 - 0.0012(ANG)	17	-0.04	0.02	-7.59 + 0.80(ANG)	16	0.96	151.1**
T_8/T_9 Interspace to T_4/T_5 Interspace	3.73 + 0.0005(ANG)	16	0.02	0.0	9.03 + 1.23(ANG)	16	0.98	282.5**
T_{12}/L_1 Interspace to T_4/T_5 Interspace	8.091 - 0.0091(ANG)	16	-0.14	0.24	ANG (see below)			

Sig. Levels:
*0.05
**0.01

ANG = Sagittal Plane Angle from Vertical (+ = forwards) of Reference Vector from T_{12}/L_1 to T_4/T_5

note: Definition of Vector Directions:

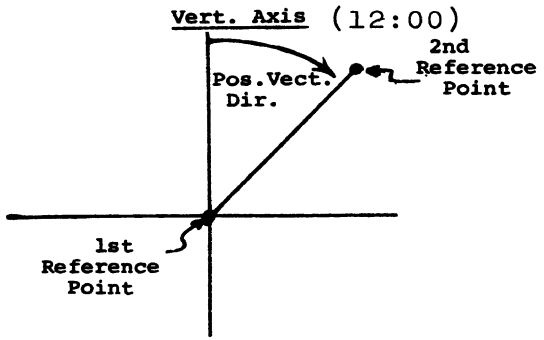

[1]The F statistic is a test of $H_0: r = 0$

(left of the sagittal plane) to +135° (right and back of the frontal plane). Also, some positions of the elbow above and below the normal horizontal plane were checked, as indicated in the procedure described at the beginning of this section.

Because of the 3-space aspects of shoulder mobility, a method of specifying the vectors of interest in three dimensions had to be devised. This was accomplished by defining two angles, ϕ and θ. Essentially, ϕ refers to the angle of the vector measured in the horizontal plane from a reference axis in the sagittal plane, with positive being measured to the left. Figure 20 displays the angles. The θ angle is measured in the vertical plane rotated through ϕ angle. In other words, it is measured in the ϕ plane from a vertical upwards reference axis.

Using this notation, the means and standard deviations of vectors connecting various surface and bone points were developed, averaged over all humeral positions. Table 14 displays these values. In general, these values represent the configuration of a seated person with his right arm abducted into a horizontal plane at a 20° angle to the right of the sagittal plane. Figures 21 and 22 display the major vectors of interest.

Examination of the mean vector locations provides the following insights:

1. With forward abduction of the arm, the acromion becomes located slightly posterior to both the center of the proximal humeral head and the acromio-clavicular junction.

2. The acromio-clavicular junction and C_7/T_1 interspace vector lies almost in the frontal plane.

3. The humeral surface marker is in a position above the projected head of the humerus, as opposed to being in line with the humeral head when the arm is at the side of the body.

The major results of the shoulder X-ray study are based upon the regression of the various vector distances and directions onto the humeral reference angle. This provides additional insight as to how the shoulder moves as a function of arm position (i.e., elbow locations). Once again, simple linear regressions were used after inspection of the plotted data presented in Appendix O. The results of these regressions are summarized in Table 15. Both a correlation coefficient, r, and an F statistic were developed to determine the possibility of an effect of the horizontal plane arm angle.*

*It should be noted that a separate statistical analysis of the the effect of being in the upper, normal, or lower elbow plane was not possible due to the high data loss in both the upper and lower planes. Inspection of the graphs, however, shows little effect.

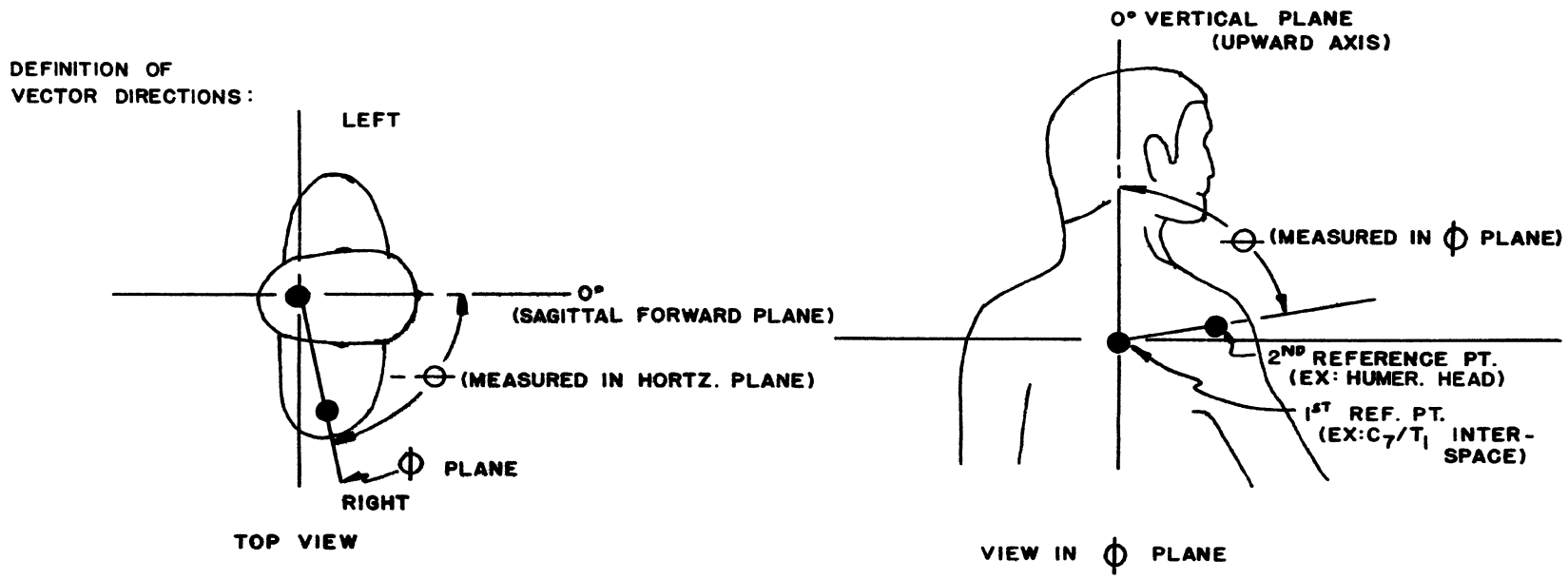

FIGURE 20

VECTOR DIRECTION NOTATIONS FOR SHOULDER STUDIES

TABLE 14

SHOULDER AND UPPER THORACIC X-RAY DATA SUMMARY

Relationship	Distances		Vector Angles			
			ϕ measured in Horizontal Plane		θ measured in ϕ plane	
	Mean	S.D.	Mean	S.D.	Mean	S.D.
T_4/T_5 Interspace to C_7/T_1 Interspace	3.51	0.10	-0.31	15.10	24.85	8.34
C_7/T_1 Interspace to Acromio-Clavicular junction	5.73	0.72	-91.08	9.03	90.08	9.32
Projected Head of Humerus to C_7/T_1 Interspace	6.47	0.55	102.13	6.67	79.47	9.26
Projected Head of Humerus to Acromio-Clavicular junction	1.62	0.24	147.29	17.70	49.39	16.83
Acromion Surface to C_7 Surface	6.84	1.21	103.26	13.61	86.47	11.82
C_7/T_1 Interspace to C_7 Surface	2.49	0.41	174.19	9.68	71.52	19.70
Acromio-Clavicular Junction to Humeral Mark	2.97	0.80	-71.40	21.11	122.60	13.75
Sterno-Clavicular Junction to Suprasternale	1.13	0.14	58.17	7.00	110.33	11.80
Projected Head of Humerus to Acromion	2.12	0.28	-3.57	31.52	47.76	35.51
Acromio-Clavicular Junction to Acromion	1.43	0.61	-151.41	18.14	27.71	25.56
Projected Head of Humerus to Humeral Mark	2.76	0.17	-83.25	22.41	52.25	12.53
Sterno-Clavicular Junction to Acromio-Clavicular Junction	6.50	0.99	-126.75	11.19	70.17	13.5

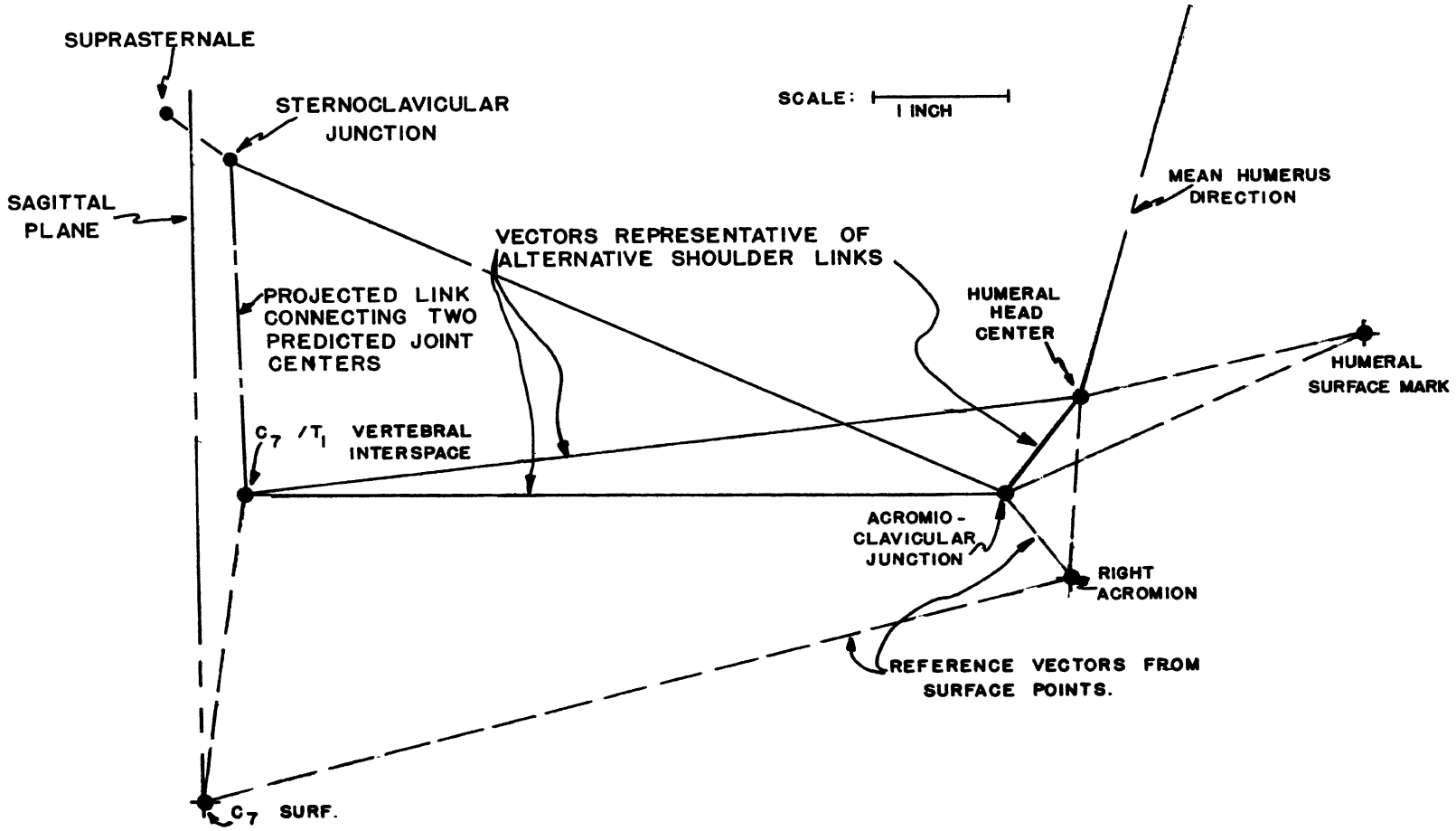

FIGURE 21

MEAN LOCATIONS OF VECTORS PROJECTED INTO HORIZONTAL PLANE FROM SHOULDER X-RAYS
(For orientation See Figure 23)
(Data in Table 14)

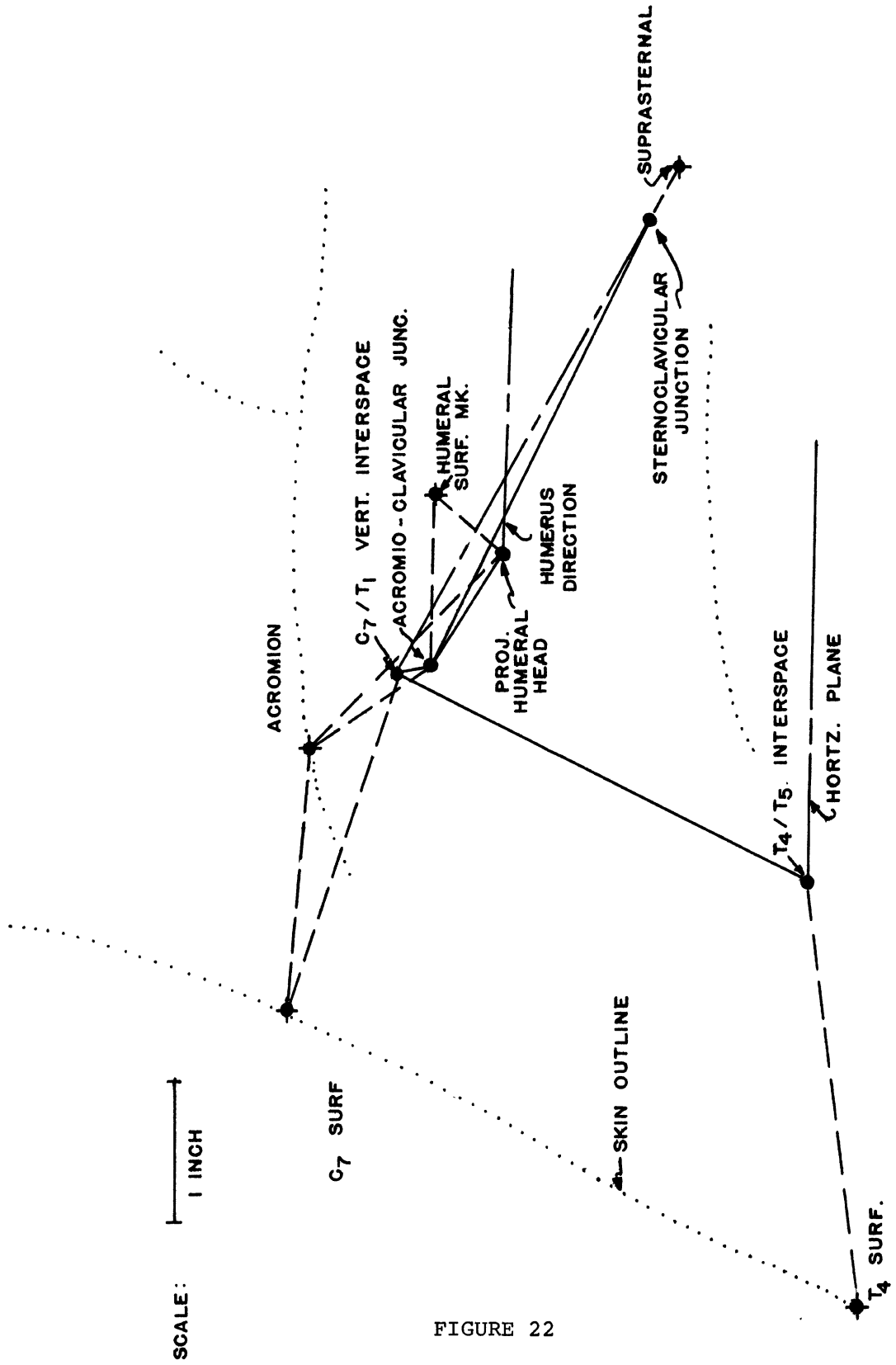

FIGURE 22

MEAN LOCATIONS OF VECTORS PROJECTED INTO SAGITTAL PLANE FROM SHOULDER X-RAYS

TABLE 15

SHOULDER VECTOR PREDICTION EQUATIONS

Reference Points:	Vector Distance (Inches)	r	F	ϕ=Vector Direction from Forward Sagittal Plane (+=left) (Degrees)	r	F	θ=Vector Direction in ϕ Plane Measured from Vertical Upwards Axis (0-180°)	r	F
T_4/T_5 Interspace to C_7/T_1 Interspace	DIST= 3.45+0.002(ANG)	0.50	3.72	ϕ = -1.49+0.034(ANG)	0.11	0.13	θ = 24.55-0.009(ANG)	0.05	0.03
C_7/T_1 Interspace to Acromio-Clavicular Junction	5.59+0.004(ANG)	0.27	0.77	-90.65-0.012(ANG)	0.06	0.04	90.41+0.013(ANG)	0.07	0.05
Projected Head of Humerus to C_7/T_1 Interspace	6.40+0.003(ANG)	0.21	0.58	102.21-0.003(ANG)	0.02	0.01	80.02-0.020(ANG)	0.11	0.15
Projected Head of Humerus to Acromio-Clavicular Junc.	1.68-0.002(ANG)	0.31	0.61	149.67-0.081(ANG)	0.16	0.38	54-78-0.185(ANG)	0.38	2.48
Acromion Surface to C_7 Surface	6.82+0.001(ANG)	0.31	0.16	105.75-0.071(ANG)	0.19	0.65	85.70+0.036(ANG)	0.11	0.22
T_4 Surface to C_7 Surface	4.35+0.002(ANG)	0.13	0.32	8.44-0.026(ANG)	0.06	0.08	21.45+0.068(ANG)	0.32	2.30
C_7/T_1 Interspace to C_7 Surface	2.56-0.003(ANG)	0.37	2.18	171.82-0.105(ANG)	0.55	5.93*	87.55-0.263(ANG)	0.67	11.53**
Acromio-Clavicular Junc. to Humeral Mark	3.02-0.004(ANG)	0.14	0.16	-66.22-0.383(ANG)	0.91	39.79**	112.02-0.035(ANG)	0.07	0.03
T_8/T_9 Interspace to T_8 Surf.	3.00-0.002(ANG)	0.15	0.25	182.55-0.083(ANG)	0.71	11.32**	32.43-0.003(ANG)	0.01	0.00
T_4/T_5 Interspace to T_4 Surf.	2.72-0.002(ANG)	0.16	0.40	181.33-0.084(ANG)	0.43	3.41	82.03-0.053(ANG)	0.14	0.31
Sterno-Clavicular Junc. to Suprasternale	1.00+0.002(ANG)	0.76	5.33	61.50-0.056(ANG)	0.34	0.51	111.75-0.024(ANG)	0.08	0.03
Projected Head of Humerus to Acromion	2.16-0.002(ANG)	0.27	1.47	-2.84-0.034(ANG)	0.04	0.03	42.31+0.208(ANG)	0.22	1.00
Acromio-Clavicular Junc. to Acromion	1.40+0.001(ANG)	0.07	0.07	-143.38-0.34(ANG)	0.65	10.92**	23.28+0.186(ANG)	0.25	1.03
Projected Head of Humerus to Humeral Mark	2.79-0.004(ANG)	0.66	7.61*	-79,61-0.48(ANG)	0.67	8.06*	50.03-0.10(ANG)	0.26	0.70
Sterno-Clavicular Junc. to Acromio-Clavicular Junc.	6.36+.0015(ANG)	0.07	0.06	-115.76-0.20(ANG)	0.83	22.02**	75.53-0.093(ANG)	-0.36	1.69

Sig. Effect Levels:
*0.05
**0.01

ANG=Humeral Arm Angle in Horizontal Plane measured from Forward Sagittal Plane (-45° Left to +135° Right)

Interpretation of Shoulder Mobility Results

The shoulder X-ray studies provide the following general results:

1. The distances for all the bone-to-bone vectors remain constant, regardless of the arm angle.

2. The lack of consistent directional movement in the horizontal plane (ϕ angle) of the two long vectors from the spine to the distal shoulder during arm horizontal movement combined with the very consistent movement of the "clavical" vector suggests that the subjects executed the movements by rotating the shoulder about a point closer to the sternum than the spine. Since the clavical forms a "hard" link for this rotation, it appears that the data is consistent with anatomical considerations.

3. The major objective of determining skin-to-bone movement was satisfied in that a large amount of consistent skin movement about the shoulder and upper thorax was documented. This is shown by the prediction equations of the vector directions of the: (a) vertebral interspaces-to-surface markers; and (b) the acromio-clavicular-to-acromion and humeral surface markers as a function of the humeral angles.

4. The one bone-to-surface vector distance that changed consistently with the arm angle was the vector from the projected humeral head to the humeral surface marker. There is a tendency for this distance to become smaller as the right arm rotates back (i.e., towards +135° from the forward sagittal plane). Because the surface marker is on the arm, its direction relative to the projected head of the humerus is directly correlated with the arm horizontal location. This skin movement is also displayed in the vector direction change from the acromio-clavicular junction.

In general, these results show that even when shoulder bone movement is not required for a large range of horizontal arm positions, consistent skin movement occurs at: (1) the C_7/T_1 level; (2) the acromion; and (3) the humeral marker. Thus, projections of bone positions with respect to these three surface points should consider the arm position. The prediction equations and associated graphs in Appendix N should assist in these developments.

Subject Anthropometry Effects on Surface-To-Bone Distances

Figure 17, presented earlier in this section, displayed the distributions of stature and weight of the subjects used to gain the X-ray data. Section II describes their specific anthropometric dimensions. In an attempt to explain the variation in the bone-to-surface distances that could not be explained by movement of the torso or arms, the following analysis of the subject effect on the data was instigated.

First, bone-to-surface marker distance data were identified that did not have any specific body position variation in them. Specifically this amounted to distance data on the following surface-to-bone vectors:

C_7 Surface-to-C_7/T_1 Interspace	i = 1
C_5 Surface-to-C_5/C_6 Interspace	i = 2
C_2 Surface-to-C_2/C_3 Interspace	i = 3
L_5 Surface-to-L_5/S_1 Interspace	i = 4
L_2 Surface-to-L_2/L_3 Interspace	i = 5
T_{12} Surface-to-T_{12}/L_1 Interspace	i = 6
T_8 Surface-to-T_8/T_9 Interspace	i = 7
T_4 Surface-to-T_4/T_5 Interspace	i = 8
Suprasternale-to-Sterno-clavicular	
Acromion-to-Acromio-clavicular	
Acromion-to-Humeral Head Center	
Humeral Surface Marker-to-Humeral Head Center	

The distance data were chosen from those studies where arm or torso positional effects were insignificant, as determined by the previous analyses (F values for body position effects were all smaller than 1.0).*

The subject effect for the spinal markers was first estimated by completing Two-Way Analysis of Variances on the data grouped into the three major spinal levels: cervical, thoracic, and lumbar. The two major effects tested were that there was no subject or reference point variance in the data, i.e.,

1. H_0: all the subjects had equal distances

2. H_0: all the reference points had equal distances

The interaction term was used as the error estimate for the F tests. The results are presented in Table 16 for an α level of 0.05.

From this analysis, it is concluded that the thoracic and

*The cervical spine data are described in the Section on Cervical Mobility. Only the resting normal position cervical data were used for this analysis.

TABLE 16

Analysis of Variance

Effect on Surface-to-Bone Dimensions

Cervical Spine Effects:	F Statistic	Sig. at =0.05
Subject	1.7	No
Point	0.8	No
Thoracic Spine Effects:		
Subject	11.3	Yes
Point	3.7	Yes
Lumbar Spine Effects:		
Subject	4.65	Yes
Point	5.23	Yes

Conclusion:

The surface-to-bone distances are significantly different for the thoracic and lumbar spines for different people and at different spinal segmental levels.

lumbar spinal columns have different surface-to-bone distances for the various subjects and at the different spinal levels. This second result was to be expected, since both the vertebra increased in size and the muscle bulk increased in mass towards the lower spinal levels. The major question relates to explaining the now-documented subject effect.

One possible explanation for varied subject distances between the spinal surface markers and the vertebra interspaces is the muscle fat variance in humans. An evaluation of this possibility was completed by regressing the lumbar and thoracic data onto five independent measures of body fat (see Section II for definition):

1. Triceps skinfold thickness
2. Subscapular skinfold thickness
3. Suprailiac skinfold thickness
4. Calf skinfold thickness
5. Heath-Carter Endomorphic Component

The results of this procedure were that only three of the ten possible relationships were significant at the $\alpha = 0.05$ level. These were:

1. Lumbar Vector Distances to Suprailiac Skinfold
2. Lumbar Vector Distances to H-C Index
3. Thoracic Vector Distances to Calf Skinfold

From a design standpoint, the suprailiac skinfold thickness provides some predictive power ($r = 0.61$). The linear regression model is (using inches)

$$\begin{bmatrix}\text{Lumbar Surface to} \\ \text{Vert. Interspaces}\end{bmatrix} = 2.9 + 1.52 \begin{bmatrix}\text{Suprailiac} \\ \text{Skinfold}\end{bmatrix}$$

The standard error estimate is still relatively large: 0.38 inches.

Another measure believed to explain some of the distance variation was the stature of the subjects, since a proportion of this dimension is due to the spinal vertebral sizes. Regressions of all of the spinal surface-to-interspace distances onto the subject statures were completed. This disclosed a significant relationship at the $\alpha = 0.05$ level. The regression equation for each i spinal level is: (see Table 17 for P_i values at each level)

$$\begin{bmatrix}\text{Spinal Surface-to-} \\ \text{Vert. Interspaces}\end{bmatrix} = -0.64 + P_i + 0.055 \begin{bmatrix}\text{Subject} \\ \text{Height}\end{bmatrix}$$

The estimate of the standard error is 0.37 inches. Considering

TABLE 17

Spinal Level Surface-to-Interspace

Correction Values for Stature Based Predictions

ith Spinal Surface-to-Vertical Interspace Distance (Inches) $= -0.64 + P_i + 0.055 \left[\begin{matrix}\text{Subject} \\ \text{Stature} \\ \text{(Inches)}\end{matrix}\right]$

i	Vertebral Levels	Mean Distances	P_i
1	C_7 Surface-to-C_7/T_1 Interspace	2.98	-.21
2	C_5 Surface-to-C_5/C_6 Interspace	3.05	-.18
3	C_2 Surface-to-C_2/C_3 Interspace	3.16	0.0
4	L_5 Surface-to-L_5/S_1 Interspace	3.70	+.48
5	L_2 Surface-to-L_2/L_3 Interspace	3.45	+.27
6	T_{12} Surface-to-T_{12}/L_1 Interspace	3.02	-.15
7	T_8 Surface-to-T_8/T_9 Interspace	3.24	0.0
8	T_4 Surface-to-T_4/T_5 Interspace	3.00	-.21

Standard Error Estimate = 0.37 inches

that this is for the surface-to-interspace distances for the entire column, the regression equation is believed to be of good enough precision to warrant its consideration in the predicting of the spinal column configuration from the various surface markers. These results, in general, indicate that the vertebral segment sizes contribute more to the surface-to-bone distances than general body fat.

The suprasternal, acromial, and humeral surface markers distances from various adjacent bone points were also regressed onto the four skinfold thickness measures, the Heath-Carter Endomorphic Component, and stature. The F statistics are given in Table 18. The conclusion is that the anthropometric dimensions which would be suspected of explaining some of the distance variations cannot be shown to affect the distances. Hence the variation in these surface-to-bone measurements must for now be attributed to such ill-defined problems as: (1) measurement error; (2) skeletal and subcutaneous tissue geometry variations; and/or (3) marker location variation. From the design standpoint, the surface-to-bone relationships expressed in Table 13 for these vectors are justified without anthropometric considerations.

Example of Use of Combined Photogrammetry and X-ray Data

To assist the person concerned with using the preceding data for engineering design, the following illustration depicting how both the photogrammetric and X-ray data can be combined is presented. The general procedure for determining such a torso configuration from the graphical data presented is:

1. Given the right elbow coordinates relative to the L_5 surface marker location, consult data in Appendix I to estimate the position of the seat or floor reference marks. (It should be noted that the seat conversion data are highly dependent on the type of seat configuration and general restraint, and that the included data is for only one particular seat.)

2. Determine the surface marker locations at L_2, T_{12}, T_8, T_4, C_7, acromion, and suprasternale from either Appendix H (for "average" seated male), Appendix I (for "average" standing male), or from Appendix J (for "tall" or "short" male).

3. Project adjacent bone reference points from surface reference points defined in Step 2, by referring to graphs in Appendices L through O. (In using these data it is recommended that the mean vector distances and directions be used (as presented in the preceding Tables 10, 12, and 14), unless the correlations in Tables 11, 13, and 15 are significant. If they are, then the general orientation of the

TABLE 18

F Statistics for Acromion, Suprasternale, and Humeral Marker Distances from Adjacent Bone Points as Related to Anthropometry

Vector Distances	SKINFOLDS				H-C Fat	Stature
	Triceps	Scapula	Suprailliac	Calf		
Suprasternale-to-Sternoclavicular joint	2.4	0.1	1.4	1.3	0.8	1.7
Acromion-to-Acromio-Clavicular Joint	0.0	0.1	4.2	0.2	0.6	0.6
Acromion-to-Acromio-Clavicular Joint	1.1	0.4	0.7	1.2	0.4	0.2
Humeral Mark-to-Center of Humeral Head	0.1	4.6*	1.8	0.9	0.2	0.8

*Sig. at 0.10 level
None sig. at 0.05 level

Conclusion: No consistent relationships exist.

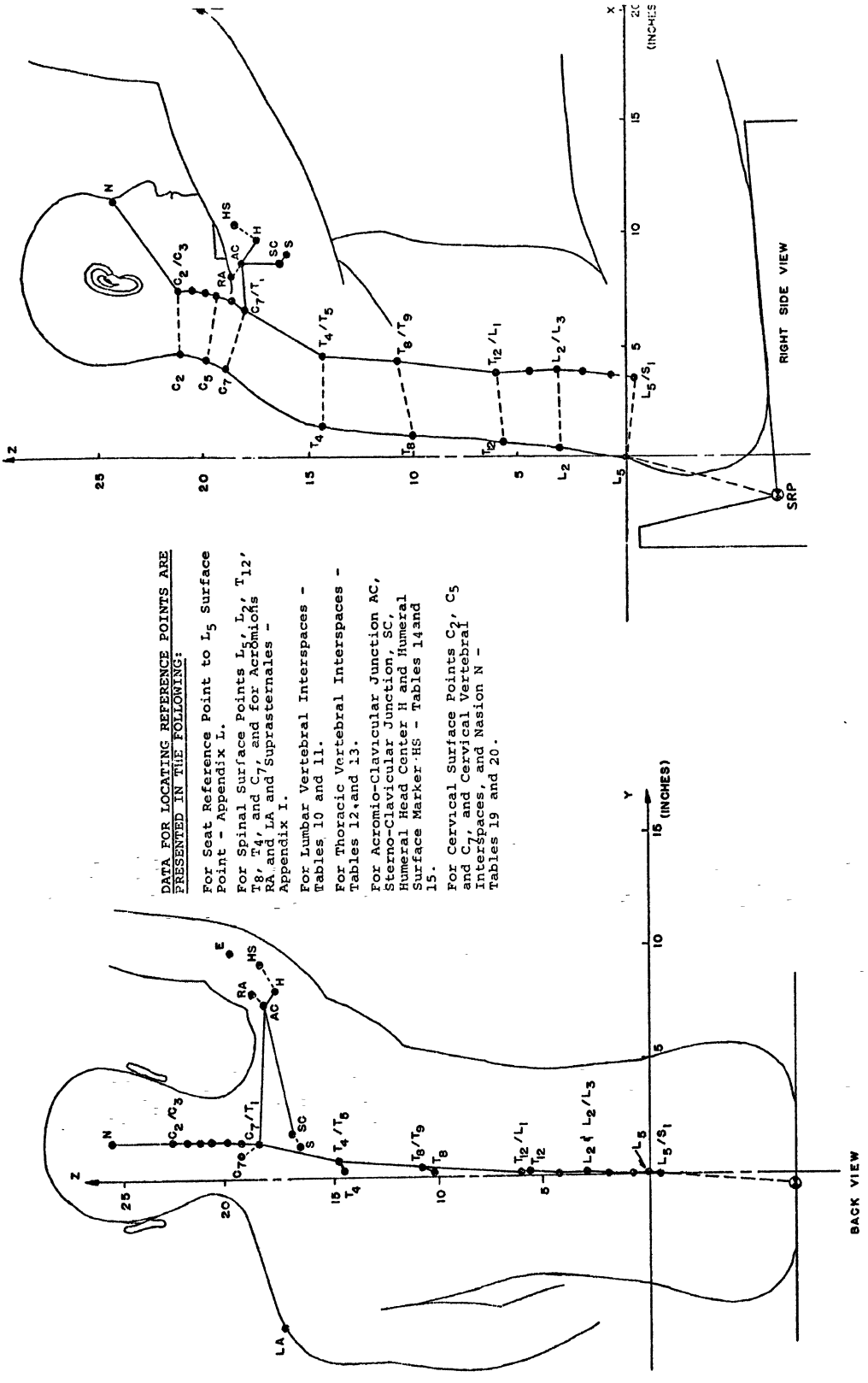

FIGURE 23

ILLUSTRATION OF REPRESENTATIVE

TORSO LINKS

various body sectors (i.e., the angle of the reference vectors) should be considered, (as depicted by the graphs associated with the prediction equations in Tables 11, 13 and 15) when projecting the adjacent bone reference point positions.) When defining a person of other than mean stature, the surface-to-bone vector distance corrections contained in Table 16 should be considered.

Because the dimensions depicted in all of the graphs are empirically defined, as opposed to assuming a set of "hard" links which have specific known degrees of freedom, the undefined variability in the data will cause some "misallignment" of the bone reference points when they are projected from two or more adjacent points. Thus a single, unique linkage describing the torso mobility is not possible from this report but rather alternative internal linkages can be defined by the designer. The complexity and accuracy of each linkage assumed by the designer will necessarily depend on the range and type of reach simulation.

To illustrate one alternative linkage the general model seated position (Appendix I) was used to determine the torso surface marker locations in Figure 23. The right elbow marker was assumed to be 20 inches above, 10 inches to the right, and 20 inches in front of the L_5 surface marker. The seat reference point was located with reference to the data in Appendix L. The internal bone reference points were projected from the surface marker locations by referring to the data presented earlier in this section. The general head position was assumed to be in the normal resting position described in the next section. For reference, the position of the greater trochanter (as defined by dimensions 66 and 68 in Appendix D) is presented as an approximate Hip Joint. The mean location is 3.96 inches above and 4.63 inches in front of the SRP.

One final comment on using the torso mobility data for design purposes. The graphical displays of the predicted torso surface marker movement may be of some assistance to a designer, but they will require both extrapolation and interpolation for different design problems. The length of the lines of the present graphs depict the excursions to which the data are amenable. The pages of comments inserted before the graphs depicting each surface marker movement describe specific factors regarding the mobility of each reference point. Because there are so many interactive factors that affect the movements of both the internal and surface reference points, it is expected that the greatest benefit from this project will be in the improvement of computerized man-geometry simulations. These models will be based on the mobility prediction equation coefficients of Appendix H, combined with internal links generated from the bone movement data presented earlier in this section. Once these models are constructed, then the trade-offs between different link representations of the torso can be researched.

SECTION V

CERVICAL SPINE MOBILITY STUDY

Like the arms, movement of the head and neck could certainly affect the surface-to-bone vectors, thus changing inferences regarding the skeletal configuration based on the location of various surface markers. The study reported in this section had this as its primary objective. In addition, cervical spine configurations were also determined for sagittal plane flexion and extension. This latter result provides further design data as to the visual area, given the upper torso location.

Procedure

The procedure followed in this study was similar to that used in the previously reported X-ray studies. The subjects were asked to position their necks into those described in Table 8 (i.e., normally seated, comfortably extended, medium flexed forward, and hyper-flexed forward).* Lateral X-rays were obtained in each position.

Mean and standard deviations of the resulting dimensions were obtained. These are displayed in Table 19.

What is of primary importance is the movement of the cervical column relative to head inclination and in particular to nasion (nasal root depression) location. To quantify this relationship, a reference vector from the C_7 surface marker (cervicale) to the nasion marker was first constructed. All of the other vectors were then regressed onto the angulations of this vector. The results of these regressions are summarized in Table 20. Plots of these data are contained in Appendix P.

Figures 24-28 illustrate four positions achieved by the subjects (as quantified by the C_7-to-Nasion vector directions). For each head position, the expected values of the cervical spine disc interspace and surface marker locations predicted from the equations in Table 20 are plotted. From inspection of this, the mobility of the various skeletal components can be noted.

Results of Cervical Spine Study

The study of movement of the cervical spine in the sagittal plane has resulted in the following:

*A few lateral flexion and cervical rotations were attempted, but the resulting X-ray data was insufficient to draw reasonable inference regarding neck mobility.

TABLE 19

Mean Cervical X-Ray Data Summary

Vectors:	Distance Mean	Distance S.D.	(+=Backwards) Direction from Vert. Upwards Axis Mean	(+=Backwards) Direction from Vert. Upwards Axis S.D.
C_7/T_1 Interspace to C_2^1/C_3 Interspace	3.56	0.15	-18.71	10.18
C_7/T_1 Interspace to C_3^1/C_4 Interspace	2.88	0.16	-21.17	10.82
C_7/T_1 Interspace to C_4^1/C_5	2.38	0.62	-26.75	14.70
C_4/C_5 Interspace to C_2/C_3 Interspace	1.51	0.60	-15.23	12.29
C_5/C_6 Interspace to C_2^6/C_3	2.13	0.13	-13.85	12.61
C_7 Surface to Nasion	9.60	0.52	-58.54	12.34
C_2/C_3 Interspace to C_2^3 Surface	3.16	0.32	+90.15	10.47
C_5/C_6 Interspace to C_5^6 Surface	2.99	0.52	+77.13	14.95
C_7/T_1 Interspace to C_7^1 Surface	2.94	0.21	+65.12	13.80
C_7/T_1 Interspace to C_5^1/C_6 Interspace	1.57	0.27	-25.64	14.82
C_3/C_4 Interspace to C_2^4/C_3 Interspace	0.72	0.05	-10.50	13.47
C_7/T_1 Interspace to C_6^1/C_7 Interspace	0.76	0.04	-24.90	9.89
C_6/C_7 Interspace to C_5^7/C_6 Interspace	0.71	0.04	-18.56	10.33
C_5/C_6 Interspace to C_4^6/C_5 Interspace	0.70	0.05	-19.26	9.82
C_4/C_5 Interspace to C_3^5/C_4 Interspace	0.70	0.04	-17.74	12.61

TABLE 20

CERVICAL VECTOR PREDICTION EQUATIONS

Reference Points	Vector Distance Prediction(Inches)	N sample size	r corr.coef.	F^1 stat.	Vector Direction in sagittal plane (degrees)	N sample size	r corr.coef.	F^1 stat.
C_7/T_1 Interspace to C_2/C_3 Interspace	3.52 - 0.0008(ANG)	16	-0.06	0.06	+19.19 + 0.64(ANG)	16	0.78	22.43**
C_9/T_1 Interspace to C_3/C_4 Interspace	2.86 - 0.0003(ANG)	16	-0.02	0.01	+11.79 + 0.56(ANG)	16	0.64	9.71**
C_7/T_1 Interspace to C_4/C_5 Interspace	3.56 + 0.020 (ANG)	16	0.40	2.63	-30.89 + 0.071(ANG)	16	-0.06	0.05
C_4/C_5 Interspace to C_2/C_3 Interspace	1.60 + 0.002 (ANG)	16	0.06	0.05	+42.82 + 0.965(ANG)	14	0.91	59.9**
C_5/C_6 Interspace to C_2/C_3 Interspace	2.11 - 0.0002(ANG)	16	-0.02	0.01	37.29 + 0.87 (ANG)	15	.85	36.75**
C_7 Surface to Nasion	10.70 + 0.019 (ANG)	16	0.45	3.47	ANG (see below)			
C_2/C_3 Interspace to C_2 Surface	3.004 - 0.003(ANG)	16	-0.10	0.14	131.75 + 0.71 (ANG)	16	0.83	31.9**
C_5/C_6 Interspace to C_5 Surface	3.63 + 0.011 (ANG)	16	0.26	1.00	+139.66 + 1.065(ANG)	16	0.88	46.8**
C_7/T_1 Interspace to C_7 Surface	3.28 + 0.006 (ANG)	16	0.32	1.65	+121.14 + 0.95 (ANG)	16	0.85	36.9**
C_7/T_1 Interspace to C_5/C_6 Interspace	1.72 + 0.0024(ANG)	16	0.11	0.16	-8.91 + 0.29 (ANG)	16	0.24	0.83
C_3/C_4 Interspace to C_2/C_3 Interspace	0.72 - 0.0001(ANG)	15	-0.04	0.02	+49.42 + 1.024(ANG)	15	0.94	96.2**
C_7/T_1 Interspace to C_6/C_7 Interspace	0.752 - 0.00021(ANG)	16	-0.06	0.04	-9.38 + 0.26 (ANG)	16	0.33	1.7
C_6/C_7 Interspace to C_5/C_6 Interspace	0.75 + 0.0006 (ANG)	14	0.22	0.63	+8.66 + 0.46 (ANG)	14	0.57	5.66*
C_5/C_6 Interspace to C_4/C_5 Interspace	0.716 + 0.0003(ANG)	14	0.07	0.05	+16.26 + 0.59 (ANG)	13	0.72	11.69**
C_4/C_5 Interspace to C_3/C_4 Interspace	0.626 - 0.0013(ANG)	13	-0.35	1.15	+36.57 + 0.90(ANG)	13	0.86	31.68**

Sig. Levels:
*0.05
**0.01

ANG = Direction in Sagittal Plane From Vertical Upward Axis of C_7 Surface Mark to Nasion Vector (+ = Backwards)

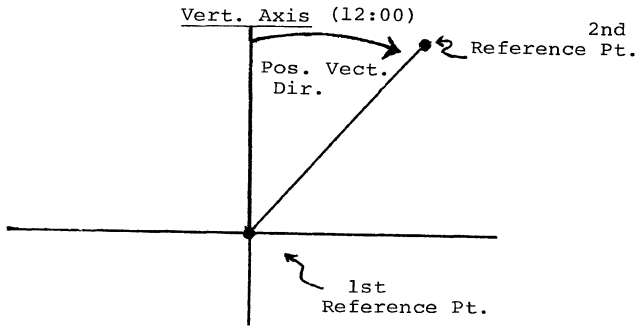

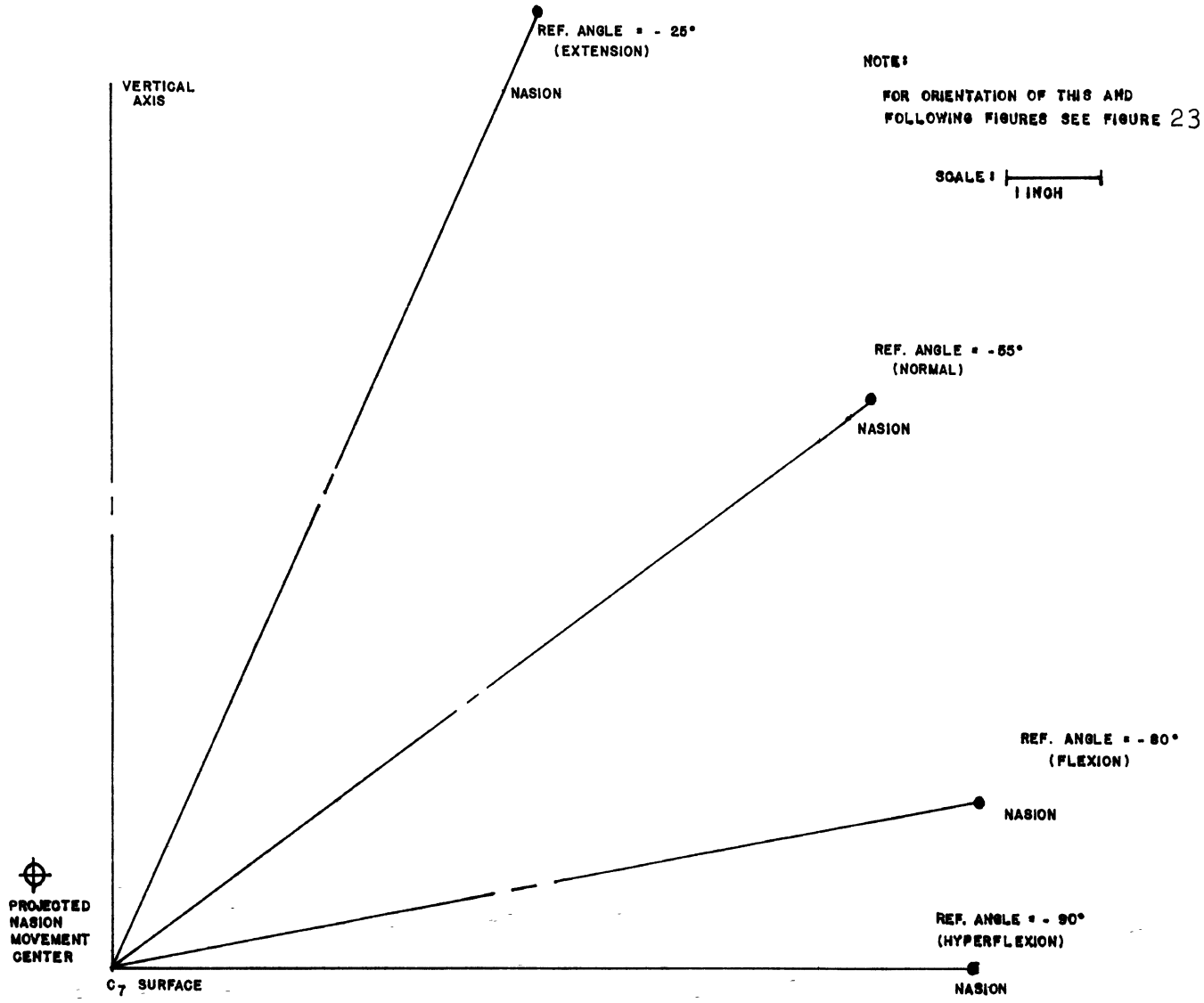

FIGURE 24

AVERAGE VALUES FOR REFERENCE
ANGLE (C_7 SURFACE TO NASION)

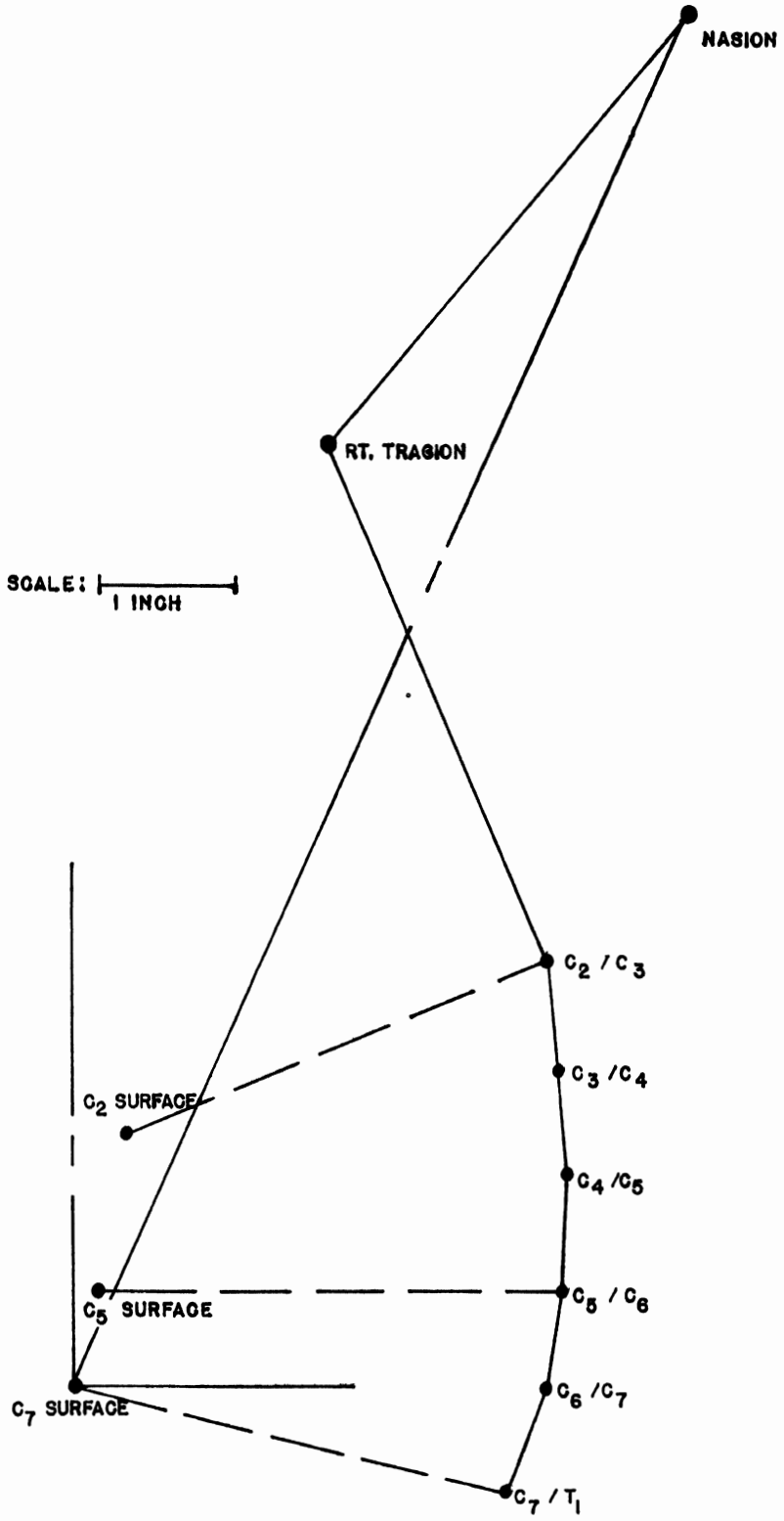

FIGURE 25

CERVICAL DISC CENTER LOCATIONS
FOR EXTENSION
(Ref. Angle = -25° from Vertical)

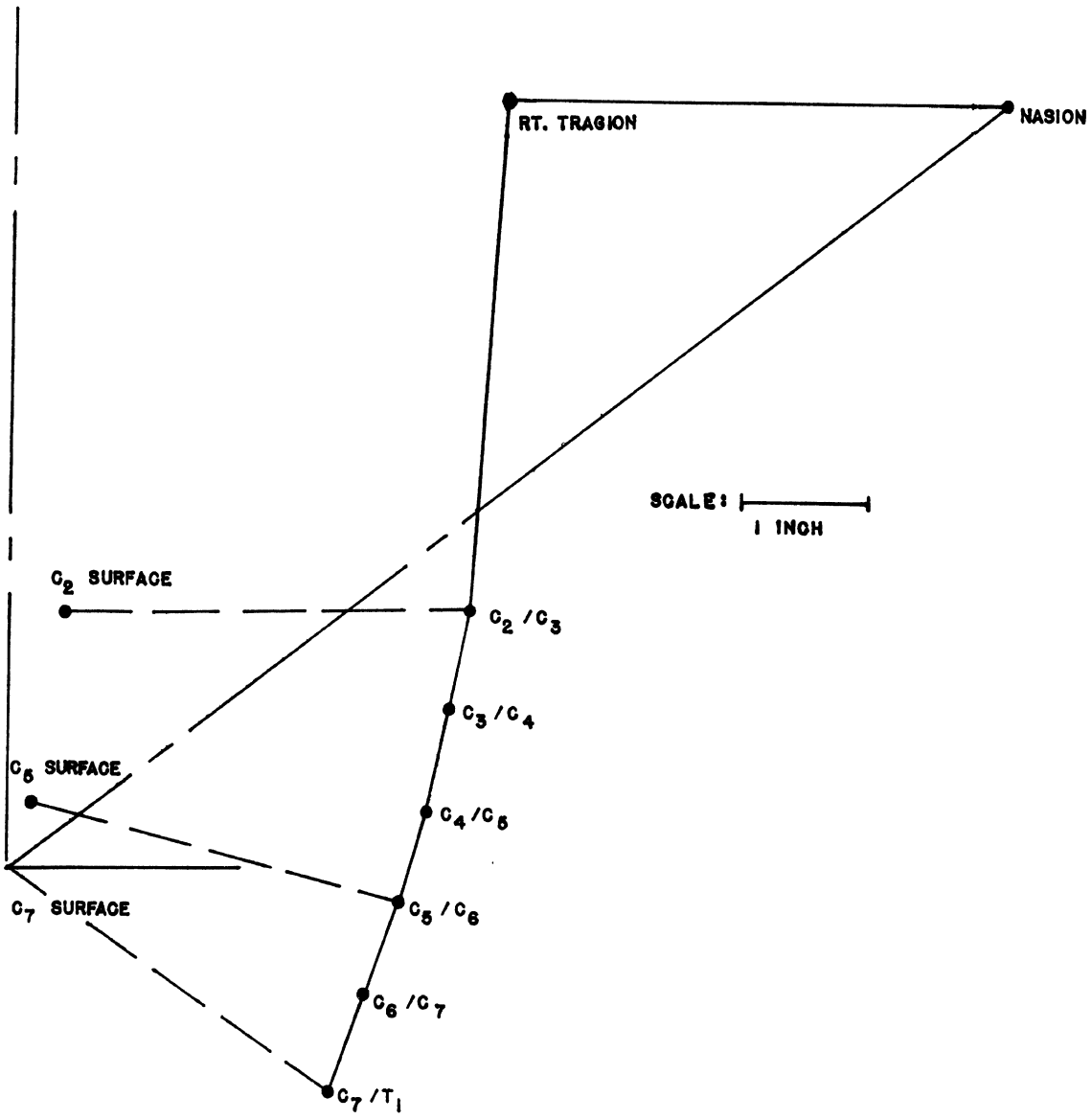

FIGURE 26

CERVICAL DISC CENTER LOCATIONS
FOR EXTENSION
(Ref. Angle = -55° from Vertical)

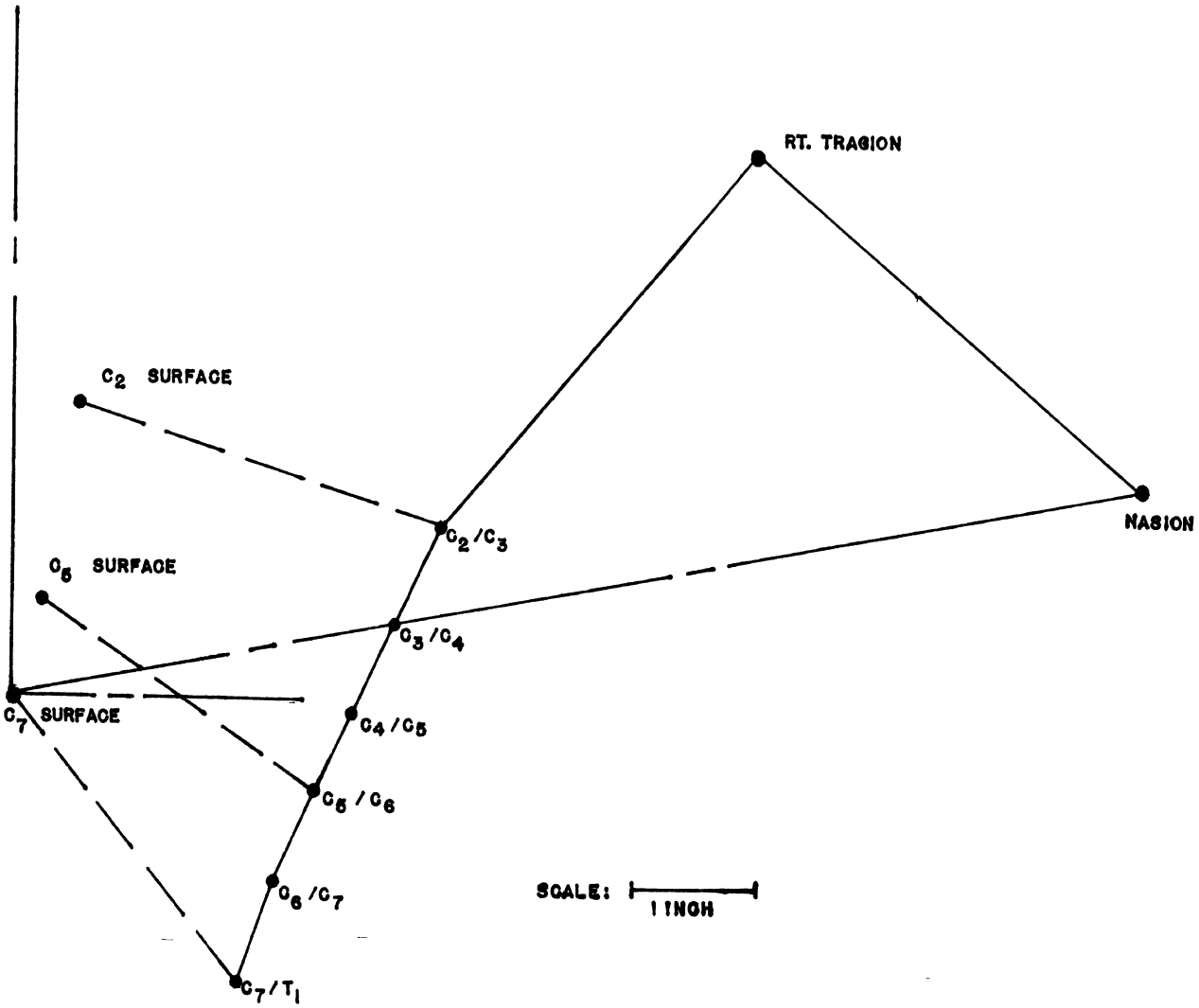

FIGURE 27

CERVICAL DISC CENTER LOCATIONS
FOR FLEXED POSITION
(Ref. Angle = -80° from Vertical)

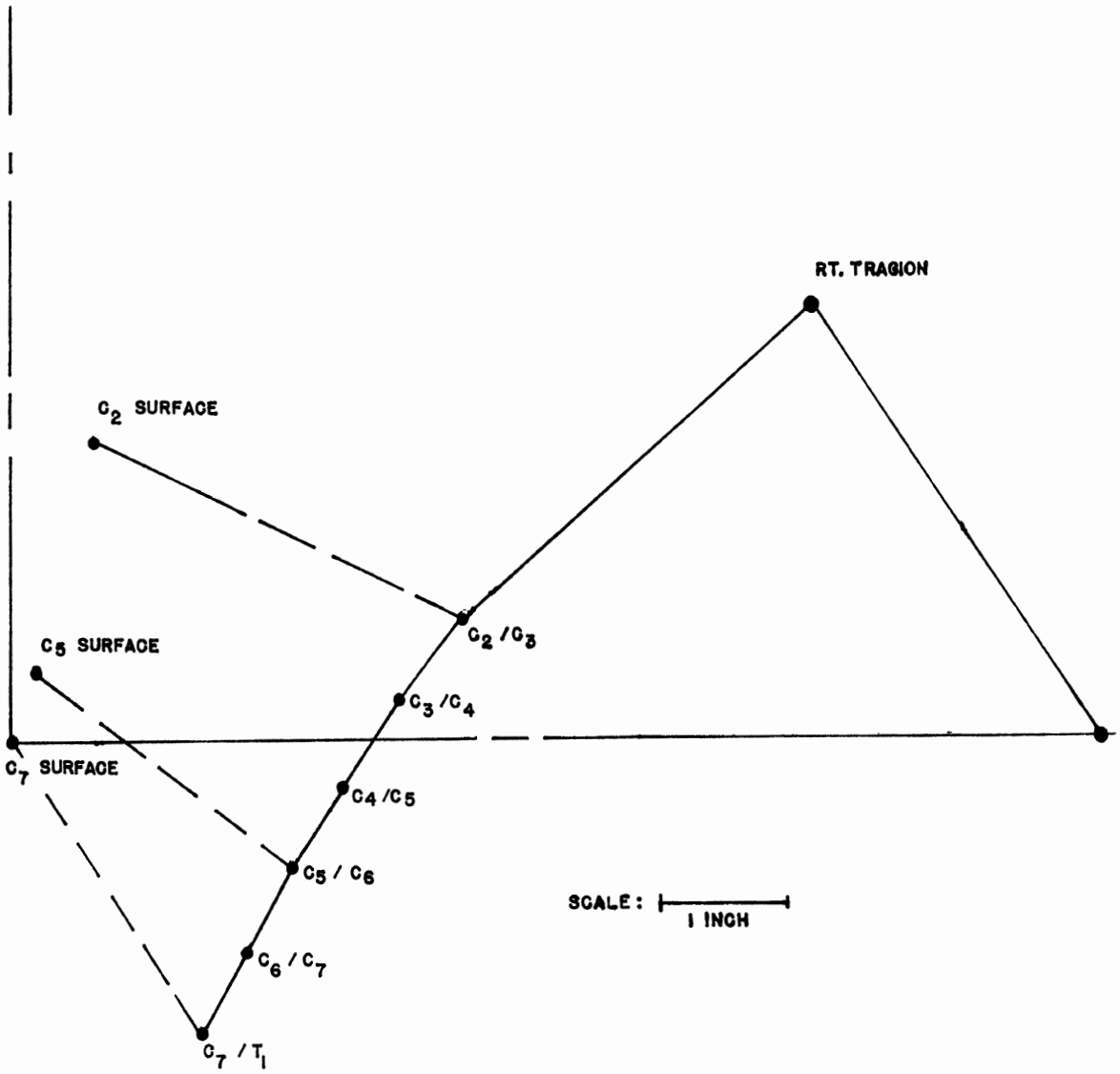

FIGURE 28

CERVICAL DISC CENTER LOCATIONS
FOR HYPERFLEXED POSITION
(Ref. Angle = -90° from Vertical)

1. The surface-to-bone distances of both the C_5 and C_2 markers do not change significantly with the head inclination, though the C_7 distance does. The directions of all three of the surface-to-bone vectors change with the inclination of the head, with the greatest change at the upper C_2 level and the least change at the C_7 level.

2. The cervical spine above the C_5/C_6 level consistently moved with the degree of head inclination. By comparing the regression coefficients of the prediction equations of vector directions in Table 20, the greatest mobility was achieved at the C_2/C_3 and C_3/C_4 levels (average 0.6 degree per degree of head tilt).

Interpretation of Cervical Study Results

The preceding results show that as the head is inclined forward from an upward gaze (neck extending position), the posterior soft tissue of the neck "tightens" in such a way as to significantly change both the distance and directions of vector from the C_7/T_1 interspace-to-C_7 surface marker. Because the C_7 surface marker (cervicale) is often used as the "top-of-the-torso" reference point, this result means that control of head position should be considered in future studies of torso surface geometry. The prediction equations given in Table 20 for this vector should be of direct assistance.

The study results also indicate that the nasion point moves in an approximate arc about a point located about 1/2 inch posterior and one inch above the C_7 surface marker, as depicted in Figures 24-28. This result, combined with the tragion-to-nasion vector plotted on Figures 24-28 (which moved directly with the line-of-sight), should be of assistance to future evaluations of visual interference problems.

P A R T II

ANTHROPOMETRIC DATA AND PHOTOGRAMMETRIC TECHNIQUE

APPENDIX A

OUTLINE OF ANTHROPOMETRIC PROCEDURES, AND DATA FORMS

1. Mark Standing Subject at Following Surface Points with a Marking Pen:
   1. Nasal root depression
   2. Chin-neck intersect
   3. Left acromion
   4. Right acromion
   5. Left sterno-clavicular
   6. Right sterno-clavicular
   7. Suprasternale
   8. Right lateral epicondyle of humerus
   9. Right medial epicondyle of humerus
   10. Greater tuberosity of right humerus (2" inferior and lateral to right acromion)
   11. C_2 spinous process
   12. C_5 spinous process
   13. Cervicale (C_7 spinous process)
   14. T_4 spinous process
   15. T_8 spinous process
   16. T_{12} spinous process
   17. L_2 spinous process
   18. L_5 spinous process
   19. Left anterior superior iliac spine
   20. Right anterior superior iliac spine
   21. Left trochanter
   22. Right trochanter
   23. Superior edge of patella
   24. Mid-patella
   25. Right lateral epicondyle of femur
   26. Right medial epicondyle of femur
   27. Right fibulare
   28. Tip styloid process of right fibula
   29. Distal tip of right lateral malleolus of fibula
   30. Right tibiale
   31 Most lateral palpable point on the right femoral greater trochanter
   32. Superior edge medial right tibia condyle
   33. Superior edge lateral right tibia condyle (lateral projection tibiale)
   34. Distal tip of tibia medial malleolus

2. Mark seated subject at following surface point with a marking pen; 35. Seated right trochanter.

3. Complete surface anthropometry according to following subject form. Add comments relative to subject, such as "weight lifter," "left-handed," or anomoly which might be important.

4. Position surface markers for photogrammetric and x-ray studies as follows:
   1. Nasal root depression
   2. Left tragion
   3. Right tragion
   4. Left acromion
   5. Right acromion
   6. Suprasternale
   7. Lateral epicondyle of the humerus
   8. Right medial epicondyle of the humerus
   9. Head of the right humerus
   10. C_2
   11. C_5
   12. Cervicale (C_7)
   13. T_4
   14. T_8
   15. T_{12}
   16. L_2
   17. L_5
   18. Left anterior superior iliac spine
   19. Right anterior superior iliac spine
   20. Left trochanter
   21. Right trochanter

5. Read and mark subject x-rays, record data.

6. Obtain computer readout for Somatotype.

SURFACE ANTHROPOMETRY FORM

Torso-Link Study

Subject No. _____

Name _____ Sex _____ N,C,M

Address (Business) _____ Telephone (bus) _____

(Residence) _____ (res) _____

Age (yr, mo) _____ Date _____

Military Service _____ Social Security No. _____

STANDING:

1.	Weight	_____
2.	Stature	_____
3.	Rt. Tragion	_____
4.	Lt. Tragion	_____
5.	Nasal Root Depression	_____
6.	Chin-Neck Intersect	_____
7.	Cervicle (C_7)	_____
8.	Suprasternale	_____
9.	Rt. Sterno-clavicular	_____
10.	Lt. Sterno-clavicular	_____
11.	Bisterno-clavicular	_____
12.	Suprasternale-acromion (Rt.)	_____
13.	Rt. Acromion	_____
14.	Lt. Acromion	_____
15.	Biacromial Breadth	_____
16.	Rt. clavical length (x-ray)	_____
17.	Nipple Height	_____
18.	Omphalion	_____
19.	Rt. Ant. Sup. Iliac Sp.	_____
20.	Lt. Ant. Sup. Iliac Sp.	_____
21.	Iliocristale Height	_____
22.	Bispinous Breadth	_____
23.	Rt. Trochanter	_____
24.	Lt. Trochanter	_____
25.	Bitrochanteric Diameter	_____
26.	Humerus Biepicondylar Diam.	_____
27.	Acromion-Radiale Length (elbow flexed 90°)	_____
28.	Head of Humerus-Radiale	_____
29.	Radius Length	_____
30.	Ulna Length	_____
31.	Forearm - Hand Length	_____
32.	Forearm-grip distance	_____

33. Wrist breadth (bone) _____
34. Hand length _____
35. Troch. - to - Lat. Fem. Condyle _____
36. Fibula length _____
37. Fibulare height _____
38. Femoral biepicondylar diameter _____
39. Mid-patella height _____
40. Tibiale Height (medial) _____
41. Tibiale Height (lateral) _____
42. Medial Sphyrion Height _____
43. Lateral Sphyrion Height _____
44. Rt. Foot Length _____
45. Lt. Foot Length _____

CIRCUMFERENCE:

46. Head Circ. _____
47. Chest Circ. _____
48. Axillary Circ. (chest) _____
49. Axillary Circ. (arm) _____
50. Biceps (relaxed) right _____
51. Biceps (relaxed) left _____
52. Biceps (flexed) right _____
53. Biceps (flexed) left _____
54. Forearm Circ. _____
55. Wrist Circ. _____
56. Calf Circ. _____
57. Ankle Circ. _____

SEATED:

58. Sitting Height _____
59. Cervicle _____
60. Suprasternale _____
61. Acromion _____
62. Buttock-Knee _____
63. Knee Height (mark) _____
64. Knee Height (actual) _____
65. Seat Back - to - Troch. (Erect)* (Trochanter palpated and marked in the erect posture.) _____
66. Seat Back - to - Troch. (Seated)* (Trochanter palpated and marked in the seated posture.) _____

* Measured with the subject in the seated posture.

67. Seat Surface - to - Trochanter (Erect)* (Troch. palpated and marked in the erect posture.) _____

68. Seated Surface - to - Trochanter (Seated)* (Troch. palpated and marked in the seated posture.) _____

SKINFOLDS:

69. Rt. Triceps _____
70. Rt. Scapula _____
71. Rt. Suprailiac _____
72. Rt. Calf _____

COMMENTS:

_____

_____

_____

_____

_____

_____

_____

_____

_____

_____

_____

_____

_____

_____

_____

_____

_____

* Measured with the subject in the seated posture.

Appendix B

DESCRIPTION OF SURFACE MARKER LOCATIONS USED AS REFERENCE POINTS FOR PHOTOMETRIC AND RADIOGRAPHIC ANALYSIS

1. Left Tragion .... On the left ear, the anterior portion of the cartiloginous notch superior to the tragus.

2. Right Tragion.... On the right ear, the anterior portion of the cartiloginous notch superior to the tragus.

3. Nasal Root Depression.....The point of greatest indentation where the bridge of the nose joins the supraorbital ridge of the forehead.

4. Head of the Humerus..... Measured from the right acromion over the lateral surface of the arm on a line projected inferiorally from the acromion to the lateral epicondyle a distance of 2 inches.

5. C_2.....The most superior dorsal point on the spinous process of the second cervical (axis) vertebra.

6. Cervicale.....The point of the spinous process of the seventh cervical vertebra.

7. T_4.....The most superior dorsal point on the spinous process of the fourth thoracic vertebra.

8. T_8..... The most superior dorsal point on the spinous process of the eighth thoracic vertebra.

9. T_{12}..... The most superior dorsal point on the spinous process of the twelfth thoracic vertebra.

10. L_2.....The most superior dorsal point on the spinous process of the second lumbar vertebra.

11. L_5.....The most superior dorsal point on the spinous process of the fifth lumbar vertebra.

12. Suprasternale.....The superior margin of the Jugular notch of the Manubrium.

13. Right Sterno-clavicular Junction.....The most superior medial point on the sternal extremity of the right clavicle.

14. Left Sterno-clavicular Junction.....The most superior medial point on the sternal extremity of the left clavicle.

15. Right Acromion.....The superior and external border of the acromion process of the right scapula.

16. Left Acromion..... The superior and external border of the acromion process of the left scapula.

17. Right Lateral Epicondyle.....The lateral epicondyle of the distal right humerus.

18. Left Lateral Epicondyle.....The lateral epicondyle of the distal left humerus.

19. Right Medial Epicondyle.....The medial epicondyle of the distal right humerus.

20. Left Medial Epicondyle.....The medial epicondyle of the distal left humerus.

21. Right Anterior Superior Iliac Spine.....The point palpable at the right anterior superior iliac spine of the pelvis.

22. Left Anterior Superior Iliac Spine.....The point palpable at the left anterior superior iliac spine of the pelvis.

23. Right Trochanter.....Most lateral palpable point on the right femoral greater trochanter. (To be located from P-A pelvis radiograph.)

24. Left Trochanter.....Most lateral palpable point on the left femoral greater trochanter. (To be located from P-A pelvis radiograph.)

Appendix C

Description of bone to bone measurements made directly from radiographs. Other measurements are defined in Appendixes B and D.

1. Acromio-clavicular Junction. Bilaterally located at the articulation of the acromion of the scapula and the acromial extremity of the clavicle.

2. Sterno-clavicular Junction. bilaterally located at the articulation of the lateral aspect of the clavicular notch of the manubrium with the sternal extremity of the clavicle.

3. Clavicle Length. The maximum distance between the sternal and acromial extremities of the right clavicle.

4. Proximal Head of the Humerus. The center of mass of the proximal (gleno-humeral) head of the humerus, as determined by the intersection of lines drawn perpendicular to the shaft and at 90° across the head of the humerus in an anterior-posterior view of the subject's radiograph.

5. Vertebral Interspaces. Located at the center of inter-vertebral discs and determined by the intersection of a perpendicular plane drawn through the center of the adjoining vertebral bodies, and a horizontal plane equally dividing the intervertebral space.

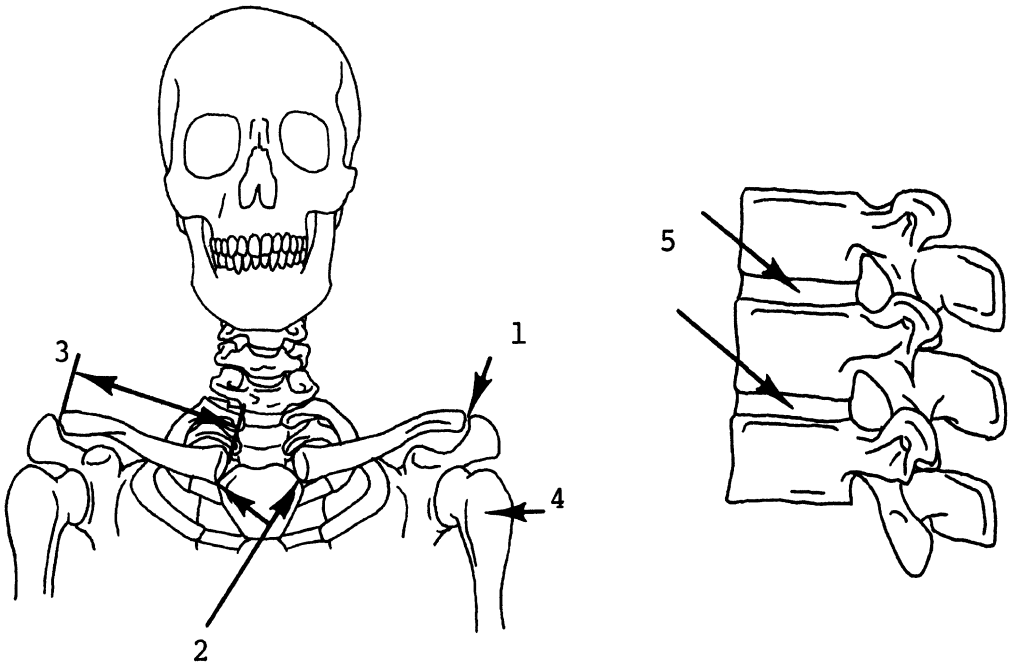

Appendix D

DESCRIPTION OF ANTHROPOMETRIC DIMENSIONS

1. WEIGHT

Taken on standard medical type scale to nearest one-half pound. Subject unclothed.

KILOGRAMS	N=28	POUNDS
79.37	Mean	174.61
12.40	SD	27.28
62.95-104.55	Range	138.5-230.0

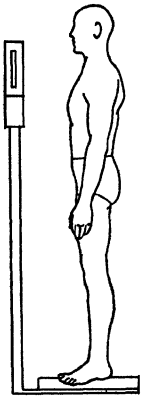

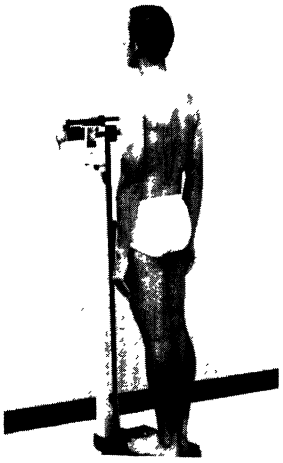

2. STATURE

The subject maintains an erect standing posture, feet together, arms hanging at his side, looking straight ahead with head held in the Frankfurt Plane*, which is determined by lining up the infra-orbital margins with tragion in the same horizontal plane. The vertical distance is measured with the anthropometer from the floor to the highest point on the subject's head with the anthropometer arm firmly contacting the scalp.

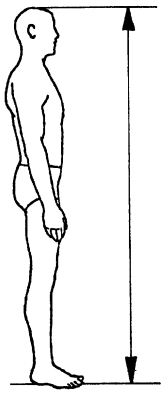

CM	N=28	IN
178.45	Mean	70.26
6.59	SD	2.59
163.5-191.4	Range	64.37-75.35

PERCENTILES

CM		IN
167.81	5th	66.07
170.20	10th	67.01
173.10	20th	68.15
175.20	30th	68.98
176.98	40th	69.68
178.65	50th	70.33
180.32	60th	70.99
182.10	70th	71.69
184.20	80th	72.52
187.10	90th	73.66
189.49	95th	74.60

*Frankfurt Plane or horizontal (F.H.) - the plane determined by the points on the infra-orbital margins and the tragion.

3. RIGHT TRAGION

The subject maintains an erect standing posture, feet together, arms hanging at his side, looking straight ahead, with head held in the Frankfurt Plane. The vertical distance is measured with an anthropometer from the floor to the anterior limit of the cartilaginous notch superior to the tragus of the right ear.

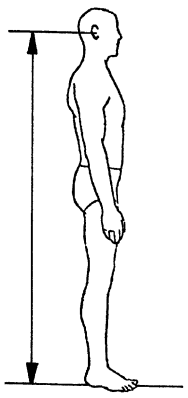

N=28

CM		IN
164.63	Mean	64.81
6.49	SD	2.56
151.2-176.5	Range	59.53-69.49

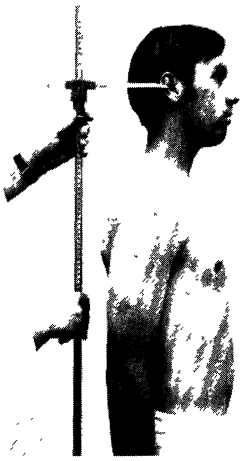

4. LEFT TRAGION

The subject maintains an erect standing posture, feet together, arms hanging at his side, looking straight ahead with head held in the Frankfurt Plane. The vertical distance is measured with an anthropometer from the floor to the anterior limit of the cartilaginous notch located superior to the tragus of the left ear.

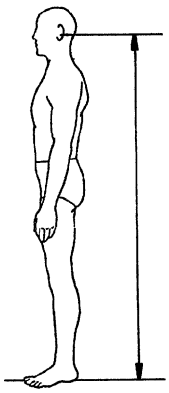

CM	N=28	IN
164.76	Mean	64.87
6.41	SD	2.52
151.0 - 176.8	Range	59.45 - 69.61

5. NASAL ROOT DEPRESSION

The subject maintains an erect posture, feet together, arms hanging at his side, looking straight ahead with head held in the Frankfurt Plane. The vertical distance is measured with an anthropometer from the floor to the point of greatest indentation where the bridge of the nose joins the supraorbital ridge of the forehead.

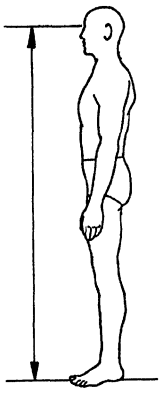

CM	N=28	IN
166.91	Mean	65.71
6.60	SD	2.60
153.4 - 180.0	Range	60.39 - 70.87

6. CHIN-NECK INTERSECT

The subject maintains an erect posture, feet together, arms hanging at his side, looking straight ahead with head held in the Frankfurt Plane. The vertical distance is measured with an anthropometer from the floor to the point of intersection of the chin and neck at the mid-line. This intersection is located by observing the subject from the side and marking the highest point on the neck intersected by the chin.

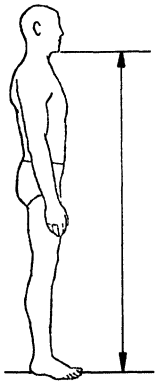

CM	N=28	IN
154.10	Mean	60.67
6.34	SD	2.50
140.1 - 166.9	Range	55.16 - 65.71

7. CERVICALE

The subject maintains an erect posture, feet together, arms hanging at his side, looking straight ahead with head held in the Frankfurt Plane. The vertical distance is measured with an anthropometer from the floor to the palpable spinous process of the seventh cervical vertebra.

CM	N=28	IN
152.74	Mean	60.13
6.26	SD	2.46
140.9 - 166.1	Range	55.47 - 65.39

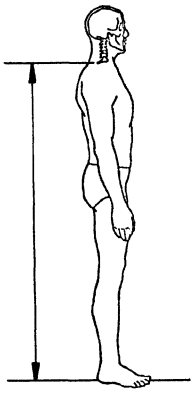

8. SUPRASTERNALE HEIGHT, STANDING

The subject maintains an erect posture, feet together, arms hanging at his side, looking straight ahead. Facing the subject, the vertical distance is measured with an anthropometer from the floor to the superior margin of the jugular notch of the manubrium.

CM	N=28	IN
145.73	Mean	57.37
5.71	SD	2.25
134.3 - 157.4	Range	52.87 - 61.97

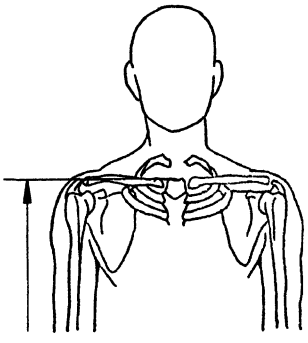

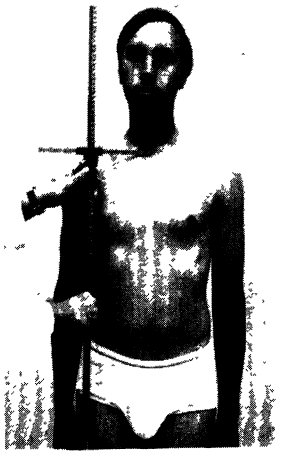

9. RIGHT STERNO-CLAVICULAR HEIGHT

The subject maintains an erect posture, feet together, arms hanging at his side, looking straight ahead. The vertical distance is measured on the subject with an anthropometer from the floor to the superior medial right sterno-clavicular prominence, as palpated on the anterior superior aspect of the proximal end of the clavicle.

CM	N=28	IN
146.78	Mean	57.79
5.80	SD	2.28
134.6 - 158.4	Range	52.99 - 62.36

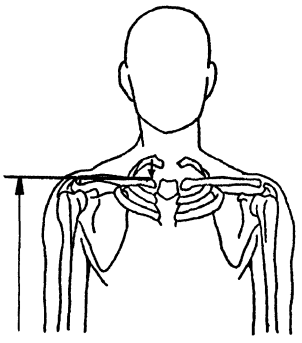

10. LEFT STERNO-CLAVICULAR HEIGHT

The subject maintains an erect posture, feet together, arms hanging at his side, looking straight ahead. The vertical distance is measured on the subject with an anthropometer from the floor to the superior medial left sterno-clavicular prominence, as palpated on the anterior superior aspect of the proximal end of the clavicle.

CM	N=28	IN
146.92	Mean	57.84
5.87	SD	2.31
134.6 - 158.8	Range	52.99 - 62.52

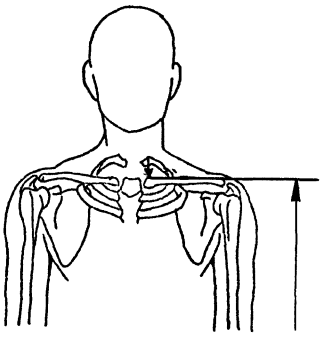

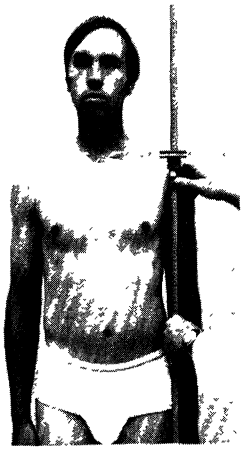

11. BISTERNO-CLAVICULAR DISTANCE

The subject maintains an erect posture, feet together, arms hanging at his side, looking straight ahead. The horizontal distance between the superior medial left and right sterno-clavicular prominences is measured with a sliding caliper.

CM	N=28	IN
4.26	Mean	1.68
0.60	SD	0.24
3.3 - 5.6	Range	1.30 - 2.20

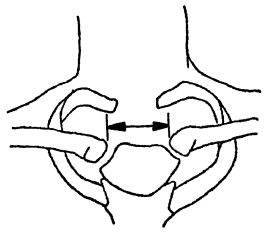

12. SUPRASTERNALE - ACROMION DISTANCE (RIGHT)

The subject maintains an erect posture, feet together, arms hanging at his side, looking straight ahead. The horizontal distance between the superior margin of the jugular notch of the manubrium and the right acromion is measured with an anthropometer.

CM	N=28	IN
20.31	Mean	8.00
1.63	SD	0.64
15.7 - 22.9	Range	6.18 - 9.02

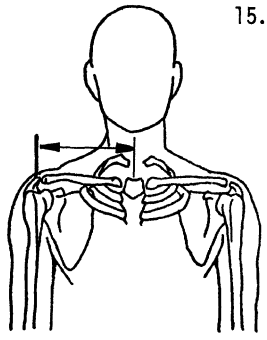

13. RIGHT ACROMION HEIGHT

The subject maintains an erect posture, feet together, arms hanging at his side, looking straight ahead. The vertical distance from the floor to the superior lateral border palpable on the margin of the acromial process of the right scapula is measured with an anthropometer.

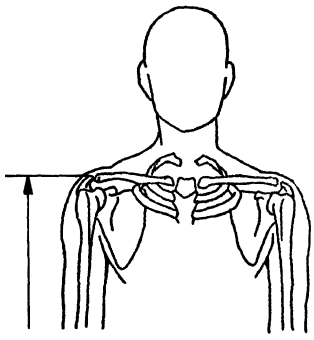

CM	N=28	IN
146.78	Mean	57.79
6.12	SD	2.41
134.6 - 160.4	Range	52.99 - 63.15

14. LEFT ACROMION HEIGHT

The subject maintains an erect posture, feet together, arms hanging at his side, looking straight ahead. The vertical distance from the floor to the superior lateral border palpable on the margin of the acromial process of the left scapula is measured with an anthropometer.

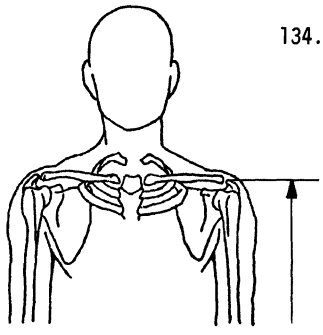

CM	N=28	IN
147.61	Mean	58.11
6.34	SD	2.50
134.6 - 161.5	Range	52.99 - 63.58

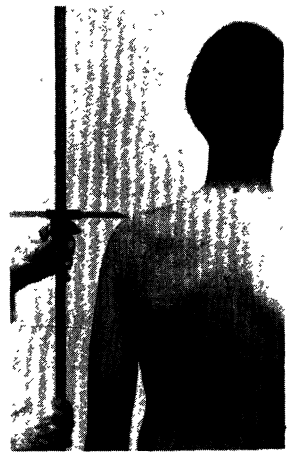

15. BIACROMIAL DIAMETER

The subject maintains an erect posture, feet together, arms hanging at his side, looking straight ahead. The horizontal distance between the superior lateral border of the acromial processes of the left and right scapulae is measured with an anthropometer.

CM	N=28	IN
39.80	Mean	15.67
2.17	SD	0.85
35.6-43.0	Range	14.02-16.93

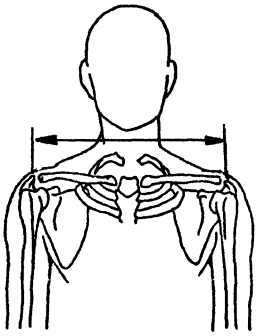

16. RIGHT CLAVICLE LENGTH

The subject maintains an erect posture, feet together, arms hanging at his side, looking straight ahead. The distance from the sternal articular surface of the right clavicle to its acromial extremity is measured with an anthropometer.

CM	N=6	IN
16.03	Mean	6.31
2.46	SD	0.97
13.9 - 20.4	Range	5.47 - 8.03

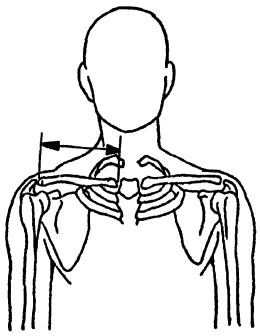

17. NIPPLE HEIGHT

The subject maintains an erect posture, feet together, arms hanging at his side, looking straight ahead. The vertical distance from the floor to the center of the right nipple is measured with an anthropometer.

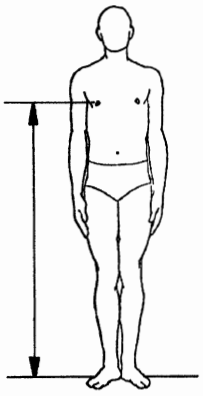

CM	N=28	IN
130.31	Mean	51.30
5.12	SD	2.02
117.9 - 140.0	Range	46.42 - 55.12

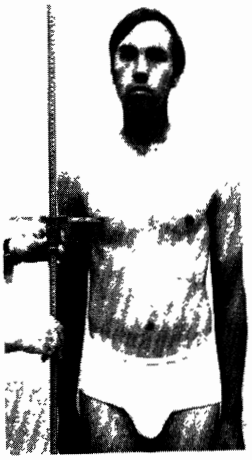

18. OMPHALION HEIGHT

The subject maintains an erect posture, feet together, arms hanging at his side, looking straight ahead. The vertical distance from the floor to the center of the umbilicus is measured with an anthropometer.

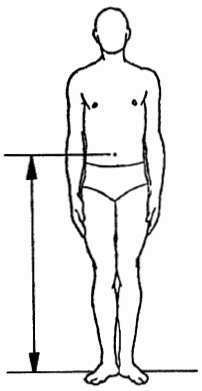

CM	N=28	IN
107.54	Mean	42.34
4.70	SD	1.85
98.8 - 116.3	Range	38.90 - 45.79

19. RIGHT ANTERIOR SUPERIOR ILIAC SPINE

The subject maintains an erect posture, feet together, arms hanging at his side, looking straight ahead. The vertical distance is measured with an anthropometer from the floor to the anterior superior iliac spine of the right ileum.

CM	N=28	IN
102.64	Mean	40.41
4.79	SD	1.89
95.7-114.9	Range	37.68-45.24

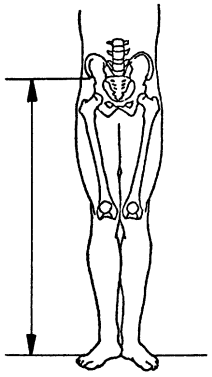

20. LEFT ANTERIOR SUPERIOR ILIAC SPINE

The subject maintains an erect posture, feet together, arms hanging at his side, looking straight ahead. The vertical distance is measured with an anthropometer from the floor to the anterior superior iliac spine of the left ileum.

CM	N=28	IN
102.65	Mean	40.41
4.83	SD	1.90
94.3 - 114.2	Range	37.13 - 44.96

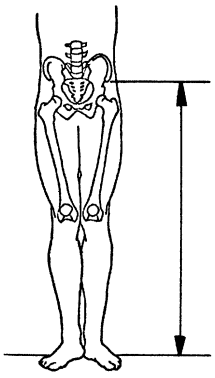

21. ILIOCRISTALE HEIGHT

The subject maintains an erect posture, feet together, arms hanging at his side, looking straight ahead. The vertical distance is measured with an anthropometer from the floor to the most laterally projecting point palpable on the crest of the right ileum.

CM	N=28	IN
108.43	Mean	42.69
4.64	SD	1.83
101.0 - 118.8	Range	39.76 - 46.77

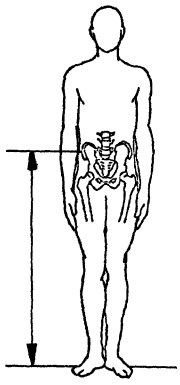

22. BISPINOUS BREADTH

The subject maintains an erect posture, feet together, arms hanging at his side, looking straight ahead. The horizontal distance is measured with an anthropometer between the lateral margins of the anterior superior iliac spines.

CM	N=27	IN
25.94	Mean	10.21
2.76	SD	1.09
22.0 - 32.3	Range	8.66 - 12.72

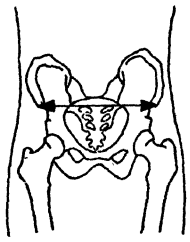

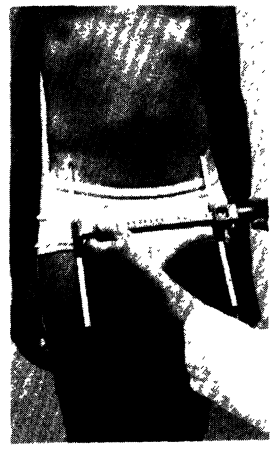

23. RIGHT TROCHANTERIC HEIGHT

The subject maintains an erect posture, feet together, arms hanging at his side, looking straight ahead. The vertical distance is measured with an anthropometer between the floor and the most lateral point palpable on the greater trochanter of the right femur.

CM	N=28	IN
92.24	Mean	36.31
4.55	SD	1.79
84.6 - 102.7	Range	33.31 - 40.43

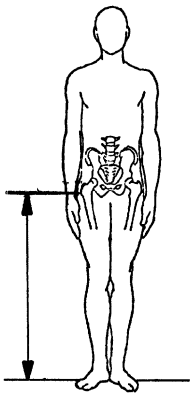

24. LEFT TROCHANTERIC HEIGHT

The subject maintains an erect posture, feet together, arms hanging at his side, looking straight ahead. The vertical distance is measured with an anthropometer between the floor and the most lateral point palpable on the greater trochanter of the left femur.

CM	N=28	IN
92.40	Mean	36.38
4.96	SD	1.95
82.7 - 104.3	Range	32.56 - 41.06

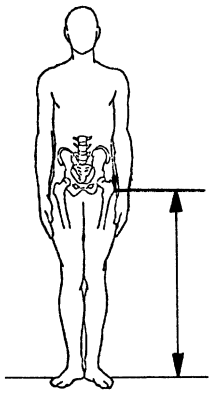

25. HIP BREADTH

The subject maintains an erect posture, feet together, arms hanging at his side, looking straight ahead. Facing the subject, the horizontal distance is measured with an anthropometer between the most lateral point palpable on the greater trochanters of the left and right femora. Firm pressure is applied to the instrument.

CM	N=28	IN
33.83	Mean	13.32
2.31	SD	0.91
29.7 - 38.3	Range	11.69 - 15.08

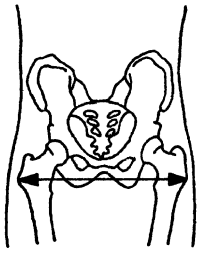

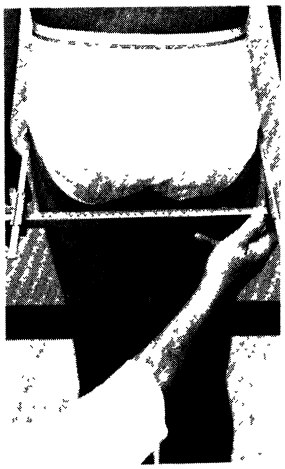

26. HUMERUS BIEPICONDYLAR DIAMETER

The distance between the lateral and medial epicondyles of the right humerus is measured with a sliding caliper with the arm hanging freely at the side.

CM	N=28	IN
7.27	Mean	2.86
0.31	SD	0.12
6.8 - 8.1	Range	2.68 - 3.19

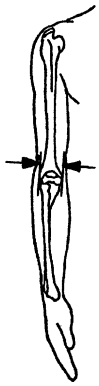

27. ACROMION-RADIALE LENGTH (ELBOW FLEXED 90°)

The subject maintains an erect posture, feet together, looking straight ahead. With the right arm hanging freely at the side, the head of the radius is located by palpation at the center of the skin dimple. The right forearm is flexed 90° so that it is horizontal with the floor. Using an anthropometer, the distance is measured between the right acromion and the head of the radius.

CM	N=28	IN
35.87	Mean	14.12
2.44	SD	0.96
29.6 - 40.2	Range	11.65 - 15.83

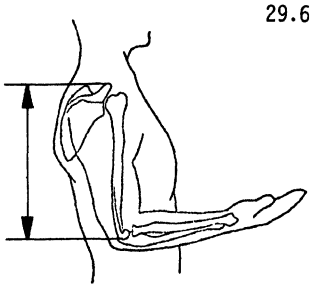

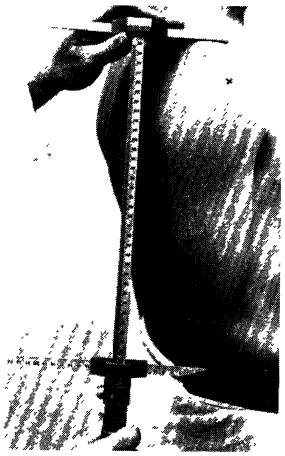

28. HEAD OF HUMERUS TO RADIALE

The subject maintains an erect posture, feet together, looking straight ahead. With the right arm hanging freely at the side, the head of the radius is located by palpation at the center of the skin dimple. The right forearm is flexed 90° so that it is horizontal with the floor. Using an anthropometer the distance is measured from the right radiale to a point corresponding to the center of rotation of the humerus. This point is located 2 inches inferior to the right acromion on the lateral surface of the upper arm.

CM	N=28	IN
31.57	Mean	12.43
2.98	SD	1.17
23.2-38.7	Range	9.13-15.24

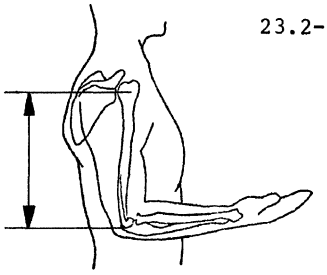

29. RADIUS LENGTH

The subject maintains an erect posture, feet together, looking straight ahead. With the right arm hanging freely at the side, the head of the radius is located by palpation at the center of the skin dimple. The right forearm is flexed 90° so that it is horizontal with the floor and the hand is supinated with the palm up. Using an anthropometer the distance is measured from the head of the radius of the right forearm to the tip of the styloid process.

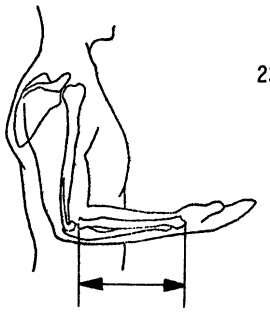

CM	N=28	IN
27.03	Mean	10.64
1.57	SD	0.62
23.6 - 30.0	Range	9.29 - 11.81

30. ULNA LENGTH

The subject maintains an erect posture, feet together, looking straight ahead. The right forearm is flexed 90° so that it is horizontal with the floor, and the hand is supinated with the palm up. Using an anthropometer on the medial aspect of the forearm, the distance is measured between the proximal tip of the olecranon of the ulna to the most distal medial palpable point of the ulna.

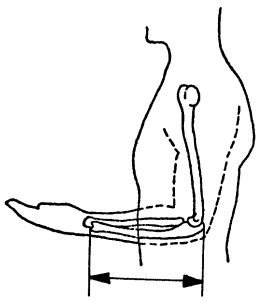

CM	N=28	IN
28.70	Mean	11.30
1.54	SD	0.61
26.0 - 31.4	Range	10.24 - 12.36

31. FOREARM - HAND LENGTH

The subject maintains an erect posture, feet together, looking straight ahead. The right forearm is flexed 90° so that it is horizontal with the floor, with the fingers extended. Using an anthropometer, the distance is measured from the tip of the right elbow (olecranon) to the tip of the longest finger.

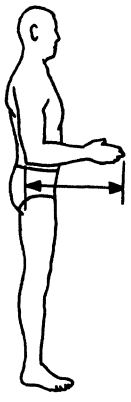

CM	N=28	IN
48.72	Mean	19.18
1.92	SD	0.76
45.4 - 52.9	Range	17.87 - 20.83

32. FOREARM GRIP DISTANCE

The subject maintains an erect posture, feet together, looking straight ahead. The right forearm is flexed 90° so that it is horizontal with the floor, and a pencil is grasped so that it is held perpendicular to the axis of the forearm and is measured with an anthropometer between the tip of the elbow (olecranon) and the center of the axis of the pencil.

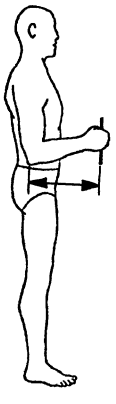

CM	N=28	IN
36.34	Mean	14.31
1.68	SD	0.66
33.4 - 39.6	Range	13.15 - 15.59

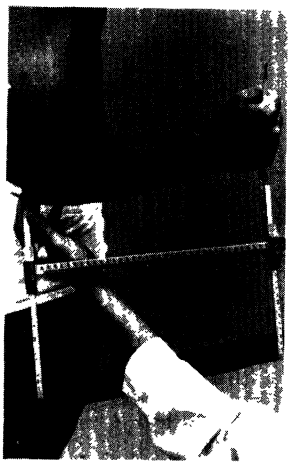

33. WRIST BREADTH (Bone)

The subject's right hand is extended with the palm up and, with a sliding caliper, the maximum diameter of the right wrist is measured from the styloid process of the radius to the styloid process of the ulna. Pressure is applied to measure bone breadth.

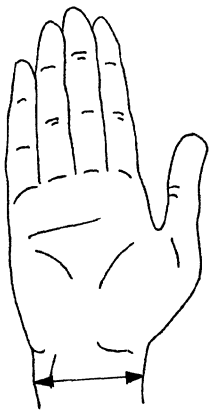

CM	N=28	IN
5.59	Mean	2.20
0.37	SD	0.15
5.0 - 6.4	Range	1.97 - 2.52

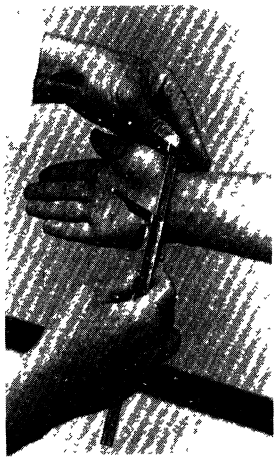

34. HAND LENGTH

The subject's hand is extended with the palm up. The distance from the proximal edge of the navicular bone at the wrist to the tip of the middle finger is measured with a sliding caliper.

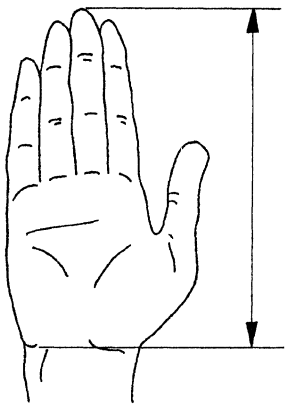

CM	N=28	IN
19.41	Mean	7.64
0.82	SD	0.32
17.7 - 20.7	Range	6.97 - 8.15

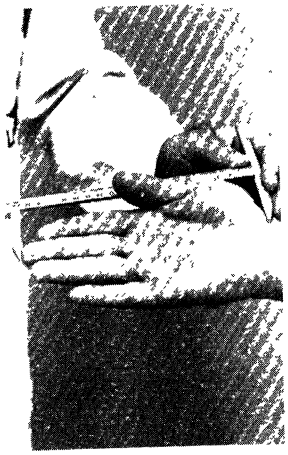

35. TROCHANTER - TO - LATERAL FEMORAL CONDYLE

The subject maintains an erect posture with feet together and weight evenly balanced. The distance is measured with an anthropometer from the most lateral point palpable on the greater trochanter of the right femur to the distal tip of the lateral condyle. To locate the latter point the lateral epicondyle is palpated and pressure is applied distally until the most distal lateral tip is found and marked for measurement.

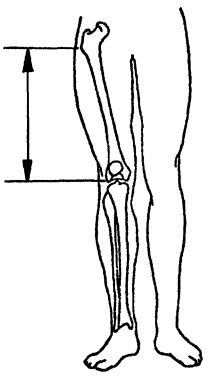

CM	N=27	IN
43.37	Mean	17.07
3.40	SD	1.34
36.1 - 50.5	Range	14.21 - 19.88

36. FIBULA LENGTH

The subject maintains an erect posture with feet together and weight evenly balanced. The vertical distance from the palpable tip of the styloid process of the right fibula to the palpable distal tip of the inferior border of the lateral malleolus is measured with an anthropometer.

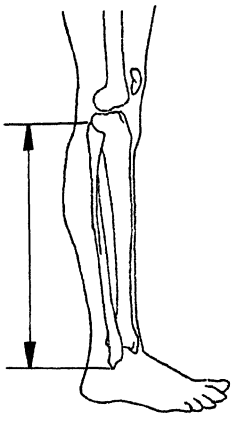

CM	N=28	IN
43.68	Mean	17.20
3.04	SD	1.20
35.0-49.7	Range	13.78-19.57

37. FIBULARE HEIGHT

The subject maintains an erect posture with feet together and weight evenly balanced. With an anthropometer, the vertical distance is measured from the floor to the most lateral projection of the head of the fibula.

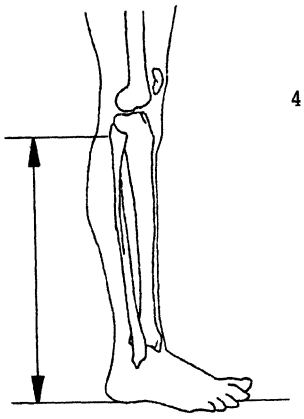

CM	N=28	IN
47.31	Mean	18.63
2.77	SD	1.09
41.9-52.5	Range	16.5-20.67

38. FEMORAL BIEPICONDYLAR DIAMETER

The subject maintains an erect posture with feet spread slightly apart. With an anthropometer, the horizontal distance is measured between the medial and lateral epicondyles of the right femur, applying firm pressure.

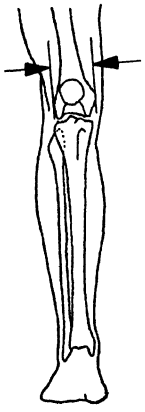

CM	N=28	IN
10.09	Mean	3.97
0.47	SD	0.19
9.0 - 11.1	Range	3.54 - 4.37

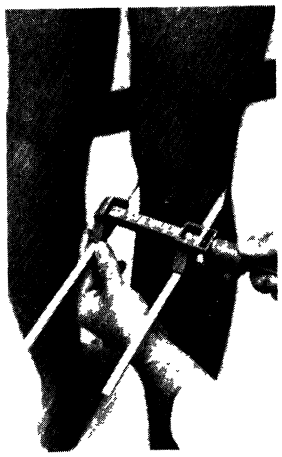

39. MID-PATELLA HEIGHT (Standing)

The subject maintains an erect posture with feet spread slightly apart. With an anthropometer, the distance is measured from the floor to the mid-patella point. This point was previously found and marked by locating the center of the patella with the rectus femoris muscle relaxed, allowing the kneecap to "drop down."

CM	N=28	IN
49.64	Mean	19.54
2.61	SD	1.03
45.8 - 55.7	Range	18.03 - 21.93

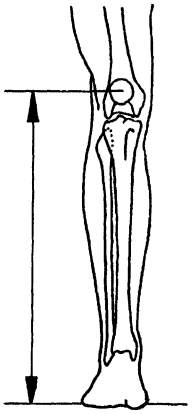

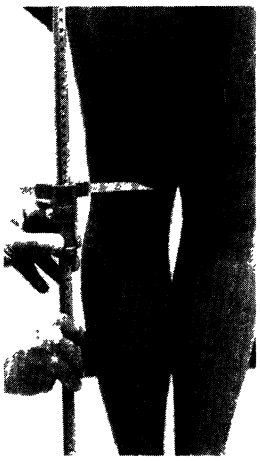

40. TIBIALE HEIGHT (Standing)

The subject maintains an erect posture with feet spread slightly apart. With an anthropometer, the vertical distance is measured from the floor to the superior tip of the medial condyle of the right tibia.

CM	N=28	IN
47.88	Mean	18.85
3.10	SD	1.22
42.2 - 54.7	Range	16.61 - 21.54

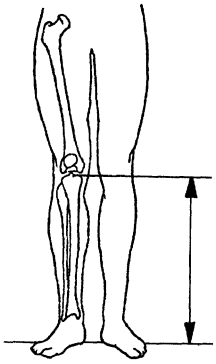

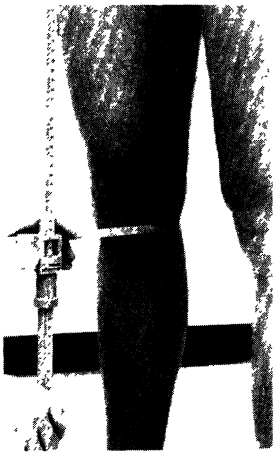

41. LATERAL TIBIAL HEIGHT (Standing)

The subject maintains an erect posture with feet spread slightly apart. Using an anthropometer, the vertical distance is measured from the floor to the superior tip of the lateral condyle of the right tibia.

CM	N=28	IN
48.09	Mean	18.93
3.22	SD	1.27
42.6 - 54.2	Range	16.77 - 21.34

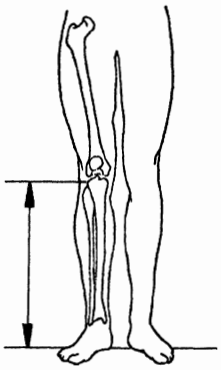

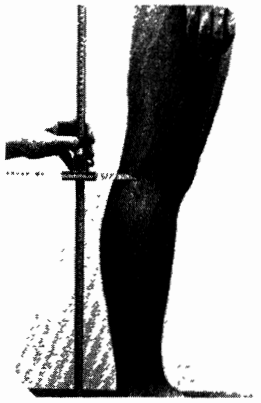

42. MEDIAL MALLEOLUS HEIGHT

The subject maintains an erect posture with feet spread slightly apart. With a foot measuring block, with millimeter scale mounted along the vertical edge, the vertical distance is measured from the floor to the most medial projection of the right medial malleolus.

CM	N=28	IN
8.34	Mean	3.28
1.03	SD	0.41
5.8 - 9.8	Range	2.28 - 3.86

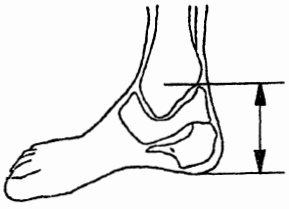

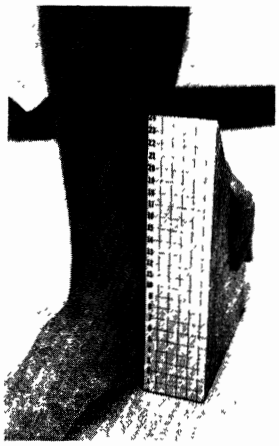

43. LATERAL MALLEOLUS HEIGHT

The subject maintains an erect posture with feet spread slightly apart. With a foot measuring board, with millimeter scale mounted along the vertical edge, the vertical distance is measured from the floor to the most lateral projection of the right lateral malleolus.

CM	N=28	IN
6.70	Mean	2.64
0.77	SD	0.30
5.5 - 7.5	Range	2.17 - 2.95

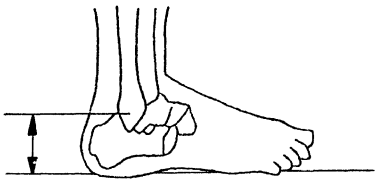

44. RIGHT FOOT LENGTH

The subject maintains an erect posture with feet spread slightly apart and weight equally distributed. With an anthropometer, the distance is measured from the heel to the most distal toe of the right foot.

CM	N=28	IN
26.68	Mean	10.50
1.06	SD	0.42
24.2 - 29.2	Range	9.53 - 11.50

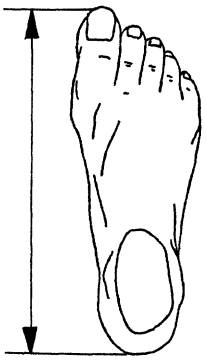

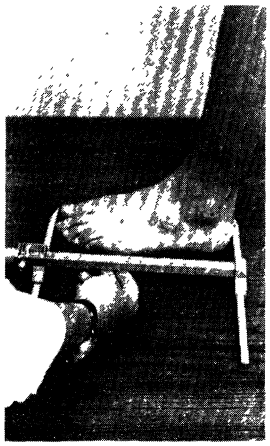

45. LEFT FOOT LENGTH

The subject maintains an erect posture with feet spread slightly apart and weight equally distributed. With an anthropometer, the distance is measured from the heel to the most distal toe of the left foot.

CM	N=15	IN
26.81	Mean	10.56
1.10	SD	0.43
24.6-28.8	Range	9.69-11.34

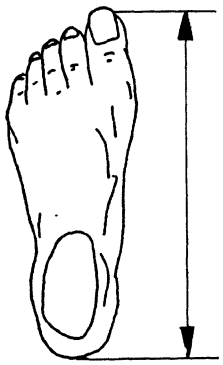

46. HEAD CIRCUMFERENCE

The subject maintains an erect posture with the head held in the Frankfurt Plane. With a steel tape positioned superior to the brow ridges, the maximum circumference of the head is measured.

CM	N=28	IN
57.73	Mean	22.73
1.29	SD	0.51
54.7 - 60.5	Range	21.54 - 23.82

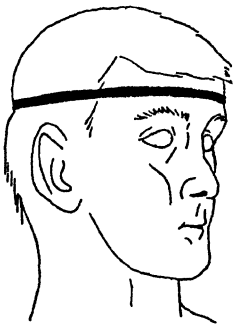

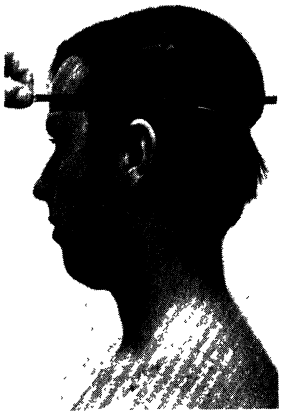

47. CHEST CIRCUMFERENCE

The subject maintains an erect posture and is required to initially raise and then lower both arms to position the tape. The circumference is taken with the tape held horizontal at nipple level, and is measured during normal breathing at maximum inspiration.

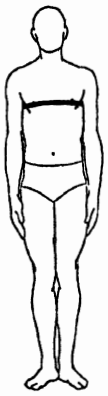

CM	N=28	IN
96.39	Mean	37.95
7.70	SD	3.03
83.0 - 113.5	Range	32.68 - 44.68

48. AXILLARY CHEST CIRCUMFERENCE

The subject maintains an erect posture and is required to initially raise and then lower both arms to allow positioning of the tape in a horizontal plane about the chest at the axillary level during normal breathing at maximum inspiration.

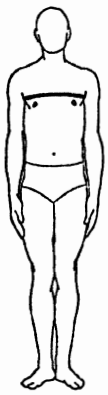

CM	N=21	IN
99.87	Mean	39.32
7.95	SD	3.13
91.1 - 115.7	Range	35.87 - 45.55

49. AXILLARY ARM CIRCUMFERENCE

The subject maintains an erect posture and raises and lowers his right arm to allow horizontal positioning to the tape. The circumference is taken at the axilla level.

CM	N=21	IN
34.38	Mean	13.54
3.56	SD	1.40
28.9 - 41.2	Range	11.38 - 16.22

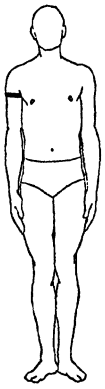

50. BICEPS RELAXED CIRCUMFERENCE (Right)

The subject maintains an erect posture with his arms hanging at the side. The circumference is measured with a steel tape at mid-point between the elbow (distal tip of the olecranon) and shoulder (acromion) of the right arm.

CM	N=27	IN
30.68	Mean	12.08
2.25	SD	0.89
26.4 - 35.0	Range	10.39 - 13.78

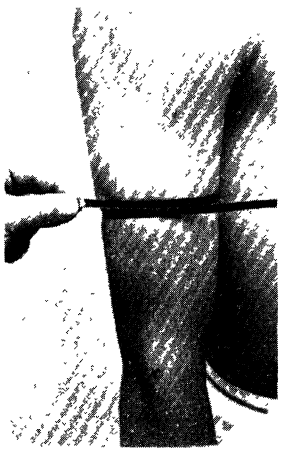

51. BICEPS RELAXED CIRCUMFERENCE (Left)

The subject maintains an erect posture with his arms hanging freely at the side. The circumference is measured with a steel tape at mid-point between the elbow (distal tip of the olecranon) and shoulder (acromion) of the left arm.

CM	N=24	IN
30.78	Mean	12.12
2.66	SD	1.05
26.4 - 36.7	Range	10.39 - 14.45

52. BICEPS FLEXED CIRCUMFERENCE (Right)

The subject maintains an erect posture with his arms hanging freely at the side. The subject flexes his right arm at least 90°, makes a fist while holding his upper arm horizontal to the floor, and flexes his biceps to the maximum. The measurement is made with a steel tape at the maximum circumference of the upper right arm.

CM	N=28	IN
33.53	Mean	13.20
2.68	SD	1.06
28.6 - 39.1	Range	11.26 - 15.39

53. BICEPS FLEXED CIRCUMFERENCE (Left)

The subject maintains an erect posture with his arms hanging freely at the side. The subject flexes his left arm at least 90°, makes a fist while holding his upper arm horizontal to the floor, and flexes his biceps to the maximum. The measurement is made with a steel tape at the maximum circumference of the upper left arm.

CM	N=28	IN
33.10	Mean	13.03
2.46	SD	0.97
29.0 - 38.0	Range	11.42 - 14.96

54. FOREARM CIRCUMFERENCE

The subject maintains an erect posture with his arms hanging freely at the side. Using a steel tape the right forearm is measured at its maximum circumference.

CM	N=28	IN
27.85	Mean	10.96
1.74	SD	0.69
25.5 - 31.9	Range	10.04 - 12.56

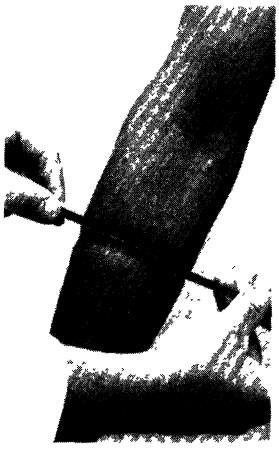

55. WRIST CIRCUMFERENCE

The subject maintains an erect posture with his arms hanging freely at the side. The circumference of the right wrist is measured with a steel tape just proximal of the styloid process of the ulna.

CM	N=28	IN
17.08	Mean	6.72
0.91	SD	0.36
15.5 - 18.7	Range	6.10 - 7.36

56. CALF CIRCUMFERENCE

The subject maintains an erect posture with his weight equally distributed and legs slightly apart. The maximum circumference of the right calf is measured with a steel tape.

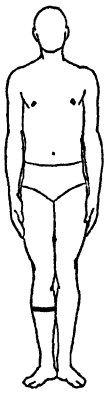

CM	N=28	IN
37.48	Mean	14.76
2.08	SD	0.82
34.2 - 43.3	Range	13.46 - 17.05

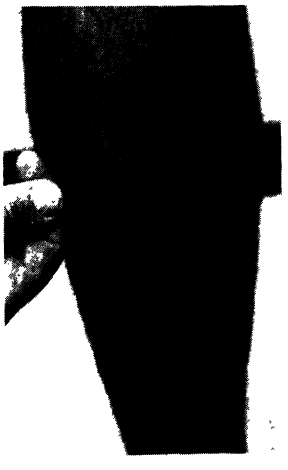

57. ANKLE CIRCUMFERENCE

The subject maintains an erect posture with his weight equally distributed and legs slightly apart. The minimum circumference of the right ankle is taken superior to the lateral malleolus projection.

CM	N=28	IN
23.28	Mean	9.17
1.52	SD	0.60
20.0 - 26.6	Range	7.87 - 10.47

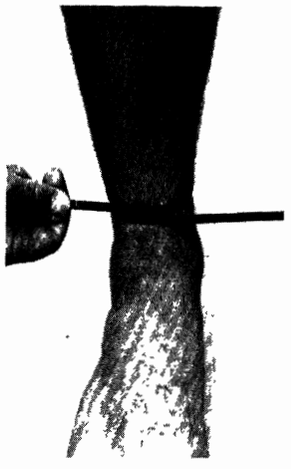

58. SITTING HEIGHT

The subject sits erect and slightly forward from back rest (to allow placement of anthropometer between seat back and subject), with arms resting on upper legs, feet together and lower legs at right angles to upper legs. The head is held in the Frankfurt Plane. The vertical distance is measured with an anthropometer from the sitting surface to vertex with the anthropometer arm firmly touching the scalp.

CM	N=28	IN
93.11	Mean	36.66
2.98	SD	1.17
84.7 - 97.0	Range	33.35 - 38.19

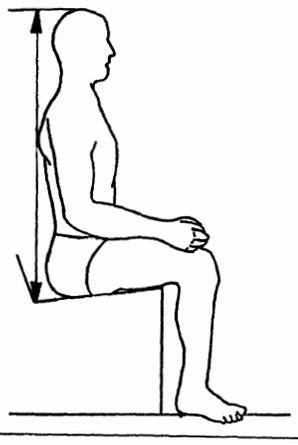

59. SITTING CERVICALE HEIGHT

The subject sits erect and slightly forward from back rest (to allow placement of anthropometer between seat back and subject), with arms resting on upper legs, feet together and lower legs at right angles to upper legs. The head is held in the Frankfurt Plane. The vertical distance is measured with an anthropometer from the sitting surface to the palpable spinous process of the seventh cervical vertebra.

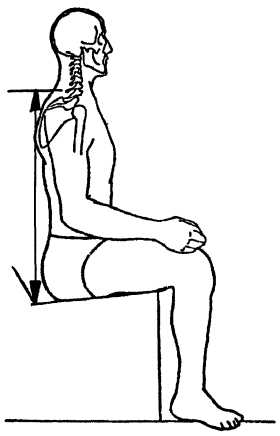

CM	N=28	IN
67.44	Mean	26.55
2.68	SD	1.06
61.7 - 71.8	Range	24.29 - 28.27

60. SITTING SUPRASTERNALE HEIGHT

The subject sits erect with buttocks against seat back, arms resting on upper legs, legs spread slightly, and head held in the Frankfurt Plane. Facing the subject, the vertical distance is measured with an anthropometer from the sitting surface to the superior margin of the jugular notch of the manubrium.

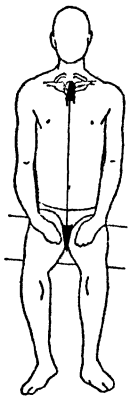

CM	N=28	IN
58.21	Mean	22.92
2.51	SD	0.99
52.5 - 64.1	Range	20.67 - 25.24

61. SITTING SHOULDER (Acromion) HEIGHT

The subject sits erect with buttocks against seat back, arms resting on upper legs, and head held in the Frankfurt Plane. The vertical distance is measured with an anthropometer from the sitting surface to right acromion.

CM	N=28	IN
60.67	Mean	23.89
3.41	SD	1.34
53.4 - 66.0	Range	21.02 - 25.98

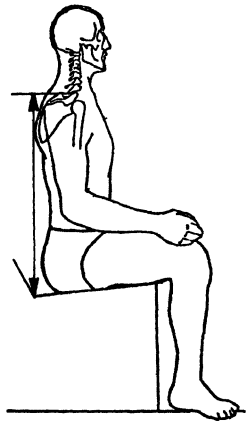

62. BUTTOCK-KNEE LENGTH

The subject sits erect with buttocks slightly forward from the seat back, arms resting on upper legs, and lower legs at a 90° angle to upper legs. The horizontal distance is measured with an anthropometer from the right buttock to the most anterior aspect of the right kneecap.

CM	N=27	IN
60.92	Mean	23.98
3.10	SD	1.22
55.1-67.6	Range	21.69-26.61

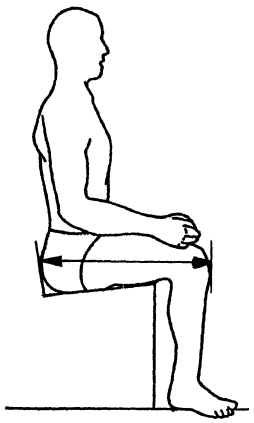

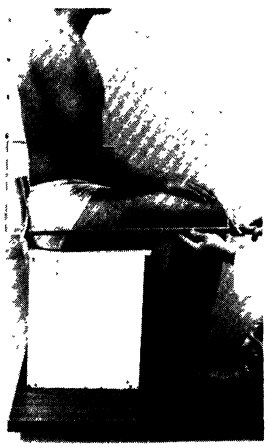

63. SITTING KNEE HEIGHT

The subject sits erect with buttocks against the seat back, arms resting on upper legs, and lower legs together and at a 90° angle to upper legs. The vertical distance is measured with an anthropometer from the floor to the superior point of the patella.

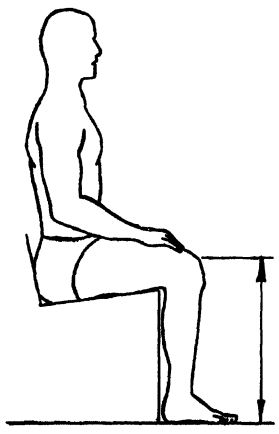

CM	N=28	IN
55.86	Mean	21.99
2.96	SD	1.17
48.8-62.8	Range	19.21-24.72

64. SITTING KNEE HEIGHT (Maximal Clearance)

The subject sits erect with buttocks against the seat back, arms resting on upper legs, and lower legs together and at a 90° angle to upper legs. The vertical distance is measured with an anthropometer from the floor to the highest point of the right knee. This point will be superior to the preceding measurement and provides maximum knee clearance distance.

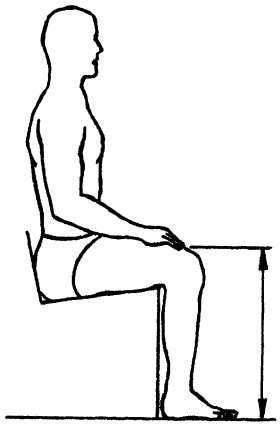

CM	N=23	IN
56.88	Mean	22.39
2.72	SD	1.07
52.8 - 63.3	Range	20.79 - 24.92

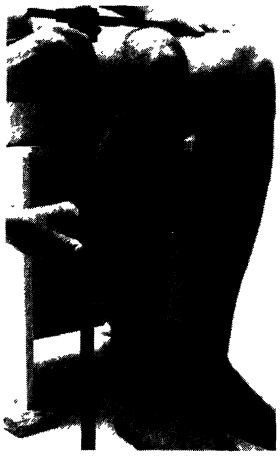

65. SEAT BACK - TO - TROCHANTER (ERECT)

The subject sits erect with buttocks against the seat back, arms resting on upper legs, and lower legs together and at a 90° angle to upper legs. The horizontal distance is measured with an anthropometer from the surface mark previously locating the trochanter while the subject was standing erect, to the anterior edge of the seat back. The seat back angle is 13° back from the vertical and the seat pan angle is 6° up from the horizontal.

CM	N=28	IN
15.13	Mean	5.96
2.20	SD	0.87
11.1 - 20.3	Range	4.37 - 7.99

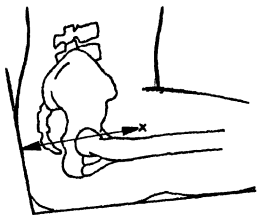

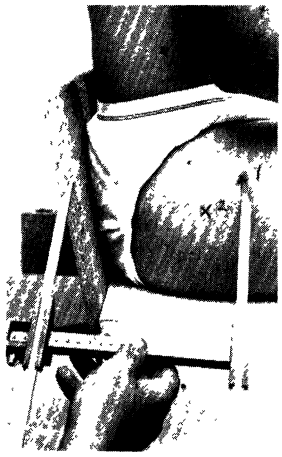

66. SEAT BACK - TO - TROCHANTER (SEATED)

The subject sits erect with buttocks against the seat back, arms resting on upper legs, and lower legs together and at a 90° angle to upper legs. The horizontal distance is measured with an anthropometer from the trochanter mark, located while the subject is seated, to the anterior edge of the seat back. The seat back angle is 13° back from the vertical and the seat pan angle is 6° up from the horizontal.

CM	N=27	IN
14.06	Mean	5.54
1.67	SD	0.66
11.1 - 19.0	Range	4.37 - 7.48

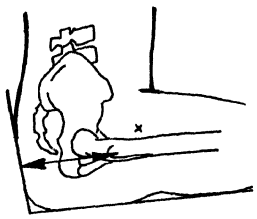

67. SEAT SURFACE - TO - TROCHANTER (ERECT)

The subject sits erect with buttocks against the seat back, arms resting on upper legs, and lower legs together and at a 90° angle to upper legs. The vertical distance is measured with an anthropometer from the surface mark previously locating the trochanter while the subject was standing erect, to the superior surface of the seat. The seat back angel is 13° back from the vertical and the seat pan angle is 6° up from the horizontal.

CM	N=28	IN
11.16	Mean	4.40
1.66	SD	0.65
8.0 - 15.0	Range	3.15 - 5.91

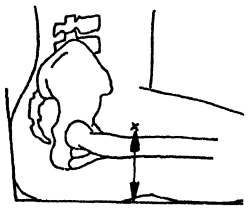

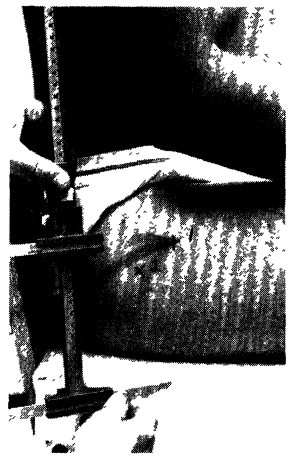

68. SEAT SURFACE - TO - TROCHANTER (SEATED)

The subject sits erect with buttocks against the seat back, arms resting on upper legs, and lower legs together and at a 90° angle to the upper legs. The vertical distance is measured with an anthropometer from the trochanter mark, located while the subject is seated, to the superior surface of the seat. The seat back angle is 13° back from the vertical and the seat pan angle is 6° up from the horizontal.

CM	N=27	IN
8.84	Mean	3.48
1.27	SD	0.50
5.7 - 11.3	Range	2.24 - 4.45

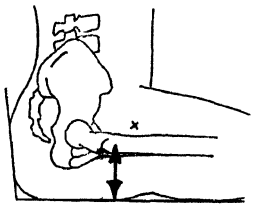

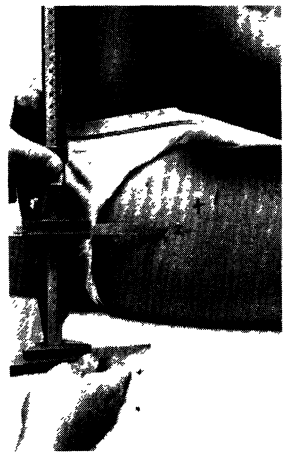

D. Skinfold Measurements:

69. RIGHT TRICEPS SKINFOLD

The point of measurement is located on the dorsal aspect of the right arm of the standing subject, midway between the acromion and tip of the elbow (olecranon) when the forearm is flexed at 90°. The subjects arm is then extended to hang freely, the skinfold is lifted parallel to the long axis of the arm by firmly grasping a fold between the thumb and forefinger about 1 centimeter from the point to which the Lange caliper is applied. A reading is made within 3 seconds after application of the caliper, and the average is taken of several readings.

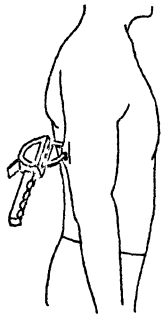

N=28

Mean 7.31 mm

SD 4.94 mm

Range 2.5-19.0 mm

70. RIGHT SUBSCAPULAR SKINFOLD

This site is located on the standing subject below the inferior angle of the right scapula. The skinfold is lifted in a direction parallel to the ribs, with the skinfold angled upward medially and downward laterally at about 45 degrees from the horizontal. A reading is made with the Lange caliper within 3 seconds after application of the caliper, and the average is taken of several readings.

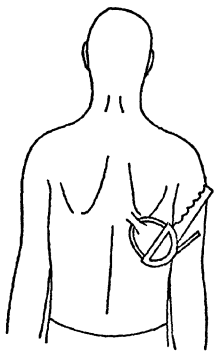

N=28

Mean 10.86 mm

SD 5.33 mm

Range 6.0-23.0 mm

71. RIGHT SUPRAILIAC SKINFOLD

This site is located on the standing subject superior to the lateral aspect of the iliac crest on the right side. The skinfold is lifted parallel to the pelvis and angled slightly upward medially. A reading is made with the Lange caliper within 3 seconds after application of the caliper, and the average is taken of several readings.

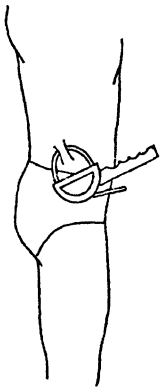

N=28

Mean 14.66 mm

SD 10.18 mm

Range 3.0-38.0 mm

72. RIGHT POSTERIOR MID-CALF

This site is located on the standing subject half way between the popliteal and alteral malleolus of the dorsal aspect of the lower leg, midway between the ankle and knee. The skinfold is lifted parallel to the leg, and a tight skin adhesion is most commonly found here. A reading is made with the Lange caliper within 3 seconds after application of the caliper, and the average is taken of several readings.

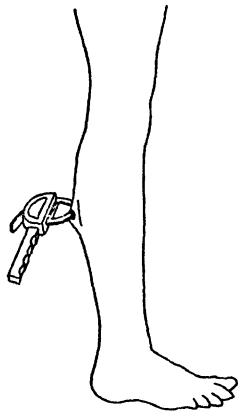

N=28

Mean 13.46 mm

SD 13.18 mm

Range 3.0-51.0 mm

APPENDIX E

Somatotype computations for each subject in 1/2 intervals on a scale from 1/2 to 9.

SUBJECT NUMBER	COMPONENT 1 ENDOMORPHY	2 MESOMORPHY	3 ECTOMORPHY
1.	3.5	6.5	1.0
2.	6.0	5.5	1.5
3.	6.0	6.0	0.5
4.	1.5	7.0	2.5
5.	4.0	4.5	2.5
6.	2.0	5.0	2.5
7.	1.5	6.5	1.5
8.	1.5	6.0	2.0
9.	2.5	7.0	1.0
10.	1.0	7.5	1.5
11.	3.0	5.0	2.5
12.	3.0	5.0	2.5
13.	3.5	5.0	2.0
14.	6.0	5.5	1.0
15.	1.0	3.5	4.0
16.	2.5	6.5	2.0
17.	1.5	4.5	3.5
18.	2.5	5.0	2.0
19.	3.5	7.0	1.0
20.	2.5	5.0	3.5
21.	1.0	2.5	5.0
22.	1.5	4.5	3.0
23.	5.0	5.5	1.0
24.	6.0	5.5	1.5
25.	6.0	6.0	1.5
26.	1.0	5.5	1.5
27.	4.0	5.5	1.5
28.	6.5	5.5	0.5

Somatype Ratings (Assement based upon measurements taken at the above four sites on each subject and calculated after Heath-Carter technique)

1. Endomorphy (relative fatness)
   N = 28
   Mean = 3.2
   Standard Deviation = 1.85
   Range = 1.0 - 6.0

2. Mesomorphy (relative musculo-skeletal development)
   N = 28
   Mean = 5.5
   Standard deviation = 1.09
   Range = 2.5 - 7.5

3. Ectomorphy (relative linearity)
   N = 28
   Mean = 2.0
   Standard deviation = 1.07
   Range = 0.5 - 5.0

Subject raw data from which somatotype for each individual was calculated by Heath-Carter Technique.

	MEASUREMENTS									
SUBJECT NO.	STATURE	WEIGHT	HUMERUS BIEPICONDYLAR DIAMETER	FEMORAL BIEPICONDYLAR DIAMETER	BICEPS CIRC. (FLEXED)	CALF CIRC.	RT. TRICEPS SKINFOLD	RT. SCAPULAR SKINFOLD	RT. SUPRAILIAC SKINFOLD	RT. CALF SKINFOLD
1.	163.5	149	7.3	9.5	30.5	34.2	10.0	10.0	12.0	6.0
2.	180.7	185.5	7.6	10.0	34.2	41.6	17.0	16.0	31.0	45.0
3.	179.0	215	7.4	10.2	36.5	38.7	13.0	23.0	24.0	34.0
4.	168.0	138.5	7.5	9.5	34.0	35.0	3.0	6.5	6.0	7.0
5.	176.5	160.0	7.1	10.0	32.0	35.1	10.0	12.5	16.5	16.0
6.	173.0	149.0	6.8	9.7	30.6	36.8	4.0	8.0	7.0	8.0
7.	171.5	163.5	7.4	10.0	33.2	35.8	2.5	7.0	8.0	4.0
8.	172.8	154.0	7.0	9.8	35.1	36.2	3.5	7.0	6.5	4.0
9.	172.9	171.0	7.6	10.8	34.3	38.5	4.0	7.0	12.0	8.0
10.	172.8	165.5	7.4	11.1	33.3	38.6	3.0	6.0	4.0	3.0
11.	176.0	154.5	6.8	10.1	32.4	35.5	8.0	11.0	12.0	6.0
12.	178.5	165.0	7.1	9.9	32.0	38.6	7.0	8.0	13.0	18.0
13.	177.5	169.5	6.9	10.3	32.5	36.1	6.0	8.0	20.0	11.0
14.	186.5	215.0	7.7	10.4	37.5	37.5	15.0	20.0	27.0	27.0
15.	178.8	145.0	7.0	9.0	29.0	34.8	3.0	7.0	4.0	3.5
16.	175.6	160.0	7.3	10.1	33.3	37.7	6.0	7.0	12.0	8.0
17.	181.6	155.5	6.8	9.8	33.5	37.5	3.5	7.0	5.0	6.0
18.	183.5	182.0	7.5	10.1	30.8	38.3	5.0	7.0	11.0	3.0
19.	181.3	196.5	7.6	10.7	37.3	39.4	2.5	10.0	20.0	5.0
20.	182.2	158.0	7.2	10.2	30.8	38.7	4.0	10.0	11.0	8.0
21.	185.0	146.5	7.2	9.7	31.5	35.3	2.5	6.0	3.0	4.0
22.	186.2	177.0	7.5	10.2	31.6	35.7	5.0	6.0	6.0	4.0
23.	185.5	221.0	7.2	10.9	37.0	38.9	19.0	16.0	17.0	25.0
24.	191.4	223.0	7.2	10.4	37.3	39.2	14.0	18.0	38.0	18.0
25.	189.7	215.5	8.1	10.7	39.1	38.2	14.0	22.0	28.0	31.0
26.	175.9	169.0	7.2	10.0	33.0	37.8	2.5	6.0	3.5	3.5
27.	197.0	210.5	7.9	10.5	33.2	42.3	3.0	7.0	11.5	6.0
28.	170.5	155.0	7.0	9.5	31.5	36.4	7.0	14.0	15.0	10.0
29.	180.3	230.0	7.1	9.9	36.5	43.3	10.0	18.0	38.0	51.0

SOMATOTYPE DATA FORM

Subject No._____ Name_____

Date_____

		MILLIMETERS	
1.	Weight_____(lbs)_____(kg)		
2.	Stature_____		(____inches)
3.	Humerus biepicondylar diameter_____		
4.	Femoral biepicondylar diameter_____		
5.	Rt. biceps circ. (relaxed, extended)_____		
6.	Rt. biceps circ. (flexed arm girth)_____		
7.	Calf circumference_____		
8.	Skinfolds: Rt. triceps_____		
9.	Rt. Subscapular_____		
10.	Rt. Suprailiac_____		
11.	Rt. Calf_____		
12.	Heath-Carter Somatotype_____		

APPENDIX F

ORTHOGONAL PHOTOGRAMMETRY[1]

Presented as part of the
Second Quarter Report for
Contract F33615-70-C-1777

Entitled:

Human Torso Link System

December, 1970

[1]The description presented in this appendix is part of a Ph.D. Dissertation now being completed by Mr. Frederick Schanne, Research Assistant in the Industrial Human Performance Research Group at The University of Michigan.

APPENDIX F

Orthogonal Photogrammetry

It is the purpose of this Appendix to provide a brief description of the technique of andrometry. The primary reference for this section is J. W. Chaffee, Andrometry: A Practical Application of Coordinate Anthropometry in Human Engineering, ASTIA Document No. 256344, April 1961.

Theory of Andrometry

Basically andrometry is a technique employing two or more orthogonal cameras each of which views the same subject and takes a photograph simultaneously. The reason that a minimum of two cameras are employed is to do away with the problem of optical parallax (linear perspective). For example, if only one camera is used and a ruler is placed next to the subject and a photograph taken, errors result. This is due to the fact that part of his body will be closer to the camera than the ruler and hence will appear larger than true size, while part of his body will lie behind the ruler and hence will appear smaller than true size. As can be readily seen in Figure AI-1, although lines y_1z_1, y_2z_2, y_3z_3 are of equal length, their representation on the film of the single camera indicates the length of y_3z_3 to be greater than y_2z_2 which also appears larger than y_1z_1, ($y_3'z_3'$, $y_2'z_2'$, $y_1'z_1'$ on the film plane). Since this error is not always small enough to ignore, the technique of additional perpendicular cameras must be employed.

Figure AI-2 depicts a photographic set-up employing two cameras, one on the x-axis and one on the y-axis. Utilizing the concepts of plane geometry it is possible to find the x and y coordinates of point P in relation to the origin, Q, from measurements taken on the focal length of the camera, lens to origin distance, and object "height" on the film. The values x and y (See Figure AI-2) are found as follows (note: x', f_y, y', f_x, d_x, d_y, are all known):

By similar triangles, we know

$$\frac{y'}{f_x} = \frac{y}{d_x - x} \quad \text{and} \quad \frac{x'}{f_y} = \frac{x}{d_y - y}$$

solving these two equations simultaneously we find:

FIGURE AI-1*
SCHEMATIC DIAGRAM OF ERROR INDUCED BY
SINGLE CAMERA PHOTOGRAPHIC TECHNIQUE

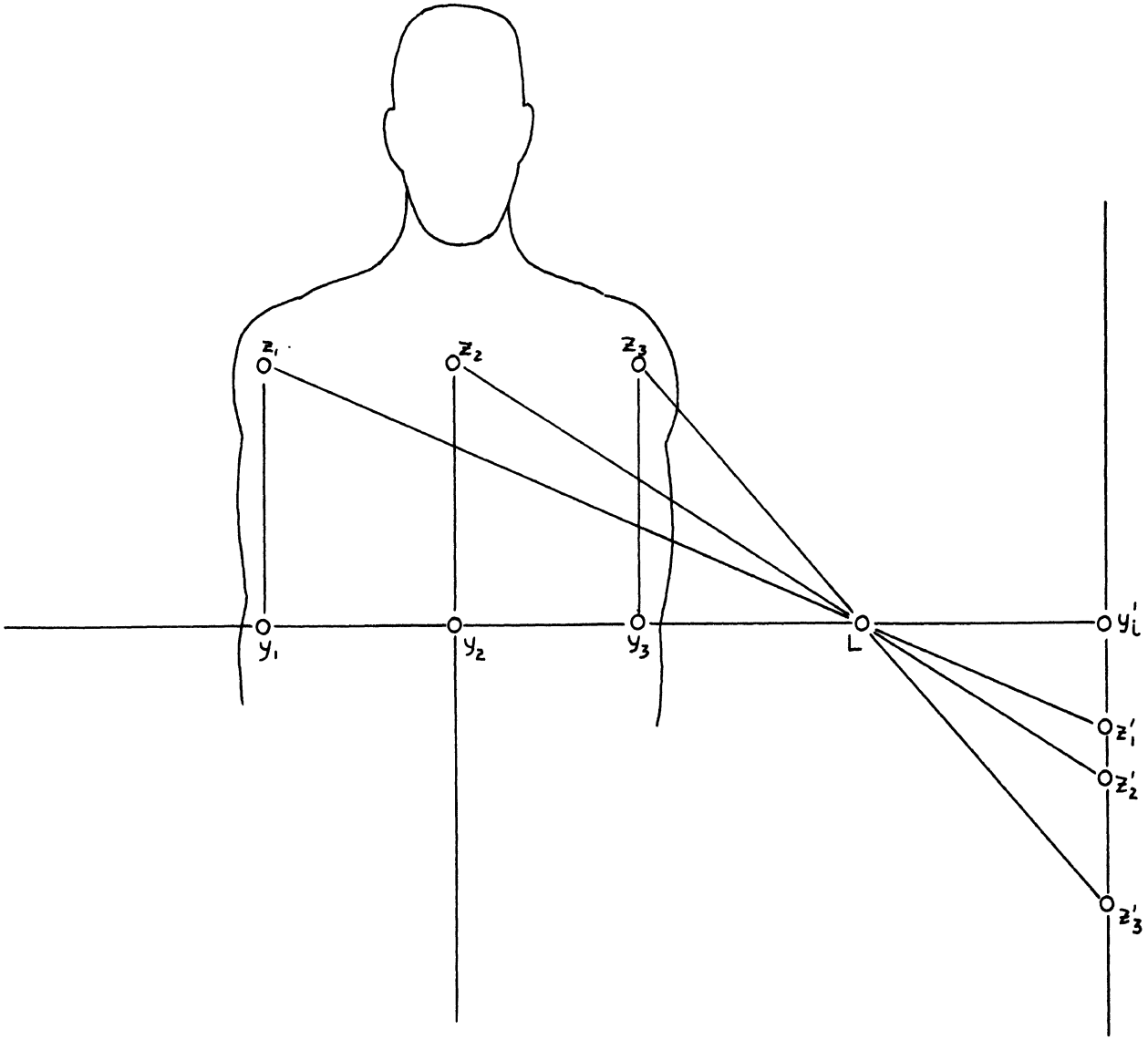

Where:

L=Lens of Camera

Lines Y_1Z_1, Y_2Z_2, Y_3Z_3 are of equal length

*Figure adapted from Chaffee

FIGURE AI-2
SCHEMATIC OF TWO ORTHOGONAL CAMERA LAYOUT

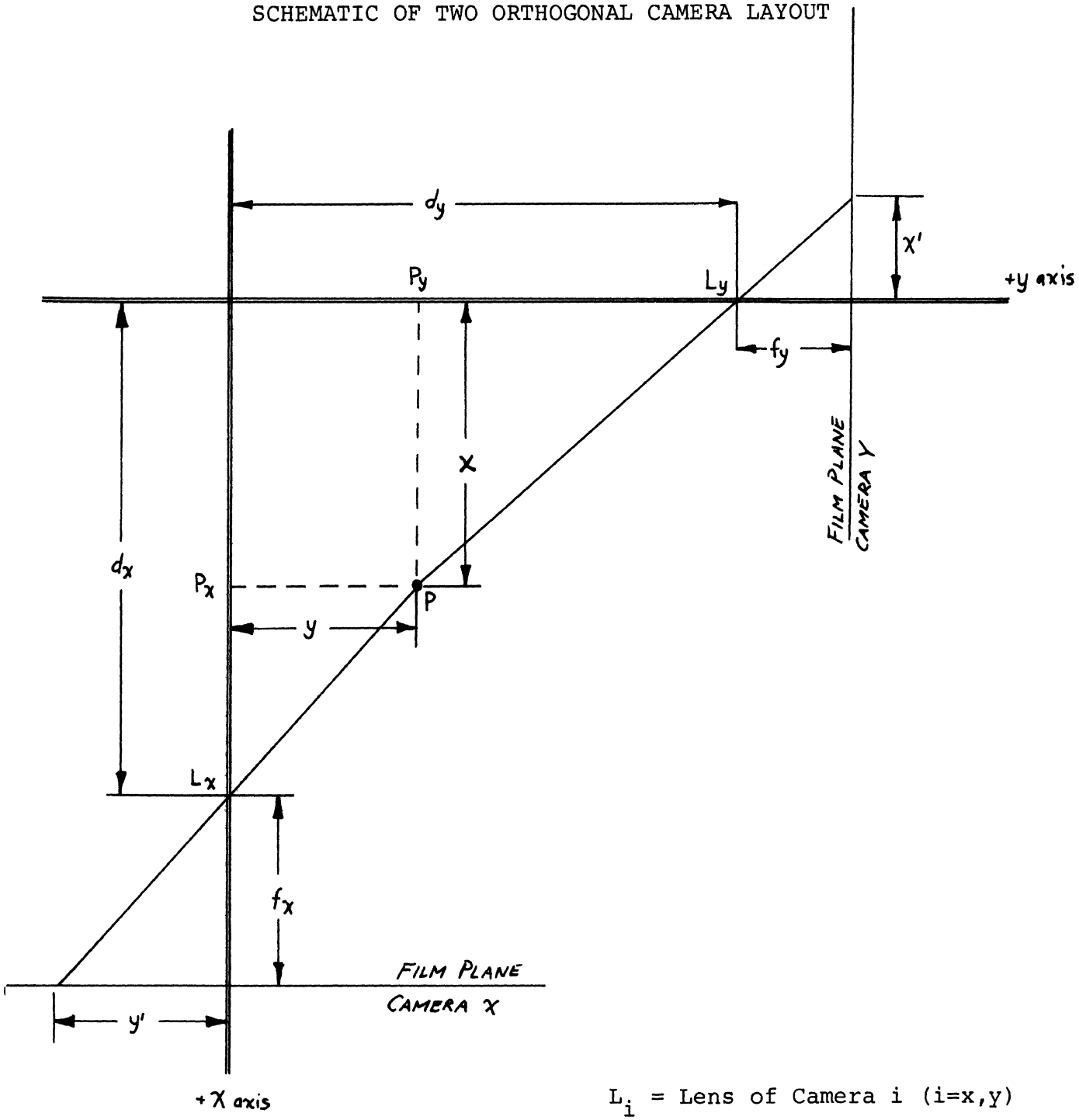

L_i = Lens of Camera i (i=x,y)
f_i = Focal length of Camera i

$$y = \frac{y'(d_x - x)}{f_x} \qquad x = \frac{x'(d_y - y)}{f_y}$$

$$y = y'/f_x \left(dx - \frac{x'(d_y - y)}{f_y} \right) = \frac{y'd_x}{f_x} - \frac{y'x'd_y}{f_x f_y} + \frac{y'yx'}{f_x f_y}$$

$$y \left(1 - \frac{y'x'}{f_x f_y} \right) = \frac{y'(f_y d_x - x'd_y)}{f_x f_y}$$

$$y(f_x f_y - y'x') = y'f_y d_x - y'x'd_y$$

$$y = y' \left[\frac{f_y d_x - x'd_y}{f_x f_y - y'x'} \right]$$

Similarly

$$x = x' \left[\frac{f_x d_y - y'd_x}{f_x f_y - y'x'} \right]$$

The z coordinate of point P can be obtained in a similar manner from the x and y cameras (see Figure AI-3) or by placing a third camera above the origin and proceeding as above using either the x or y camera data in addition to that of the z camera.

To obtain the z coordinate of point P from the data of the x and y cameras alone we proceed as follows:

Let z_x = estimate of z coordinate from camera x

z_y = estimate of z coordinate from camera y

Employing a similar triangle methodology as above , we find

$$z_x = z'_x \left[\frac{f_y d_x - x'd_y}{f_x f_y - x'y'} \right]$$

or

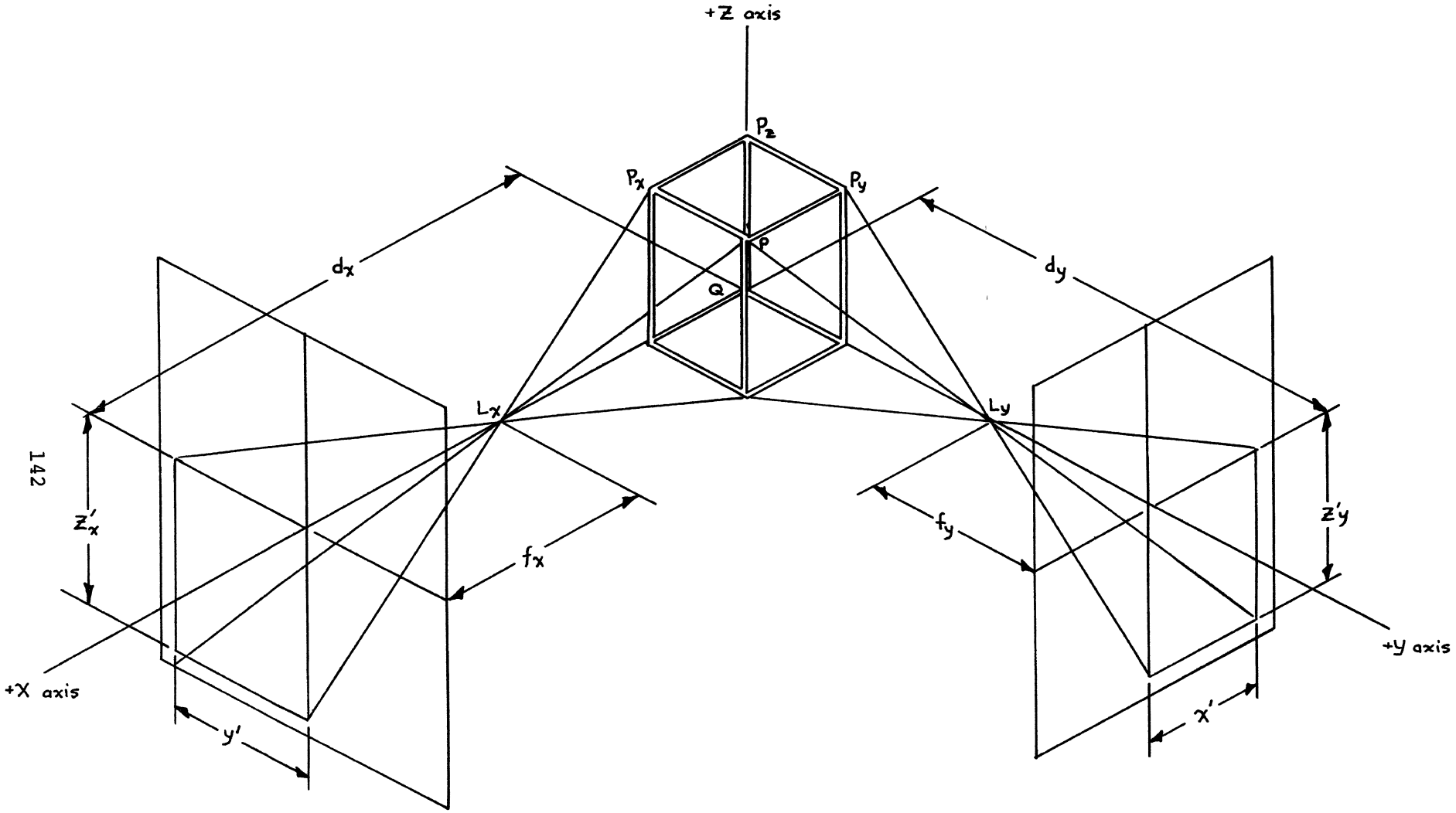

FIGURE AI-3
SCHEMATIC OF Z-COORDINATE CALCULATION GEOMETRY

$$z_y = z'_y \frac{f_x d_y - y' d_x}{f_x f_y - x' y'}$$

Since only a view of the point in two of the cameras is needed to predict the coordinates of the point in three-space, it becomes readily apparent that a z camera (third camera) must serve a function other than for determination of the z coordinate. A z-camera, or any additional orthogonal camera, is utilized to insure that the subject's own body configuration does not obscure any point of interest. For this project, because so many different body surface markers are present, a third and fourth camera insures that each point is visible in at least two of the four views.

Using this method Chaffee has found that over 90% of the coordinates estimated via this procedure are within 0.12 inch of the actual value. Hence the results are quite accurate. Precision (standard deviation of estimated values) was found to be 0.036 inch, by actual tests of our system.

Determination of Focal Lengths of Cameras

To determine the focal length of any one of the cameras the procedure employed is relatively simple. Referring to Figure AI-4, the reader can readily see how easily the geometry of the situation lends itself to computation of the focal length if the original object height, x, projected object height, x', and distance from object of film plane, d, are known. Hence:

$$\frac{f_x}{x'} = \frac{d - f_x}{x}$$

or

$$f_x = \frac{x'(d - f_x)}{x}$$

$$f_x(x + x') = dx'$$

$$f_x = \frac{dx'}{x + x}$$

Data Collection

It should be apparent to the reader that direct measurement

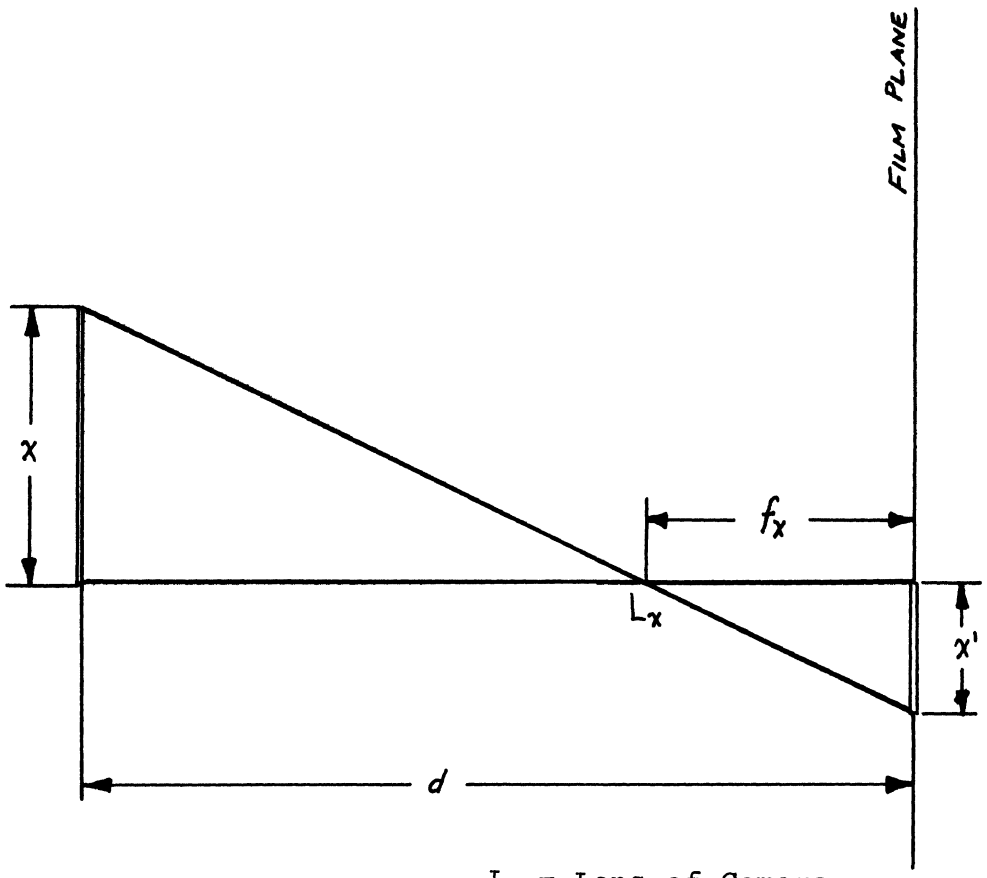

L_X = Lens of Camera

FIGURE A1-4
SCHEMATIC FOR DETERMINATION OF FOCAL LENGTH, f_x

of the various distances represented on the film itself is a laborious, time-consuming task. Because of this, another, more feasible, method of data collection from the film had to be developed.

Data Reduction

Figure AI-5 presents a general flow chart of the data collection technique employed.

Data Coder Coordinates

As shown, the data are first recorded on the films of the four orthogonal cameras. Each film is then projected on to the Bolt Beranek and Newman Data Coder screen and the various articulation surface markers on the body are recorded by moving a hairline cursor over the desired point, inputting this point in grey code to either a Hewlett-Packard 2115A Digital Computer or directly to a paper punch tape which is then punched in decimal form on a paper tape. Figure AI-6 is a schematic of the actual physical setup for this part of the data reduction.

Conversion of Data Coder Coordinates to Actual Dimensions

The data coder coordinates are in terms of divisions from the data coder origin. A simple conversion factor in the form of a ratio (inches per data coder division) is multiplied times the data coder coordinates to obtain values for the actual distances on the negatives. The only difference being that instead of measuring the negatives directly, the data are obtained in an indirect manner.

Computation of Three-Space Coordinates

The three-space coordinates are then computed on the 360/67 IBM computer by a program originally written by a staff researcher, Dr. Kerry Kilpatrick, and modified by another researcher, Mr. Fred Schanne, to take the misalignment roll into consideration.

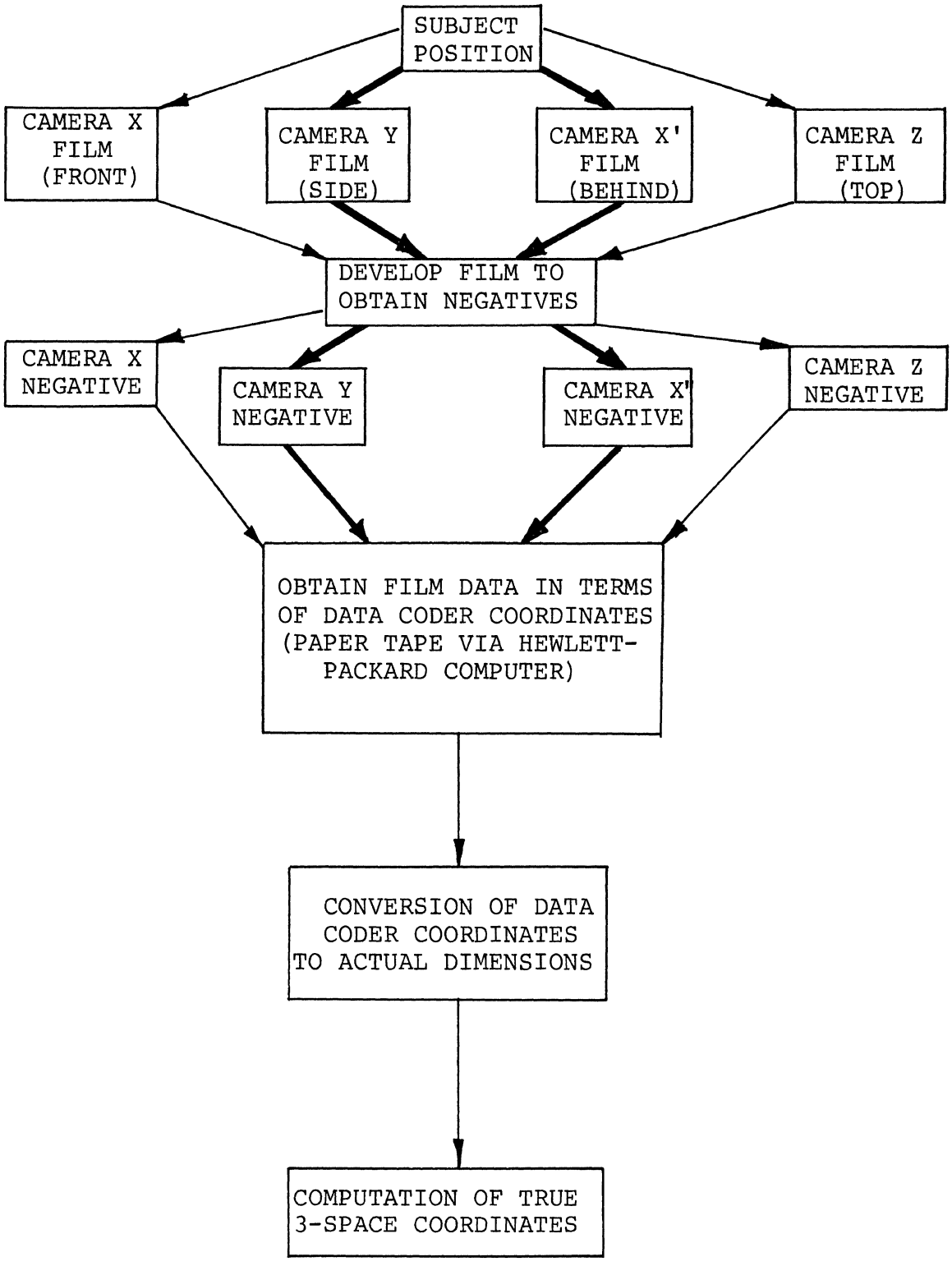

FIGURE AI-5
FLOW CHART OF DATA COLLECTION TECHNIQUES

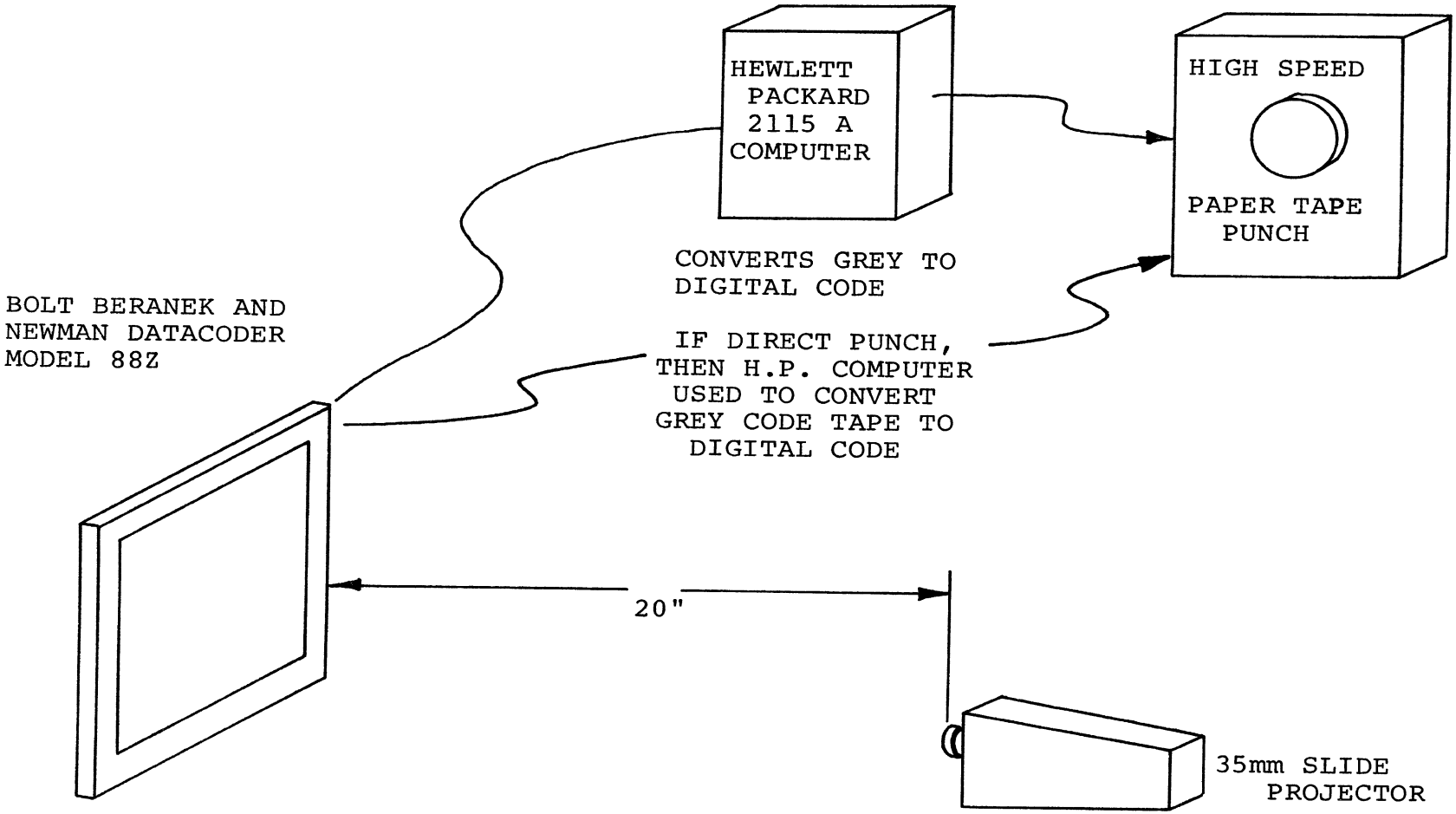

FIGURE AI-6
SCHEMATIC OF DATACODER SETUP

P A R T I I I

SURFACE MARKER MOVEMENT AND RADIOGRAPHIC RESULTS OF SKELETAL MOBILITY

APPENDIX G

TABLES OF PREDICTION EQUATION COEFFICIENTS

The following tables contain the least-squared error coefficients for the variables that significantly contributed to the prediction accuracy of each surface marker location. If a variable does not have a coefficient listed in one of the columns, it means that it did not significantly affect the surface marker data in that particular X, Y, or Z coordinates. Note: All coordinate predictions are relative to the L_5 surface marker. Each surface marker has four sets of prediction equations presented on two pages:

Seated - General Model
Seated - Anthropometric Model
Standing - General Model
Standing - Anthropometric Model

The actual derivation of the equations was performed by using step-wise regression. An important trade-off is involved in deciding at which step to terminate the sequential regression procedure. If the sequential inclusion of variables is halted prematurally, the resulting equations will not account for many of the localized, but important, idiosyncrasies of the response surface. Conversely, if the accumulation of variables is not curtailed soon enough, the prediction equations will over-specify the true relationship between the dependent and independent variables. The empirical equations will begin to accommodate pure random variations in the data. Over fitting will usually cause the prediction equations to become completely erroneous outside the range of the data. Extrapolation becomes impossible. In fact, sharp discontinuities may be created for segments inside the data sphere over which no data was recorded.

The decision as to when to halt the step-wise regression was made on the basis of the values of R^2, the coefficient of determination, and T, the standard error of estimation. As stated in the text, critical values on the order of $*R^2$ equal to .7 and *T equal to 1.5 inches were used. The value of R^2 specifies the percentage of the variability explained by the regression equation. The inclusion of variables was halted when the percentage of the variability accounted for by the equations exceeded $*R^2$ (usually set at 70%). Similarly, the iterative regression procedure was terminated when the standard error of estimation fell below *T. It is futile or erroneous to continue to add terms if the absolute

size of the equation variance is almost equal to the inherent variance of the data or is already below the level of practical significance. Note, the goodness of fit of a regression equation cannot be based solely on R^2 or determined solely from T. Situations where R^2 equals 90% and T is 3 inches and cases where R^2 equals 20% and T is 1/4 inch are very realistic.

The specific values used for the critical points, $*R^2$ and *T, depended on which surface marker was being considered and on whether the general or anthropometric model was being analyzed. The value used for *T decreased in size when surface markers having less inherent variability, such as the lower spine, were being analyzed. A different strategy was used in fitting the general model and the anthropometric model. The value of $*R^2$ was smaller and *T was larger for the general model. Exactness was sacrificed for simplicity in the model. For the anthropometric model, $*R^2$ was raised drastically and *T was lowered almost to the 'within subject' value. In addition to introducing anthropometric variables, the prediction accuracy that was required for the equations was increased.

SURFACE LANDMARK: Right Acromion POSITION: Standing

Independent Variable (Inches or Pounds)	SURFACE MARKER COORDINATES					
	General Model			Anthropometric Model		
	X	Y	Z	X	Y	Z
Constant	-0.483	6.30	15.07	-0.483	6.30	8.878
X - elbow	0.376	0.111		0.376	0.111	
X - elbow squared *		0.00695	-0.00560		0.00695	-0.00637
X - elbow cubed *	0.000337	-0.000368		0.000337	-0.000368	
Y - elbow	-0.184	0.260		-0.184	0.260	
Y - elbow squared	0.0204	-0.0250	-0.00363	0.0204	-0.0250	-0.00421
Y - elbow cubed	-0.000491	0.000887		-0.000491	0.000887	
Z - elbow	-0.183	-0.170	0.267	-0.183	-0.170	0.495
Z - elbow squared						-0.00908
Z - elbow cubed						
Stature						
Stature squared						0.000156
Stature cubed						
Sitting height						
Sitting height squared						
Sitting height cubed						
Weight						
Weight squared						
Weight cubed						
Chest circumference						
Chest cir. squared						
Chest cir. cubed						
Biacromial breath						
Biacromial breath squared						
Biacromial breath cubed						
Humeral length						
Humeral length squared						
Humeral length cubed						

* The terms "squared" and "cubed" designate that the prediction equations contain the second and third power terms of a dimension.

SURFACE LANDMARK: Right Acromion POSITION: Seated

Independent Variable (Inches or Pounds)	SURFACE MARKER COORDINATES					
	General Model			Anthropometric Model		
	X	Y	Z	X	Y	Z
Constant	-2.81	4.71	15.83	-2.81	4.71	9.13
X - elbow	0.410	0.129		0.410	0.129	
X - elbow squared *		0.0126			0.0126	
X - elbow cubed *	0.000312	-0.000592	-0.000197	0.000312	-0.000592	-0.000207
Y - elbow	-0.155	0.335	-0.0758	-0.155	0.335	
Y - elbow squared	0.0220	-0.0250		0.0220	-0.0250	-0.00396
Y - elbow cubed	-0.000479	0.000957		-0.000479	0.000957	
Z - elbow		-0.104	0.244		-0.104	0.242
Z - elbow squared						
Z - elbow cubed						
Stature						
Stature squared						
Stature cubed						
Sitting height						
Sitting height squared						
Sitting height cubed						0.000139
Weight						
Weight squared						
Weight cubed						
Chest circumference						
Chest cir. squared						
Chest cir. cubed						
Biacromial breath						
Biacromial breath squared						
Biacromial breath cubed						
Humeral length						
Humeral length squared						
Humeral length cubed						

* The terms "squared" and "cubed" designate that the prediction equations contain the second and third power terms of a dimension.

SURFACE LANDMARK: Left Acromion POSITION: Seated

Independent Variable (Inches or Pounds)	SURFACE MARKER COORDINATES					
	General Model			Anthropometric Model		
	X	Y	Z	X	Y	Z
Constant	2.93	-8.16	15.979	-156.79	-2.77	8.137
X - elbow	0.0590		-0.0237	0.0528	-0.0627	-0.0259
X - elbow squared *		0.00214			0.0147	
X - elbow cubed *	0.000311			0.000312	0.000356	
Y - elbow	0.240	0.139		0.238	0.138	
Y - elbow squared		-0.0114	-0.00414		-0.0138	
Y - elbow cubed		0.000636	0.000246		0.000762	0.0000616
Z - elbow	-0.418		0.196	-0.405	-0.271	0.233
Z - elbow squared	0.0103		-0.00502	0.0102		-0.00639
Z - elbow cubed					0.000307	
Stature						
Stature squared						
Stature cubed						
Sitting height						
Sitting height squared						
Sitting height cubed						0.000139
Weight						
Weight squared				0.00000312		0.0000000986
Weight cubed						
Chest circumference						
Chest cir. squared						
Chest cir. cubed						
Biacromial breath				16.22		
Biacromial breath squared				-0.0245	-0.000956	
Biacromial breath cubed						
Humeral length						
Humeral length squared				-0.000728		
Humeral length cubed						

* The terms "squared" and "cubed" designate that the prediction equations contain the second and third power terms of a dimension.

SURFACE LANDMARK: Left Acromion

POSITION: Standing

Independent Variable (Inches or Pounds)	SURFACE MARKER COORDINATES					
	General Model			Anthropometric Model		
	X	Y	Z	X	Y	Z
Constant	-0.377	-6.22	16.95	-149.85	-3.36	-3.716
X - elbow	-0.204	-0.0947	0.024	-0.214	-0.0821	
X - elbow squared *	-0.0123	0.0232		-0.0115	0.0221	
X - elbow cubed *	0.00119	-0.000610	-0.0000931	0.00115	-0.000533	-0.000149
Y - elbow	0.247			0.224		
Y - elbow squared			-0.00365	0.0210		
Y - elbow cubed		0.000430	0.000227	-0.000777	0.000469	
Z - elbow	-0.140	-0.332	0.241	-0.368	-0.306	
Z - elbow squared			-0.0203	0.00817		-0.00180
Z - elbow cubed		0.000403	0.000426		0.000367	
Stature						
Stature squared						
Stature cubed						
Sitting height						
Sitting height squared						0.544
Sitting height cubed						
Weight						
Weight squared						0.0124
Weight cubed				0.000000350		
Chest circumference						
Chest cir. squared						
Chest cir. cubed						
Biacromial breath				15.429		
Biacromial breath squared						
Biacromial breath cubed				-0.0239	-0.000915	
Humeral length						
Humeral length squared						
Humeral length cubed				-0.000920		

* The terms "squared" and "cubed" designate that the prediction equations contain the second and third power terms of a dimension.

SURFACE LANDMARK: Supersternale POSITION: Seated

Independent Variable (Inches or Pounds)	SURFACE MARKER COORDINATES					
	General Model			Anthropometric Model		
	X	Y	Z	X	Y	Z
Constant	2.55	0.368	13.09	2.55	0.882	80.93
X - elbow	0.241			0.241		
X - elbow squared *	-0.0113			-0.0113		
X - elbow cubed *	0.000518		-0.000193	0.000518		-0.000214
Y - elbow	0.145	0.214		0.145	0.208	
Y - elbow squared		-0.0143	-0.00257		-0.0135	-0.00308
Y - elbow cubed		0.000652			0.000636	
Z - elbow			0.533		-0.235	0.565
Z - elbow squared			-0.0128			-0.0139
Z - elbow cubed					0.000268	
Stature						-1.588
Stature squared						0.000113
Stature cubed						
Sitting height						
Sitting height squared						
Sitting height cubed						0.0000862
Weight						
Weight squared						
Weight cubed						
Chest circumference						
Chest cir. squared					0.0000241	
Chest cir. cubed						
Biacromial breath						
Biacromial breath squared						
Biacromial breath cubed						
Humeral length						
Humeral length squared						
Humeral length cubed						

* The terms "squared" and "cubed" designate that the prediction equations contain the second and third power terms of a dimension.

SURFACE LANDMARK: Suprasternale POSITION: Standing

Independent Variable (Inches or Pounds)	SURFACE MARKER COORDINATES					
	General Model			Anthropometric Model		
	X	Y	Z	X	Y	Z
Constant	3.21	2.30	13.30	23.02	2.30	
X - elbow	0.0989	-0.118		0.0981	-0.118	0.0466
X - elbow squared *	-0.00792	0.0158		-0.00794	0.0158	-0.00614
X - elbow cubed *	0.000634	-0.000427		0.000594	-0.000427	
Y - elbow	0.149			0.124		0.0326
Y - elbow squared						-0.00419
Y - elbow cubed		0.000515			0.000515	
Z - elbow	-0.0582	-0.520	0.149	-0.0761	-0.520	0.753
Z - elbow squared		0.158			0.158	-0.0469
Z - elbow cubed						0.000969
Stature						
Stature squared						
Stature cubed						0.00000972
Sitting height				0.560		0.390
Sitting height squared						
Sitting height cubed						
Weight						
Weight squared						
Weight cubed				0.000000160		
Chest circumference						4.294
Chest cir. squared						
Chest cir. cubed						-0.00103
Biacromial breath						
Biacromial breath squared				0.0000376		0.00140
Biacromial breath cubed						
Humeral length						
Humeral length squared						0.00213
Humeral length cubed						

* The terms "squared" and "cubed" designate that the prediction equations contain the second and third power terms of a dimension.

SURFACE LANDMARK: C_7 POSITION: Seated

Independent Variable (Inches or Pounds)	SURFACE MARKER COORDINATES					
	General Model			Anthropometric Model		
	X	Y	Z	X	Y	Z
Constant	-3.59	0.810	17.94	-3.59	0.810	129.72
X - elbow	0.243	0.111		0.243	0.111	
X - elbow squared *						
X - elbow cubed *	0.000288		-0.000105	0.000288		-0.000139
Y - elbow	-0.0148	0.0778		-0.0148	0.0778	-0.0371
Y - elbow squared	0.0102	0.0134		0.0102	0.0134	
Y - elbow cubed	-0.000148	-0.000219		-0.000148	-0.000219	
Z - elbow		-0.424	0.0569		-0.424	0.0493
Z - elbow squared		0.0113			0.0113	
Z - elbow cubed						
Stature						-2.506
Stature squared						0.000187
Stature cubed						
Sitting height						
Sitting height squared						
Sitting height cubed						
Weight						
Weight squared						
Weight cubed						
Chest circumference						
Chest cir. squared						
Chest cir. cubed						
Biacromial breath						
Biacromial breath squared						
Biacromial breath cubed						
Humeral length						
Humeral length squared						
Humeral length cubed						

* The terms "squared" and "cubed" designate that the prediction equations contain the second and third power terms of a dimension.

SURFACE LANDMARK: C_7 POSITION: Standing

Independent Variable (Inches or Pounds)	SURFACE MARKER COORDINATES					
	General Model			Anthropometric Model		
	X	Y	Z	X	Y	Z
Constant	-1.03	-0.617	18.35	-1.03	-0.617	51.10
X - elbow	0.158	0.0638		0.158	0.0638	
X - elbow squared *		0.0132	-0.00331		0.0132	-0.00418
X - elbow cubed *	0.000335	-0.000439	-0.00000792	0.000335	-0.000439	-0.0000321
Y - elbow		0.0666			0.0666	
Y - elbow squared	0.0159	-0.0114		0.0159	-0.0114	
Y - elbow cubed	-0.000485	0.000738	-0.0000619	-0.000485	0.000738	-0.000109
Z - elbow	-0.286	0.257	0.0376	-0.286	0.257	0.0356
Z - elbow squared		-0.0364			-0.0364	
Z - elbow cubed	0.000253	0.00102		0.000253	0.00102	
Stature						
Stature squared						0.0000224
Stature cubed						
Sitting height						-0.391
Sitting height squared						
Sitting height cubed						
Weight						-0.170
Weight squared						
Weight cubed						0.00000182
Chest circumference						0.122
Chest cir. squared						
Chest cir. cubed						
Biacromial breath						-0.743
Biacromial breath squared						
Biacromial breath cubed						
Humeral length						
Humeral length squared						
Humeral length cubed						

* The terms "squared" and "cubed" designate that the prediction equations contain the second and third power terms of a dimension.

SURFACE LANDMARK: T_4 POSITION: Seated

Independent Variable (Inches or Pounds)	SURFACE MARKER COORDINATES					
	General Model			Anthropometric Model		
	X	Y	Z	X	Y	Z
Constant	-4.77	-2.02	14.74	-4.77	-6.46	66.87
X - elbow	0.188	0.0955		0.188	0.0962	
X - elbow squared *		0.0115			0.0125	
X - elbow cubed*	0.000264	-0.000384	-0.0000651	0.000264	-0.000420	
Y - elbow		0.0730	-0.0234		0.0806	
Y - elbow squared	0.0163	-0.0105		0.0163	-0.0120	
Y - elbow cubed	-0.000440	0.000641		-0.000440	0.000694	
Z - elbow			0.0238			0.226
Z - elbow squared						-0.00624
Z - elbow cubed						
Stature						
Stature squared						
Stature cubed						
Sitting height						
Sitting height squared						
Sitting height cubed						0.000107
Weight						
Weight squared					0.000465	
Weight cubed					-0.00000175	
Chest circumference						
Chest cir. squared						
Chest cir. cubed						
Biacromial breath						
Biacromial breath squared						
Biacromial breath cubed						
Humeral length						-6.077
Humeral length squared						
Humeral length cubed						0.00923

* The terms "squared" and "cubed" designate that the prediction equations contain the second and third power terms of a dimension.

SURFACE LANDMARK: T_4 POSITION: Standing

Independent Variable (Inches or Pounds)	SURFACE MARKER COORDINATES					
	General Model			Anthropometric Model		
	X	Y	Z	X	Y	Z
Constant	-4.94	-0.427	14.15	-1.55	-12.06	3.35
X - elbow	0.137	0.0770		0.137	0.0718	
X - elbow squared*		0.0107	-0.00128		0.0106	-0.00381
X - elbow cubed *	0.000341	-0.000338		0.000338	-0.000324	
Y - elbow				-0.0524	0.0456	
Y - elbow squared	0.0123			0.0148	-0.00935	
Y - elbow cubed	-0.000328	0.000299		-0.000349	0.000578	-0.0000894
Z - elbow		-0.0618		-0.133	-0.0501	
Z - elbow squared						-0.00159
Z - elbow cubed				0.000193		
Stature						0.199
Stature squared				-0.00000702		
Stature cubed						
Sitting height						
Sitting height squared						
Sitting height cubed						
Weight					0.106	
Weight squared						
Weight cubed					-0.00000011	
Chest circumference						
Chest cir. squared						
Chest cir. cubed						
Biacromial breath						
Biacromial breath squared						
Biacromial breath cubed						
Humeral length						
Humeral length squared						
Humeral length cubed						-0.000696

* The terms "squared" and "cubed" designate that the prediction equations contain the second and third power terms of a dimension.

SURFACE LANDMARK: T_8 POSITION: Seated

Independent Variable (Inches or Pounds)	SURFACE MARKER COORDINATES					
	General Model			Anthropometric Model		
	X	Y	Z	X	Y	Z
Constant	-4.00	-0.987	9.78	-4.87	-7.28	10.83
X - elbow	0.143	0.0870	0.0268	0.141	0.0922	0.0412
X - elbow squared *						
X - elbow cubed *	0.000148			0.000149		
Y - elbow						
Y - elbow squared	0.0126			0.0123	-0.00378	
Y - elbow cubed	-0.000350	0.000213		-0.000335	0.000364	
Z - elbow						
Z - elbow squared					0.00618	
Z - elbow cubed					0.000274	
Stature						
Stature squared						
Stature cubed						
Sitting height						
Sitting height squared						
Sitting height cubed						0.000145
Weight					0.0608	
Weight squared						
Weight cubed					-0.000000675	
Chest circumference				-0.0704		
Chest cir. squared						
Chest cir. cubed						
Biacromial breath						
Biacromial breath squared						
Biacromial breath cubed						
Humeral length				0.253		-0.605
Humeral length squared						
Humeral length cubed						

* The terms "squared" and "cubed" designate that the prediction equations contain the second and third power terms of a dimension.

SURFACE LANDMARK: T_8 POSITION: Standing

Independent Variable (Inches or Pounds)	SURFACE MARKER COORDINATES					
	General Model			Anthropometric Model		
	X	Y	Z	X	Y	Z
Constant	-2.88	0.440	9.21	-1.23	-10.09	65.81
X - elbow		0.0698	0.0161		0.0739	
X - elbow squared *					0.00640	
X - elbow cubed *	0.000304			0.000311	-0.000212	
Y - elbow						
Y - elbow squared	0.0102			0.00976		
Y - elbow cubed	-0.000359	0.000132		-0.000333	0.000161	
Z - elbow		-0.0389				
Z - elbow squared					-0.00637	
Z - elbow cubed					0.000240	
Stature					-0.0905	0.113
Stature squared						
Stature cubed						
Sitting height						
Sitting height squared						
Sitting height cubed					0.0000654	0.0000410
Weight					0.0717	
Weight squared						
Weight cubed					-0.000000782	
Chest circumference					0.0254	
Chest cir. squared						
Chest cir. cubed						
Biacromial breath					0.255	
Biacromial breath squared						
Biacromial breath cubed				-0.000463		
Humeral length						-6.816
Humeral length squared						
Humeral length cubed						0.0105

* The terms "squared" and "cubed" designate that the prediction equations contain the second and third power terms of a dimension.

SURFACE LANDMARK: T_{12} POSITION: Seated

Independent Variable (Inches or Pounds)	SURFACE MARKER COORDINATES					
	General Model			Anthropometric Model		
	X	Y	Z	X	Y	Z
Constant	-2.18	-0.724	4.91	13.45	-0.758	151.99
X - elbow	0.0821	0.0506	0.0508	0.0827	0.0572	
X - elbow squared *						
X - elbow cubed*	0.0000764			0.0000811		0.0512
Y - elbow						
Y - elbow squared	0.00681		0.00101	0.00625		0.000679
Y - elbow cubed	-0.000190	0.000131		-0.000160	0.000144	
Z - elbow						
Z - elbow squared						
Z - elbow cubed				0.0000219	0.0000395	
Stature						
Stature squared						
Stature cubed						-6.305
Sitting height						
Sitting height squared						0.00174
Sitting height cubed						
Weight				-0.0992		
Weight squared				0.000000964	-0.0000000548	
Weight cubed				-0.0149		
Chest circumference						
Chest cir. squared						-0.0000310
Chest cir. cubed						
Biacromial breath				-0.236		
Biacromial breath squared						
Biacromial breath cubed						
Humeral length						
Humeral length squared						
Humeral length cubed						

* The terms "squared" and "cubed" designate that the prediction equations contain the second and third power terms of a dimension.

SURFACE LANDMARK: T_{12} POSITION: Standing

Independent Variable (Inches or Pounds)	SURFACE MARKER COORDINATES					
	General Model			Anthropometric Model		
	X	Y	Z	X	Y	Z
Constant	-1.260	-0.0682	4.925	-50.59	-6.84	-65.61
X - elbow			0.0226		0.0203	0.0152
X - elbow squared *		0.00156			0.00379	
X - elbow cubed *	0.000148			0.000162	-0.0000986	
Y - elbow						
Y - elbow squared	0.00505			0.00451		
Y - elbow cubed	-0.000162	0.0000624		-0.000125	0.0000861	
Z - elbow		-0.00844				
Z - elbow squared				0.000777	-0.00473	
Z - elbow cubed					0.000206	
Stature						1.461
Stature squared						-0.0000872
Stature cubed						
Sitting height						
Sitting height squared				0.0000165	0.0000134	
Sitting height cubed						
Weight				-0.0950	0.0450	
Weight squared				0.000000975	-0.000000508	
Weight cubed						
Chest circumference				2.304		
Chest cir. squared				-0.000549		
Chest cir. cubed						
Biacromial breath						
Biacromial breath squared						
Biacromial breath cubed						
Humeral length						
Humeral length squared				0.000761		+0.000600
Humeral length cubed						

* The terms "squared" and "cubed" designate that the prediction equations contain the second and third power terms of a dimension.

SURFACE LANDMARK: L_2 POSITION: Seated

Independent Variable (Inches or Pounds)	SURFACE MARKER COORDINATES					
	General Model			Anthropometric Model		
	X	Y	Z	X	Y	Z
Constant	-0.874	-0.146	2.48	0.927	-0.0704	47.19
X - elbow	0.0414	0.0124	0.0307	0.0407	0.0191	0.0451
X - elbow squared *	0.000545			0.000635		-0.000659
X - elbow cubed *						
Y - elbow	0.0188			0.0204		
Y - elbow squared		0.00112	0.000694		0.00245	0.000408
Y - elbow cubed					-0.0000278	
Z - elbow						
Z - elbow squared						
Z - elbow cubed					0.0000147	
Stature						-0.145
Stature squared						
Stature cubed						
Sitting height						-5.956
Sitting height squared						0.00167
Sitting height cubed						
Weight						-0.000363
Weight squared						0.00000143
Weight cubed						
Chest circumference				-0.049		4.983
Chest cir. squared						-0.00118
Chest cir. cubed						
Biacromial breath						-2.665
Biacromial breath squared						0.00428
Biacromial breath cubed						
Humeral length						
Humeral length squared					-0.000142	
Humeral length cubed						0.00232

* The terms "squared" and "cubed" designate that the prediction equations contain the second and third power terms of a dimension.

SURFACE LANDMARK: L_2 POSITION: Standing

Independent Variable (Inches or Pounds)	SURFACE MARKER COORDINATES					
	General Model			Anthropometric Model		
	X	Y	Z	X	Y	Z
Constant	0.00220	-0.212	2.45	7.24	-43.28	-46.96
X - elbow						
X - elbow squared *		0.000810			0.000770	0.000401
X - elbow cubed *	0.0000593		0.0000317	0.0000628		
Y - elbow						
Y - elbow squared				0.00281		
Y - elbow cubed	-0.0000108	0.0000364		-0.000112	0.0000368	
Z - elbow						
Z - elbow squared						
Z - elbow cubed						
Stature						
Stature squared						
Stature cubed						-0.00000397
Sitting height						-4.472
Sitting height squared						0.00122
Sitting height cubed						
Weight				-0.048		-0.0439
Weight squared				0.000000493		0.000000681
Weight cubed						
Chest circumference				-0.0260	0.743	6.019
Chest cir. squared					-0.000927	-0.00143
Chest cir. cubed						
Biacromial breath						0.149
Biacromial breath squared						
Biacromial breath cubed						
Humeral length					2.923	
Humeral length squared				-0.000372	-0.00476	0.00238
Humeral length cubed						

* The terms "squared" and "cubed" designate that the prediction equations contain the second and third power terms of a dimension.

SURFACE LANDMARK: L_5 POSITION: Seated

Independent Variable (Inches or Pounds)	SURFACE MARKER COORDINATES					
	General Model			Anthropometric Model		
	X	Y	Z	X	Y	Z
Constant	-1.45	-1.67	4.61	-0.716	-343.67	26.42
X - elbow	0.0389	0.0258	0.0367	0.0395	0.0312	0.0388
X - elbow squared *		0.00330			0.00326	
X - elbow cubed *	0.000120	-0.0000733	0.0000632	0.000120	-0.0000821	0.0000645
Y - elbow					0.0167	
Y - elbow squared	0.00166		0.00141	0.00171		0.00154
Y - elbow cubed		0.000111			0.0000915	
Z - elbow	0.0261	0.0276		0.0259	0.0302	
Z - elbow squared						
Z - elbow cubed			0.0000439			0.0000402
Stature					1.826	0.820
Stature squared				-0.00000210	-0.000129	-0.0000663
Stature cubed						
Sitting height					-0.138	0.161
Sitting height squared						
Sitting height cubed						
Weight					0.0126	-0.0807
Weight squared						0.000199
Weight cubed						
Chest circumference					2.961	
Chest cir. squared						
Chest cir. cubed					-0.000671	
Biacromial breath					11.239	-5.710
Biacromial breath squared						
Biacromial breath cubed					-0.0158	0.00882
Humeral length					7.296	
Humeral length squared						
Humeral length cubed					-0.0111	0.000437

* The terms "squared" and "cubed" designate that the prediction equations contain the second and third power terms of a dimension.

SURFACE LANDMARK: L_5 POSITION: Standing

Independent Variable (Inches or Pounds)	SURFACE MARKER COORDINATES (Relative to SRP)					
	General Model			Anthropometric Model		
	X	Y	Z	X	Y	Z
Constant	-2.92	-2.89	40.95	-34.57	58.97	40.37
X - elbow	0.0559	0.0889	0.0100	0.0699	0.0884	0.00834
X - elbow squared *	0.00338		-0.000502	0.00608		-0.000772
X - elbow cubed *			0.0000718	-0.000111		0.0000752
Y - elbow	0.189	0.0930		0.0207	0.0893	
Y - elbow squared	0.00156		0.000358	0.00162	0.00245	
Y - elbow cubed		0.0000667				
Z - elbow	0.0908	0.0420	0.00672	0.0941	0.0547	0.0713
Z - elbow squared						-0.00755
Z - elbow cubed						0.000218
Stature				5.479	-3.224	
Stature squared				-0.000355	0.000241	
Stature cubed						
Sitting height						
Sitting height squared						
Sitting height cubed				-0.000143		
Weight				-0.608	0.122	
Weight squared				0.00157		
Weight cubed					-0.00000140	
Chest circumference				0.253		
Chest cir. squared					-0.0000648	0.0000123
Chest cir. cubed						
Biacromial breath				-17.590		
Biacromial breath squared				0.0264		
Biacromial breath cubed						
Humeral length					7.0910	
Humeral length squared						
Humeral length cubed				-0.000661	-0.0104	

* The terms "squared" and "cubed" designate that the prediction equations contain the second and third power terms of a dimension.

SURFACE LANDMARK: Right Anterior Superior Iliac POSITION: Seated

Independent Variable (Inches or Pounds)	SURFACE MARKER COORDINATES					
	General Model			Anthropometric Model		
	X	Y	Z	X	Y	Z
Constant	5.89	6.57	1.25	52.23	58.93	103.52
X - elbow		-0.0365	-0.0673		-0.0417	-0.0651
X - elbow squared *	-0.00338			-0.00348		
X - elbow cubed *	0.0000901		-0.0000465	0.0000887		-0.0000587
Y - elbow	-0.0291	0.105	-0.0430	-0.0351	0.0855	-0.0448
Y - elbow squared		-0.00904	-0.00528		-0.00741	-0.00539
Y - elbow cubed		0.000196	0.000160		0.000162	0.000163
Z - elbow	0.122		0.229	0.0214		
Z - elbow squared	-0.00282		-0.00680			
Z - elbow cubed						
Stature						
Stature squared						
Stature cubed				0.0000115		0.0000191
Sitting height					-4.923	-4.231
Sitting height squared						
Sitting height cubed				-0.0000605	0.00136	0.000968
Weight					-0.0577	
Weight squared						
Weight cubed				0.000000268	0.000000825	
Chest circumference				3.632	0.0668	
Chest cir. squared						
Chest cir. cubed				-0.000863		
Biacromial breath					7.532	
Biacromial breath squared						
Biacromial breath cubed				-0.000586	-0.0126	
Humeral length				-14.74	-0.441	
Humeral length squared						
Humeral length cubed				0.0255		

* The terms "squared" and "cubed" designate that the prediction equations contain the second and third power terms of a dimension.

SURFACE LANDMARK: Right Anterior Superior Iliac POSITION: Standing

Independent Variable (Inches or Pounds)	SURFACE MARKER COORDINATES					
	General Model			Anthropometric Model		
	X	Y	Z	X	Y	Z
Constant	6.55	4.946	-1.67	102.48	26.97	289.06
X - elbow	0.0545	-0.0864		0.0739	-0.0624	
X - elbow squared *	-0.00500	0.00361		-0.00266	0.00616	
X - elbow cubed *	0.000162		-0.000127		-0.000145	-0.000143
Y - elbow	-0.0623	0.130		-0.0286	0.110	
Y - elbow squared	0.00606	-0.0135	0.00500			
Y - elbow cubed	-0.000146	0.000479	-0.000229			-0.0000534
Z - elbow			0.0802			0.0686
Z - elbow squared						
Z - elbow cubed			-0.000161			-0.000150
Stature					-0.198	
Stature squared						
Stature cubed				0.0000129		0.0000339
Sitting height				0.0168		-0.842
Sitting height squared						
Sitting height cubed					0.0000982	
Weight				0.0168	-0.128	
Weight squared						
Weight cubed					0.00000144	0.000000177
Chest circumference				0.0489		-0.251
Chest cir. squared						
Chest cir. cubed						
Biacromial breath				-9.00127		-1.223
Biacromial breath squared						
Biacromial breath cubed				0.0126		
Humeral length						-25.56
Humeral length squared						
Humeral length cubed						0.0411

* The terms "squared" and "cubed" designate that the prediction equations contain the second and third power terms of a dimension.

APPENDIX H

GRAPHS OF SURFACE MARKER COORDINATES FOR THE SEATED PERSON

Without Anthropometric Variable (General Model)

The following graphs depict the predicted coordinates of the torso surface markers (relative to the L_5 surface marker) for various elbow positions. For each surface marker two of the following three types of graphs are presented:

1. Top View - Y versus X with Z held constant. A value of Z=20.0 inches (relative to L_5 surface) is used which corresponds to a transverse (horizontal) plane at shoulder height.

2. Side View - Z versus X with Y held constant. A value of Y = 10.0 inches (relative to L_5 surface) is used which corresponds to the sagittal plane just to the right of the right shoulder.

3. Back View - Z versus Y with X held constant. A value of X=10.0 inches (relative to L_5 surface) was used which corresponds to a frontal plane several inches in front of the chest.

The abscissa and ordinate of the graph give the coordinates of the surface marker while the coordinates of the elbow are specified by the contour lines on the graph. For example, using elbow coordinates of X_e=20.0, Y_e=10.0, and Z_e=10.0, the X and Y coordinates of the surface marker can be determined from a top view graph (Z_e=10.0). The X coordinate of the surface marker is determined by projecting the intersection of the X_e=20 and y_e=10 contours onto the ordinate. A similar projection onto the abscissa yields the Y coordinate of the surface marker. A diagnostic summary sheet accompanies each pair of graphs for the various surface markers. These summary sheets interpret and specify the limitations of the graph.

The graphs are for general design purposes and are given to supplement, not supplant, the equations given in Appendix G. The graphs can be used to intuitively verify the derived equations. The graphs also allow the designer to visualize and interpret the implications of the prediction equations. The interrelationships among the X, Y, and Z equations is depicted. However, the graphs were not intended to be used to estimate specific numerical values for the surface marker coordinates. Numerical predictions should be calculated directly from the original equations. It is very

difficult to accurately interpolate between contour lines or between individual graphs.

A second caution, the graphs specify the torso positions for fixed reach target positions. Torso position during dynamic movement was not within the scope of the present investigation. The contour lines on the graphs should not be misinterpreted. The contour lines represent the locus of fixed point positions, not pathes of motion.

SUMMARY SHEET FOR RIGHT ACROMION

GENERAL-SEATED MODEL

Positioning Pattern

1. Increasing X_e, elbow moving forward, causes the right acromion to move forward and to become lower. The left and right deviations in the right acromion is irregular and can best be ascertained by referring to the top-view graph. In general, the right acromion deviates slightly to the right and then drastically to the left as the target moves forward.

2. Increasing Y_e, elbow movement from left to right across the body, causes the right acromion to move from left to right. There is a mid-range where the right acromion remains relatively stable as the arm rotates from left to right about the shoulder. Transverse movement of the elbow causes the right acromion to move backwards and subsequently forward again in an elongated 'U' shaped pattern. The base of the 'U' corresponds to the previously mentioned mid-range position. The right acromion remains deflected backwards as the arm revolves from left to right about the shoulder. It is not depicted on the graphs, but the right acromion drops as the elbow moves from the left to directly in front of the shoulder. As the elbow moves further to the right, the Z coordinate of the right acromion remains relatively constant.

3. Increasing Z_e, elbow movement upward, causes a uniform upward movement of the right acromion and little or no variation in Y_{RA}. It is not depicted in the graphs, but there is a tendency for the right acromion to move to the left (X_{RA} decreases). As the elbow is raised, the shoulder tilts and forces the right acromion to the left.

Limitations in the Prediction Equation

There does not appear to be any range of extrapolated reach positions for which the prediction equations are inconsistent.

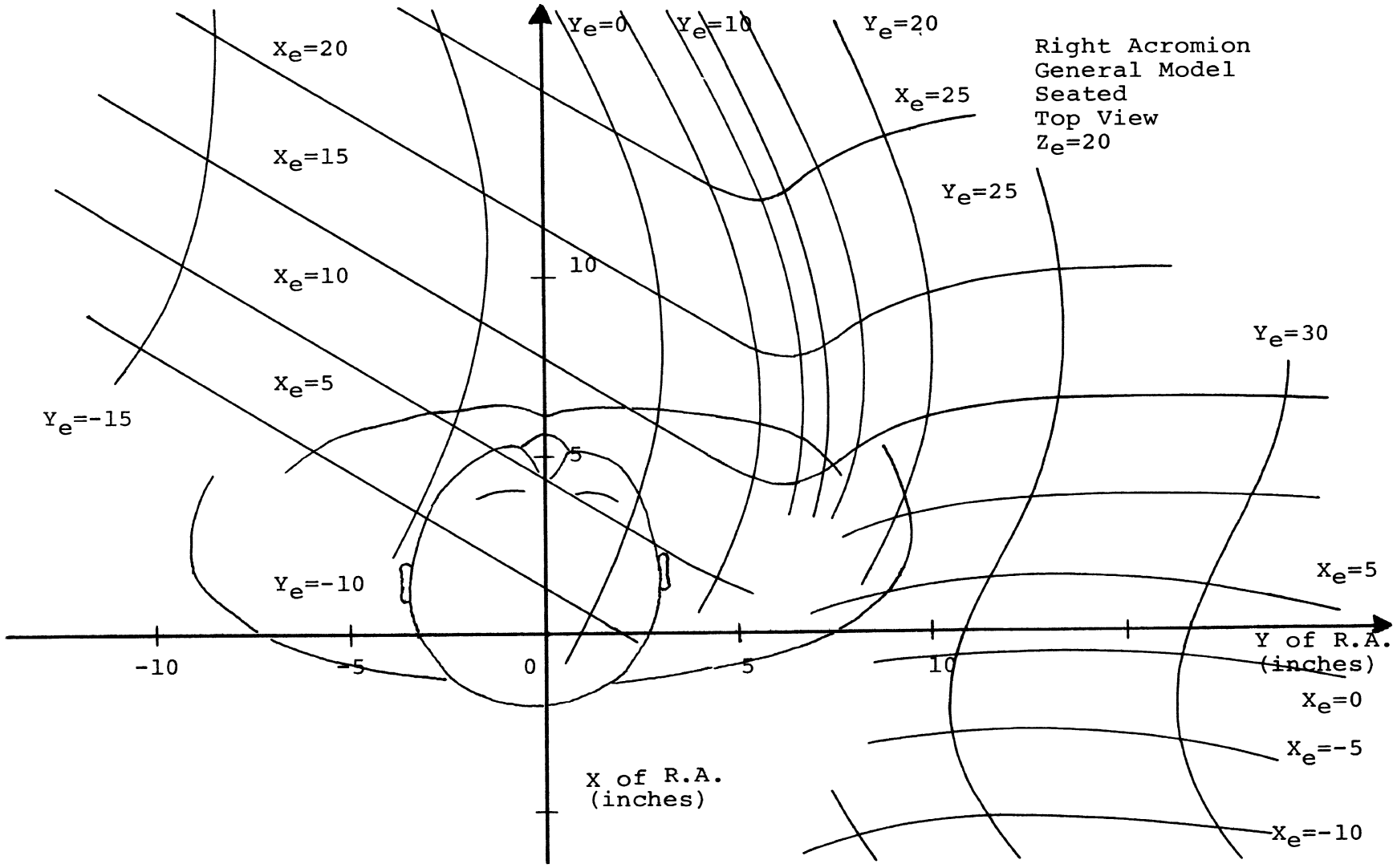
Right Acromion
General Model
Seated
Top View
Z_e=20
Y_e=0
Y_e=10
Y_e=20
Y_e=25
Y_e=30
Y_e=-15
Y_e=-10
X_e=20
X_e=15
X_e=10
X_e=5
X_e=25
X_e=5
X_e=0
X_e=-5
X_e=-10
10
5
-10
-5
0
5
10
Y of R.A.
(inches)
X of R.A.
(inches)

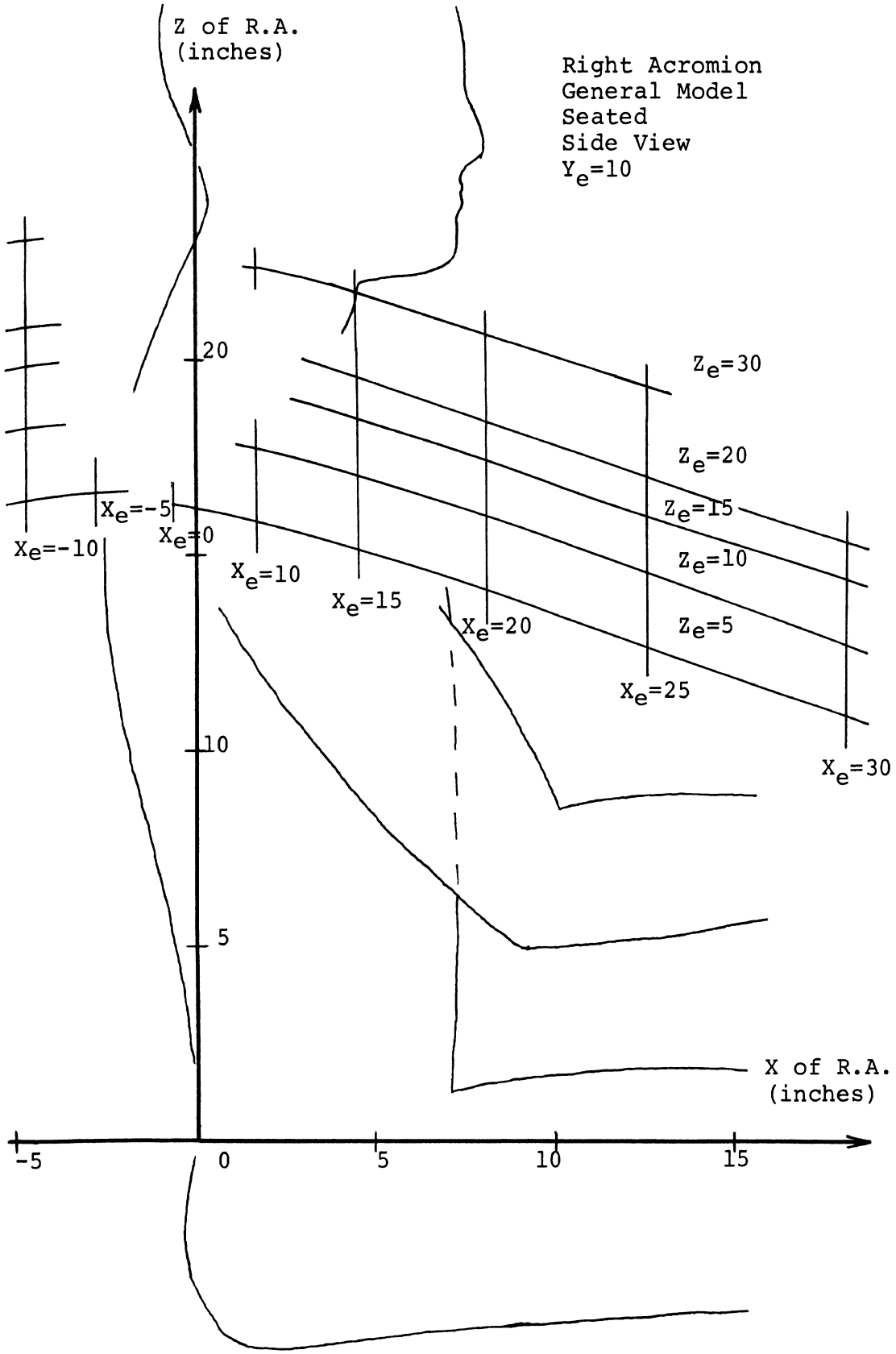
Z of R.A.
(inches)
Right Acromion
General Model
Seated
Side View
Y_e=10
20
10
5
Z_e=30
Z_e=20
Z_e=15
Z_e=10
Z_e=5
X_e=-10
X_e=-5
X_e=0
X_e=10
X_e=15
X_e=20
X_e=25
X_e=30
X of R.A.
(inches)
-5
0
5
10
15

SUMMARY SHEET FOR LEFT ACROMION

GENERAL-SEATED MODEL

Positioning Pattern

1. Increasing X_e, elbow moving forward, causes the left acromion to move forward. There is very little change in the Z or Y coordinates. The increase in the X coordinate of the left acromion tends to increase as the forward movement of the elbow becomes maximal.

2. Increasing Y_e, elbow moving from left to right across the body, causes the left acromion to move from left to right. For the mid-range of reach positions, the increase in Y_{LA} is minor. Reach position in the mid-range in front of the body are accomplished primarily by changing the transverse angle of the arm with respect to the shoulder. The left acromion gradually moves forward as the elbow moves in front of and across the body. This forward movement is accelerated for the mid-range of elbow positions in front of the body. As the right arm rotates clockwise about the shoulder, the trunk and consequently the left acromion are rotated forward. It is not depicted on the graphs, but the left acromion rises uniformly for left to right transverse movement of the elbow. The lateral movement of the left acromion causes the left shoulder to rotate slightly upward.

3. Increasing Z_e, elbow movement upward, causes the left acromion to first rise and then gradually lower. The initial rise in the left acromion results because the entire torso is raised as the elbow moves from waist level to shoulder level. The secondary lowering of the left shoulder results as the elbow continues to rise to eye level. The right shoulder rises which in turn causes the left shoulder to tilt downward. For identical reasons the movement in the sagittal plane is first backward and then forward. It is not depicted in the graphs, but the movement of the left acromion in the Y direction is negligible, only a very slight shift to the left.

Limitations in the Prediction Equation

There does not appear to be any ranges of extrapolated reach position for which the prediction equations become inconsistent.

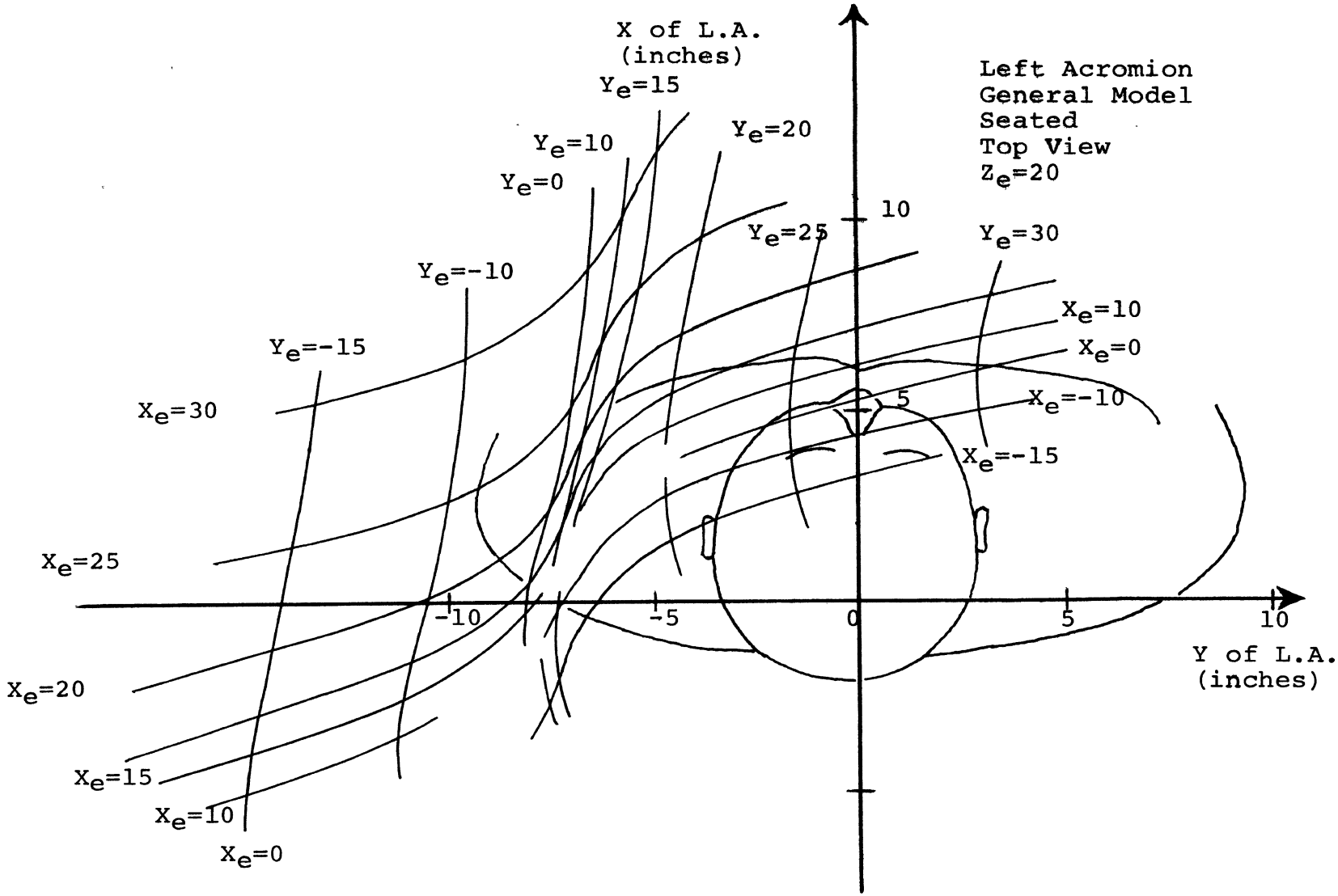
X of L.A.
(inches)
Left Acromion
General Model
Seated
Top View
Z_e=20
Y_e=15
Y_e=10
Y_e=0
Y_e=-10
Y_e=-15
Y_e=20
Y_e=25
Y_e=30
X_e=30
X_e=25
X_e=20
X_e=15
X_e=10
X_e=0
X_e=10
X_e=0
X_e=-10
X_e=-15
10
5
-10
-5
0
5
10
Y of L.A.
(inches)

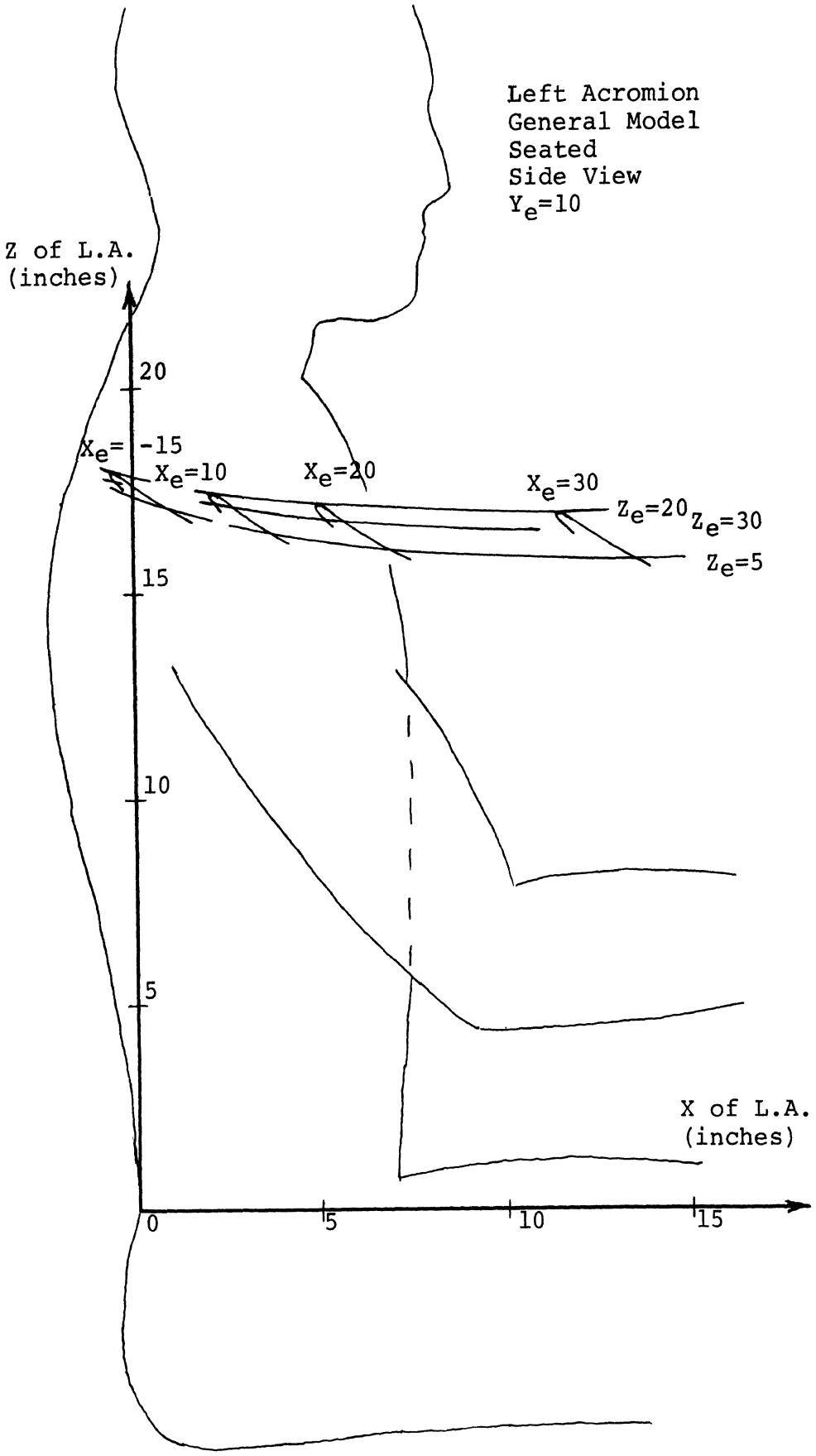
Left Acromion
General Model
Seated
Side View
Y_e=10
Z of L.A.
(inches)
20
15
10
5
X_e= -15
X_e=10
X_e=20
X_e=30
Z_e=20
Z_e=30
Z_e=5
X of L.A.
(inches)
0
5
10
15

SUMMARY SHEET FOR SUPRASTERNALE

GENERAL-SEATED MODEL

Positioning Pattern

1. Increasing X_e, elbow moving forward, causes the suprasternale to move forward. There is no noticeable deviation of the suprasternale to the left or right as the torso bends forward. The vertical height of the suprasternale gradually decreases. The decrease in Z_s becomes pronounced as the torso bends forward to accommodate submaximal forward reaches.

2. Increasing Y_e, elbow moving from left to right across the body, causes the suprasternale to move to the right. The lateral movement of the suprasternale becomes attenuated for the mid-range of reach positions. Reach positions in front of the right shoulder are accomplished by holding the Y coordinates of the torso relatively fixed and positioning the arm at different angles with respect to the right shoulder. The suprasternale moves slightly forward as Y_e increases. When reaching to the left (with the right arm) the torso is pushed slightly backward and when reaching to the right, the torso is pulled slightly forward. The increase in X_s is the largest as the elbow moves from left to right in front of the shoulder. It is not depicted on the graphs, but the suprasternale first rises and then falls as Y_e increases. The vertical height of the suprasternale is the largest when the elbow target is in front of the right shoulder. A back view of the torso shows that there is a slight clockwise rotation of the shoulder girdle as the elbow moves laterally across the front of the body.

3. Increasing Z_e, elbow moving upward, causes the suprasternale to rise. There is no deviation in the X or Y coordinates of the suprasternale as the elbow is raised.

Limitations in the Prediction Equations

There does not appear to be any ranges of extrapolated reach positions for which the prediction equations become inconsistent.

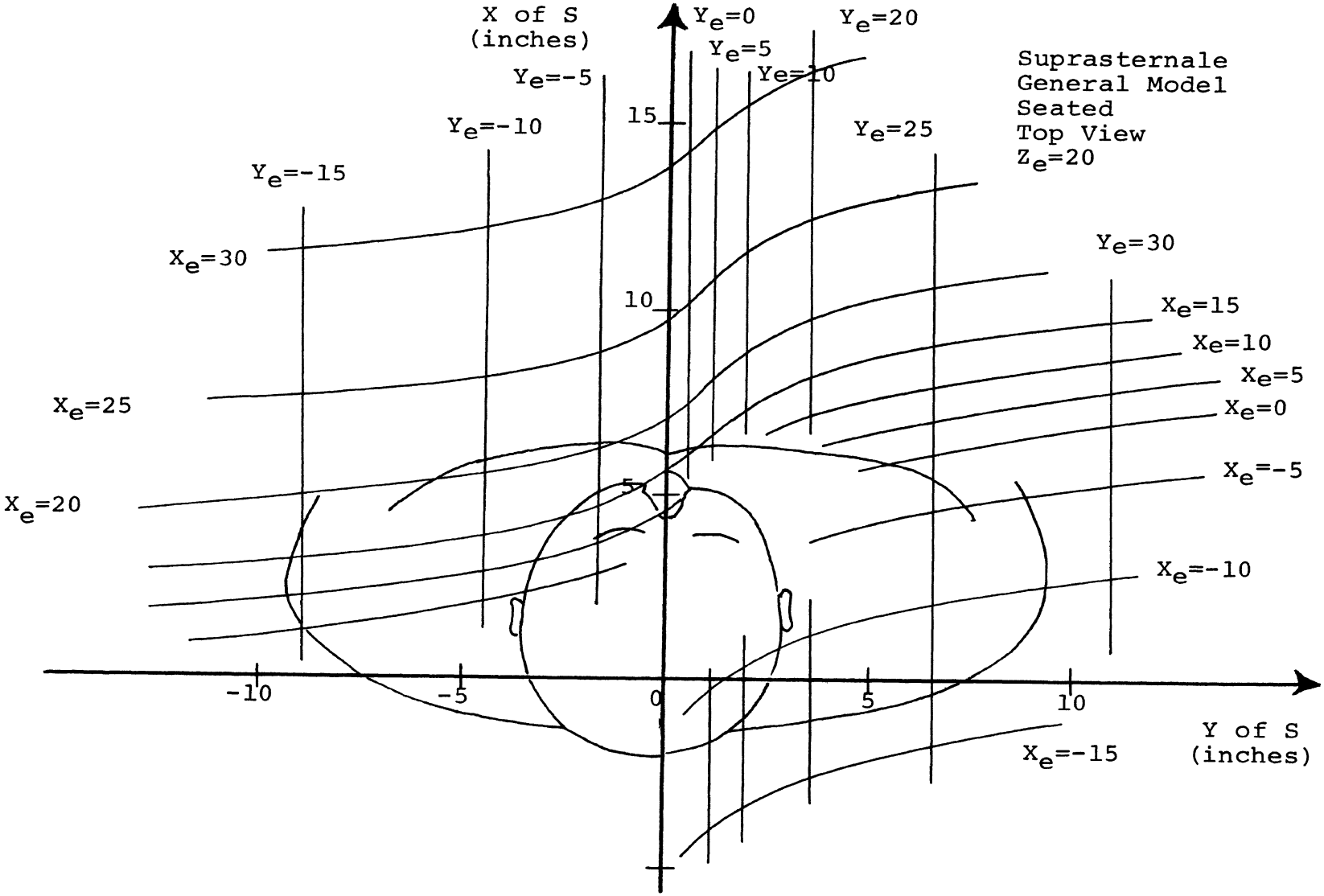
X of S
(inches)
Ye=0
Ye=20
Ye=5
Ye=-5
Ye=10
Ye=-10
15
Ye=25
Ye=-15
Suprasternale
General Model
Seated
Top View
Ze=20
Xe=30
Ye=30
10
Xe=15
Xe=10
Xe=5
Xe=25
Xe=0
Xe=-5
Xe=20
5
Xe=-10
-10
-5
0
5
10
Xe=-15
Y of S
(inches)

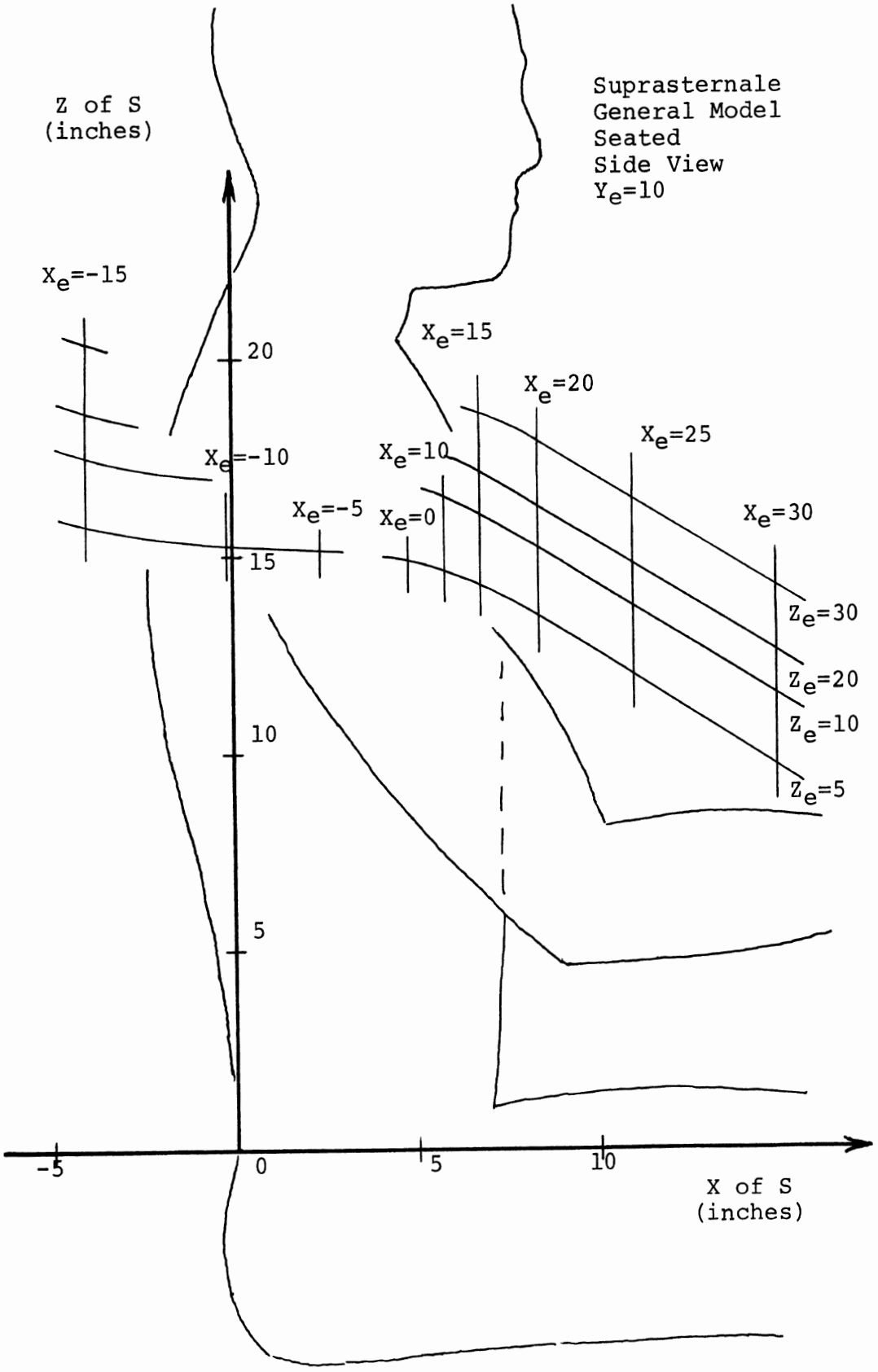
Z of S
(inches)
Suprasternale
General Model
Seated
Side View
Y_e=10
X_e=-15
X_e=15
X_e=20
X_e=25
X_e=10
X_e=-10
X_e=-5
X_e=0
X_e=30
Z_e=30
Z_e=20
Z_e=10
Z_e=5
20
15
10
5
-5
0
5
10
X of S
(inches)

SUMMARY SHEET FOR C_7 SURFACE

GENERAL-SEATED MODEL

Positioning Pattern

1. Increasing X_e, elbow moving forward, causes C_7 to move forward and slightly downward. The magnitude of the downward movement increases as the torso bends forward to perform sub-maximal reaches. Moving the elbow forward also causes the C_7 surface marker to be deflected to the right.

2. Increasing Y_e, elbow movement from left to right across the body, causes C_7 to move in an unconventional 'U' shaped pattern. As the elbow moves from in front of the left shoulder to directly in front of the chest, the X and Y coordinates of C_7 decrease. C_7 is pushed back and to the left. As the elbow continues to move to the right, C_7 reverses direction and moves forward and to the right so as to track the elbow movement pattern. It is not depicted on the graphs, but C_7 first rises slightly and then falls slightly as the elbow is moved laterally from left to right. This up and down deflection is caused by the slight rotation of the entire upper torso in the frontal plane.

3. Increasing Z_e, elbow movement upward, causes C_7 to rise at a uniform rate. There is negligible movement for C_7 forward or backwards as the elbow is raised. It is not depicted on the graphs, but there is some minor movement of C_7 in the Y direction associated with alleviating the elbow. As the elbow moves from waist level to shoulder level, the shoulders are tilted slightly to the left which causes C_7 to move to the left. As the elbow moves above shoulder height, the torso and C_7 are pulled to the right in order to track the elbow.

Limitations in the Prediction Equations

There does not appear to be any range of extrapolated reach positions for which the prediction equations become inconsistent. On first inspection it may appear that the movement patterns for C_7 and suprasternale are not consistent for reach positions in front of and to the left of the body (negative Y_e). As the elbow moves from left to right in this quadrant of the reach sphere, the suprasternale moves forward and to the right while C_7 moves backwards and to the left. This is not an inconsistency. A top view of the shoulder girdle shows that the torso is rotating clockwise.

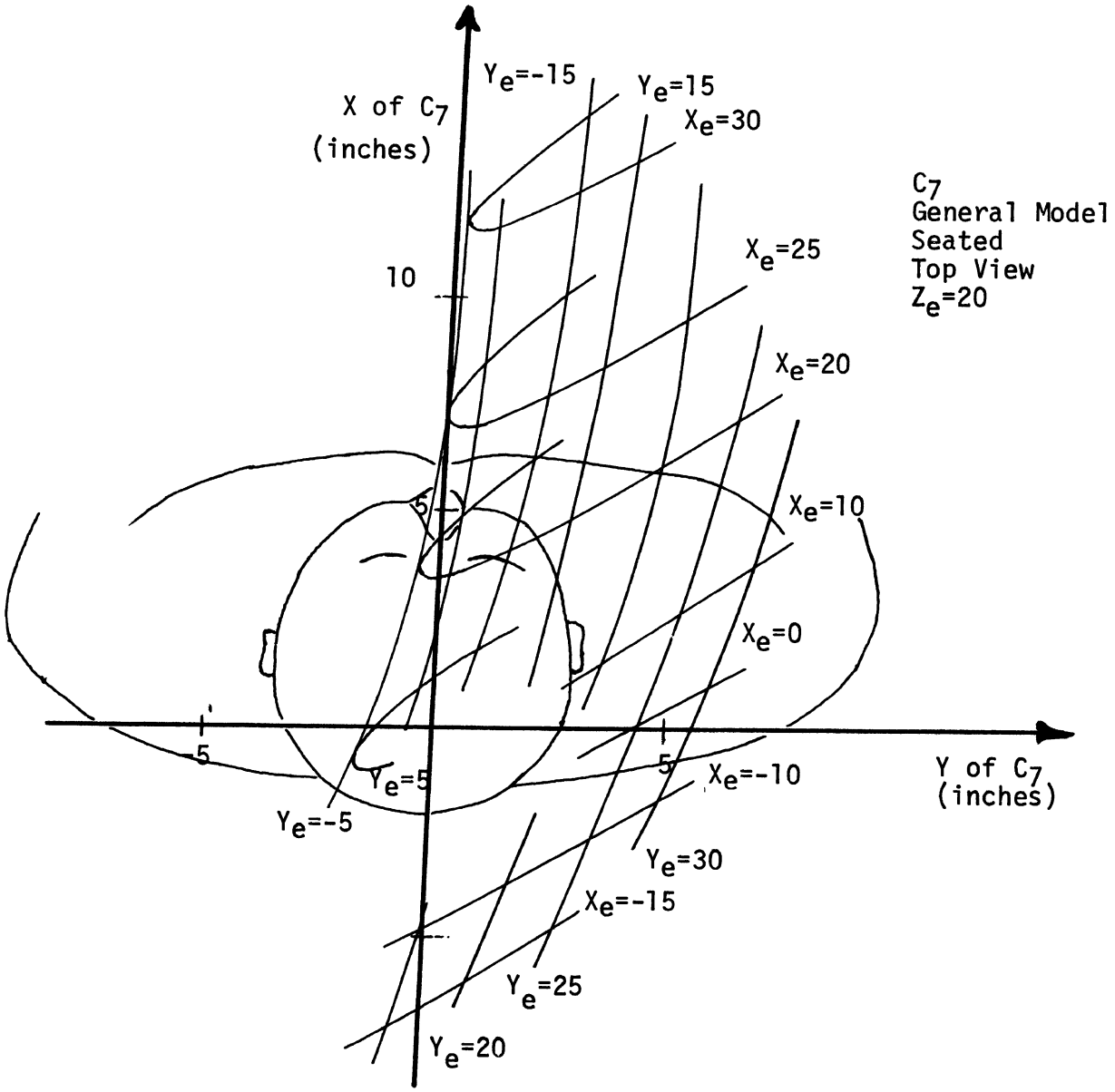
X of C_7
(inches)
Y_e=-15
Y_e=15
X_e=30
X_e=25
10
X_e=20
X_e=10
5
X_e=0
5
5
Y_e=5
X_e=-10
Y_e=-5
Y_e=30
X_e=-15
Y_e=25
Y_e=20
Y of C_7
(inches)
C_7
General Model
Seated
Top View
Z_e=20

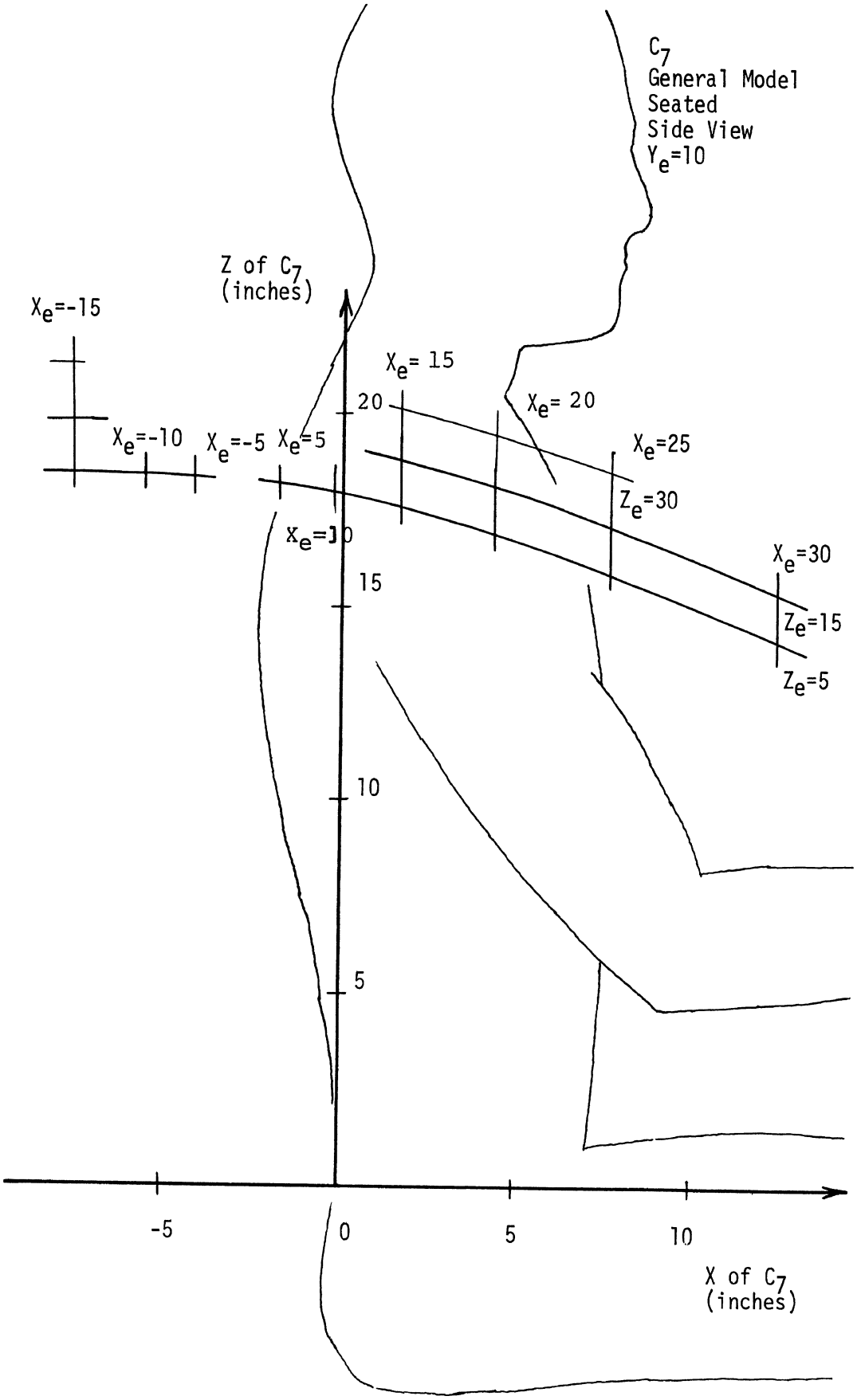
C7
General Model
Seated
Side View
Ye=10
Z of C7
(inches)
Xe=-15
Xe=-10
Xe=-5
Xe=5
Xe=10
Xe= 15
Xe= 20
Xe=25
Xe=30
Ze=30
Ze=15
Ze=5
20
15
10
5
-5
0
5
10
X of C7
(inches)

SUMMARY SHEET FOR THORACIC AND LUMBAR SPINE

GENERAL-SEATED MODEL

Positioning Pattern

The movement pattern for the surface markers T_4, T_8, T_{12}, and L_2 can be visualized quite readily from the graphs.

1. Increasing X_e, elbow movement forward, causes the lower spine to be pulled forward. The deflections to the left and right of the lower spine as X_e increases are negligible and could not be detected by the regression equations. The important contrast to be made concerns the Z coordinates for the spinal markers. As the elbow moves forward, the vertical distances for T_4 (and C_7) decrease whereas the vertical distances for T_8, T_{12}, and L_2 increase. The torso bends forward as it rotates forward. This bending of the torso causes the Z coordinates of the shoulder girdle and upper spine to decrease.

2. Increasing Y_e, elbow movements from left to right across the body, causes the spine to rotate and thereby causes the spinal marker to move from left to right. There is no significant change in the X coordinates of the spine as the elbow moves laterally. There is some increase in the Z coordinate of T_{12} and L_2 as the elbow moves from in front of the right shoulder to the far right. The previously semi-relaxed lower back stretches in response to sub-maximal reaching with the elbow.

3. Increasing Z_e, elbow movement upward, only effect T_4. There is no significant change in X, Y, or Z for T_8, T_{12}, and L_2 as Z_e increases. The only change in T_4 is in the Z direction and the increase in $^{Z}T_4$ appears to be fairly uniform.

Limitations in the Prediction Equations

There does not appear to be any ranges of extrapolated reach positions for which the prediction equations become inconsistent.

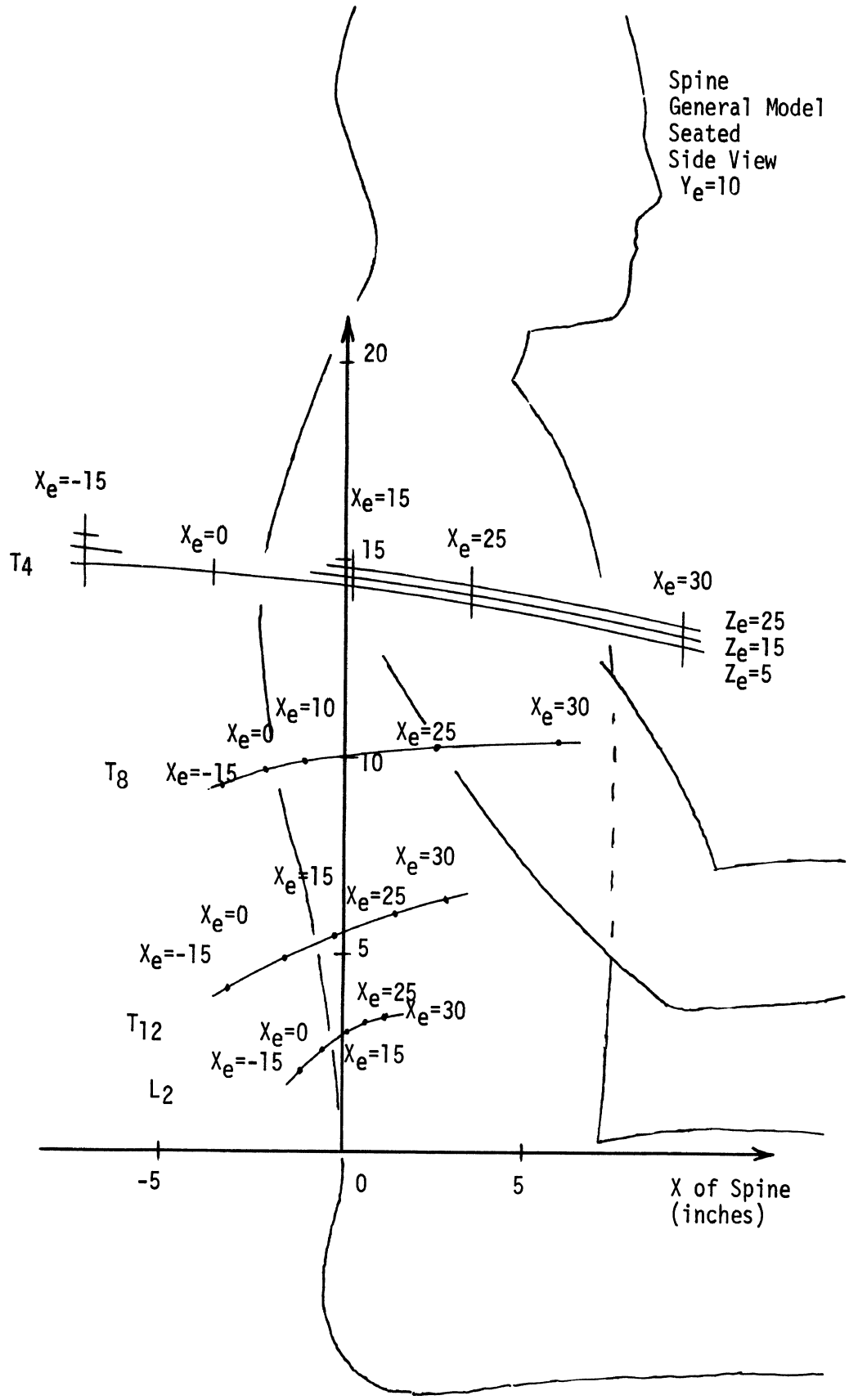
Spine
General Model
Seated
Side View
Y_e=10
20
X_e=-15
X_e=15
X_e=0
15
X_e=25
T_4
X_e=30
Z_e=25
Z_e=15
Z_e=5
X_e=10
X_e=30
X_e=0
X_e=25
T_8
X_e=-15
10
X_e=30
X_e=15
X_e=25
X_e=0
X_e=-15
5
X_e=25
X_e=30
T_{12}
X_e=0
X_e=15
X_e=-15
L_2
-5
0
5
X of Spine
(inches)

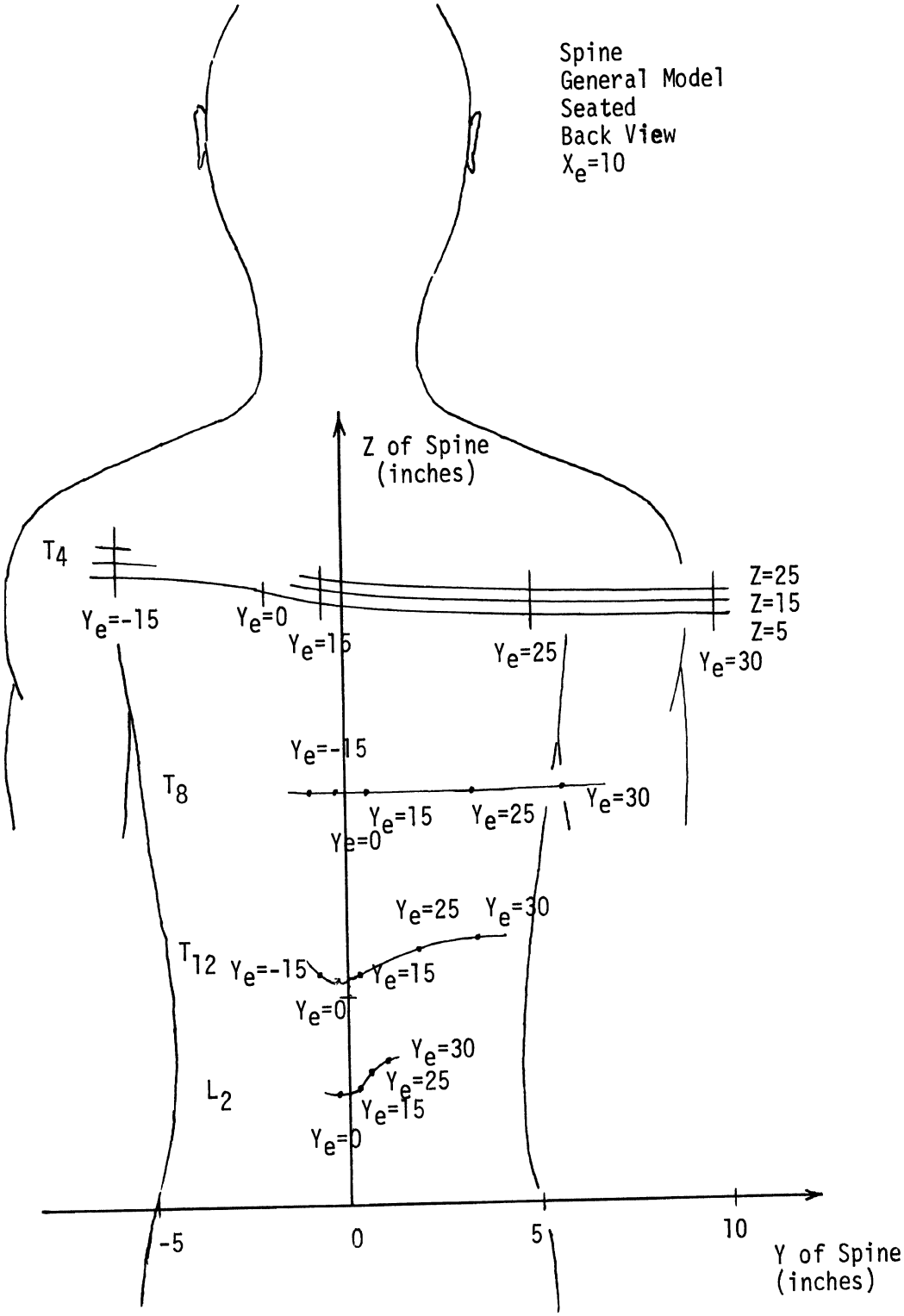
Spine
General Model
Seated
Back View
X_e=10
Z of Spine
(inches)
T_4
Y_e=-15
Y_e=0
Y_e=15
Y_e=25
Y_e=30
Z=25
Z=15
Z=5
T_8
Y_e=-15
Y_e=0
Y_e=15
Y_e=25
Y_e=30
T_{12}
Y_e=-15
Y_e=0
Y_e=15
Y_e=25
Y_e=30
L_2
Y_e=0
Y_e=15
Y_e=25
Y_e=30
-5
0
5
10
Y of Spine
(inches)

APPENDIX I

GRAPHS OF SURFACE MARKER COORDINATES FOR THE STANDING PERSON

Without Anthropometric Variables
(General Model)

The same introductory comments given at the beginning of Appendix I apply to this Appendix.

SUMMARY SHEET FOR SHOULDER GIRDLE: RIGHT ACROMION, LEFT ACROMION, SUPRASTERNALE AND C_7

GENERAL-STANDING MODEL

Positioning Pattern

The descriptions of the movement pattern of the shoulder girdle given in the summary sheets in Appendix I also apply to the present standing model. There are only two noticeable distinctions between the seated and standing models. First, movement patterns are, in general, slightly broader for the standing model. The distance between contour lines tends to increase slightly because the standing subject has more freedom of movement. The second distinction concerns reach positions in front of and to the left of the body (negative Y_e). For the seated subject reach positions in this quadrant of the reach sphere were achieved by rotating the torso (counter clockwise in top view), this rotation caused the left acromion and suprasternale to be displaced back and to the left with respect to the normal sitting position. C_7 in contrast was positioned forward and to the right due to the rotation. For the standing subject this rotation of the torso was not observed. The greater freedom of movement of the standing position allows the subject to lean to the left. The elimination of the torso rotation is depicted in the graphs by having the left acromion, suprasternale and C_7 move forward and to the left in order to attain reach targets in the second quadrant (top view) of the reach sphere.

Limitations in the Prediction Equations

There does not appear to be any ranges of extrapolated reach positions for which the prediction equations become inconsistent.

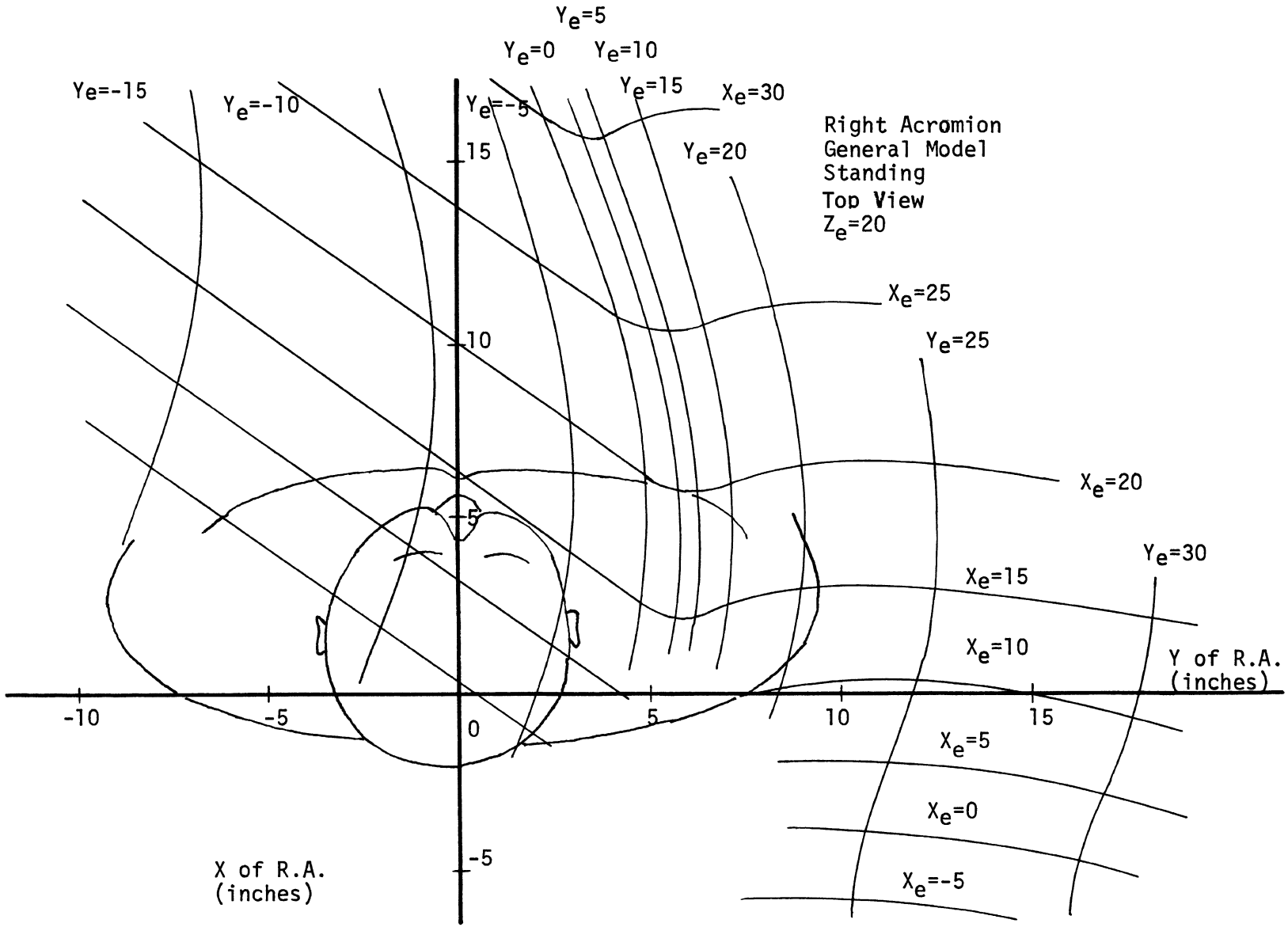
Ye=5
Ye=0
Ye=10
Ye=15
Xe=30
Ye=-15
Ye=-10
Ye=-5
Ye=20
Right Acromion
General Model
Standing
Top View
Ze=20
Xe=25
Ye=25
Xe=20
Ye=30
Xe=15
Xe=10
Y of R.A.
(inches)
15
10
5
-10
-5
0
5
10
15
Xe=5
Xe=0
Xe=-5
-5
X of R.A.
(inches)

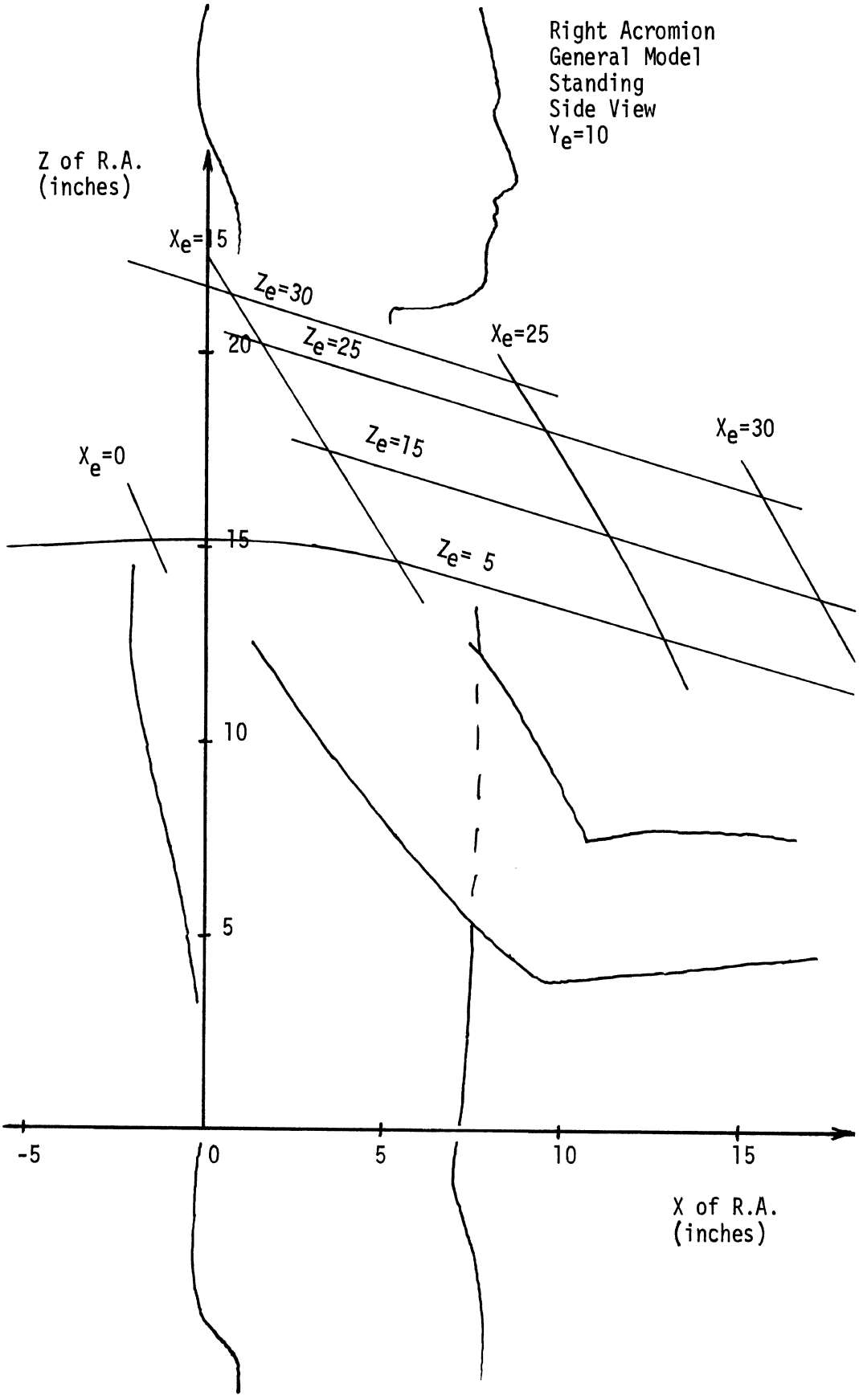
Right Acromion
General Model
Standing
Side View
Ye=10
Z of R.A.
(inches)
Xe=15
Ze=30
Ze=25
20
Xe=25
Xe=30
Ze=15
Xe=0
15
Ze= 5
10
5
-5
0
5
10
15
X of R.A.
(inches)

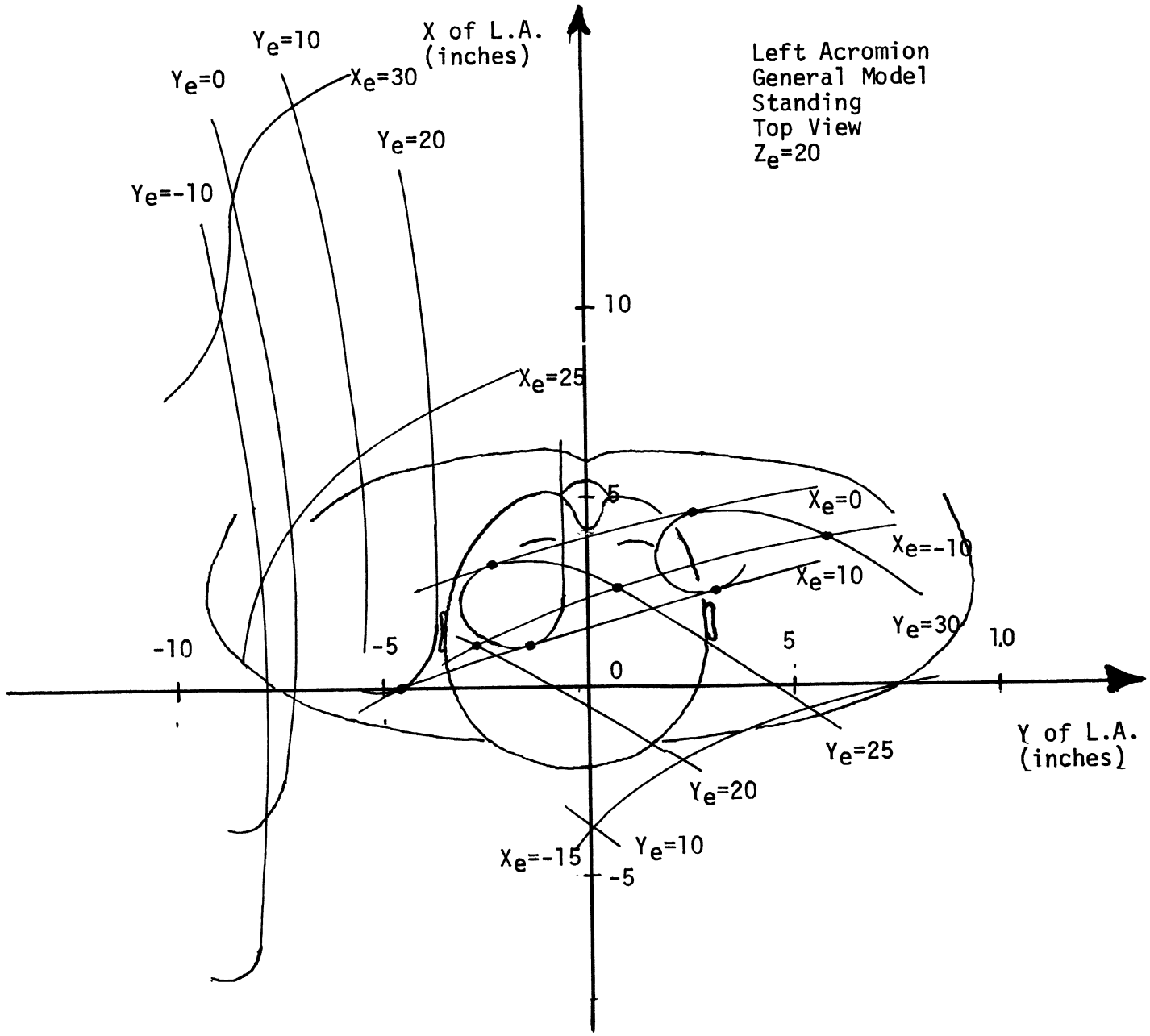
Left Acromion
General Model
Standing
Top View
Z_e=20
X of L.A. (inches)
Y of L.A. (inches)
Y_e=10
Y_e=0
X_e=30
Y_e=20
Y_e=-10
10
X_e=25
5
X_e=0
X_e=-10
X_e=10
Y_e=30
-10
-5
5
10
0
Y_e=25
Y_e=20
Y_e=10
X_e=-15
-5

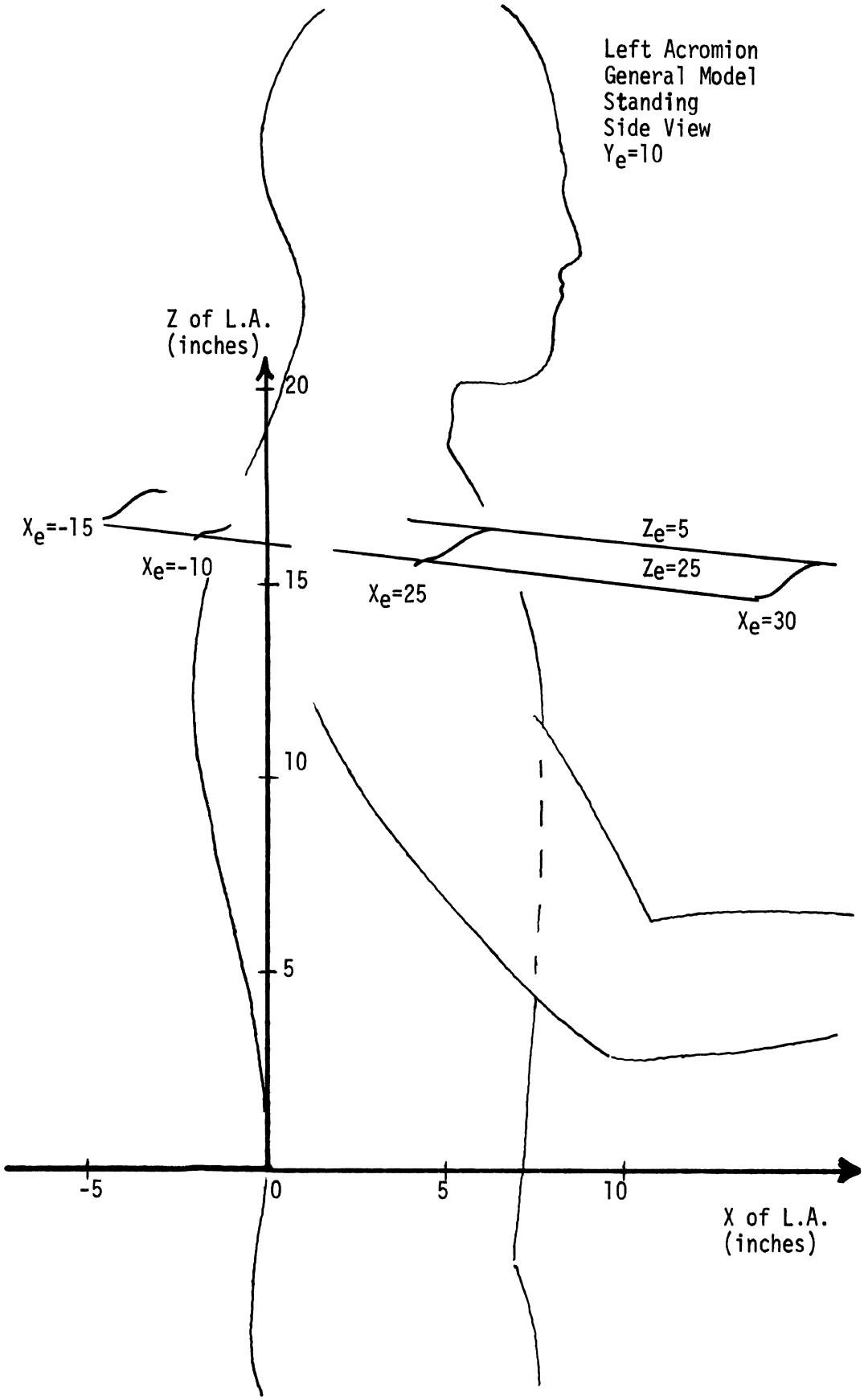
Left Acromion
General Model
Standing
Side View
Y_e=10
Z of L.A.
(inches)
20
15
10
5
X_e=-15
X_e=-10
Z_e=5
Z_e=25
X_e=25
X_e=30
-5
0
5
10
X of L.A.
(inches)

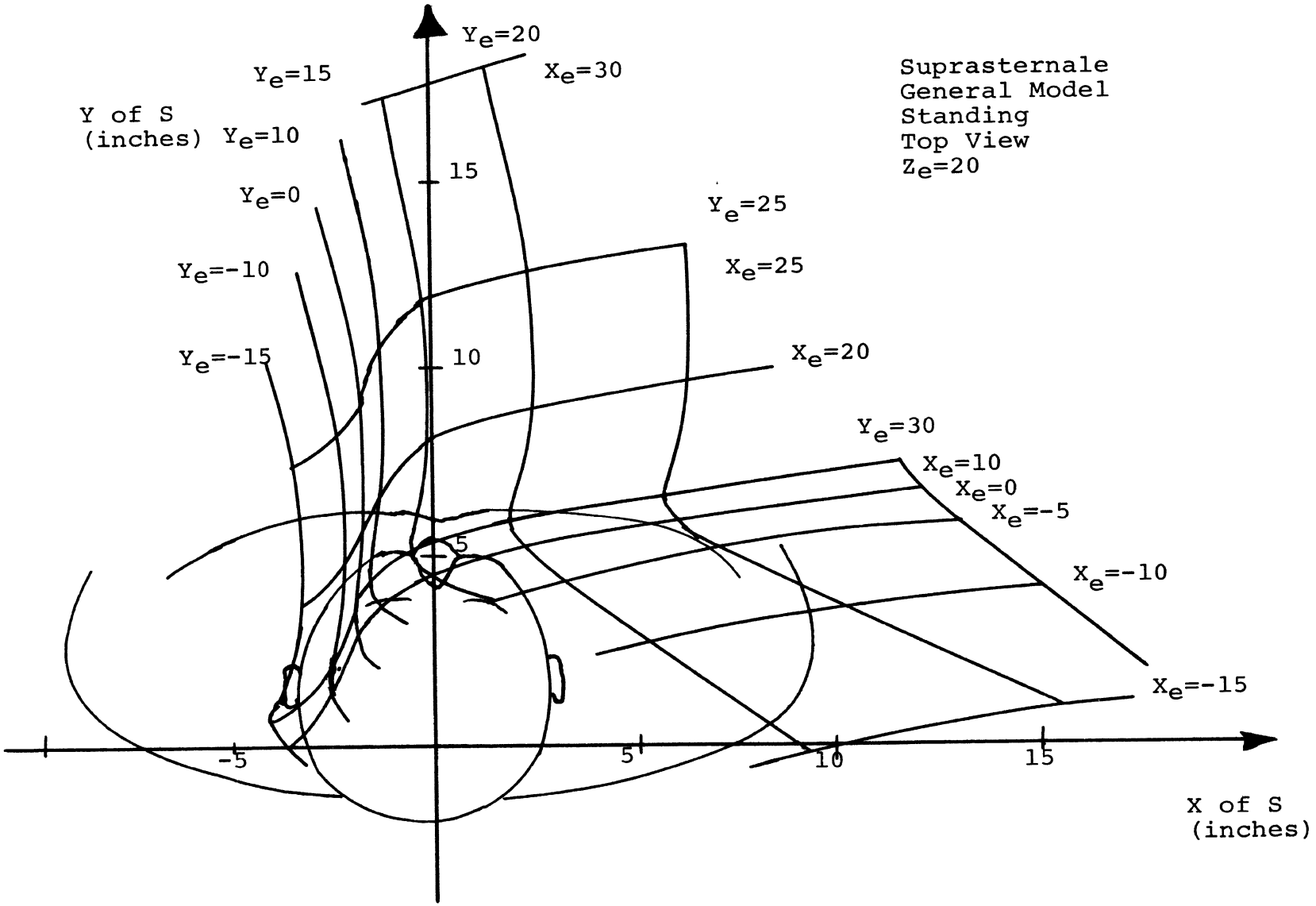
Suprasternale
General Model
Standing
Top View
Ze=20
Y of S
(inches)
Ye=20
Ye=15
Xe=30
Ye=10
15
Ye=0
Ye=25
Ye=-10
Xe=25
Ye=-15
10
Xe=20
Ye=30
Xe=10
Xe=0
Xe=-5
5
Xe=-10
Xe=-15
-5
5
10
15
X of S
(inches)

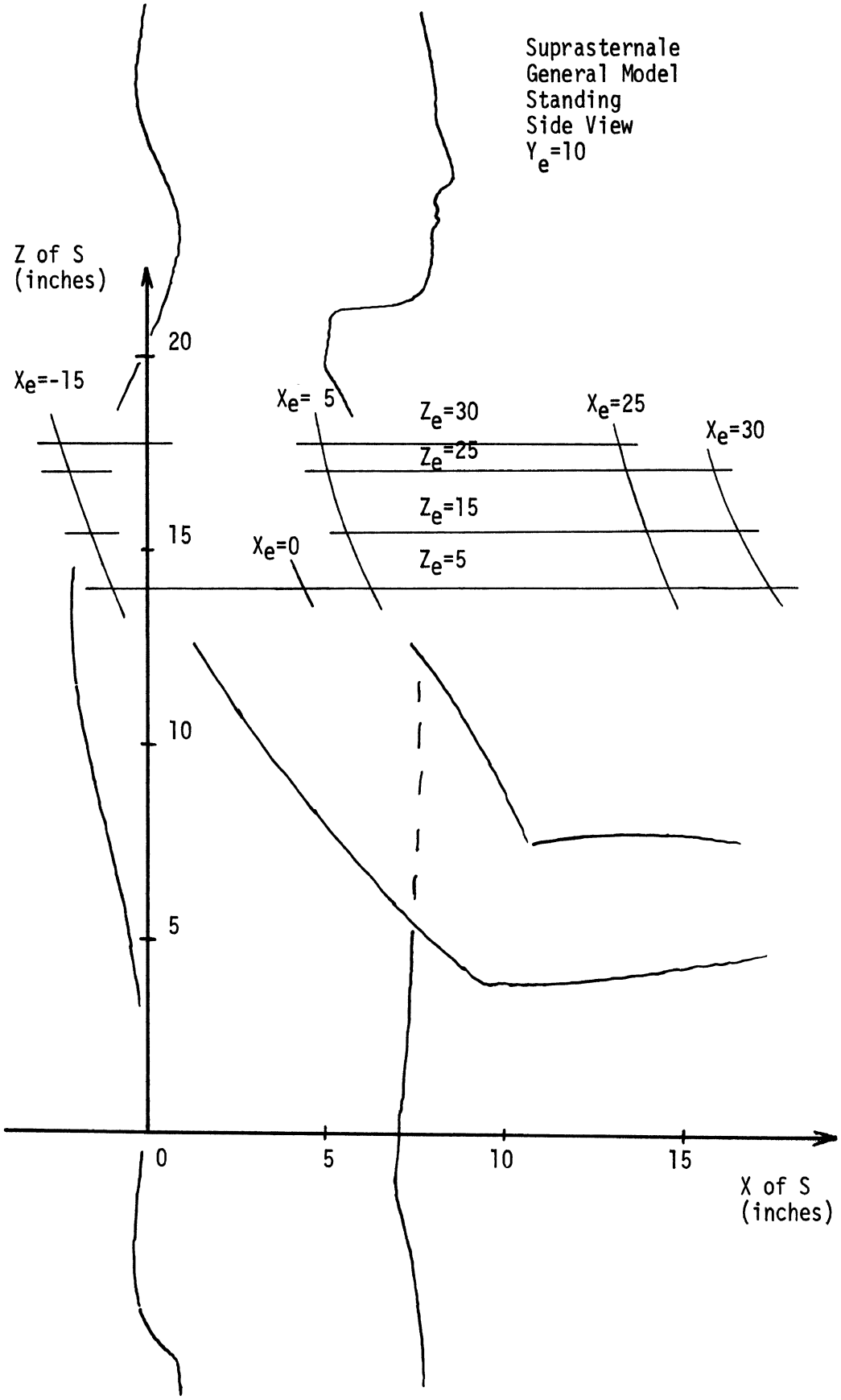
Suprasternale
General Model
Standing
Side View
Y_e=10
Z of S
(inches)
20
15
10
5
X_e=-15
X_e= 5
Z_e=30
X_e=25
X_e=30
Z_e=25
Z_e=15
X_e=0
Z_e=5
0
5
10
15
X of S
(inches)

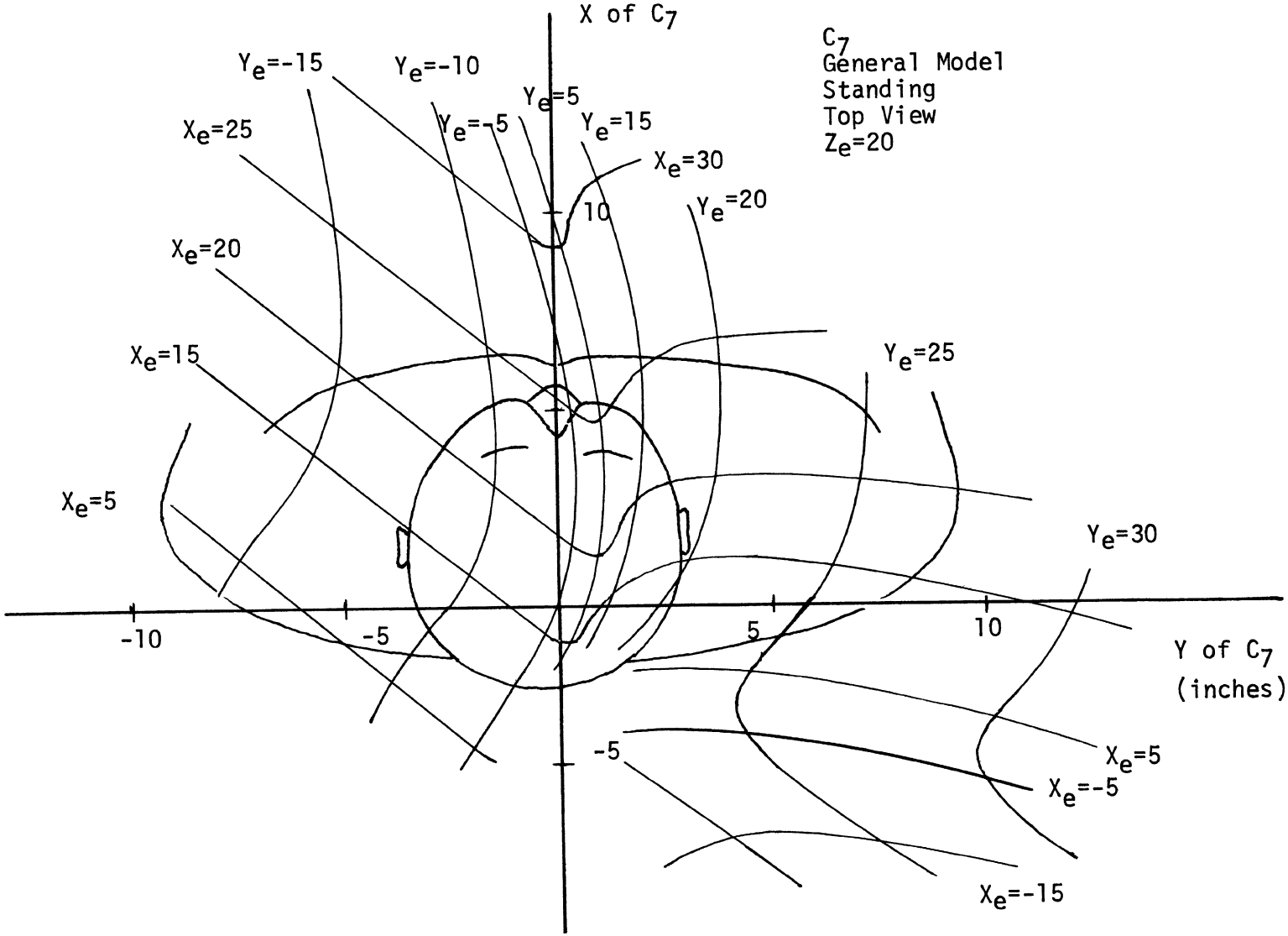
X of C_7
C_7
General Model
Standing
Top View
Z_e=20
Y_e=-15
Y_e=-10
Y_e=5
Y_e=-5
Y_e=15
X_e=25
X_e=30
10
Y_e=20
X_e=20
X_e=15
Y_e=25
X_e=5
Y_e=30
-10
-5
5
10
Y of C_7
(inches)
-5
X_e=5
X_e=-5
X_e=-15

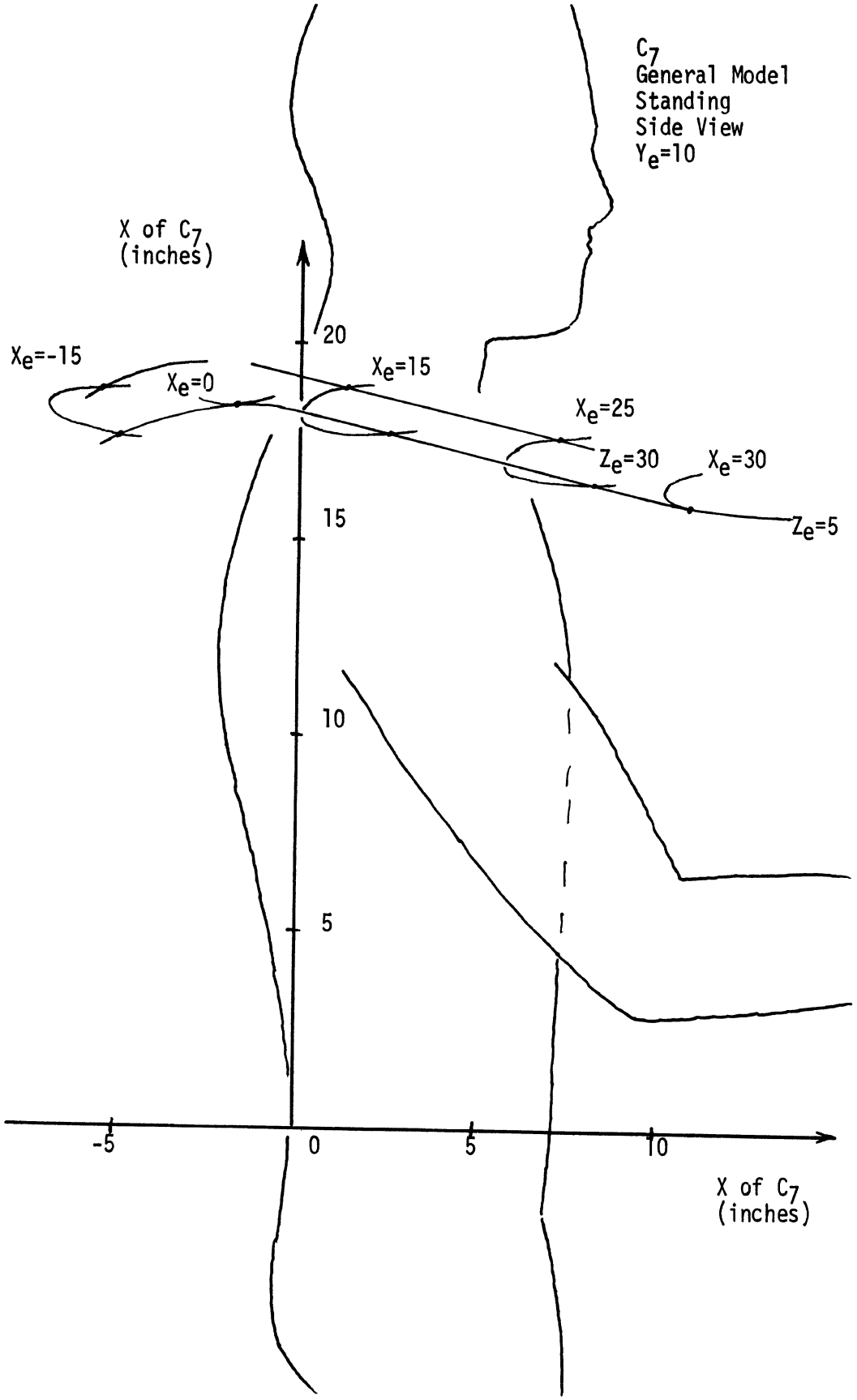
C7
General Model
Standing
Side View
Ye=10
X of C7
(inches)
20
15
10
5
Xe=-15
Xe=0
Xe=15
Xe=25
Ze=30
Xe=30
Ze=5
-5
0
5
10
X of C7
(inches)

SUMMARY SHEET FOR LOWER SPINE: T_4, T_8, T_{12} and L_2 SURFACE MARKERS

GENERAL-STANDING MODEL

Positioning Pattern

The summary sheet given in Appendix I for the lower spine is generally valid for the present standing model and will not be repeated here.

Limitations in the Prediction Equations

For the lower spine, the prediction equations for the standing model may not be as accurate as for the seated model. This possible inaccuracy is caused by three interrelated factors. First, the sample size of the data base is smaller. Second, the subject variability is much larger for standing reach tests. When standing, the subject has far greater freedom in positioning because he can bend and rotate on his legs. Third, the underlying true relationship which is being predicted is much more complicated for standing tests. When standing, the subject has two objectives. His primary objective is to reach the target. But unlike the seated tests, he must also concentrate on keeping his balance. This secondary objective of balance adds another order of complexity to the prediction equations.

In the seated tests, the positioning pattern is completely consistent with the target position. If the target moves forward (or to the right), the spine shifts forward (or to the right). For the standing tests, the positioning pattern becomes inconsistent. For sub-maximal reaches forward (or to the right) the subject will actually push his lower spine back (or to the left) to keep his balance as he bends or tilts his torso. These detailed variations in lower spine position are not adequately shown on the graphs since the Z coordinates of the spinal markers are constants. The subject variability is so large that the regression equation cannot account for variation in the Z coordinate. Constant Z values create horizontal lines on the graphs and individual, overlapping segments of that line cannot be detected graphically. However, the actual regression equation does in fact partially access and record the influence of balance when predicting the X and Y coordinates.

Note: These possible inaccuracies for the lower spine are not as pronounced for the shoulder girdle. The mobility of the shoulder girdle is much larger and it is far easier to detech the variations in position. The adjustments for balance are negligible when considered with respect to shoulder girdle movement.

A quarter inch shift in L_2 for balance does not have a significant effect on an 18 inch movement of the right acromion. Balancing is achieved by moving the center of gravity of the body, that is by moving or flexing the lower spine. There is no direct effect on shoulder girdle because the coordinates of the markers on the upper torso are given with respect to the observed coordinates of L_5 surface.

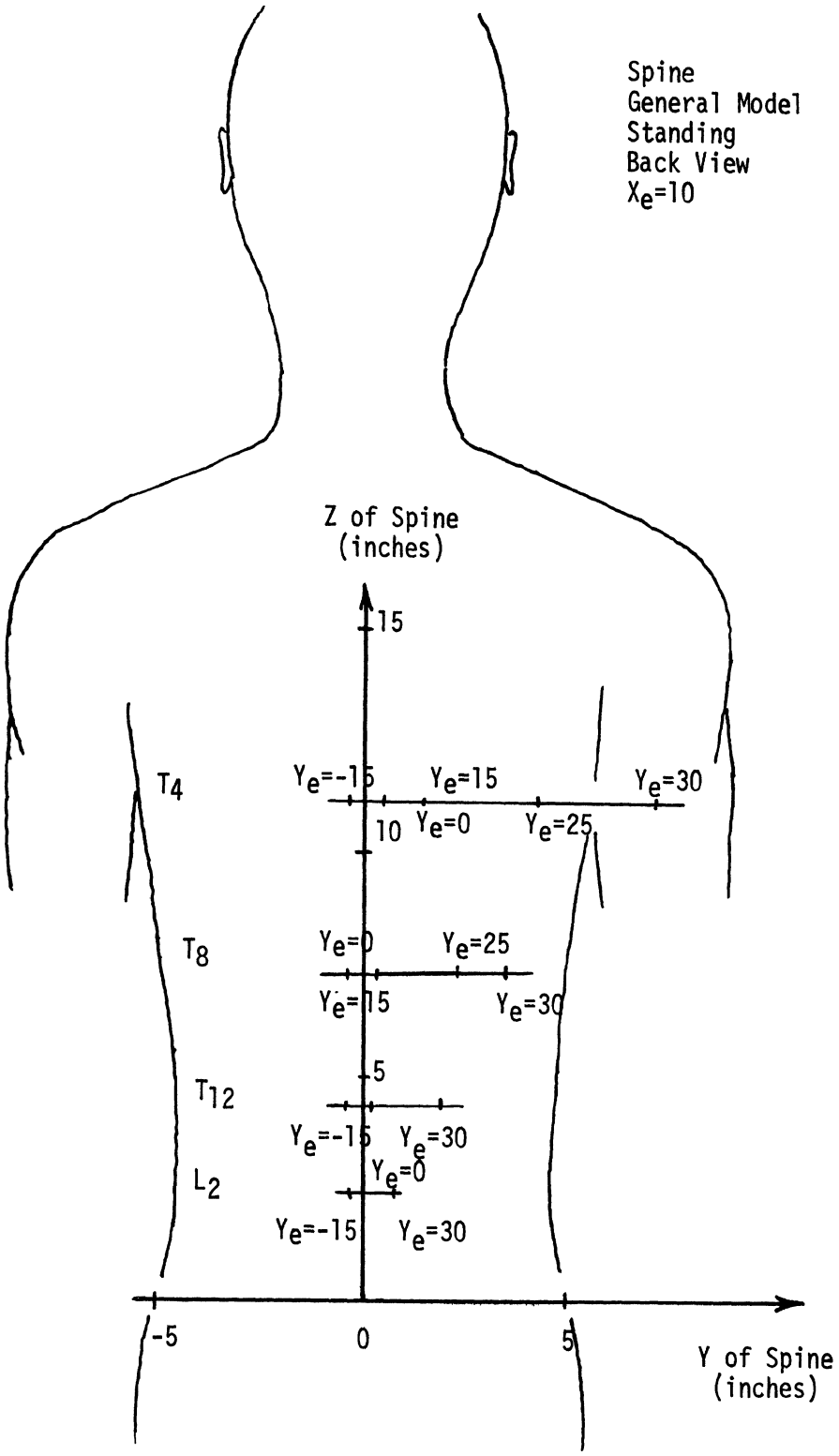
Spine
General Model
Standing
Back View
X_e=10
Z of Spine
(inches)
15
10
5
T_4
T_8
T_{12}
L_2
Y_e=-15
Y_e=15
Y_e=30
Y_e=0
Y_e=25
Y_e=0
Y_e=25
Y_e=15
Y_e=30
Y_e=-15
Y_e=30
Y_e=0
Y_e=-15
Y_e=30
-5
0
5
Y of Spine
(inches)

Spine
General Model
Standing
Side View
Y_e=10

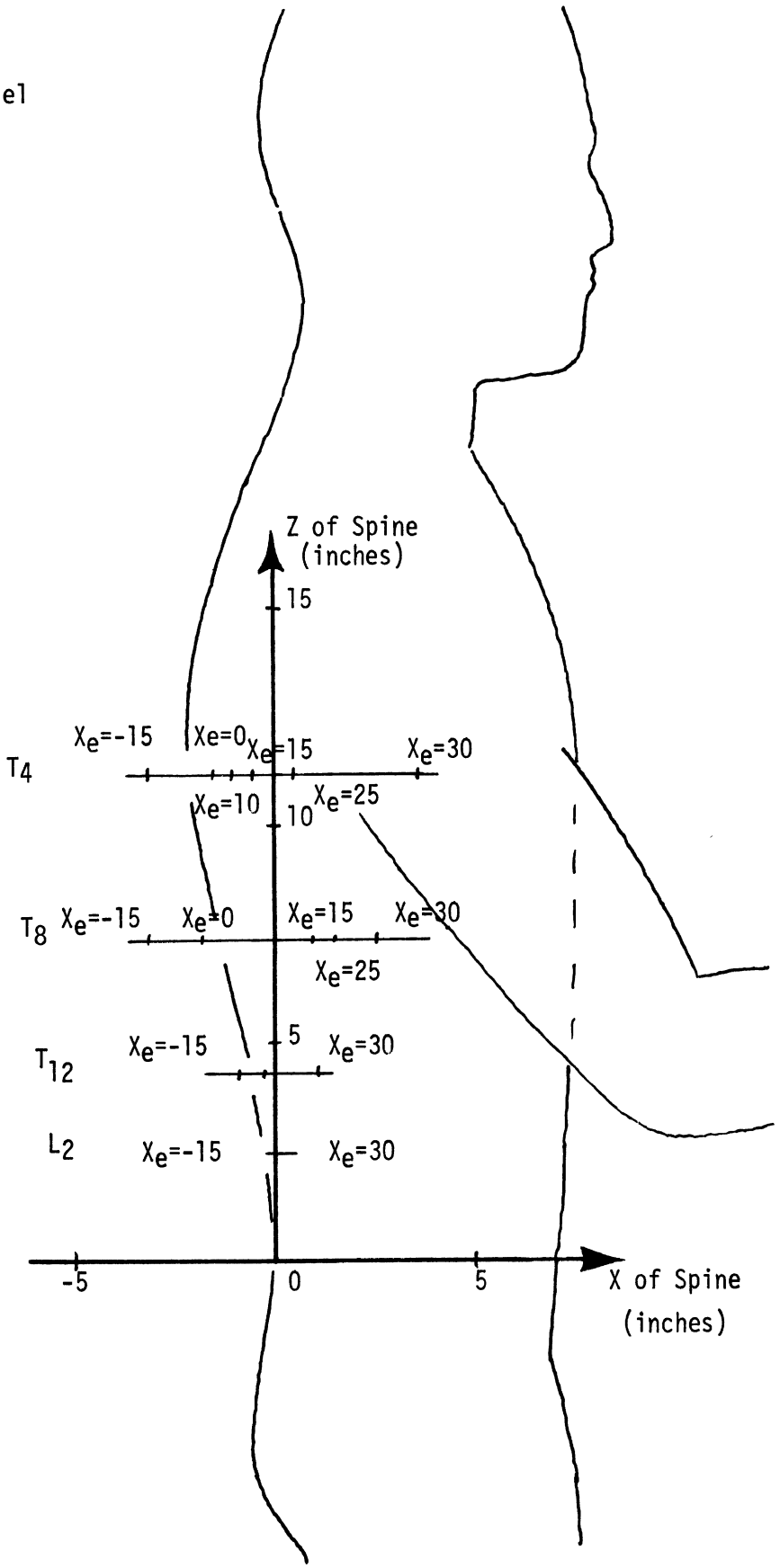

APPENDIX J

GRAPHS OF SURFACE MARKER COORDINATES FOR BOTH SEATED AND STANDING SUBJECTS

With Selected Anthropometry (Anthropometric Model)

The following graphs depict the predicted coordinates of the torso surface markers (relative to the L_5 surface marker) for various elbow positions and specified anthropometric dimensions. The seated and standing anthropometric models were evaluated using 5 percentile and 95 percent anthropometry. The anthropometric values used are (in inches and pounds):

Variable	5%	95%
Stature	65.86	73.89
Sitting Height	34.70	38.80
Chest Circumference	34.86	43.08
Biacromial Breadth	16.04	17.26
Humeral Length	11.87	14.08
Body Weight	140.15	210.76

These values are based on the 1967 USAF Anthropometric Survey. Only the graphs for 95 percentile standing model are presented. The 5 percentile and sitting graphs are completely analogous.

The same introductory comments given at the beginning of Appendix I apply to this Appendix.

SUMMARY SHEET FOR TORSO SURFACE MARKERS
ANTHROPOMETRIC MODEL

95 PERCENTILE - STANDING SUBJECT

Positioning Pattern

The conclusions concerning how torso position is affected by elbow position for the 95 percentile--standing subject are, in general, completely analogous to the results observed for the general models discussed in Appendixes I and J. The inclusion of anthropometric variables in the prediction equations proved significant only for estimating the Z coordinates of the surface landmarks. In some cases, the anthropometric variables are not included at all in the prediction equation for X and Y. In the case where the step-wise regression procedures incorporated anthropometric variables in the X and Y equation, the contribution of these terms is marginal.

Two factors are responsible for the lack of significance of the anthropometric variables in estimating the X and Y coordinates. First, the subject pool used in deriving the regression equations is relatively uniform. The extremes of the general population are not present in the much more selective USAF population. This selectivity effect is magnified because the size of the actual sample population is relatively small. The second and more important factor responsible for the lack of significance of anthropometry is the range of reach position. The influence of anthropometry on the X and Y coordinates is of major significance only for maximal reaches. The top views of a tall subject and a short subject sitting normally are almost identical when the X and Y coordinates of the surface markers are considered with respect to L_5. Differences are only noticeable if the subjects have to twist or extend their upper torsos.

The data base for the present analysis was confined to reach positions on the surface of or inside of a sub-maximal reach sphere; consequently, the reach positions capable of generating maximum anthropometric differences in the X and Y direction are not included in the present analysis.

For the Z coordinates of the surface landmarks, the exact opposite condition was realized. The anthropometric variables (particularly stature and sitting height) always proved to be significant. The increase increase in precision of the anthropometric model over the general model is primarily due to a reduction in the Z-component of the residual vector.

Limitations in the Prediction Equations

The predictions from the anthropometric models appear to be consistent and rational throughout the entire reach sphere.

However, there are some restrictions on the range of anthropometric values which can be substituted into the equations. The predictions will become completely erroneous if anthropometric dimensions less than the 5 percentile limit or greater than the 95 percentile limit are used. This restriction is not as critical for stature and weight. The sample population was partially stratified to include subjects approaching the 5 and 95 percentile limits. The restriction is needed primarily when using chest circumference and humeral length measurements. These two anthropometric variables appear as squared and cubed terms in a large majority of the equations. These terms will blow up if the 5 and 95 percentile limits are exceeded.

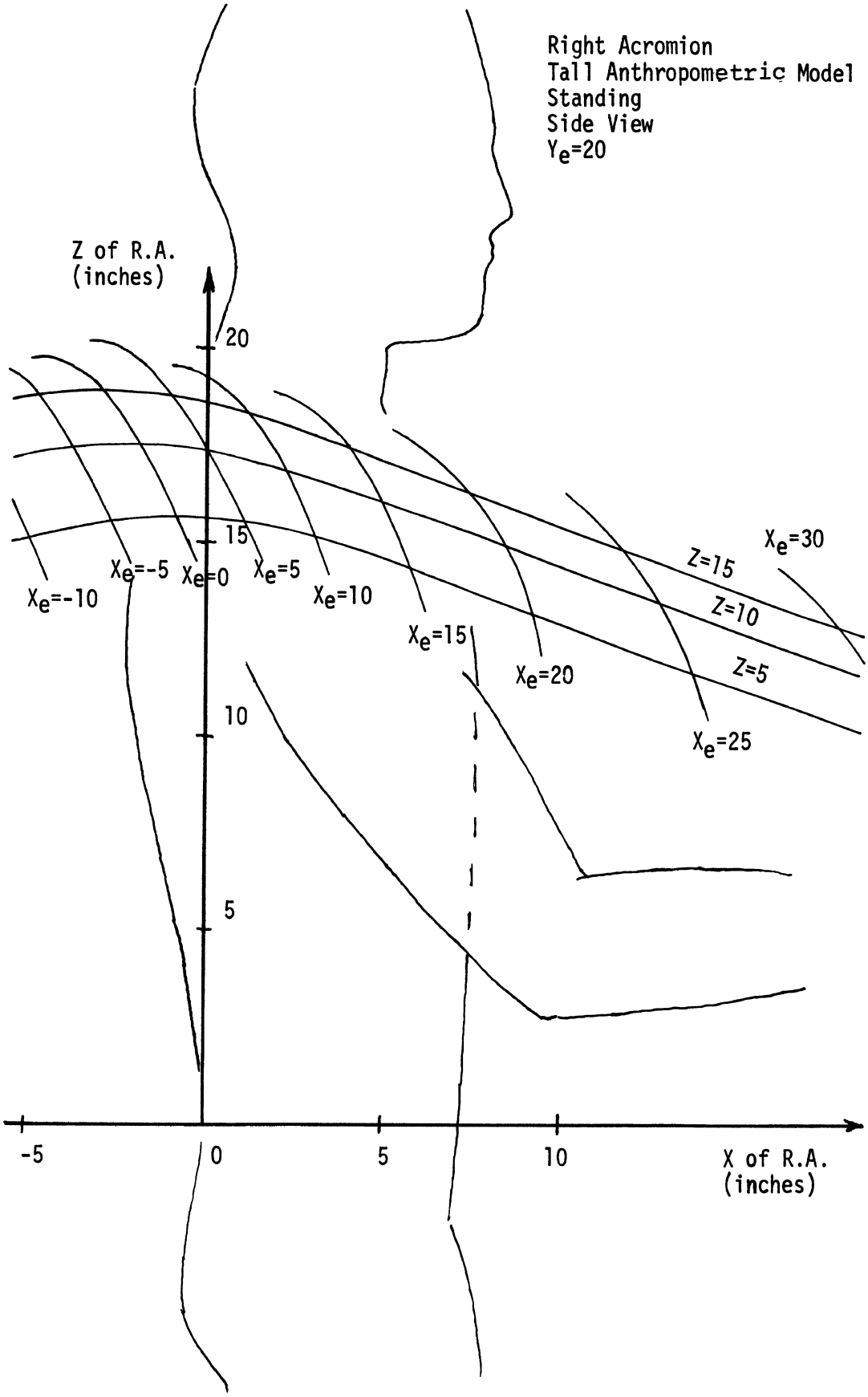
Right Acromion
Tall Anthropometric Model
Standing
Side View
Y_e=20
Z of R.A.
(inches)
20
15
10
5
X_e=-10
X_e=-5
X_e=0
X_e=5
X_e=10
X_e=15
X_e=20
X_e=25
X_e=30
Z=15
Z=10
Z=5
-5
0
5
10
X of R.A.
(inches)

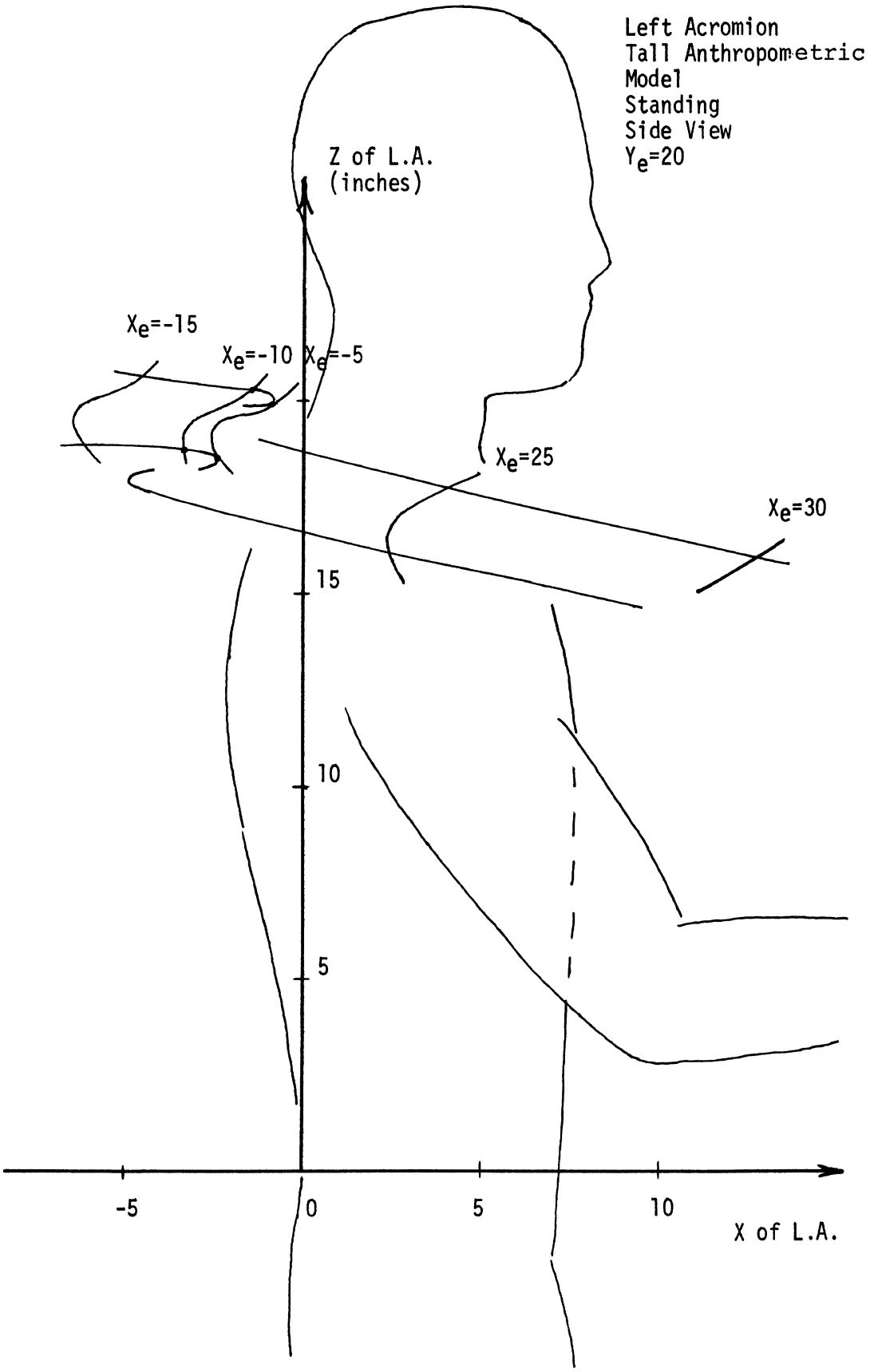
Left Acromion
Tall Anthropometric
Model
Standing
Side View
Y_e=20
Z of L.A.
(inches)
X_e=-15
X_e=-10
X_e=-5
X_e=25
X_e=30
15
10
5
-5
0
5
10
X of L.A.

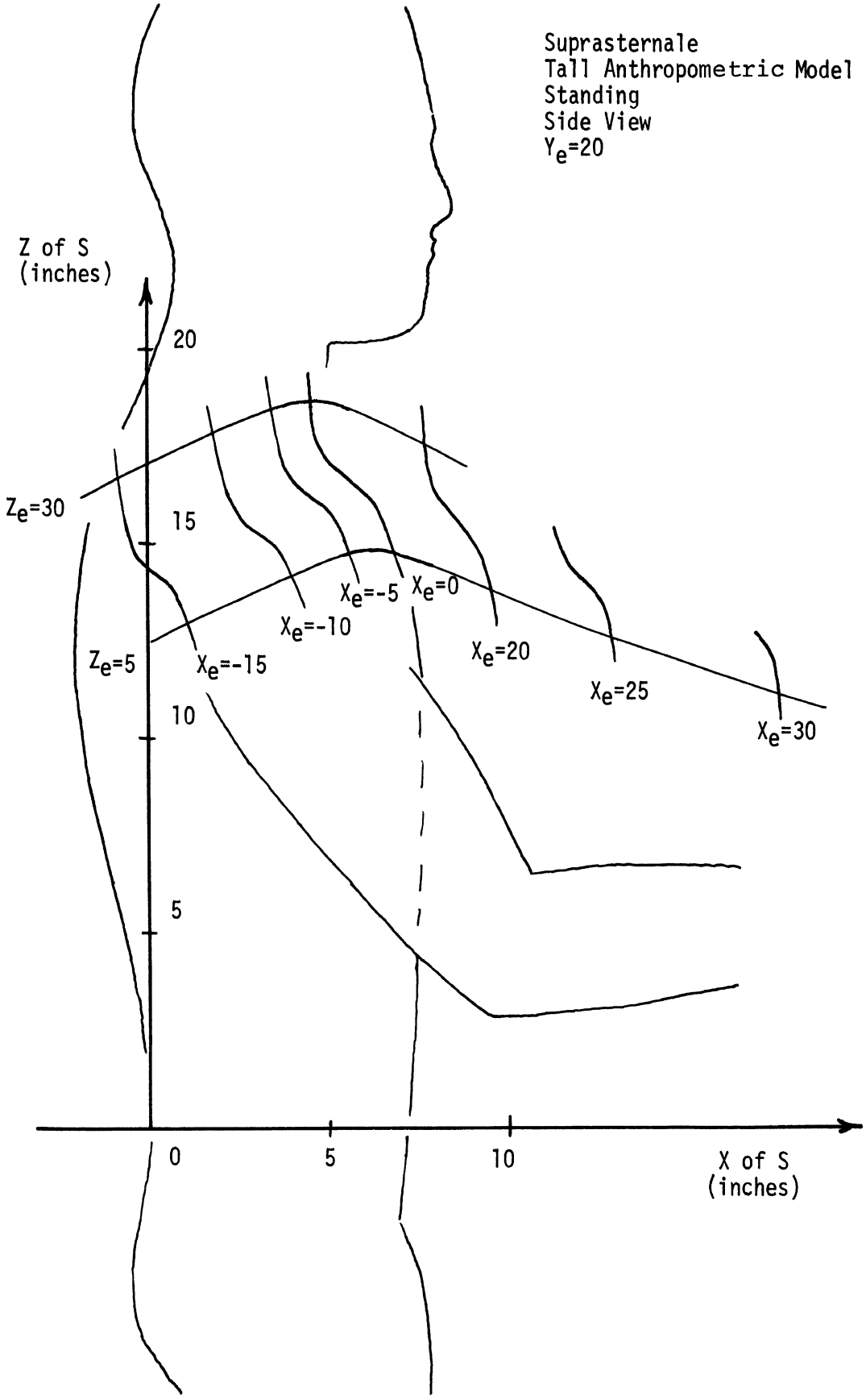
Suprasternale
Tall Anthropometric Model
Standing
Side View
Y_e=20
Z of S
(inches)
20
15
10
5
Z_e=30
Z_e=5
X_e=-15
X_e=-10
X_e=-5
X_e=0
X_e=20
X_e=25
X_e=30
0
5
10
X of S
(inches)

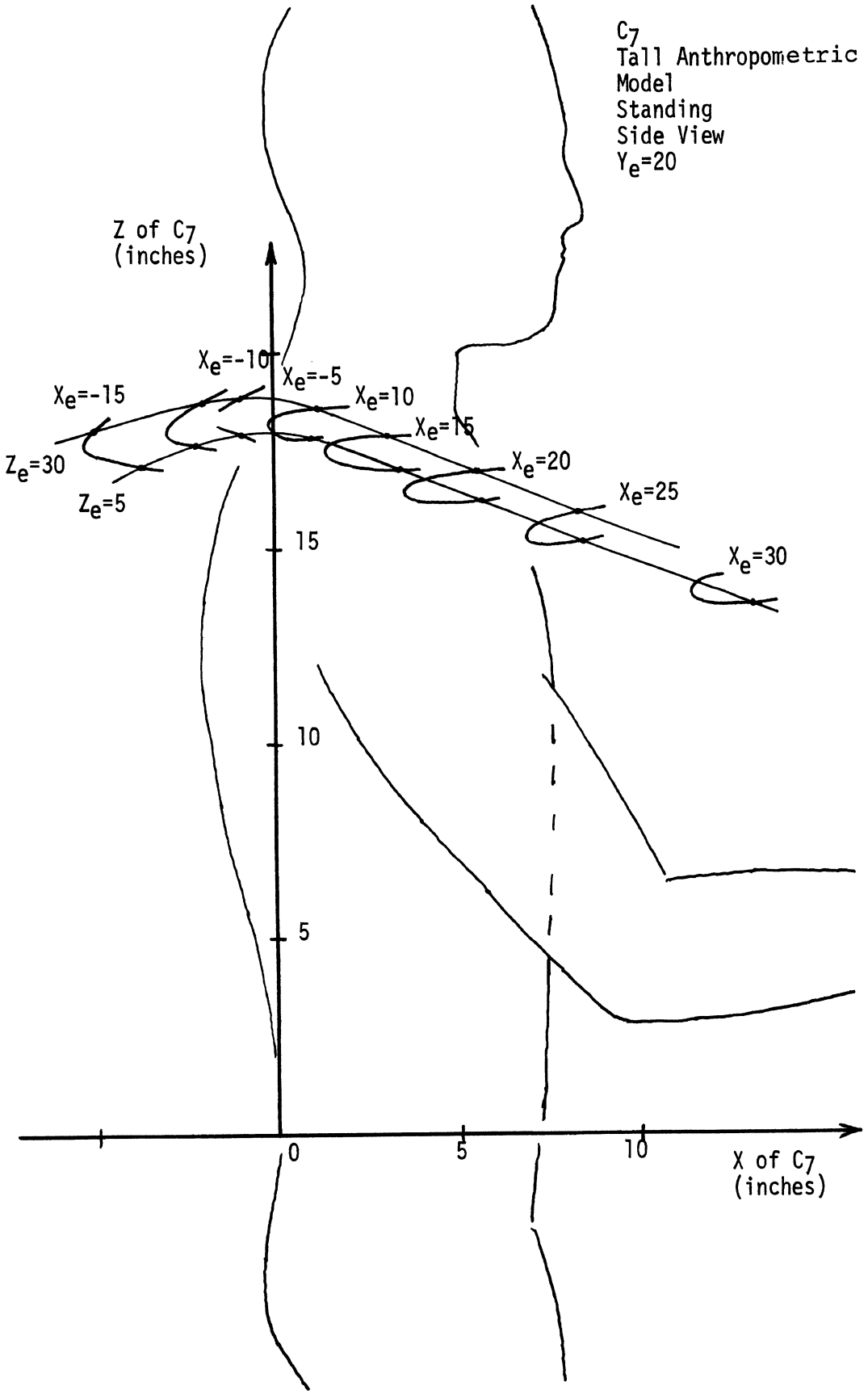
C7
Tall Anthropometric
Model
Standing
Side View
Ye=20
Z of C7
(inches)
Xe=-10
Xe=-5
Xe=-15
Xe=10
Xe=15
Xe=20
Xe=25
Xe=30
Ze=30
Ze=5
15
10
5
0
5
10
X of C7
(inches)

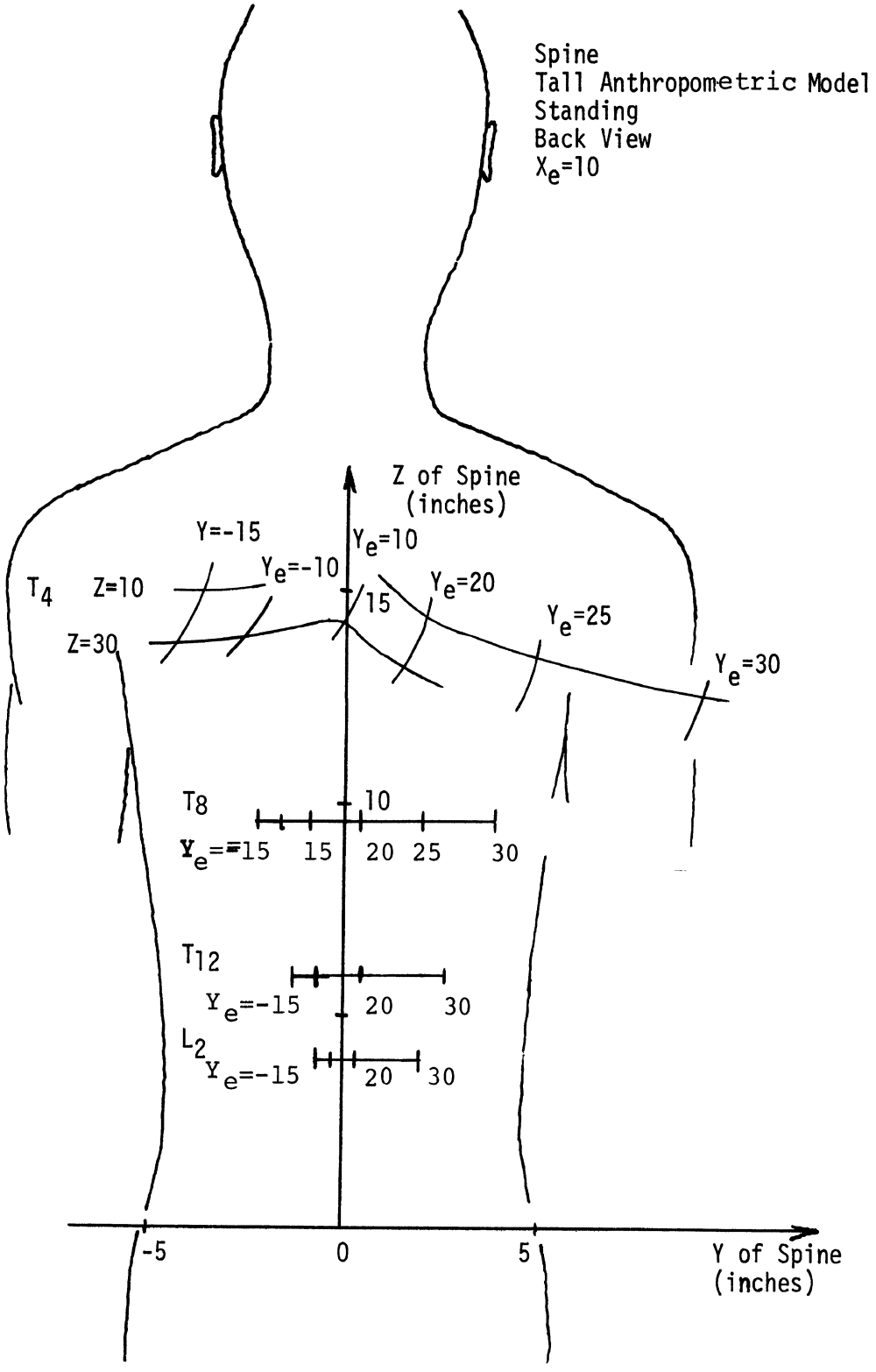
Spine
Tall Anthropometric Model
Standing
Back View
X_e=10
Z of Spine
(inches)
Y=-15
Y_e=10
Y_e=-10
Y_e=20
Y_e=25
Y_e=30
T_4 Z=10
Z=30
15
T_8
10
Y_e=-15 15 20 25 30
T_{12}
Y_e=-15 20 30
L_2
Y_e=-15 20 30
-5
0
5
Y of Spine
(inches)

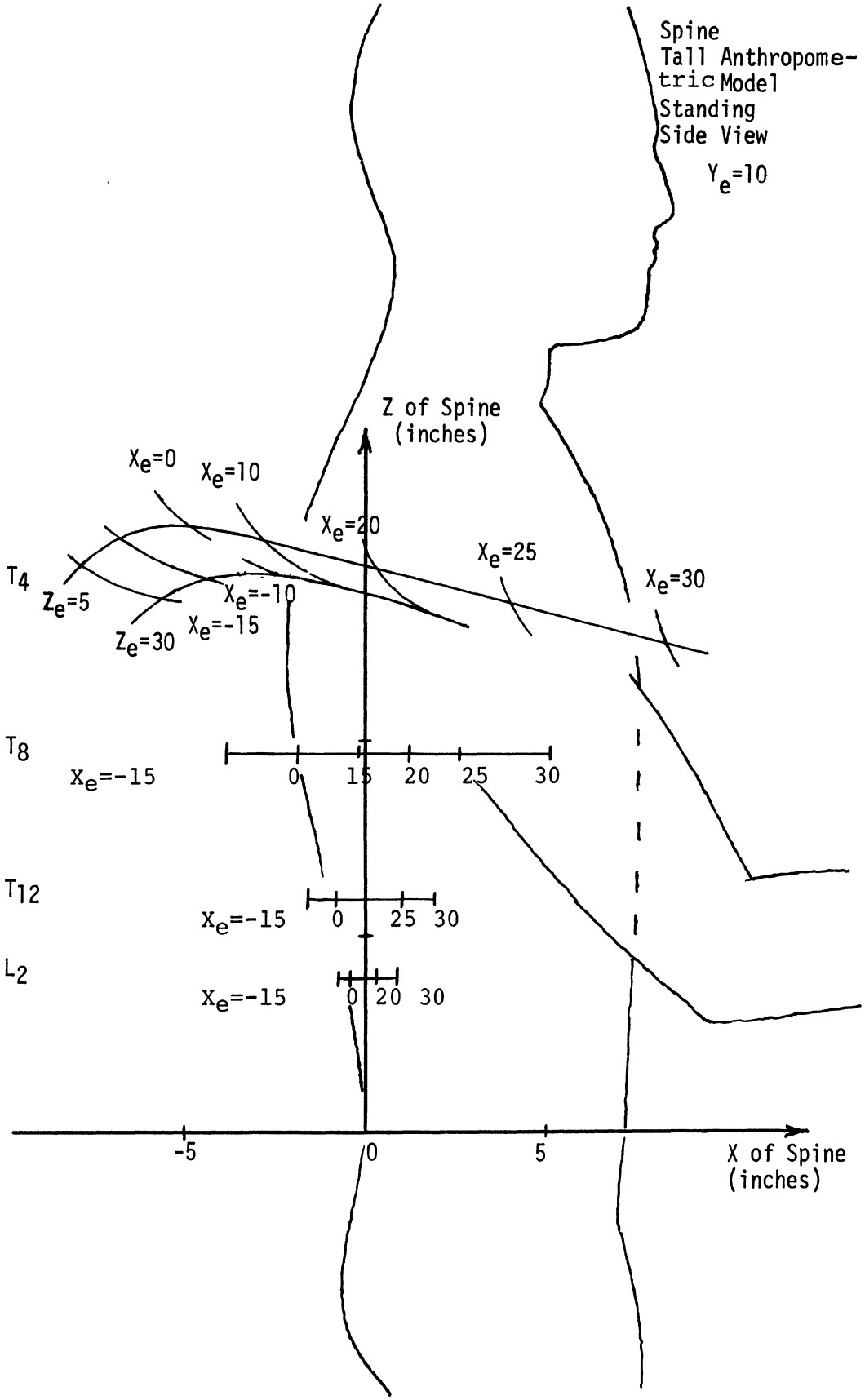
Spine
Tall Anthropometric Model
Standing
Side View
Y_e=10
Z of Spine
(inches)
X_e=0
X_e=10
X_e=20
X_e=25
X_e=30
X_e=-10
X_e=-15
Z_e=5
Z_e=30
T4
T8
X_e=-15
0
15
20
25
30
T12
X_e=-15
0
25
30
L2
X_e=-15
0
20
30
-5
0
5
X of Spine
(inches)

SUMMARY SHEET FOR L_5 SURFACE MARKER

Positioning Pattern

There are individual variations between the standing and the sitting results and between the general and the anthropometric models, but the conclusions stated below tend to hold in all cases.

1. Increasing X_e, elbow movement forward, causes L_5 to move forward. The forward deviation in L_5 increases in size as the forward reach distance becomes maximal. There is also a tendency for the L_5 surface marker to be deflected to the right as X_e increases. The movement in the X and Y directions results from the torso bending forward and rotating slightly. There is a relatively large increase in the Z coordinate of the L_5 surface marker as the elbow moves forward. The usually relaxed and semi-compressed lower back extends and stretches to accommodate maximal forward reaches.

2. Increasing Y_e, elbow movement from left to right across the body, causes the L_5 surface marker to shift to the right and to move slightly forward. These movements occur because the upper torso is rotating from left to right in response to the elbow movement. The change in the Z coordinate of the L_5 surface marker is negligible for lateral movement of the elbow.

3. Increasing Z_e, elbow movement upward, causes the L_5 surface marker to rise slightly. The increase in the vertical height of L_5 becomes significant for reach targets above shoulder level. A forward deflection in L_5 is also noticed when the elbow is elevated. The rate of increase in the X coordinate of L_5 is the largest when the elbow is moving from waist level to chest level. The forward deflection in L_5 is almost maximum when the elbow attains shoulder level. There is no significant variation in the Y coordinate of L_5 as Z_e increases.

Limitations in the Prediction Equations

There does not appear to be any ranges of extrapolated reach positions for which the prediction equations become inconsistent.

APPENDIX K

GRAPHS OF THE L_5 SURFACE MARKER WITH RESPECT TO AN EXTERNAL REFERENCE MARKER

Reference Point Conversion Model

The movement of the L_5 surface marker with respect to the seat reference point (seated subject) and with respect to the floor reference point (standing subject) is depicted in the enclosed graphs. Four models or sets of prediction equations were derived for the L_5 surface marker. Top and side view graphs are presented for the general-seated model, the general-standing model and the anthropometric-standing model. Graphs are not presented for the anthropometric-seated model and only the 95 percentile subject graphs are displayed for the anthropometric-standing model. Completely analogous conclusions are derived for the anthropometric graphs which have been omitted.

The same introductory comments given at the beginning of Appendix I apply to this Appendix.

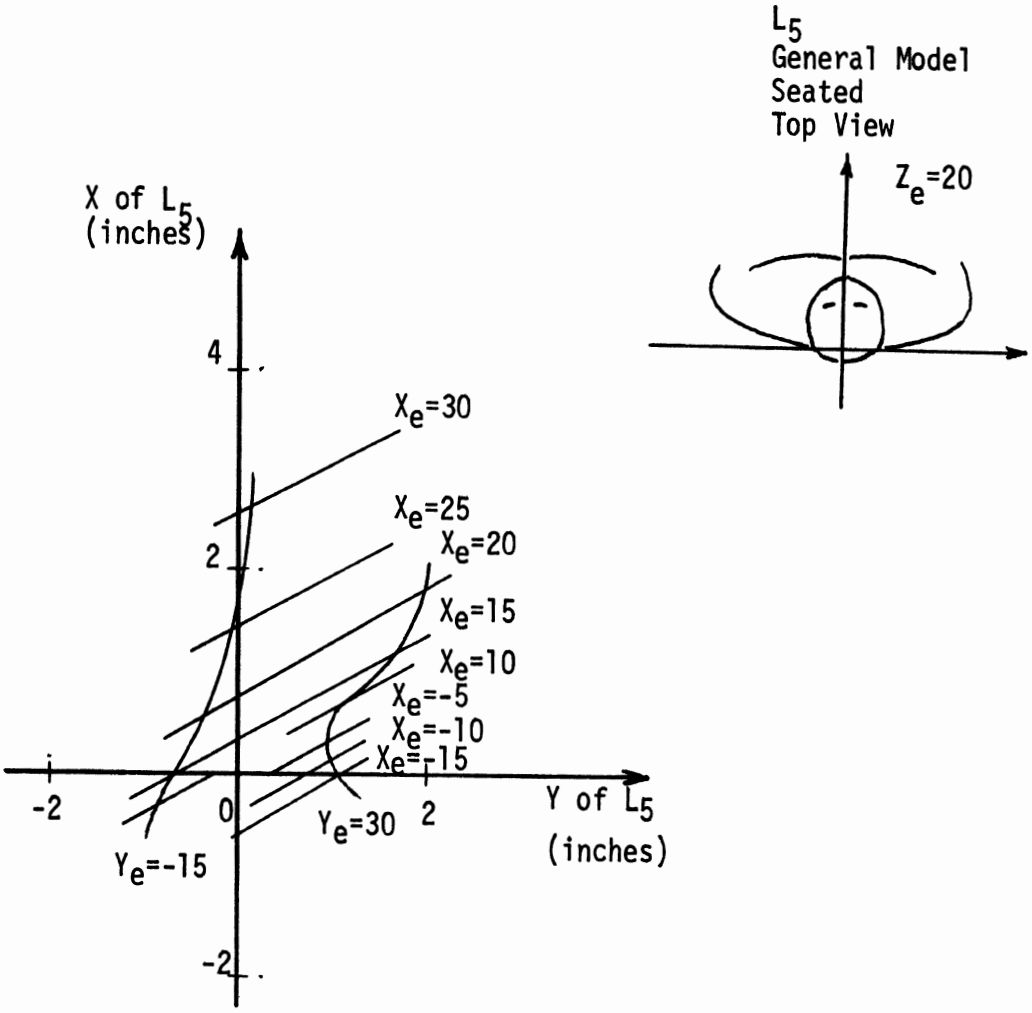
L_5
General Model
Seated
Top View
Z_e=20
X of L_5
(inches)
4
2
-2
-2
0
2
X_e=30
X_e=25
X_e=20
X_e=15
X_e=10
X_e=-5
X_e=-10
X_e=-15
Y_e=30
Y_e=-15
Y of L_5
(inches)

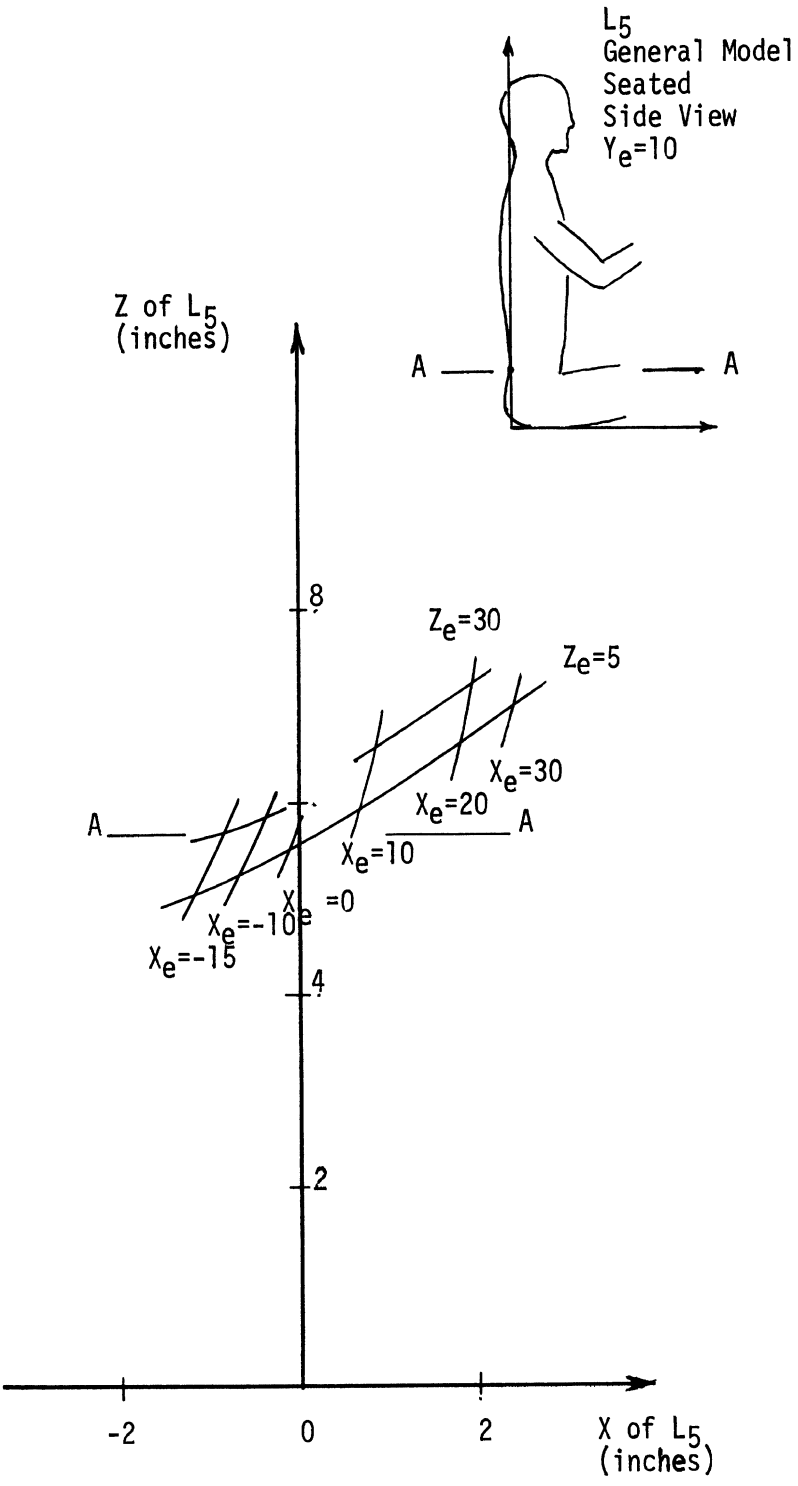
L_5
General Model
Seated
Side View
Y_e=10
A
A
Z of L_5
(inches)
8
4
2
Z_e=30
Z_e=5
X_e=30
X_e=20
X_e=10
X_e=0
X_e=-10
X_e=-15
A
A
-2
0
2
X of L_5
(inches)

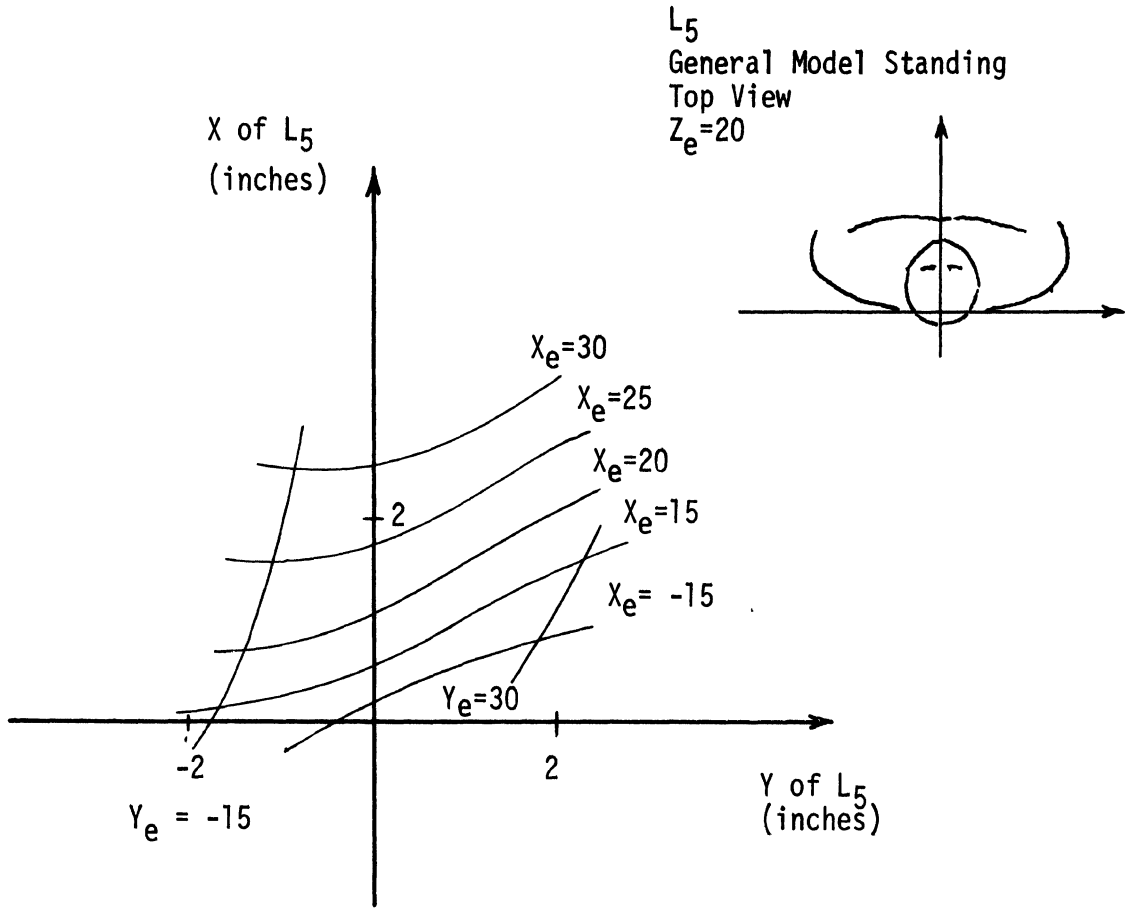
L_5
General Model Standing
Top View
Z_e=20
X of L_5
(inches)
X_e=30
X_e=25
X_e=20
X_e=15
X_e= -15
Y_e=30
2
-2
2
Y_e = -15
Y of L_5
(inches)

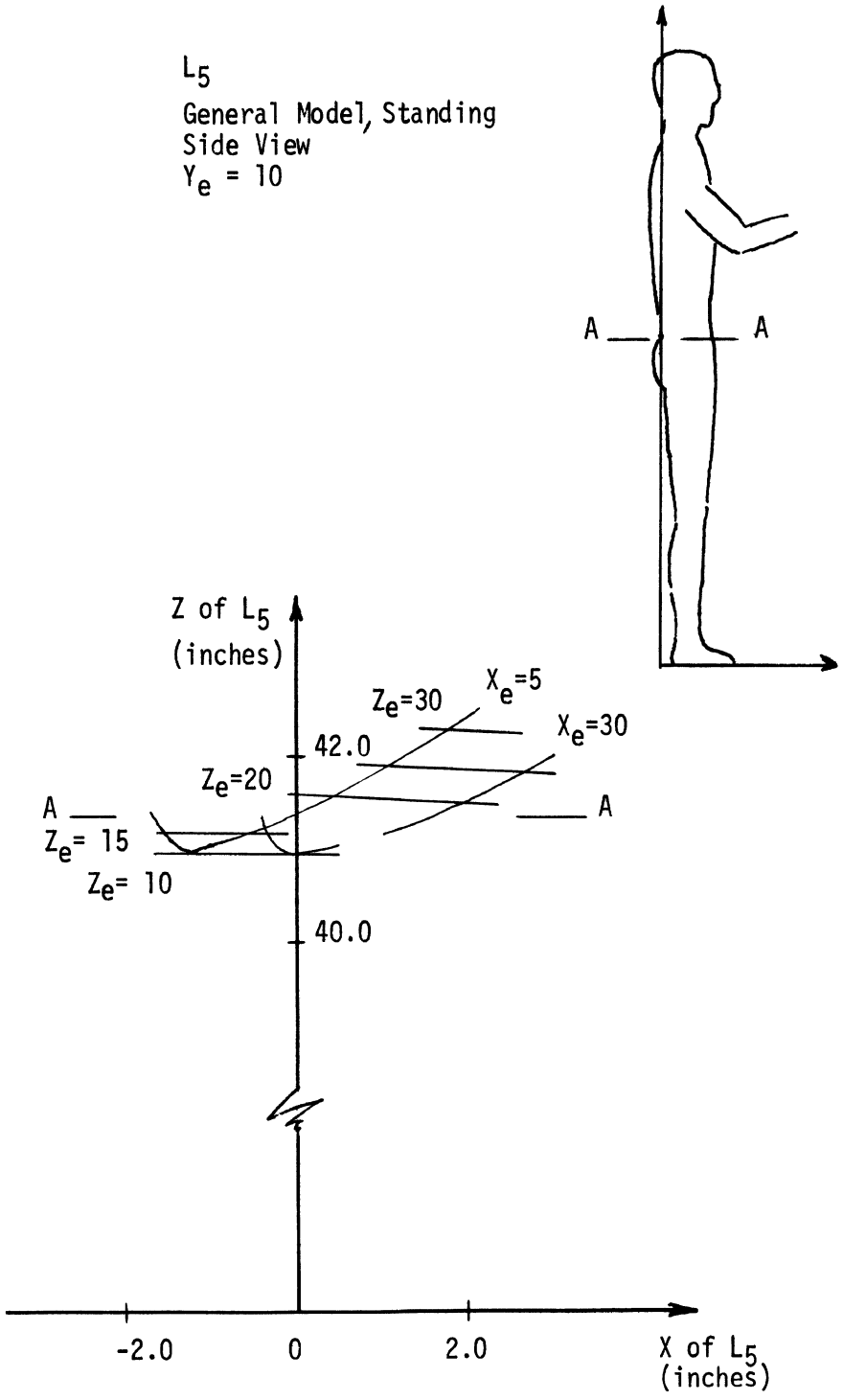
L_5
General Model, Standing
Side View
Y_e = 10
A
A
Z of L_5
(inches)
Z_e=30
X_e=5
X_e=30
42.0
Z_e=20
A
A
Z_e= 15
Z_e= 10
40.0
-2.0
0
2.0
X of L_5
(inches)

L_5

Tall Anthropometric Model
Standing
Top View
Z_e=20

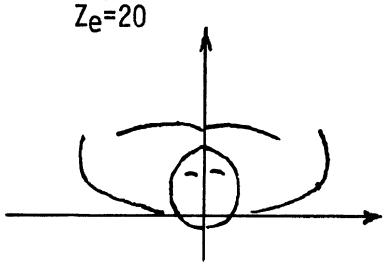

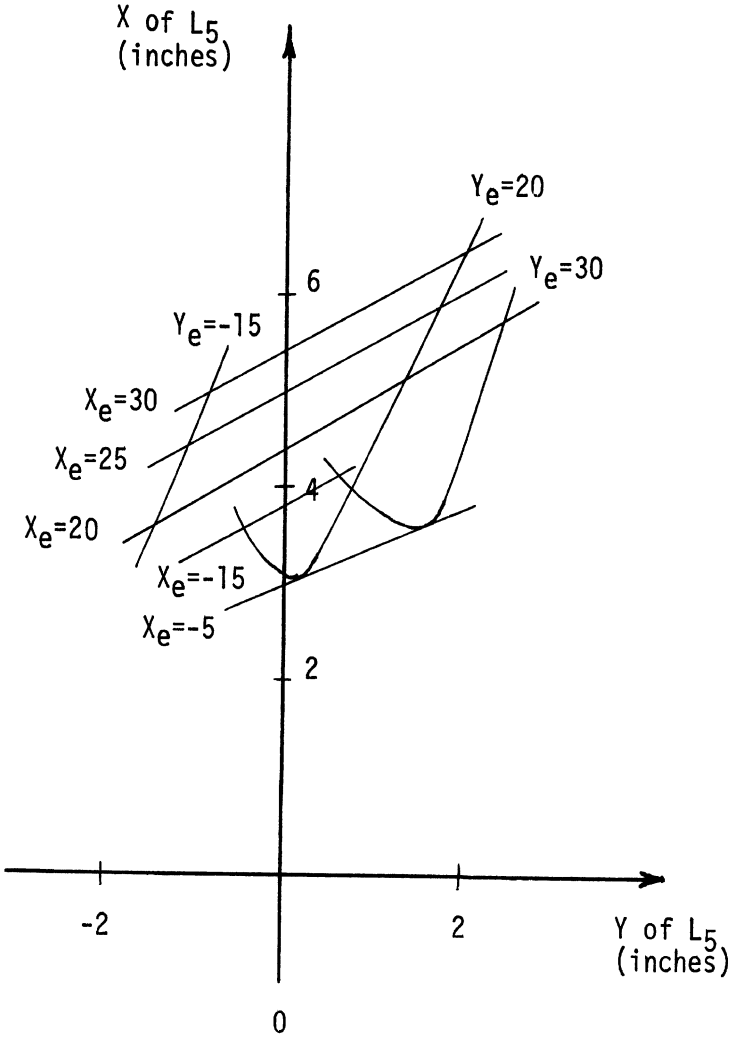

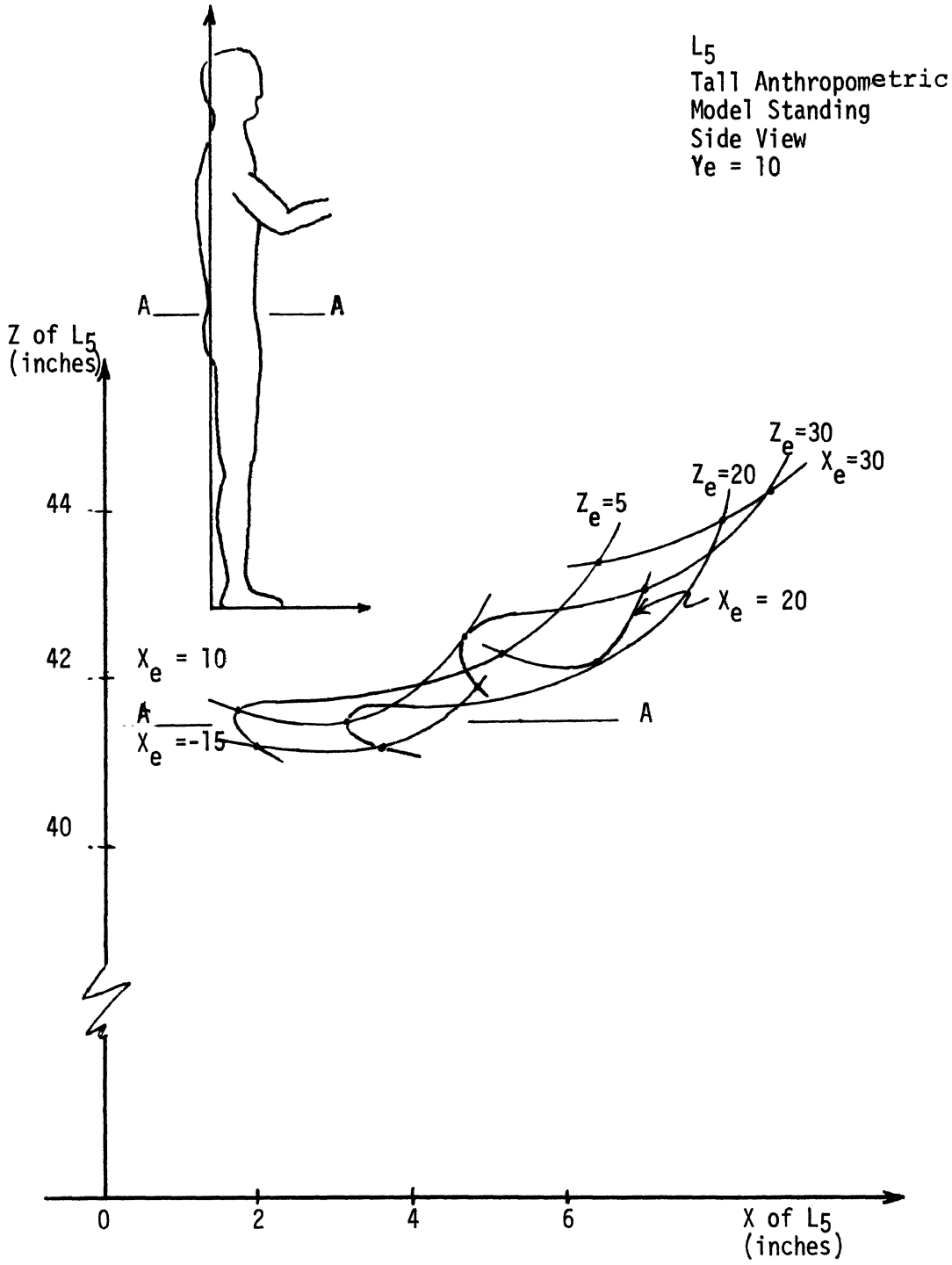
L_5
Tall Anthropometric
Model Standing
Side View
Ye = 10
A
A
Z of L_5
(inches)
44
42
40
Z_e=30
X_e=30
Z_e=20
Z_e=5
X_e = 20
X_e = 10
A
A
X_e =-15
0
2
4
6
X of L_5
(inches)

APPENDIX L

Plots of Lumbar Vectors

vs.

Angle of Lumbar Reference Vector ANG

NOTE: Surface-to-bone interspace vectors are plotted from horizontal reference axis rather than standard vertical axis.

Relationship: L_5/S_1 Interspace to L_5 Surface Mark

LAT:

Distance from L_5 Surface Mark (Inches)

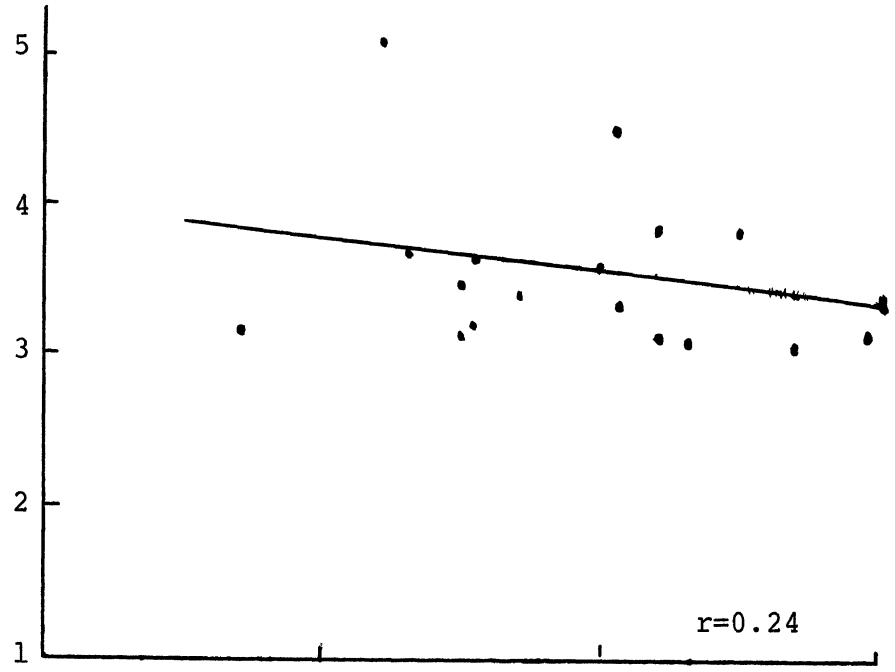

Vector Direction from Horizontal Plane of L_5/S_1 to L_5 Surface Mark (Degrees)

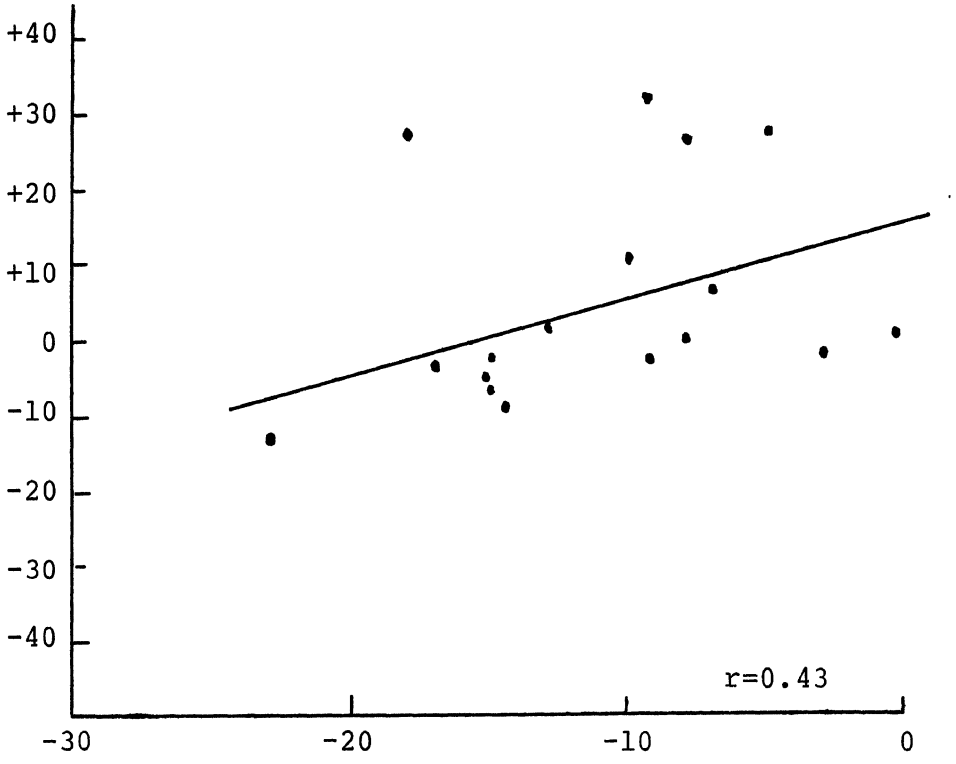

ANG = Reference Angle of Vector from L_5/S_1 to L_1/L_2 Interspaces, (positive=forward)

Relationship: L_2/L_3 Interspace to L_2 Surface Mark

LAT:

Distance from L_2/L_3 Interspace to L_2 Surface Mark

(Inches)

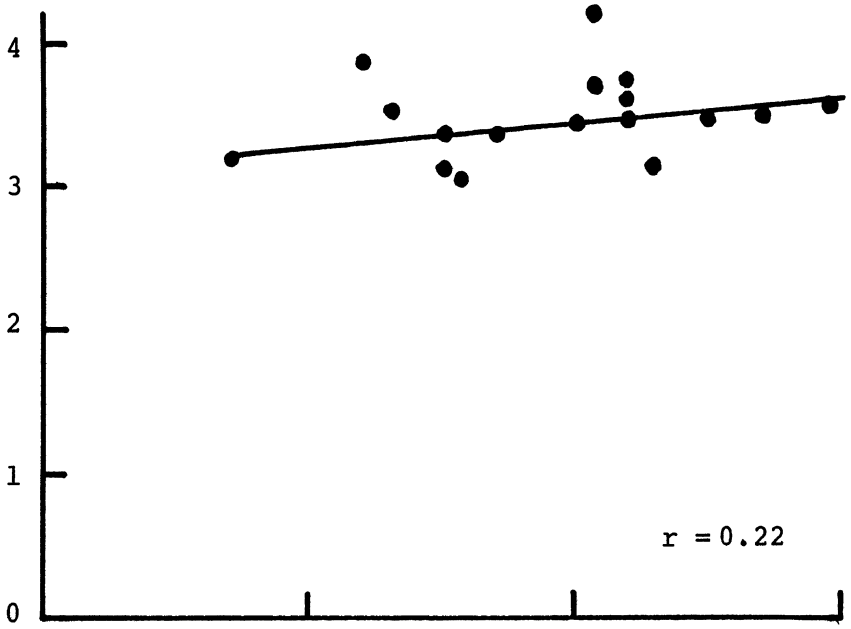

Vector Direction from Horizontal Plane of L_2/L_3 to L_2 Surface Mark

(Degrees)

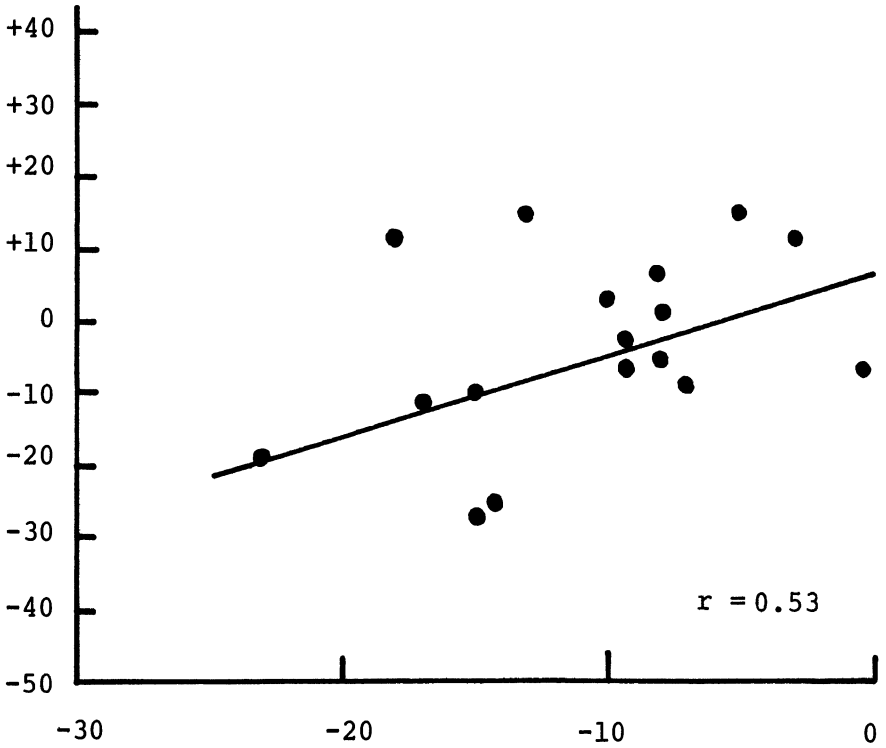

ANG = Reference Angle of Vector from L_5/S_1 to L_1/L_2 Interspaces, (positive=forward)

Relationship: L_5 Surface Mark to L_2 Surface Mark

LAT:

Distance from L_5 to L_2 Surface Mark (Inches)

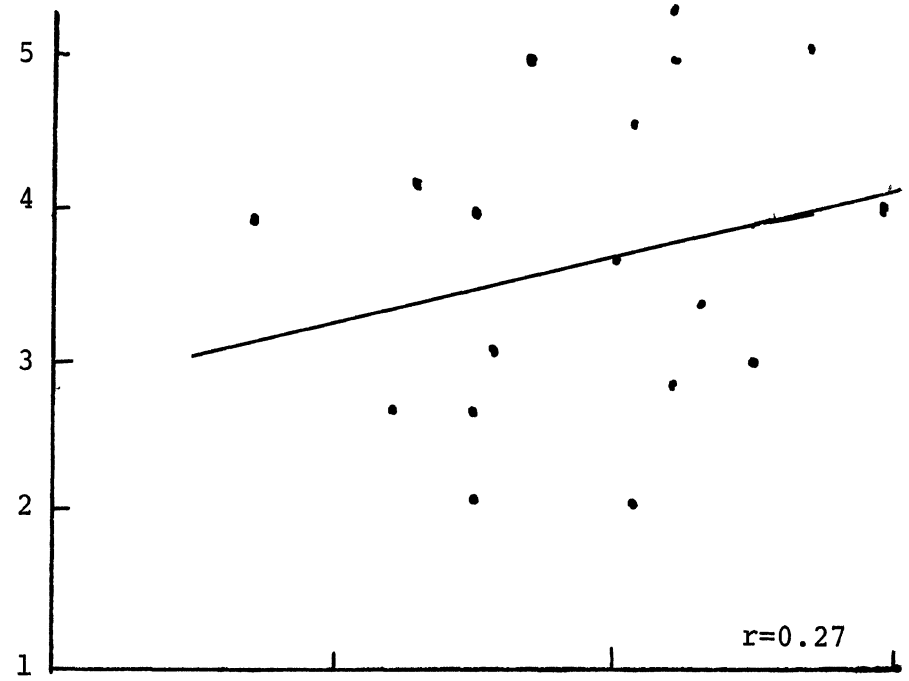

Vector Direction from Frontal Plane of L_5 to L_2 Surface Mark

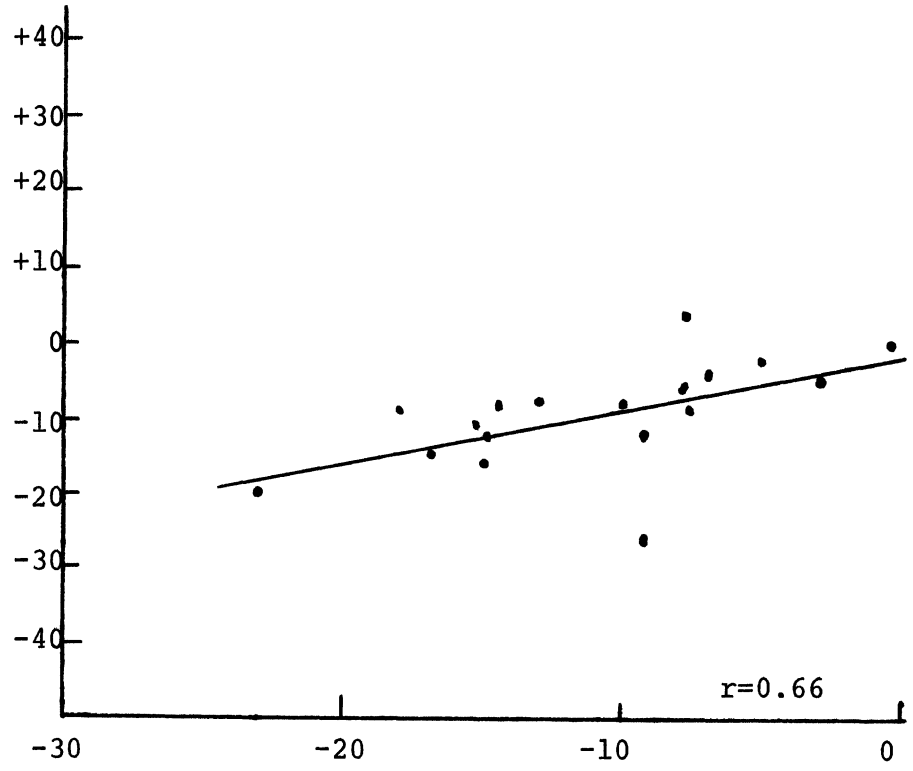

ANG = Reference Angle of Vector from L_5/S_1 to L_1/L_2 Interspaces, (positive=forward)

Relationship: L_5/S_1 Interspace to L_2/L_3 Interspace

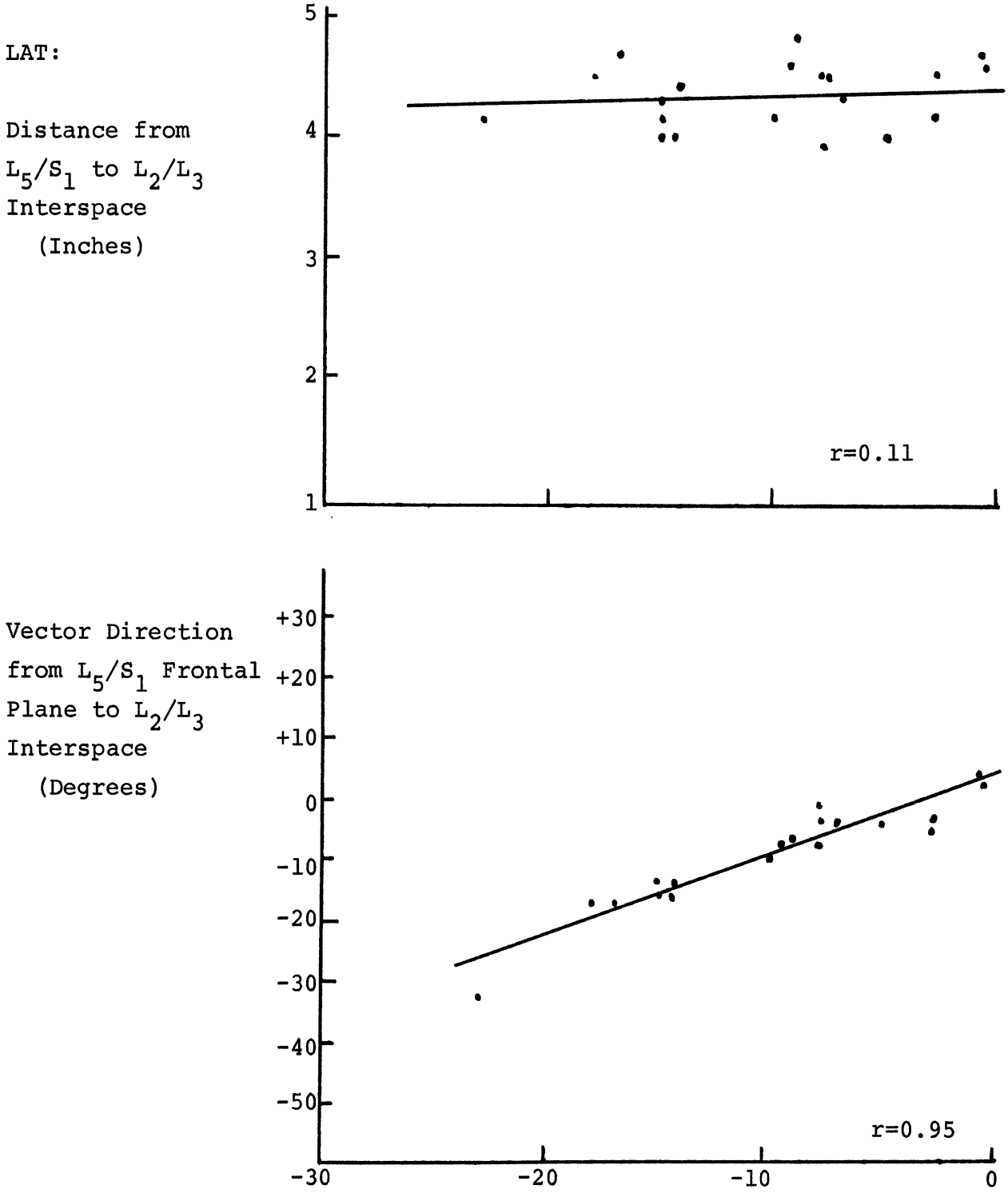

ANG = Reference Angle of Vector from L_5/S_1 to L_1/L_2 Interspaces, (positive=forward)

(See Figure 18)

Relationship: L_5/S_1 Interspace to L_4/L_5 Interspace

LAT:

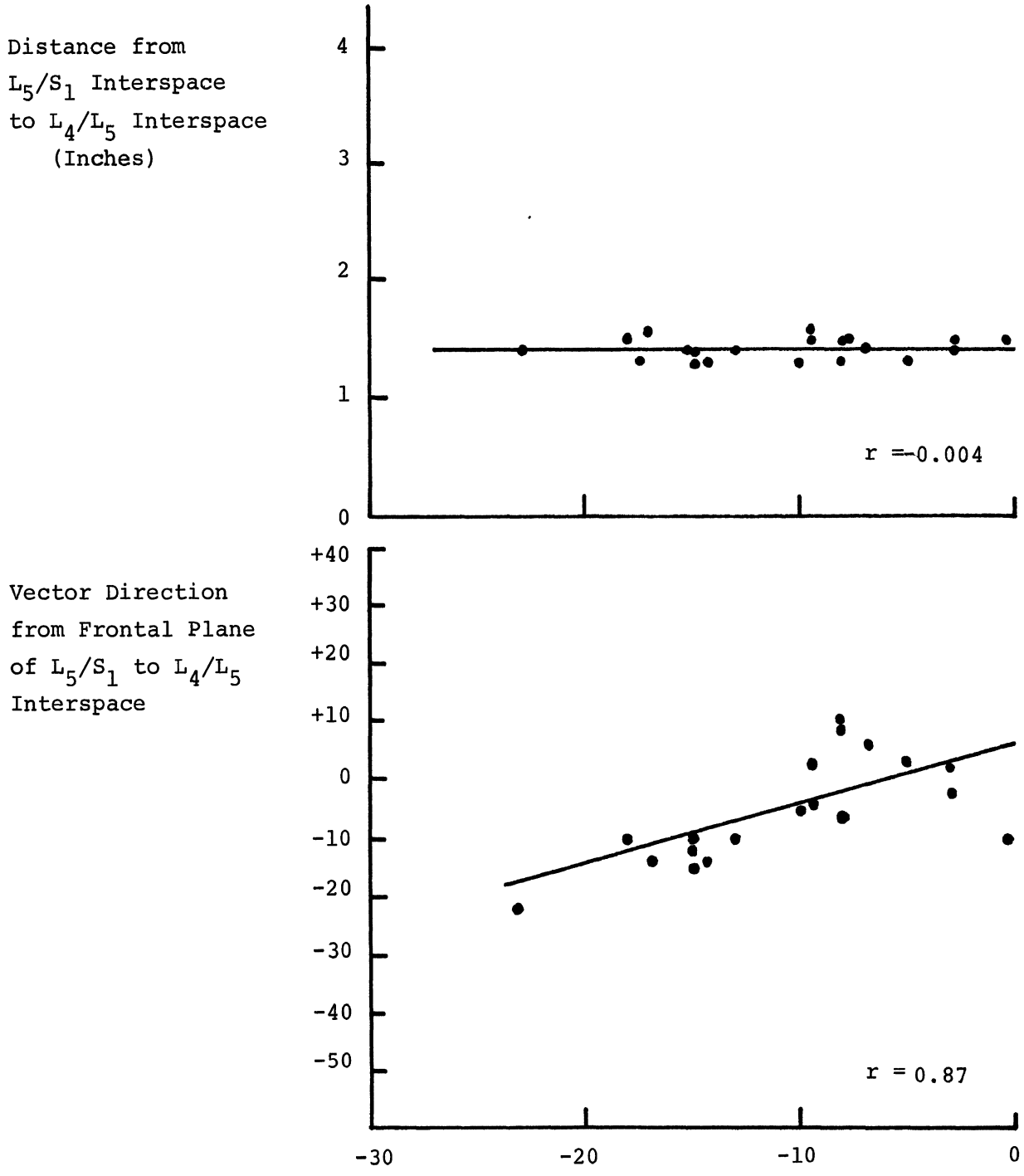

Relationship: L_4/L_5 Interspace to L_3L_4 Interspace

LAT:

Distance from L_4/L_5 to L_3/L_4 Interspace (Inches)

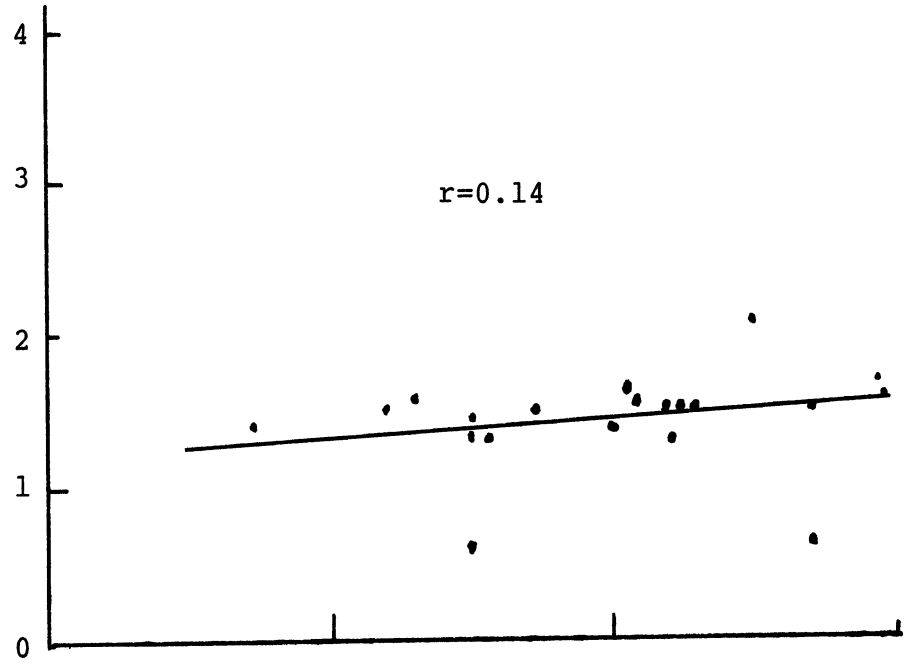

Vector Direction from Frontal Plane of L_4/L_5 to L_3/L_4 Interspace (Degrees)

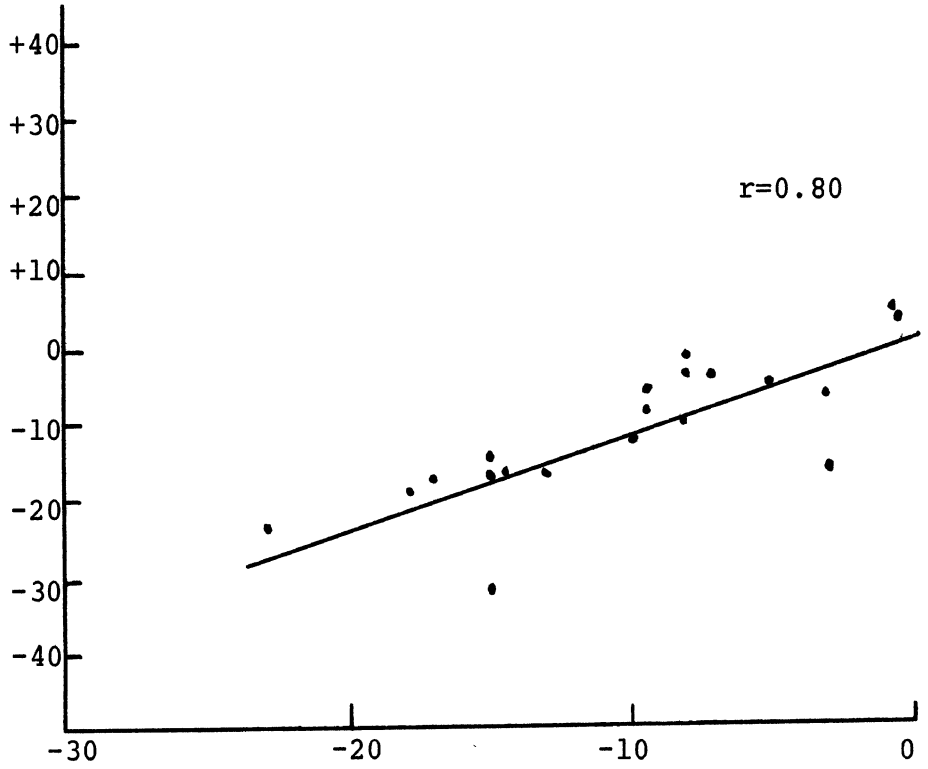

ANG = Reference Angle of Vector from L_5/S_1 to L_1/L_2 Interspaces, (positive=forward)

Relationship: L_3/L_4 Interspace to L_2/L_3 Interspace

LAT:

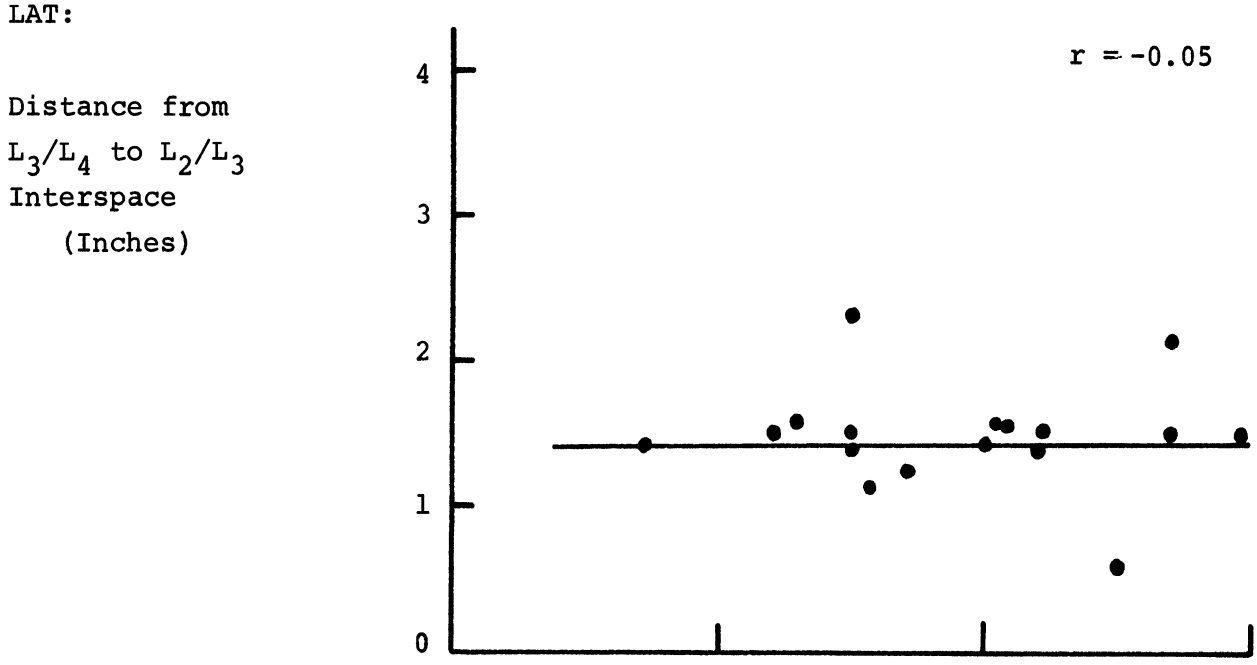

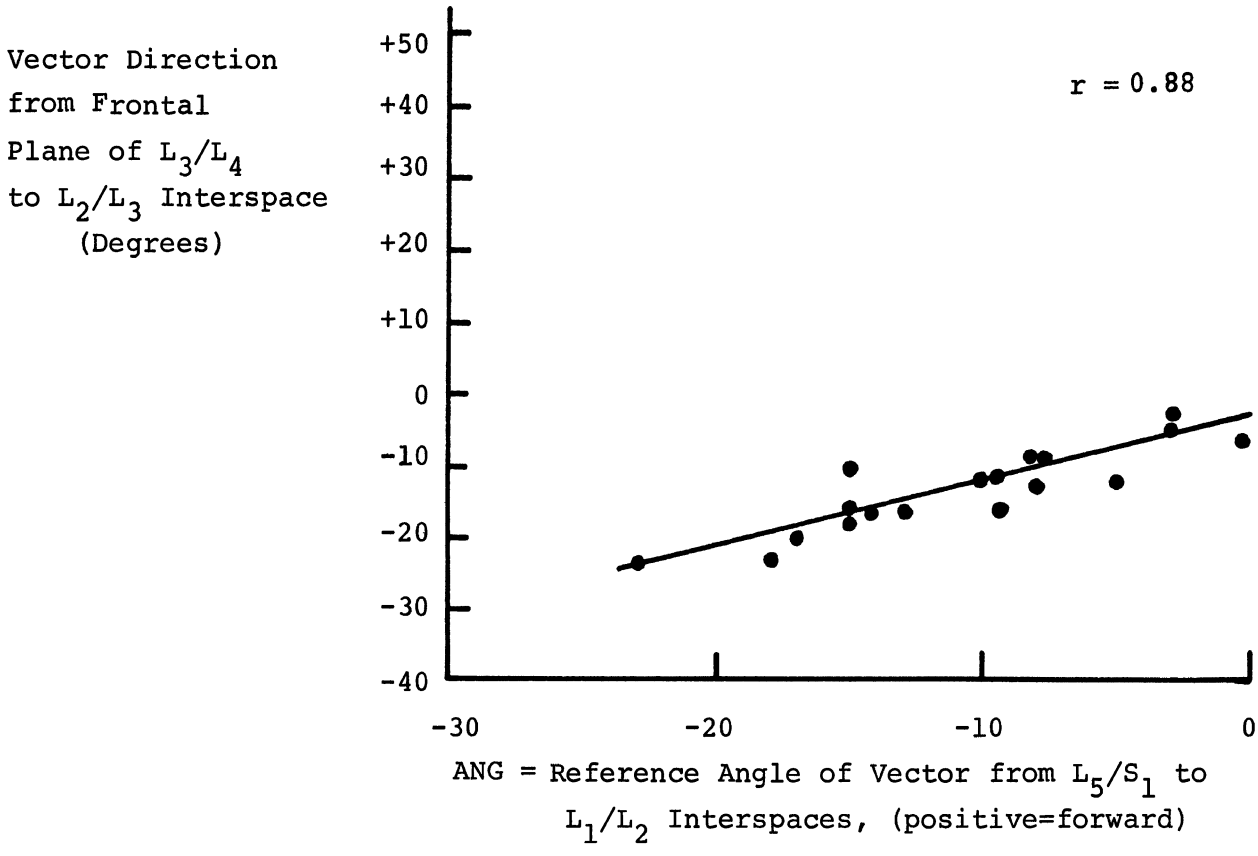

Relationship: L_2/L_3 Interspace to L_1/L_2 Interspace

LAT:

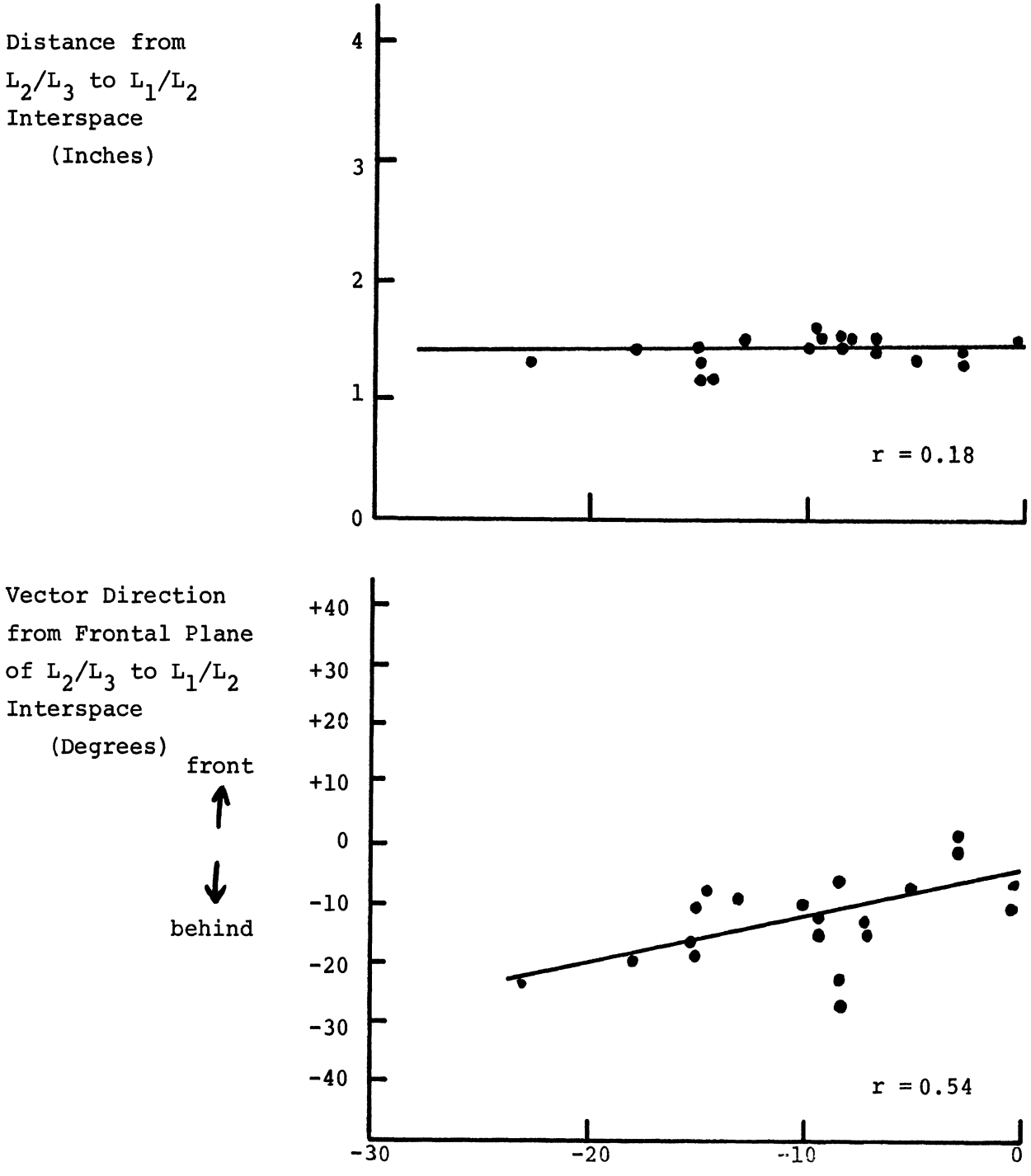

APPENDIX M

Plots of Thoracic Vectors

vs.

Angle of Thoracic Reference Vector ANG

Note: Some surface-to-bone articulations are plotted in reference to the horizontal reference axis rather than the standard vertical axis.

Relationship: T_{12}/L_1 Interspace to T_{12} Surface Mark

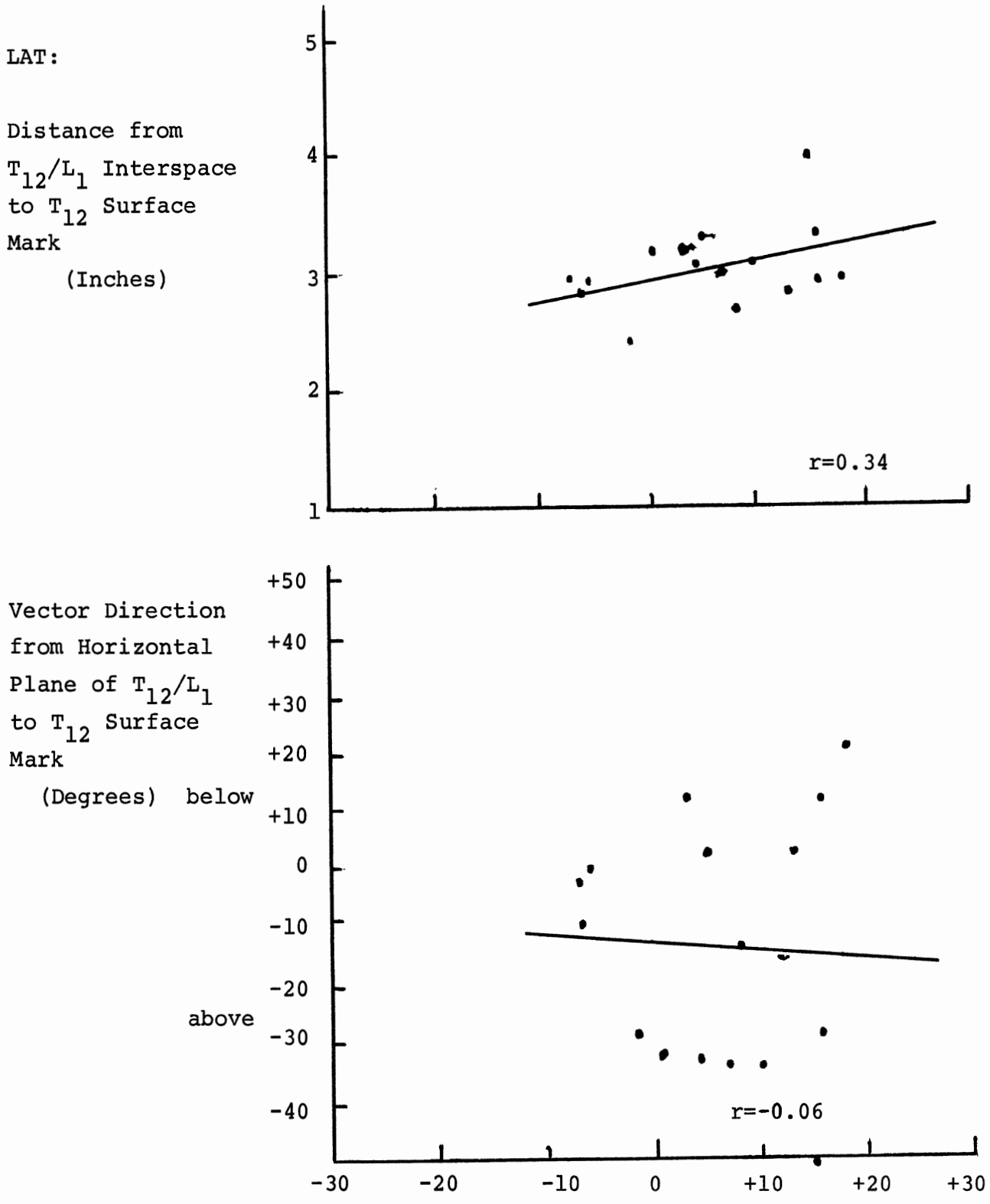

ANG = Reference Angle of Vector from T_{12}/L_1 to T_4/T_5 Interspace, (positive=forward)

Relationship: T_8/T_9 Interspace to T_8 Surface Mark

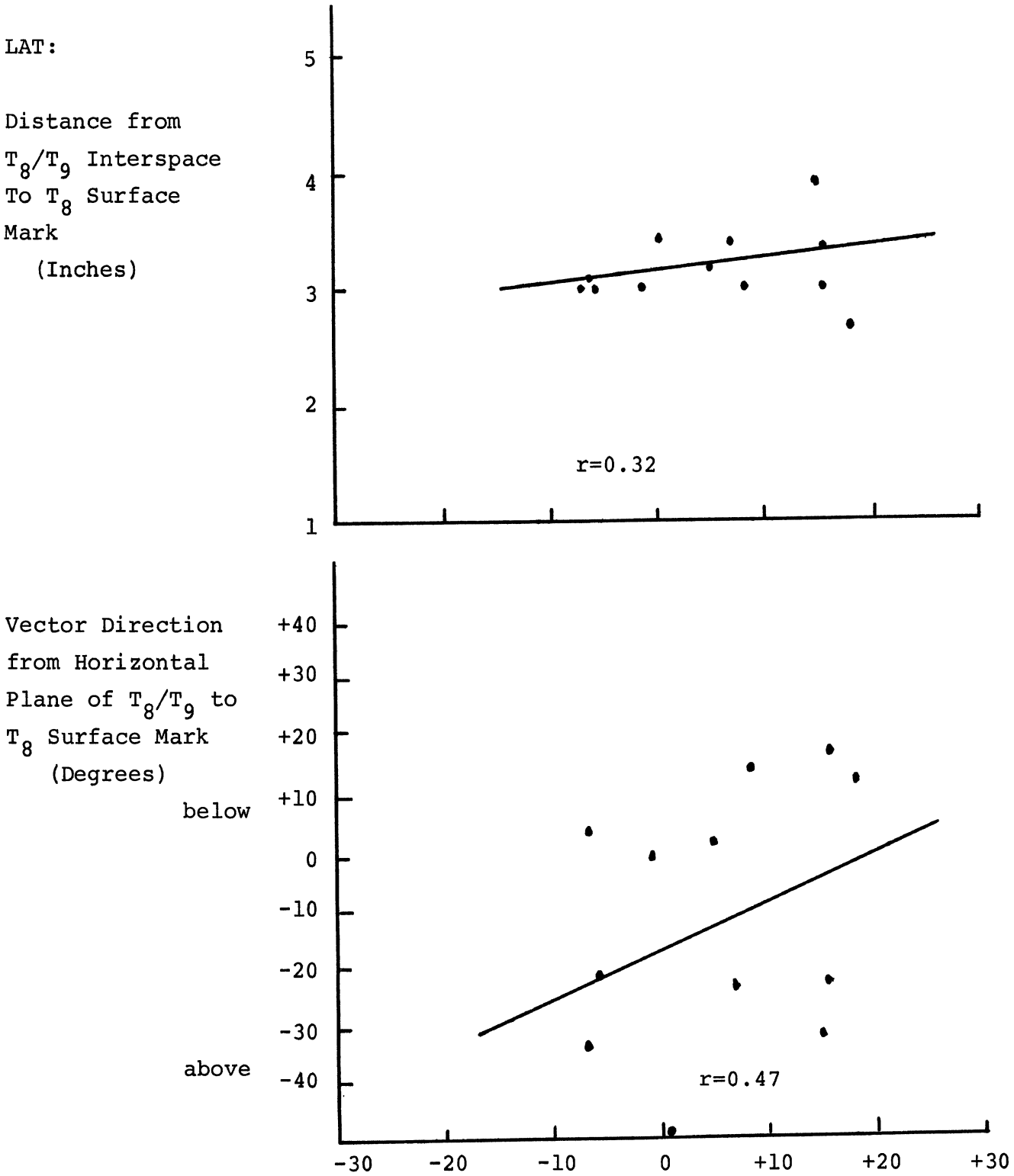

ANG = Reference Angle of Vector from T_{12}/L_1 to T_4/T_5 Interspace, (positive=forward)

(See Figure 19)

Relationship: T_4/T_5 Interspace to T_4 Surface Mark

LAT:

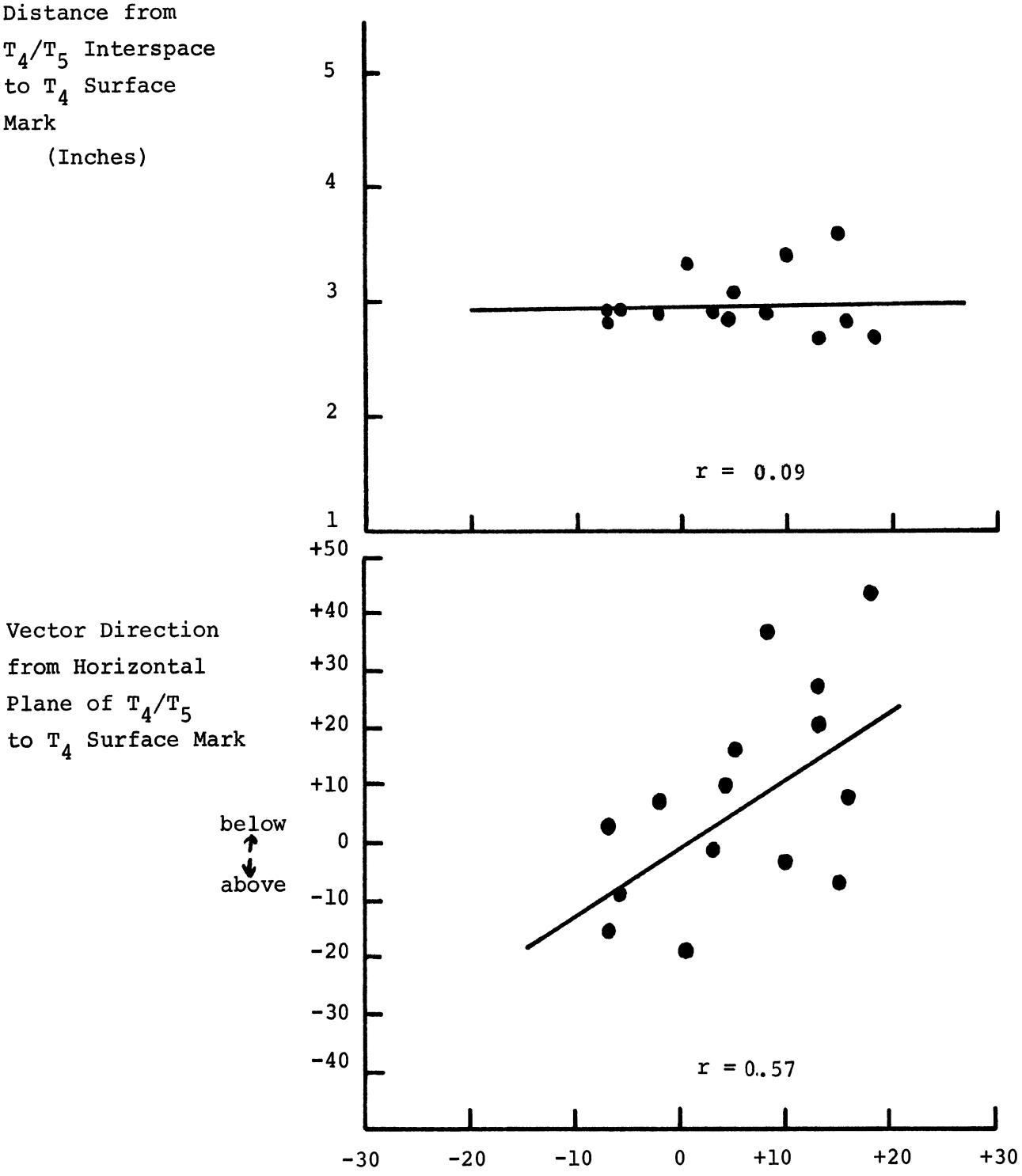

ANG = Reference Angle of Vector from T_{12}/L_1 to T_4/T_5 Interspaces, (positive=forward)

Relationship: T_{12} Surface Mark to T_8 Surface Mark

LAT:

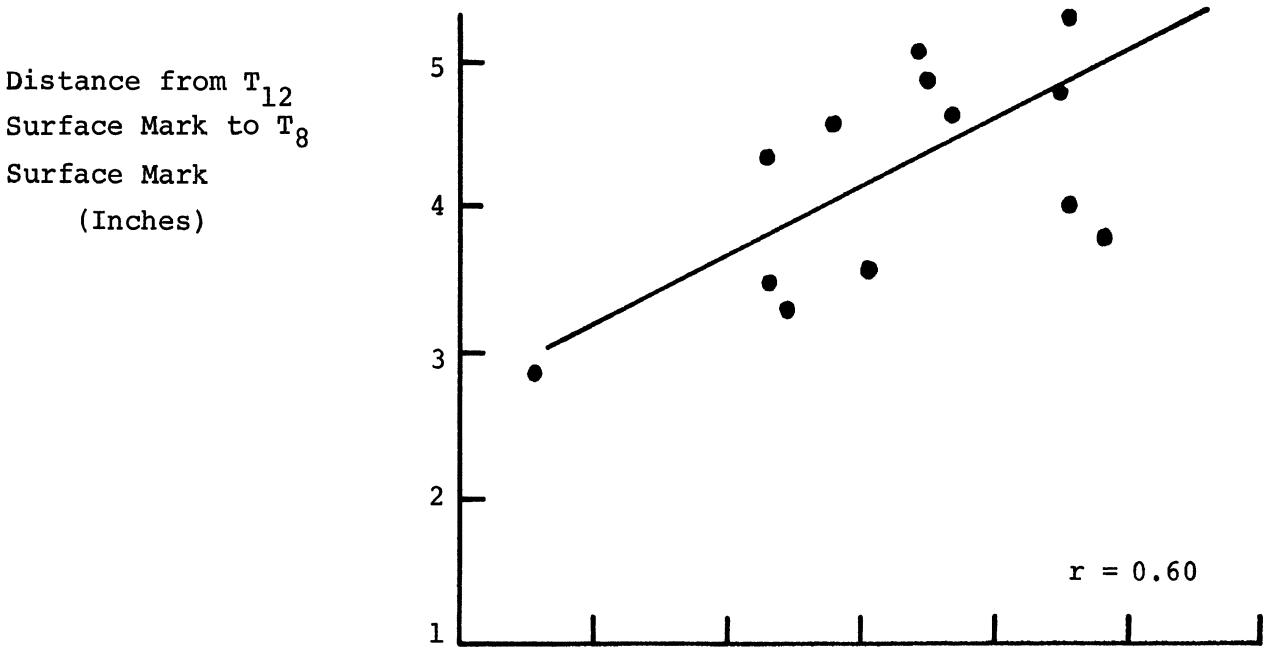

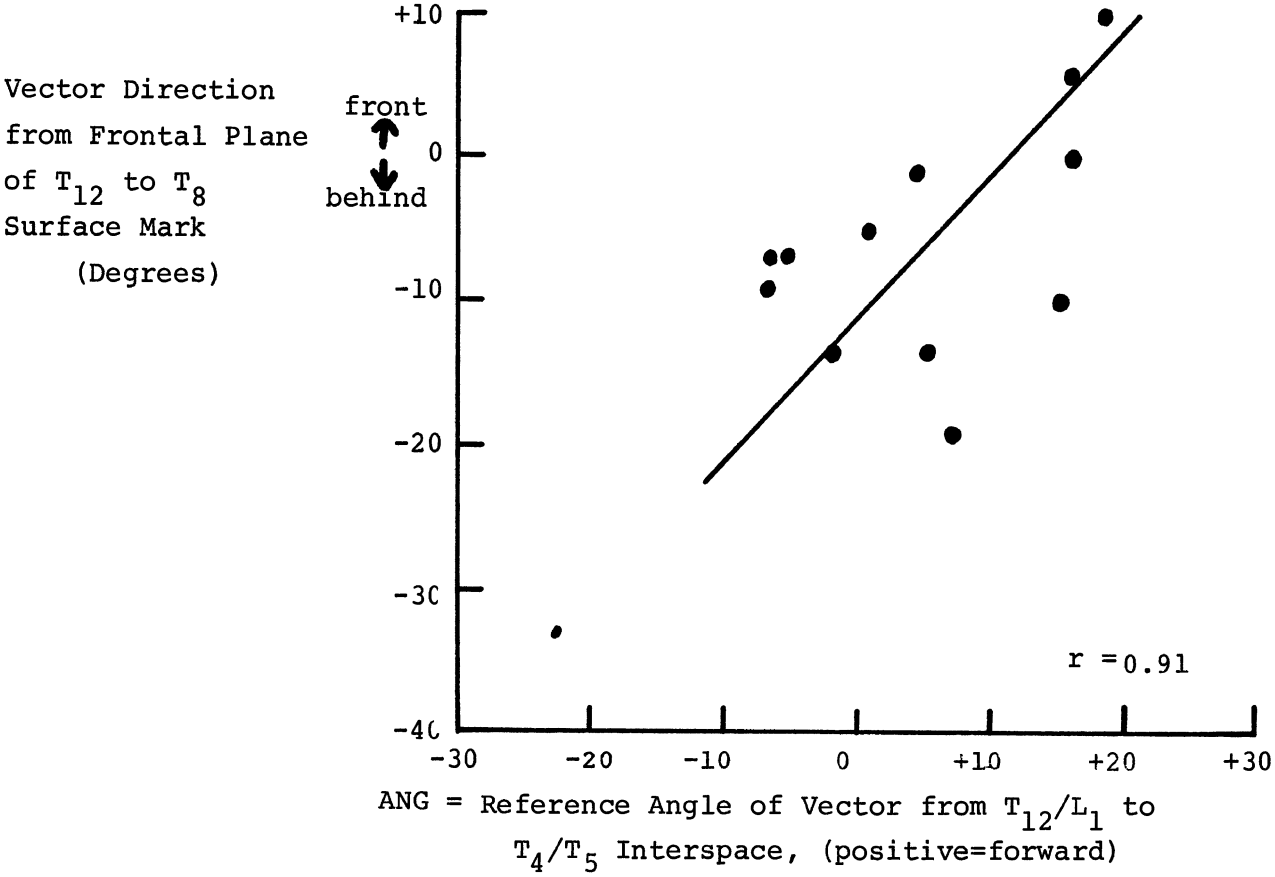

ANG = Reference Angle of Vector from T_{12}/L_1 to T_4/T_5 Interspace, (positive=forward)

Relationship: T_8 Surface Mark to T_4 Surface Mark

LAT:

Distance from T_8 to T_4 Surface Mark (Inches)

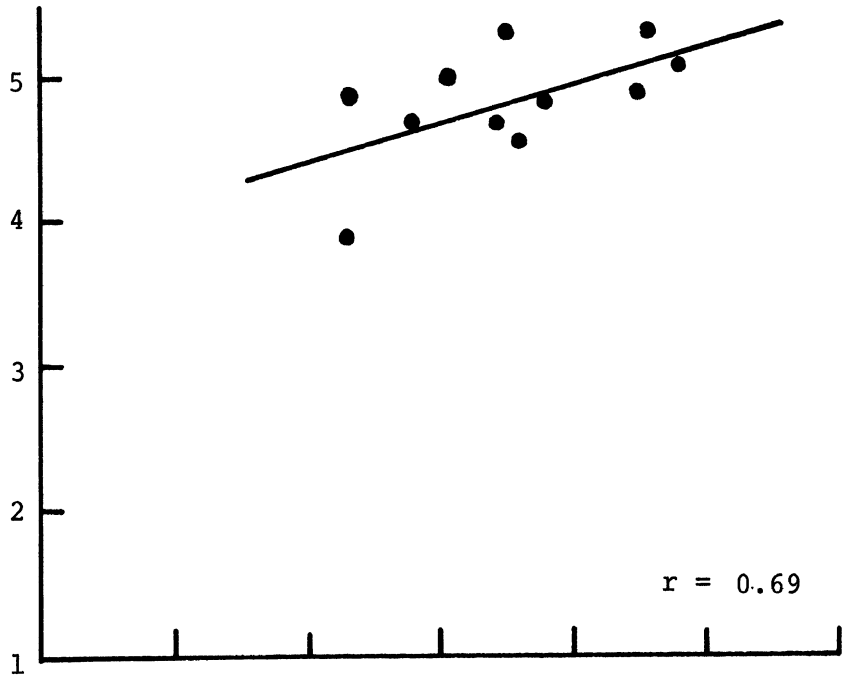

Vector Direction from Frontal Plane of T_8 to T_4 Surface Mark (Degrees)

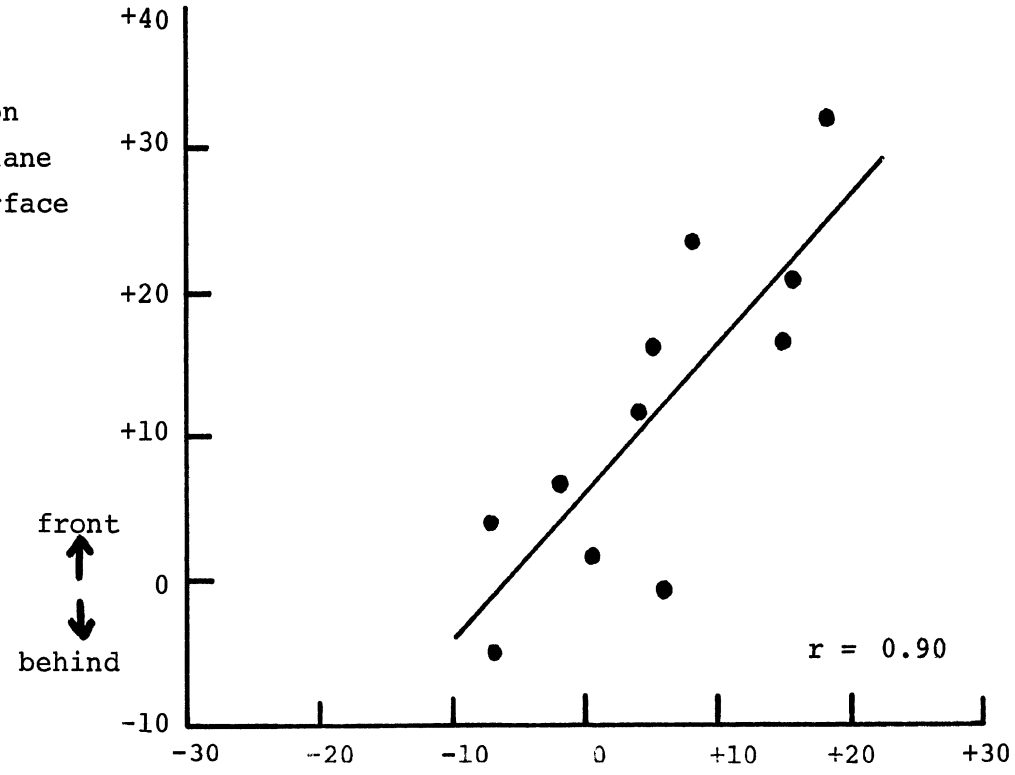

ANG = Reference Angle of Vector from T_{12}/L_1 to T_4/T_5 Interspace, (positive=forward)

Relationship: T_{12}/L_1 Interspace to T_8/T_9 Interspace

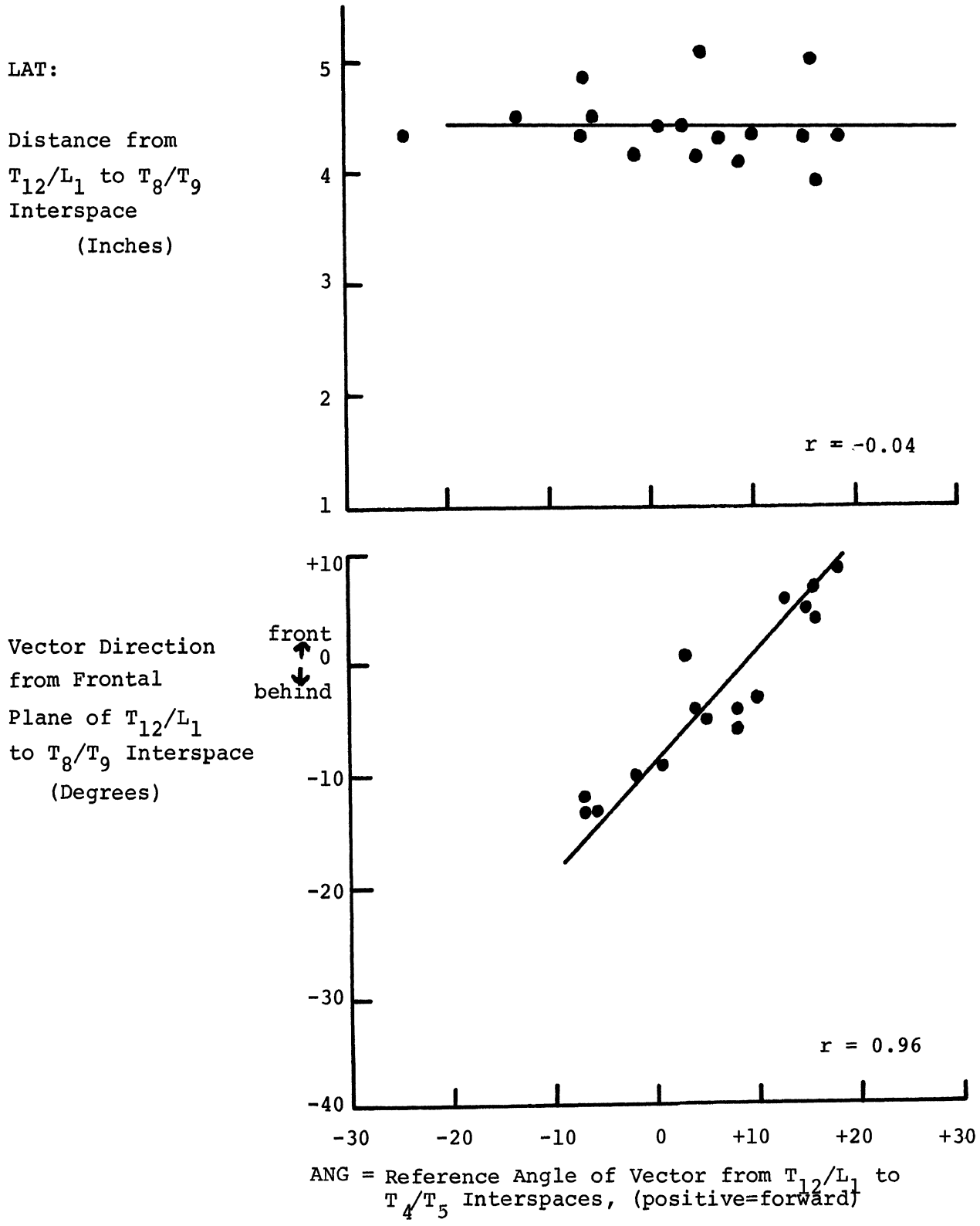

Relationship: T_8/T_9 Interspace to T_4/T_5 Interspace

LAT:

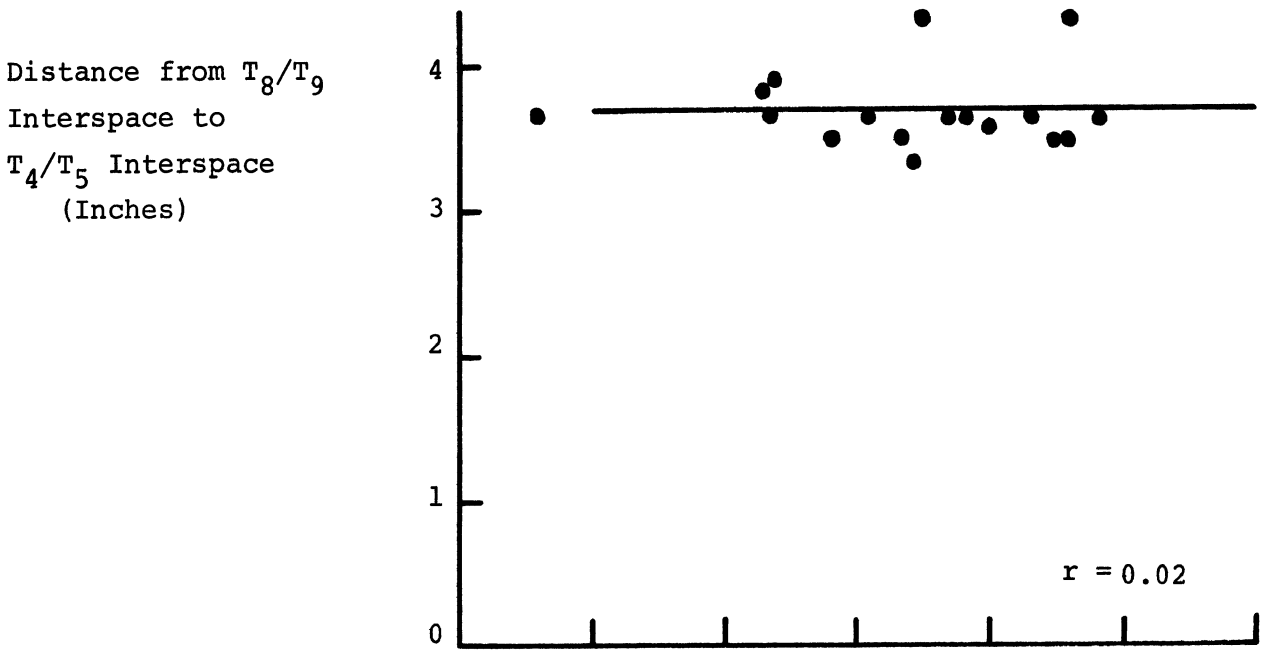

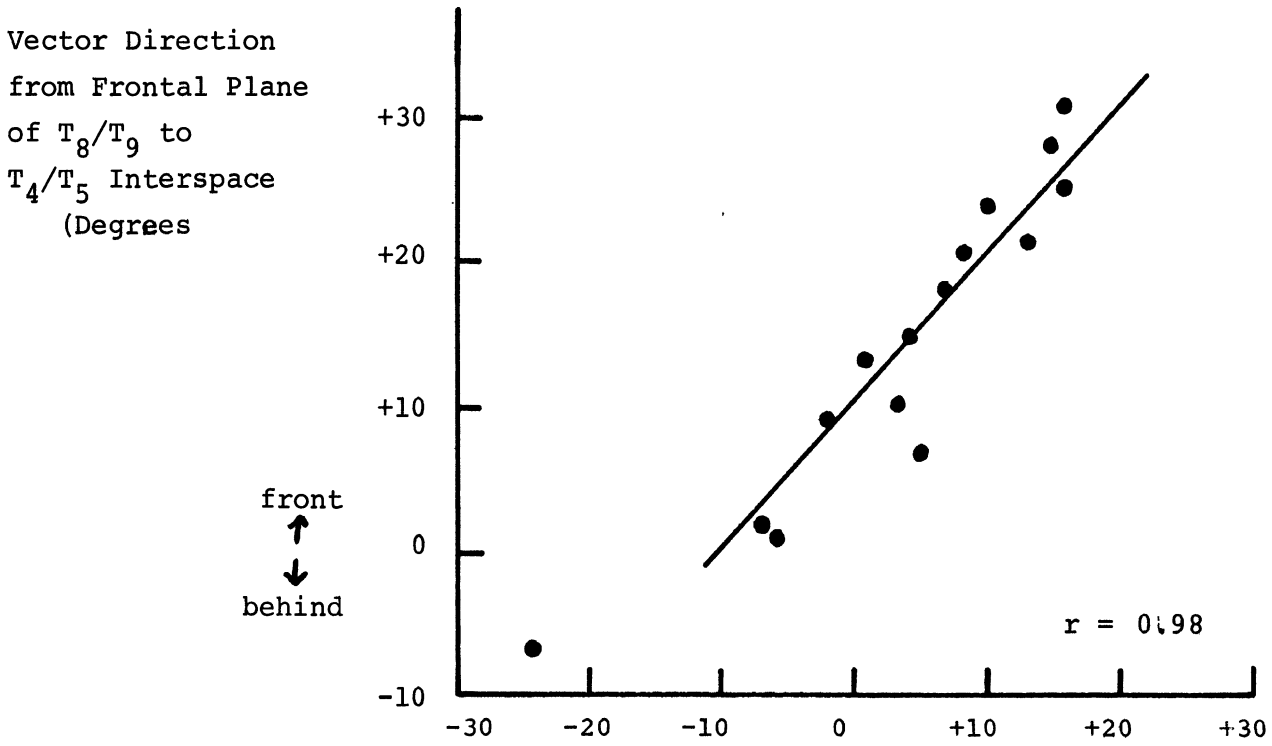

ANG = Reference Angle of Vector from T_{12}/L_1 to T_4/T_5 Interspaces, (positive=forward)

APPENDIX N

Plots of Shoulder Vectors

vs.

Horizontal Plane Angle of Arm

Note: For definition of directional axis, see Section IV.

Relationship: Sterno-Clavicular Junction
to Suprasternale

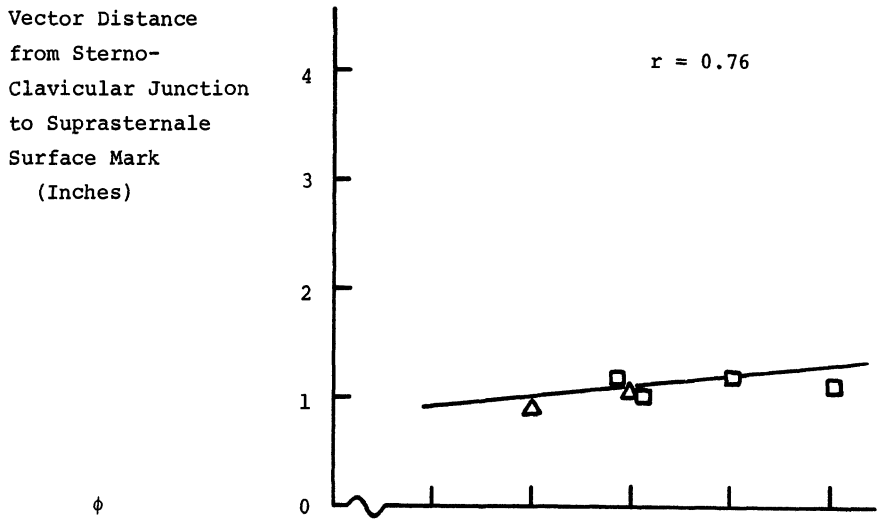

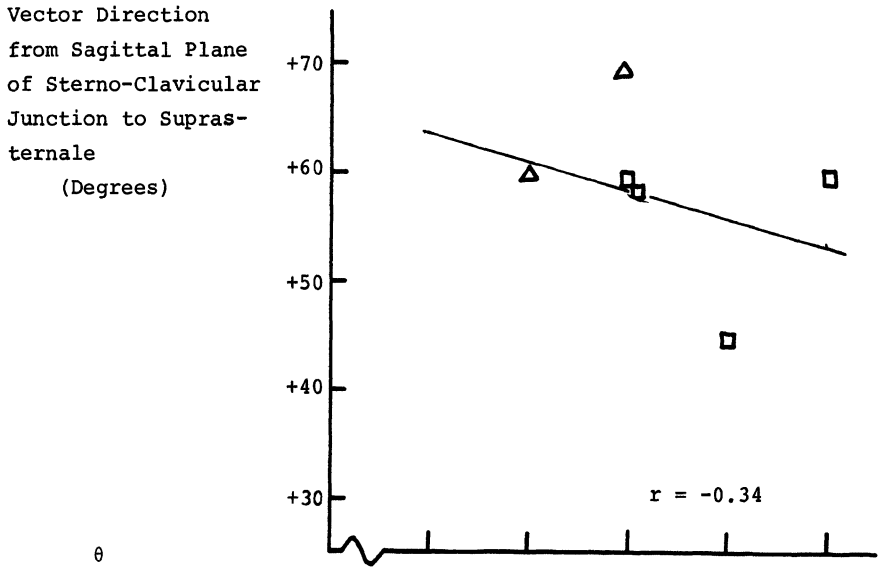

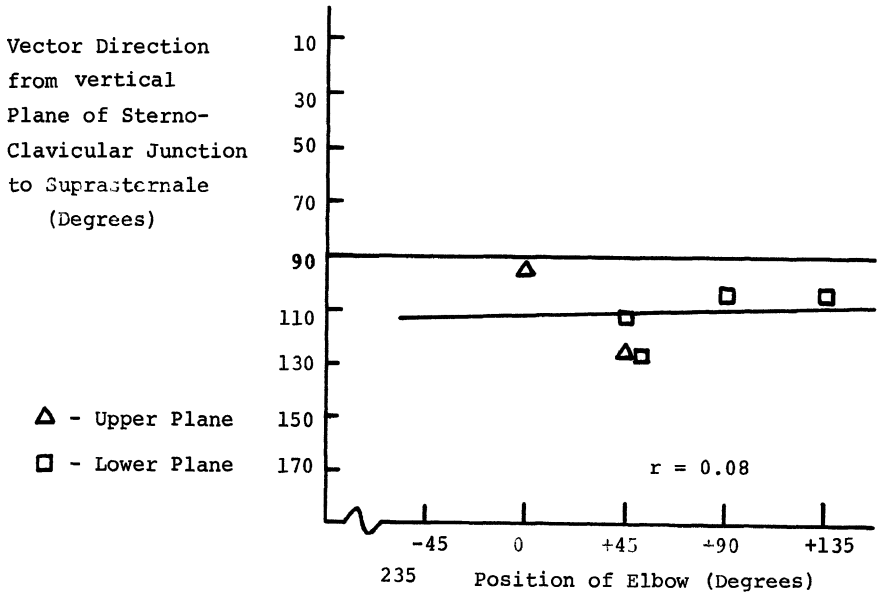

Relationship: T_4/T_5 Interspace to T_4 Surface Mark

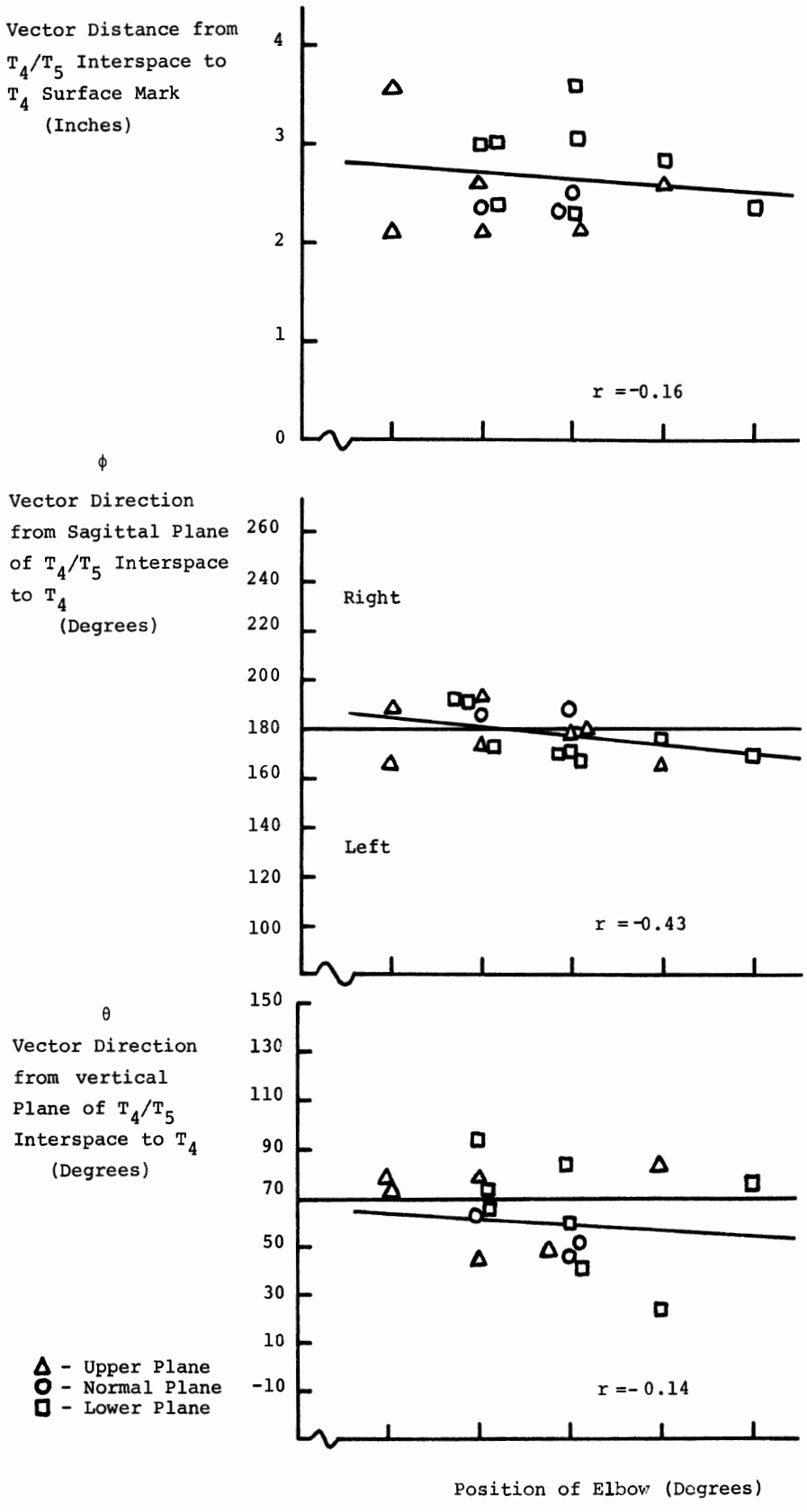

Relationship: Interspace C_7/T_1 to Surface C_7

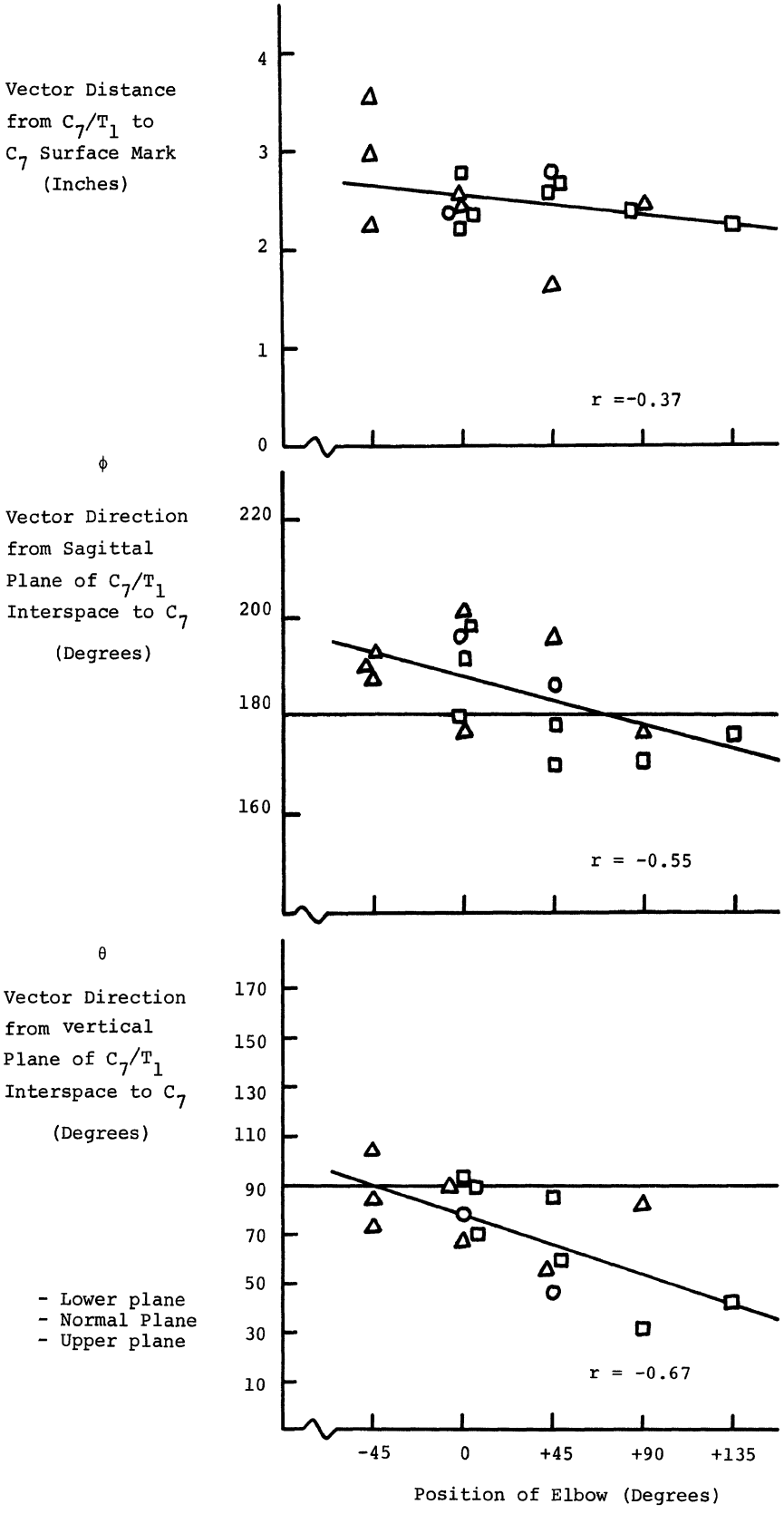

Relationship: T_8/T_9 Interspace to T_8 Surface Mark

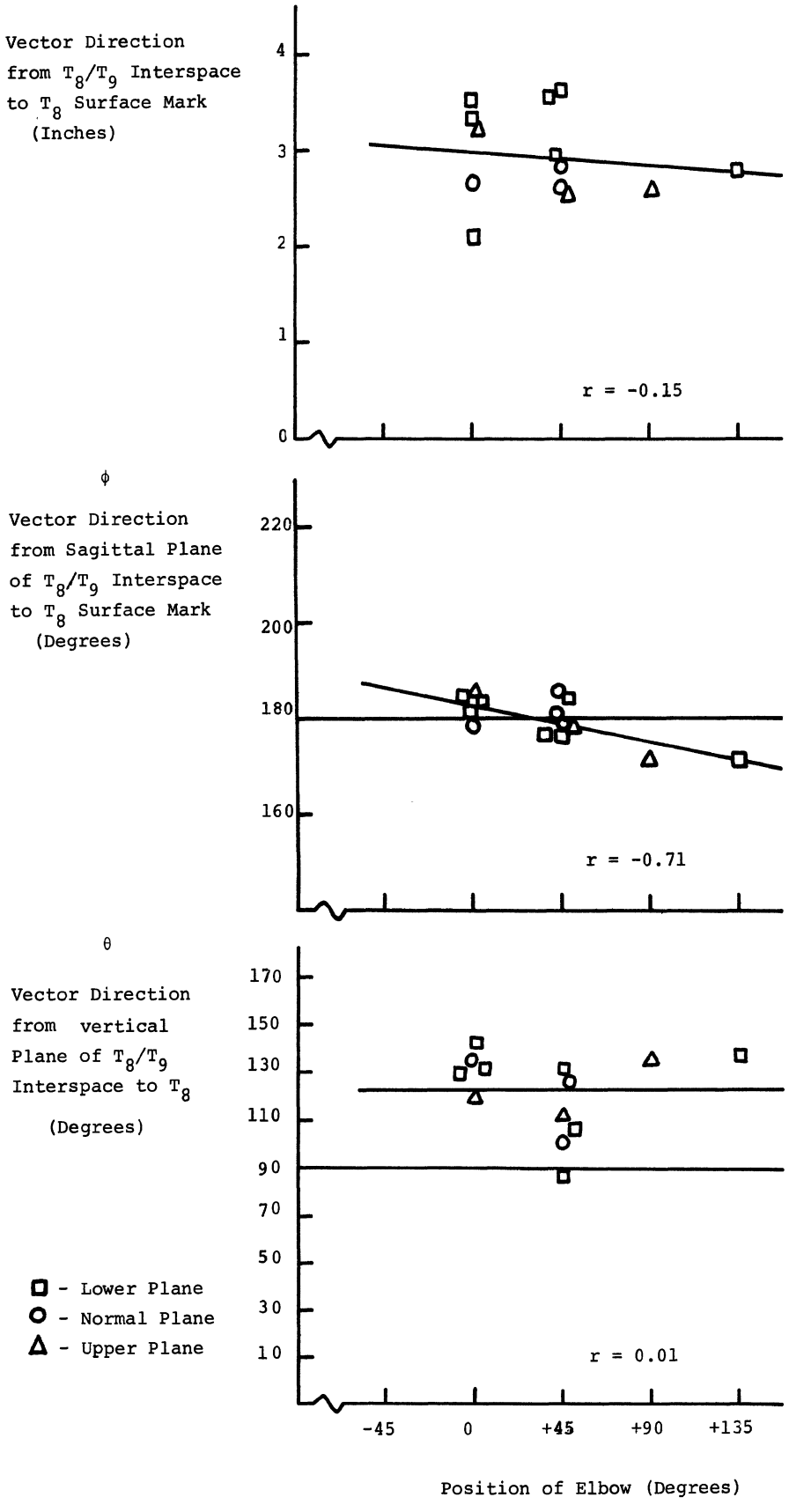

Relationship: T_4/T_5 Interspace to C_7/T_1 Interspace

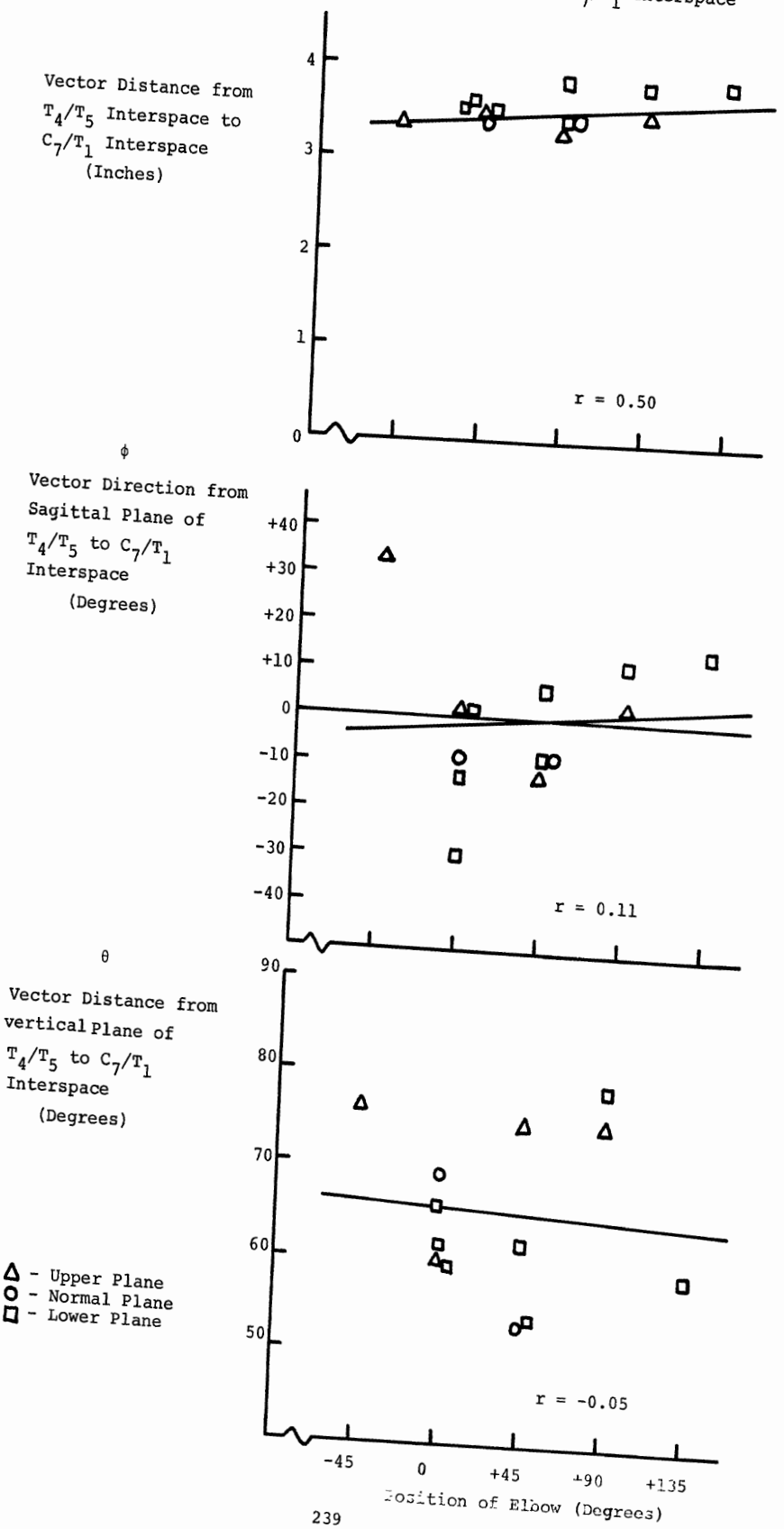

Relationship T_4 Surface to C_7 Surface

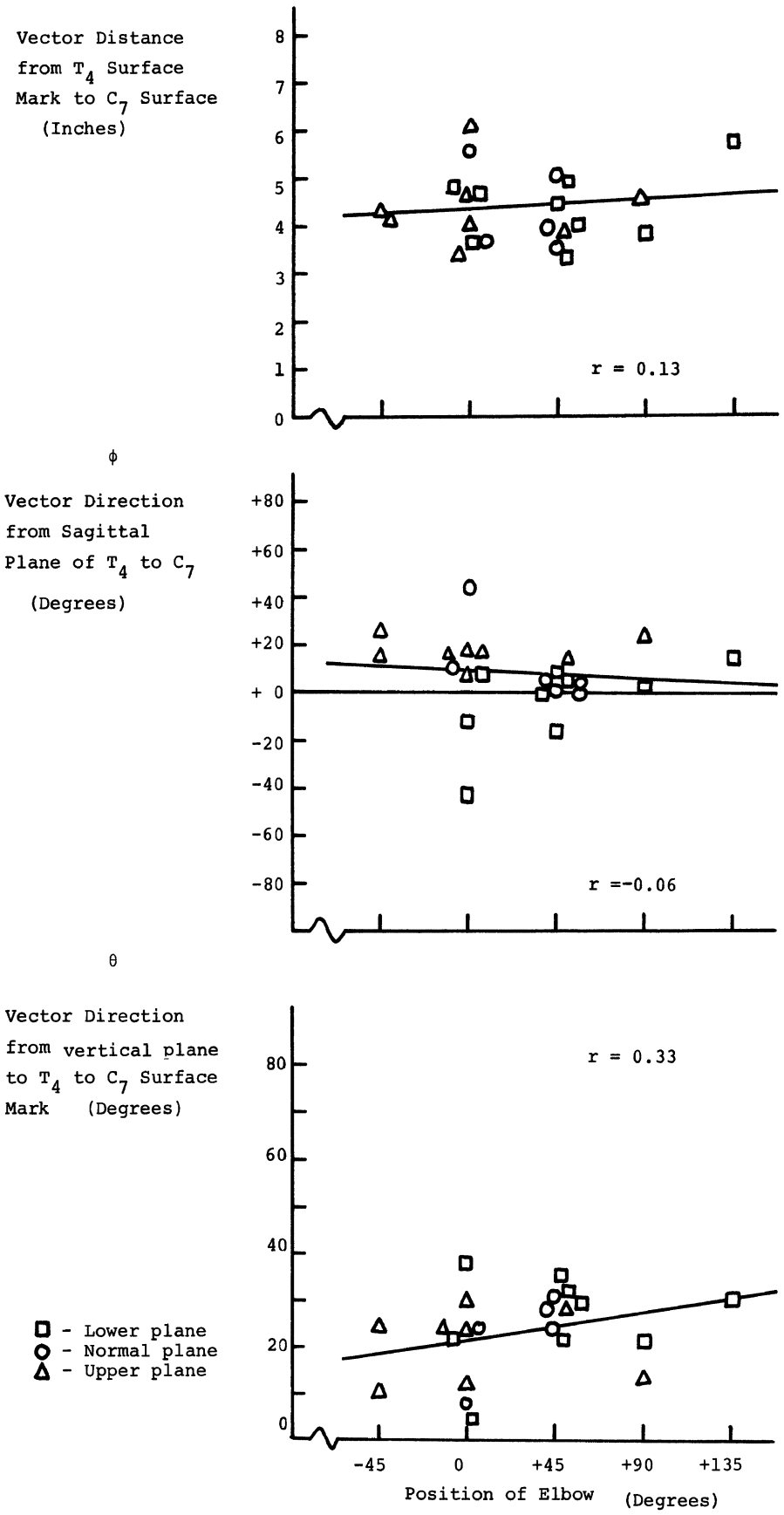

Relationship: Acromion Surface Mark to C_7 Surface Mark

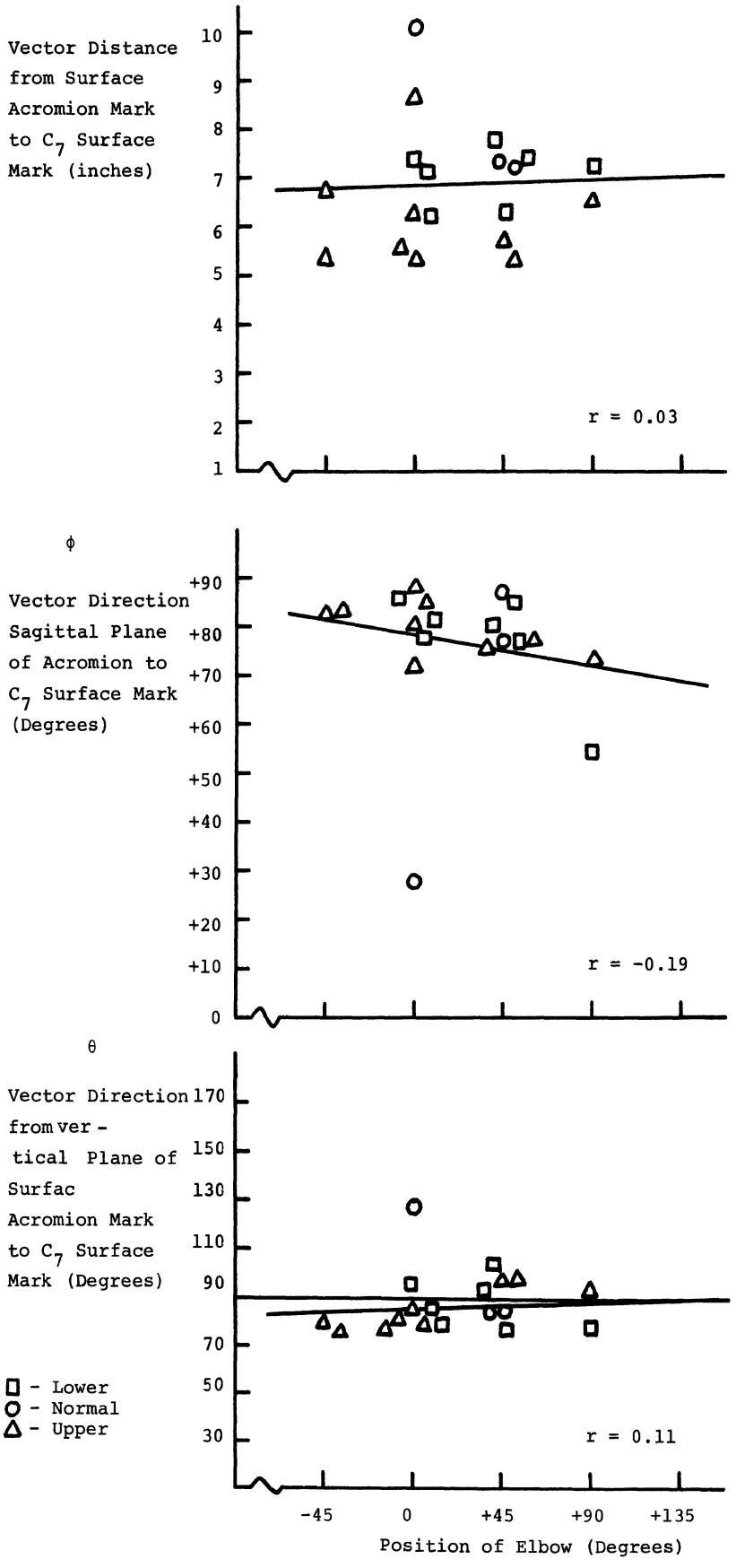

Relationship: C_7/T_1 Interspace to Acromio-Clavicular Junction

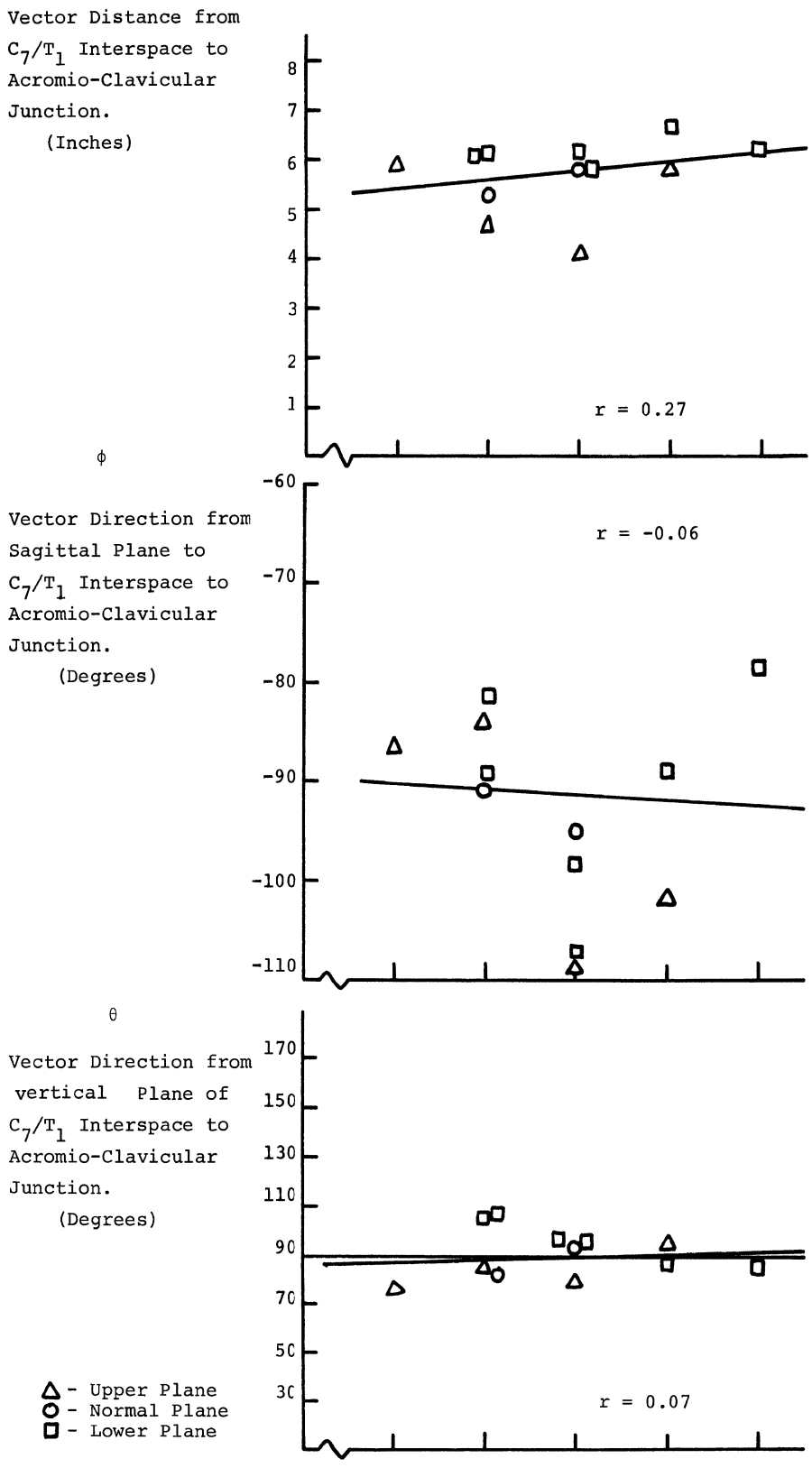

Relationship: Projected Head of Humerus to Humeral Mark

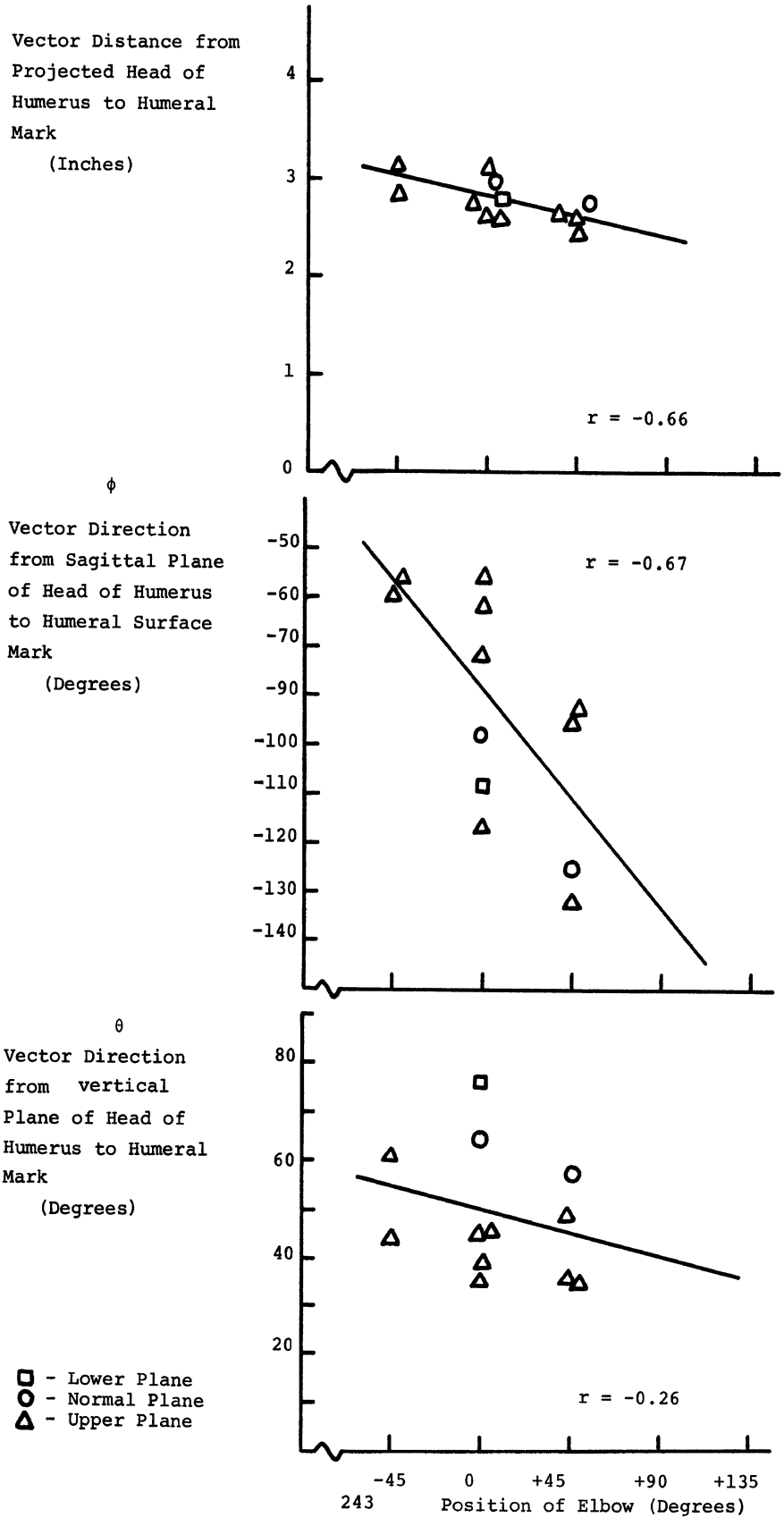

Relationship: Acromio-Clavicular Junction to Humeral Mark

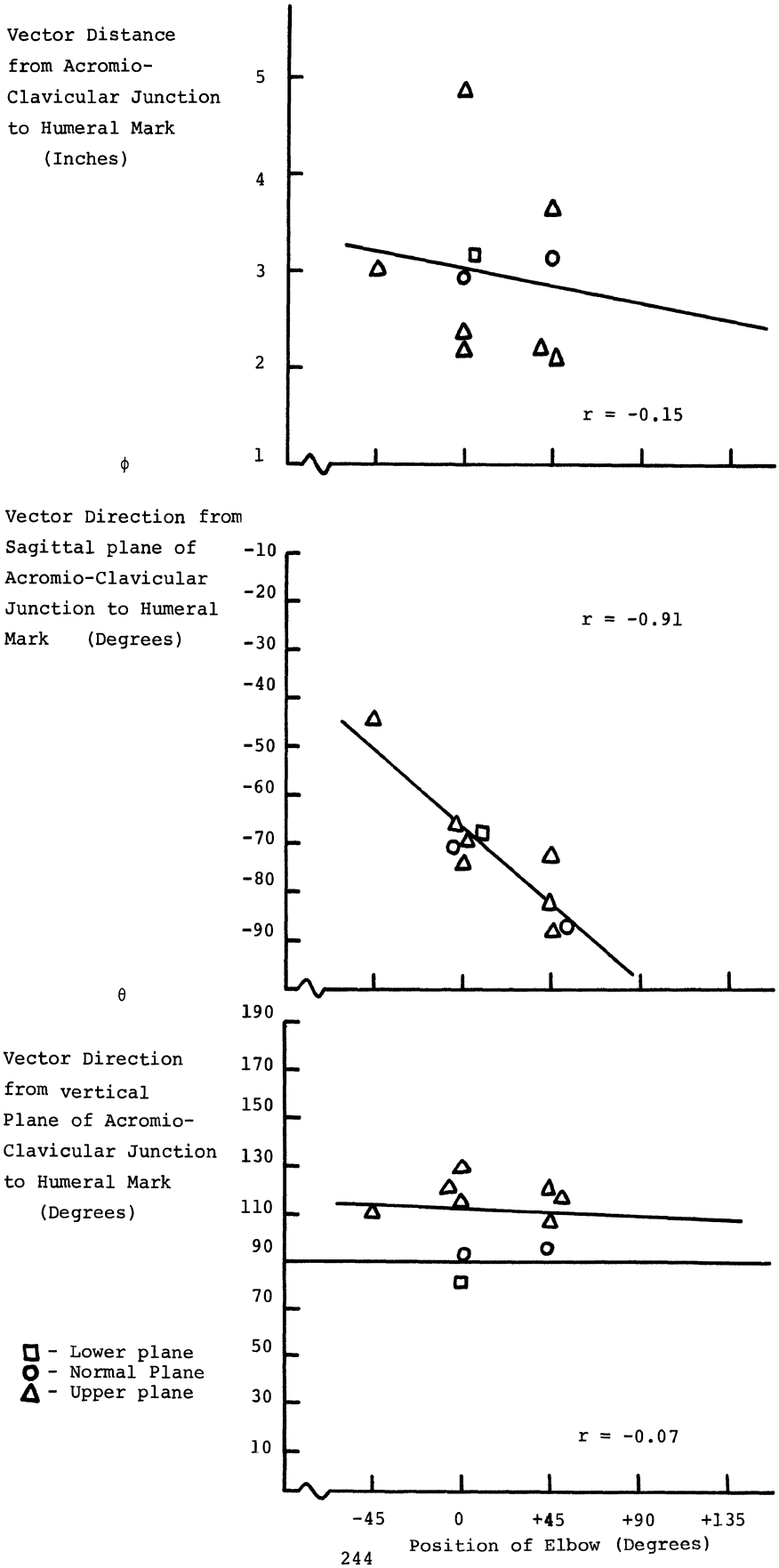

Relationship: Head of Humerus to C_7/T_1 Interspace

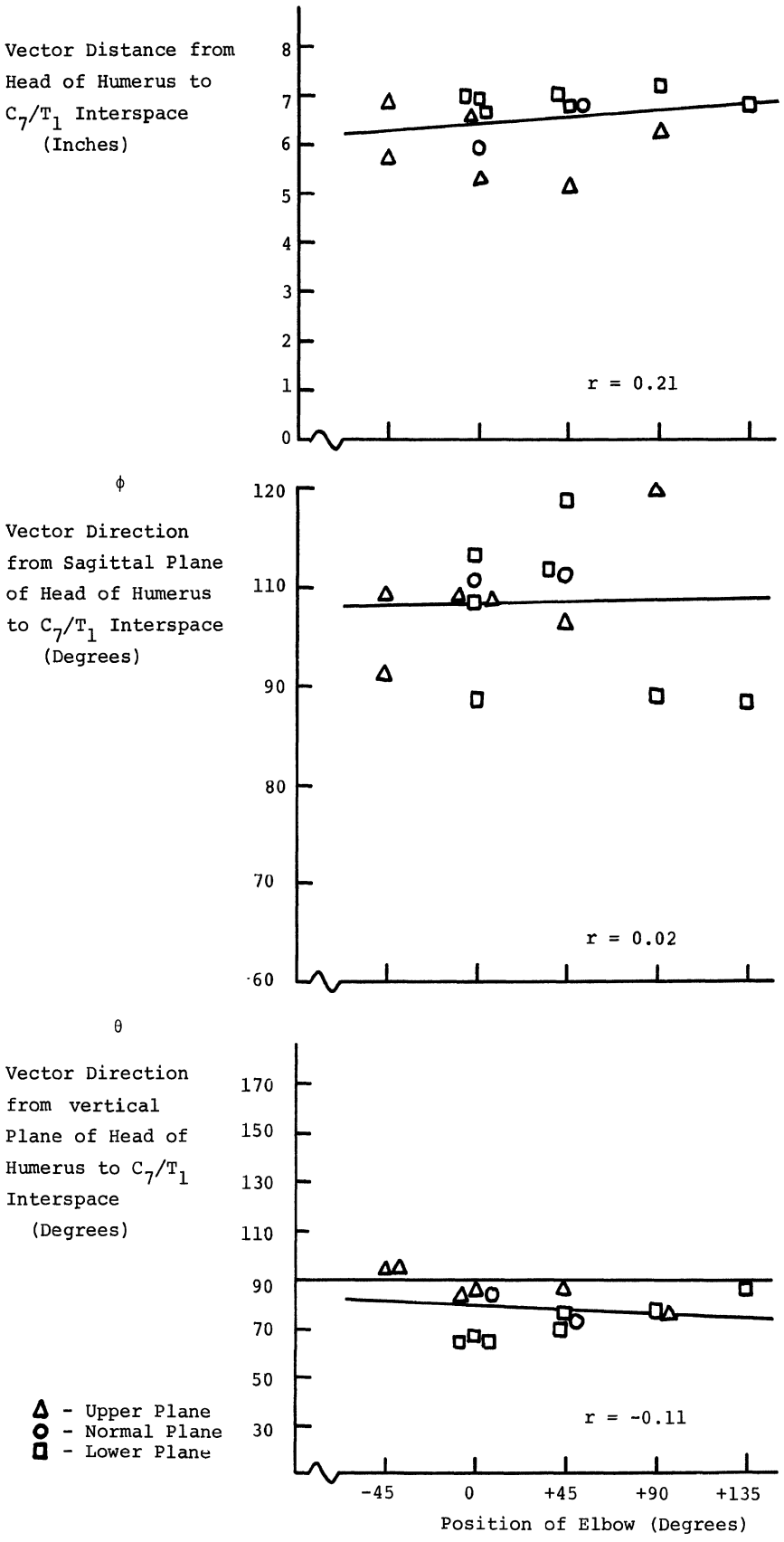

Relationship: Acromio-Clavicular Junction to Acromion

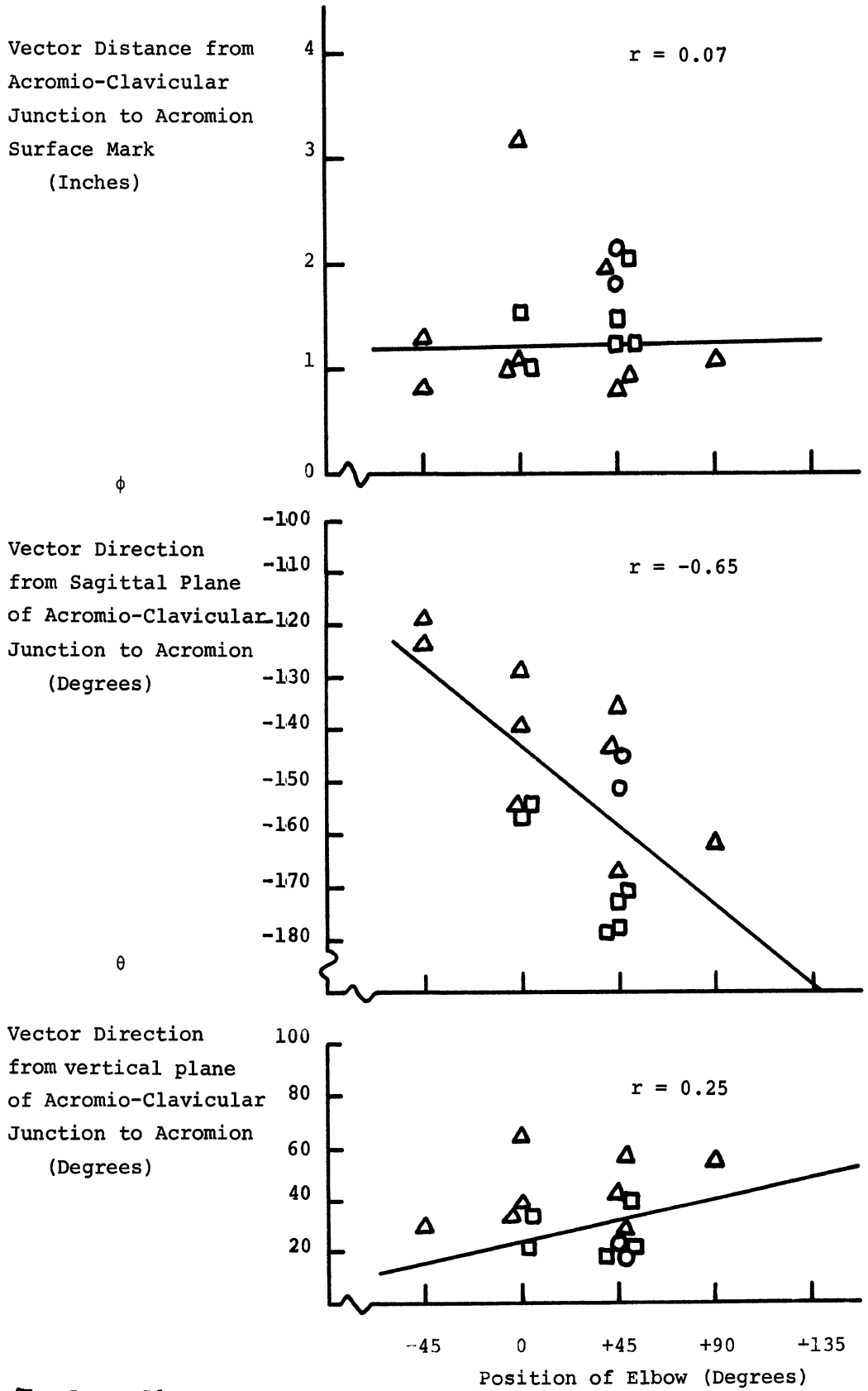

□ - Lower Plane
○ - Normal Plane
△ - Upper Plane

Relationship: Projected Head of Humerous
to Acromio-Clavicular Junction

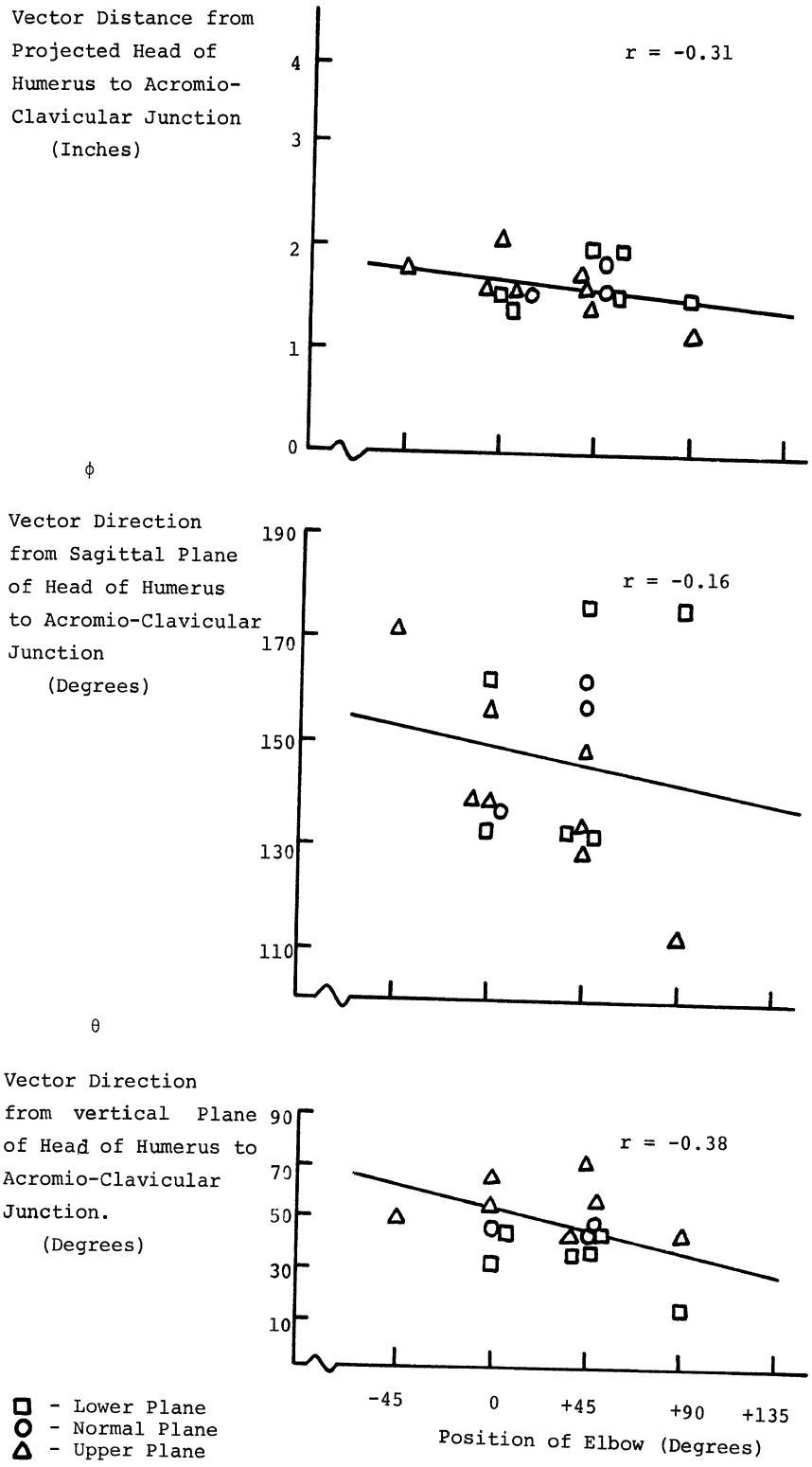

Relationship: Projected Head of Humerus to Acromion

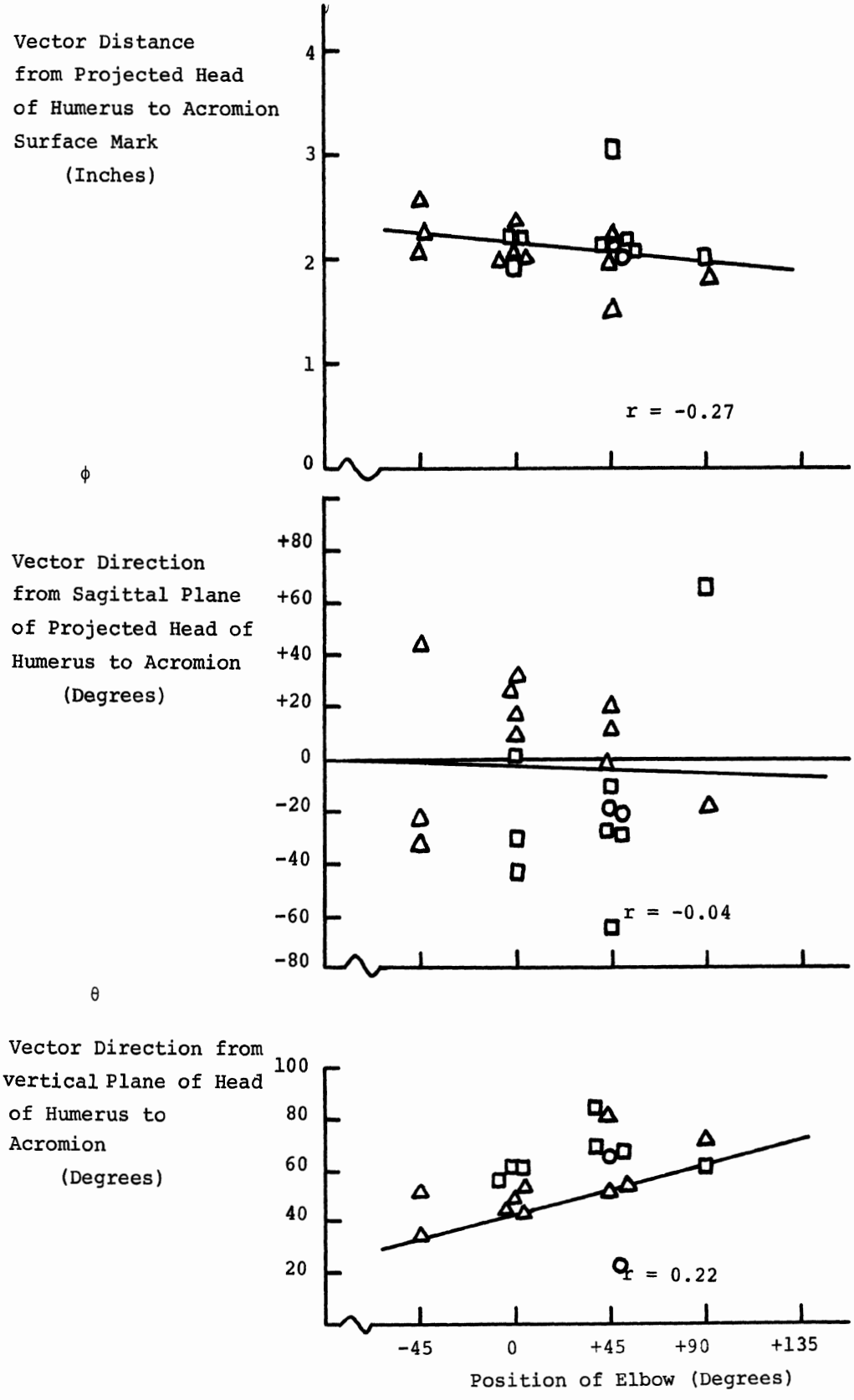

□- Lower Plane
○- Normal Plane
△- Upper Plane

Relationship of Vector from Sternoclavicular Junction to Acromioclavicular Junction

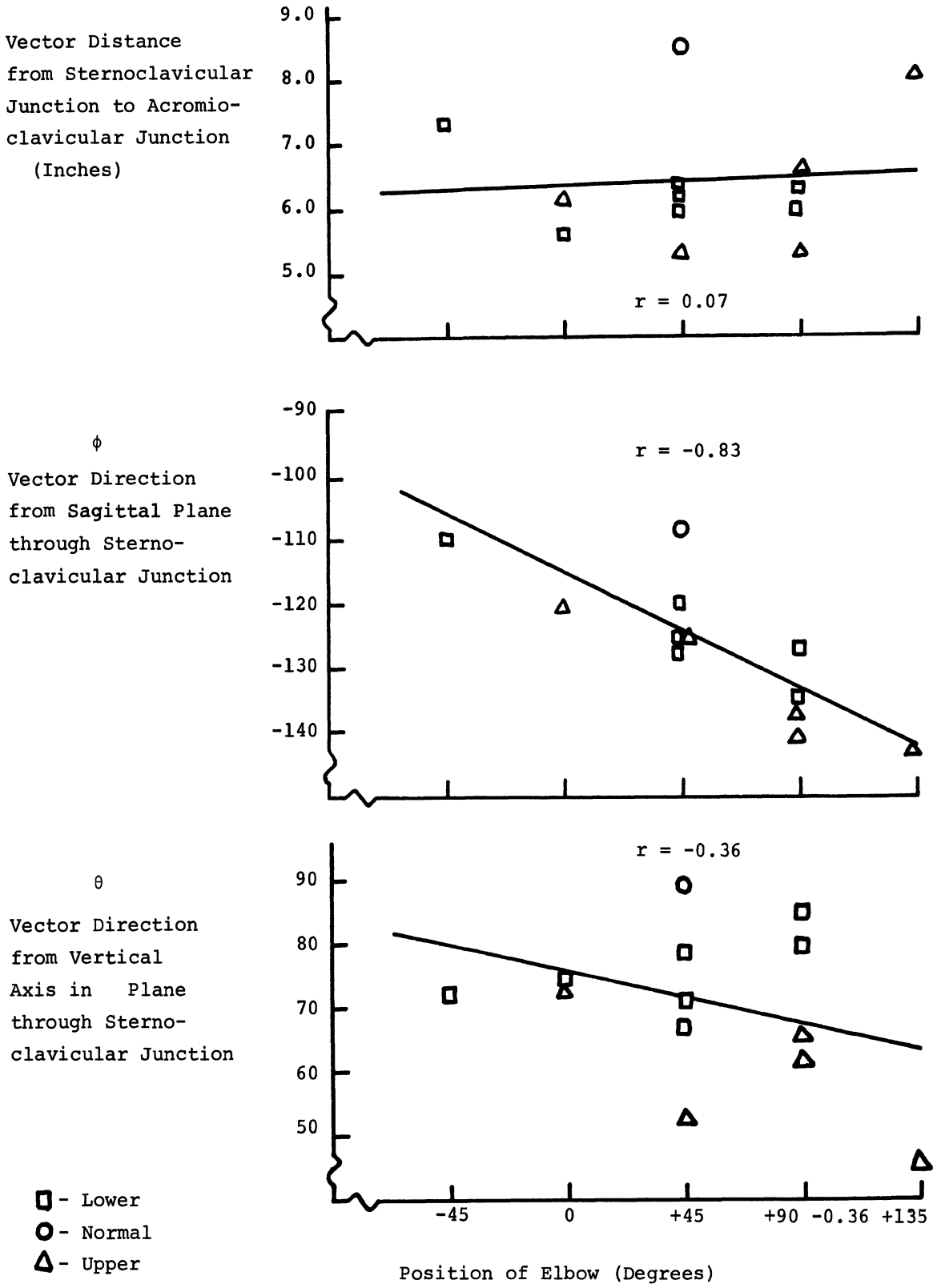

APPENDIX O

Plots of Cervical Vectors

vs.

Angle of Cervical Reference Vector ANG

C_7/T_1 To C_2/C_3 VS. Vector Direction
From C_7 Surface to Nasion

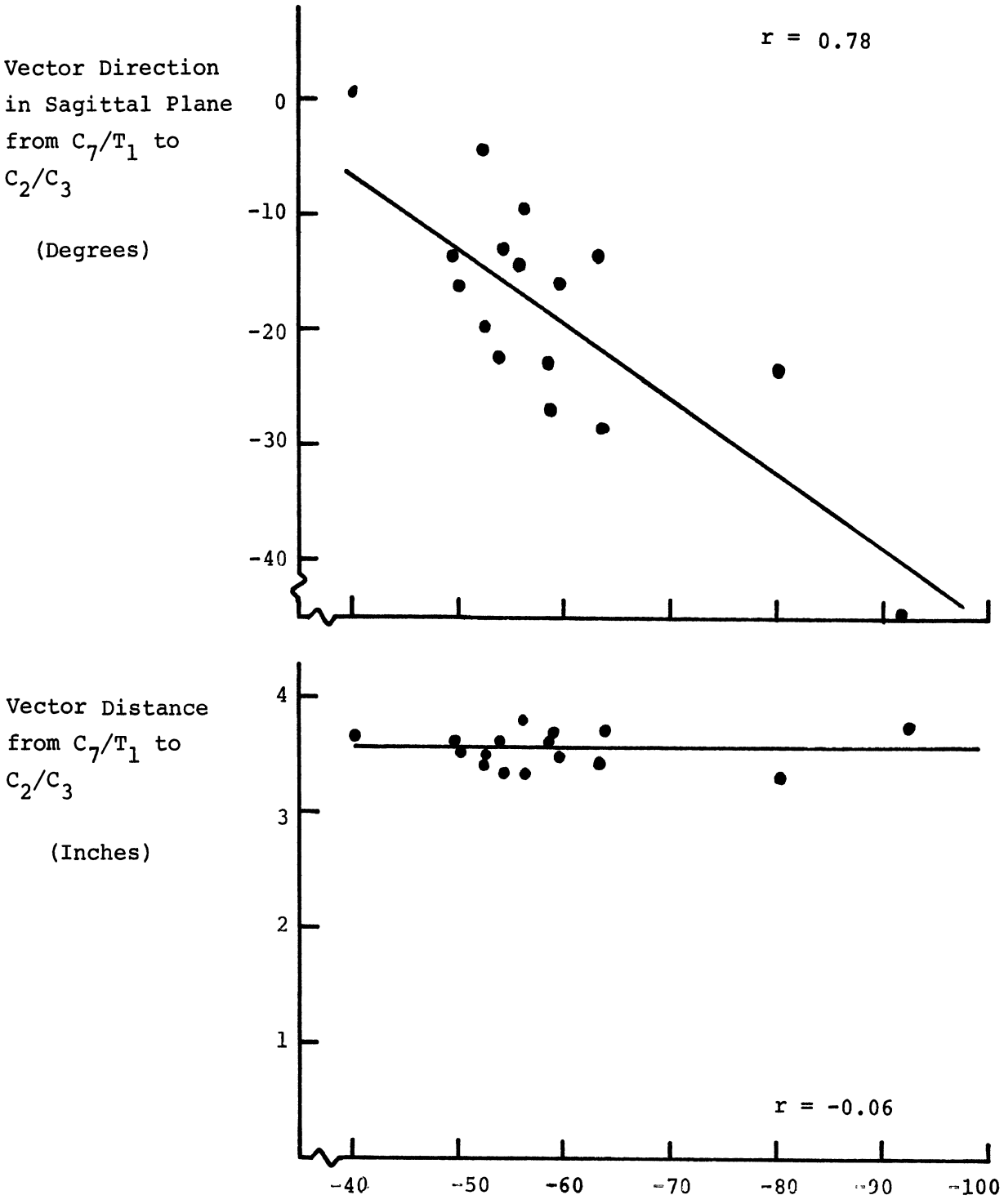

C_7/T_1 To C_3/C_4 VS. Vector Direction
From C_7 Surface to Nasion

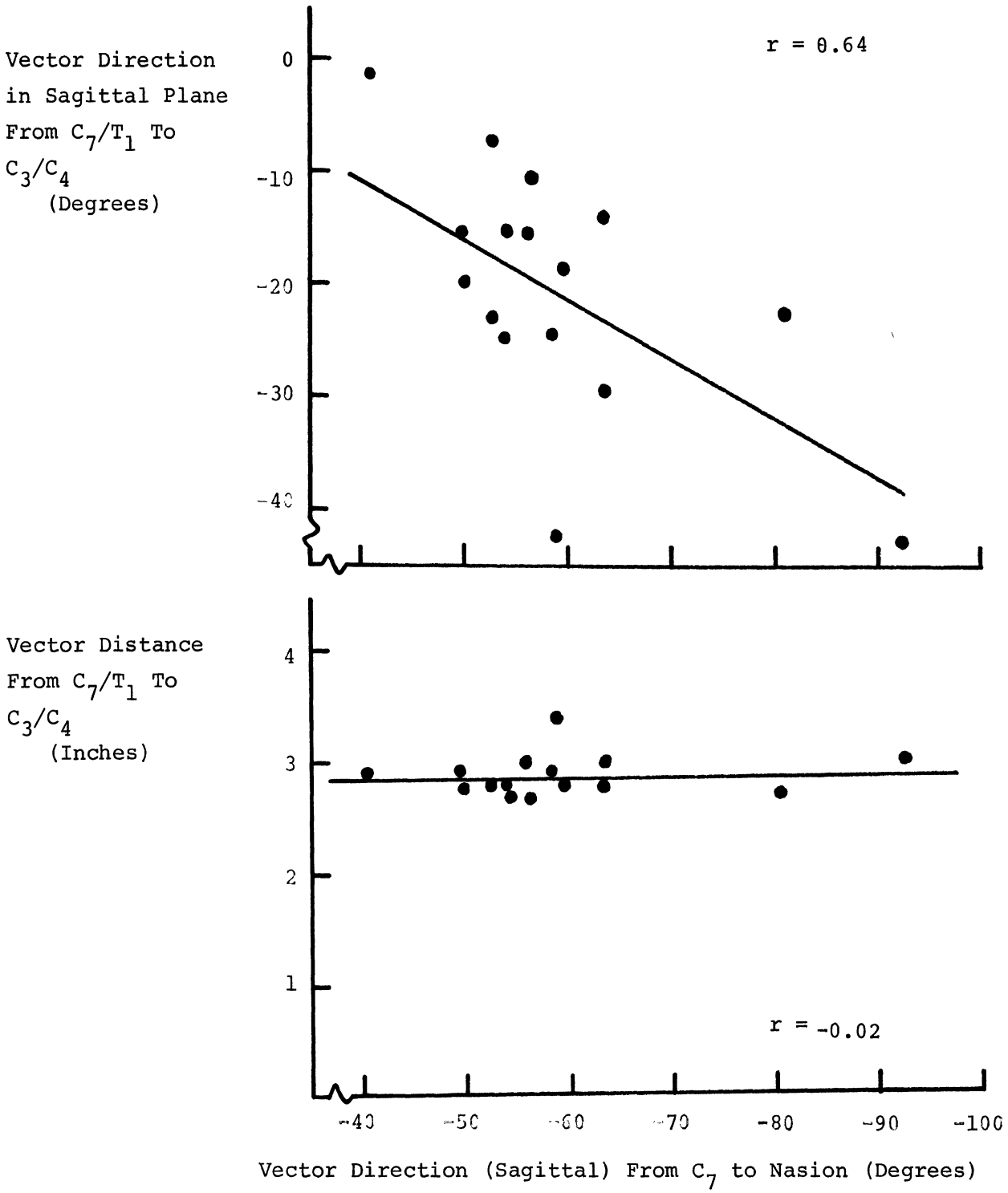

C_7/T_1 To C_4/C_5 vs. Vector Direction

From C_7 Surface to Nasion

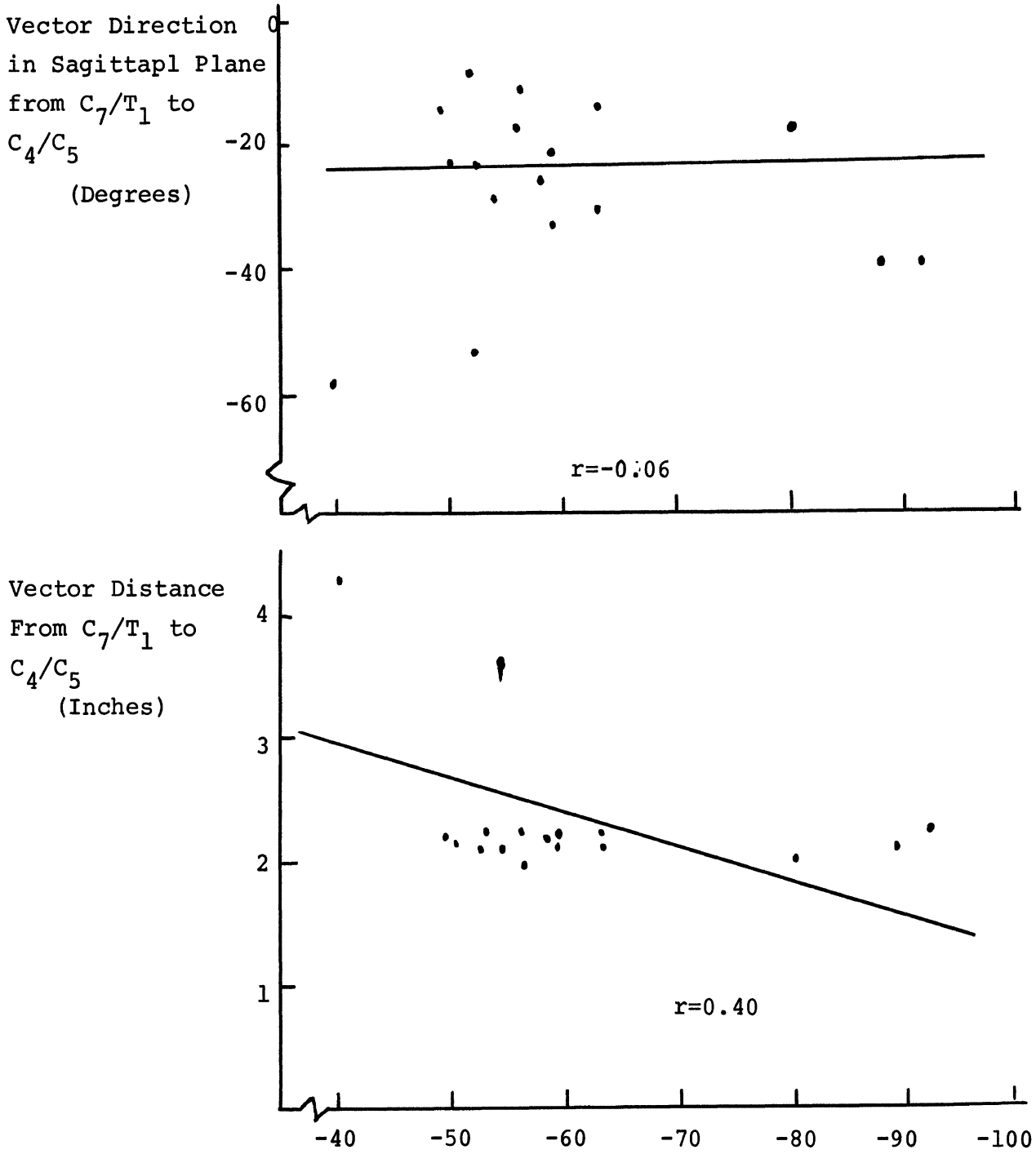

C_4/C_5 To C_2/C_3 vs. Vector Direction

From C_7 Surface to Nasion

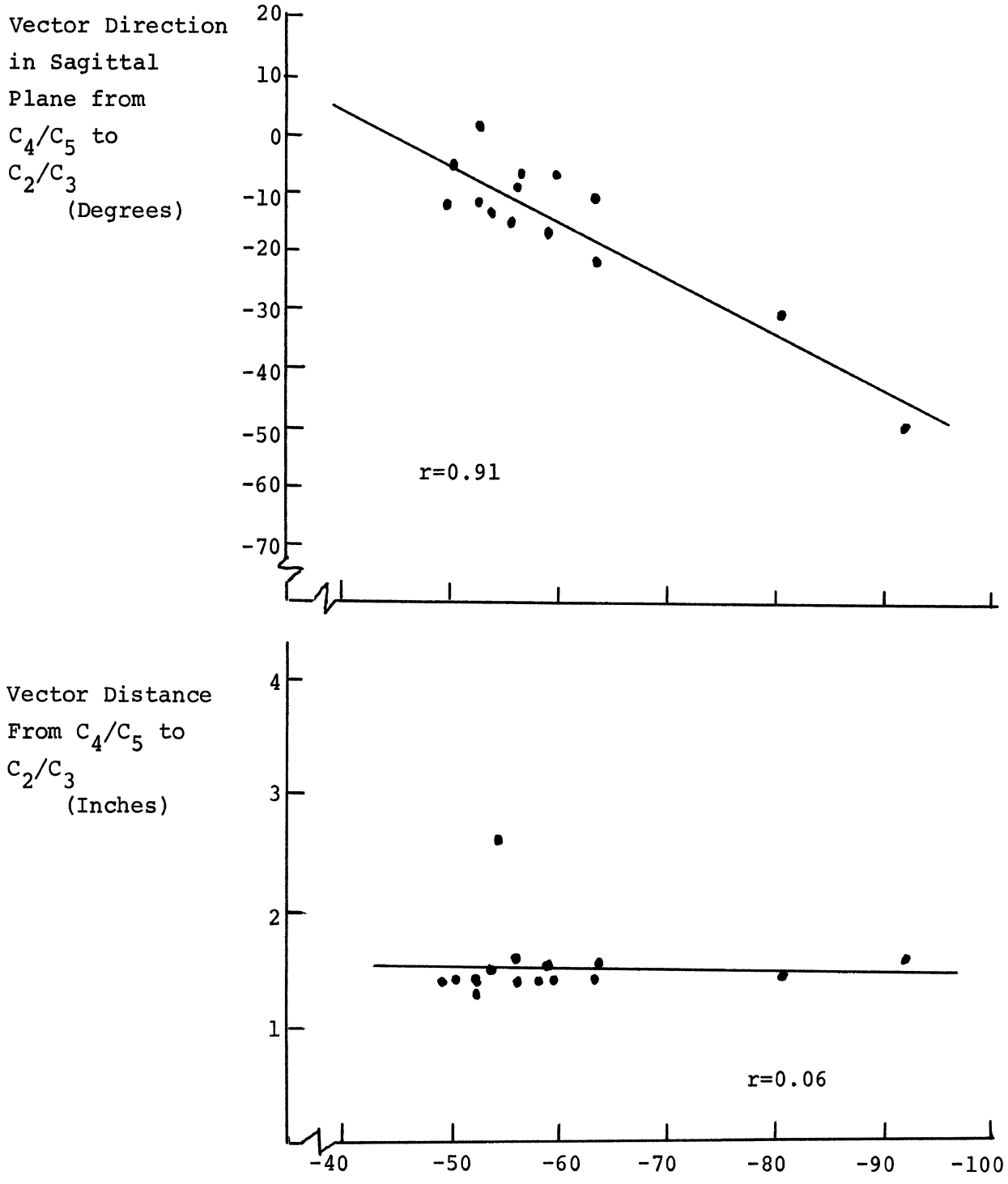

C_5/C_6 To C_2/C_3 vs. Vector Direction
From C_7 Surface to Nasion

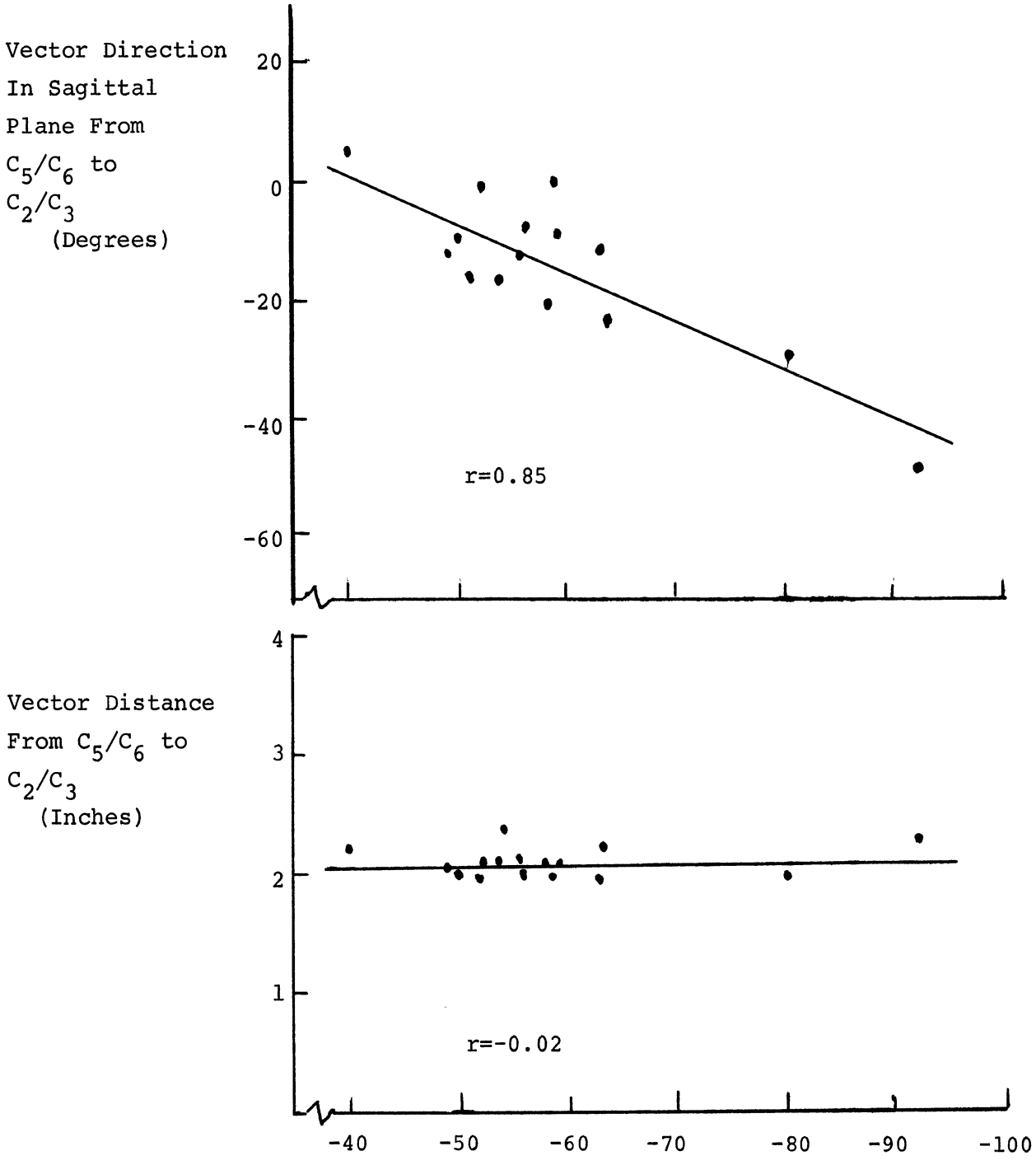

C_2/C_3 to C_2 Surface vs. Vector Direction

From C_7 Surface to Nasion

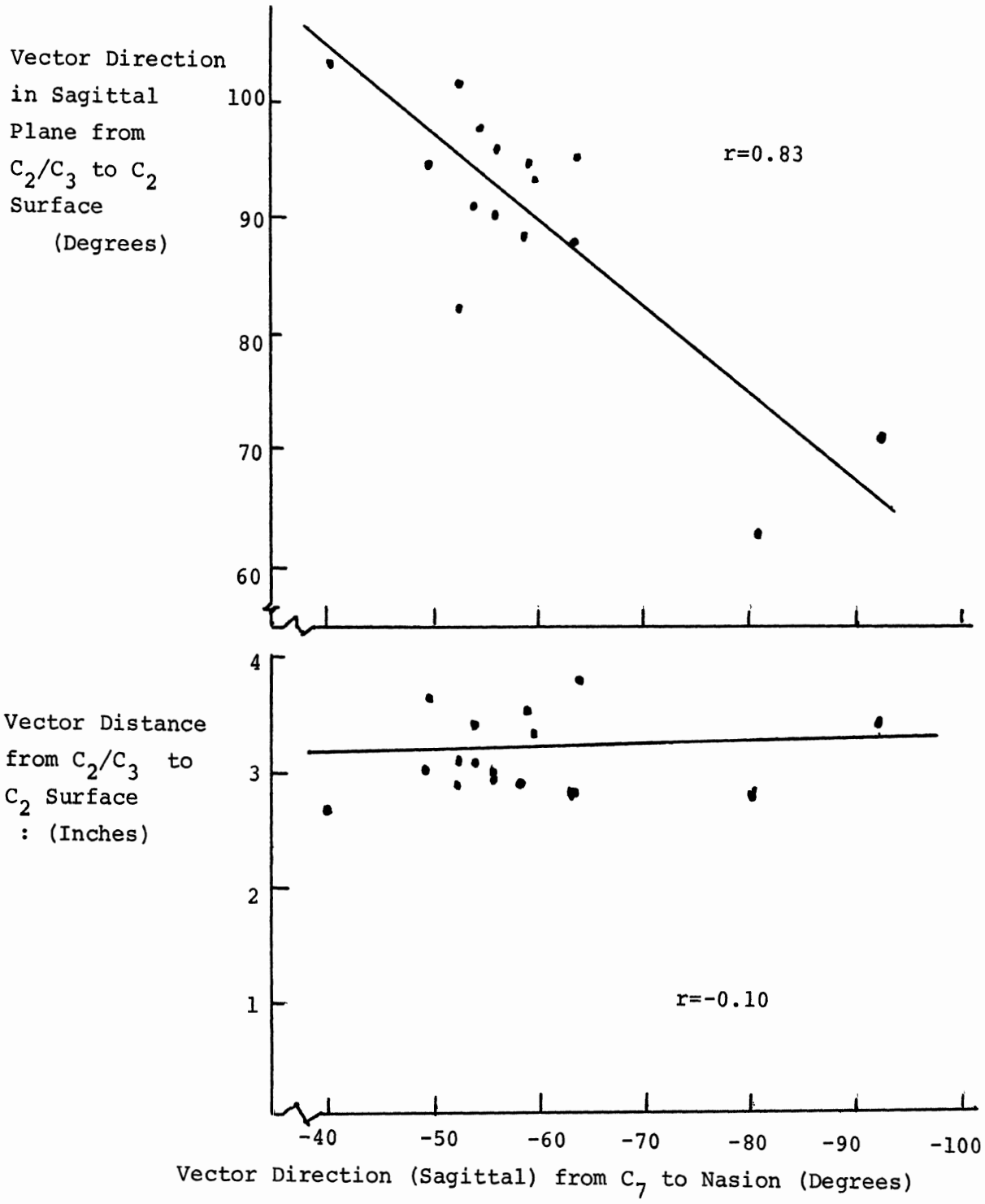

C_5/C_6 to C_5 Surface vs. Vector Direction
From C_7 Surface to Nasion

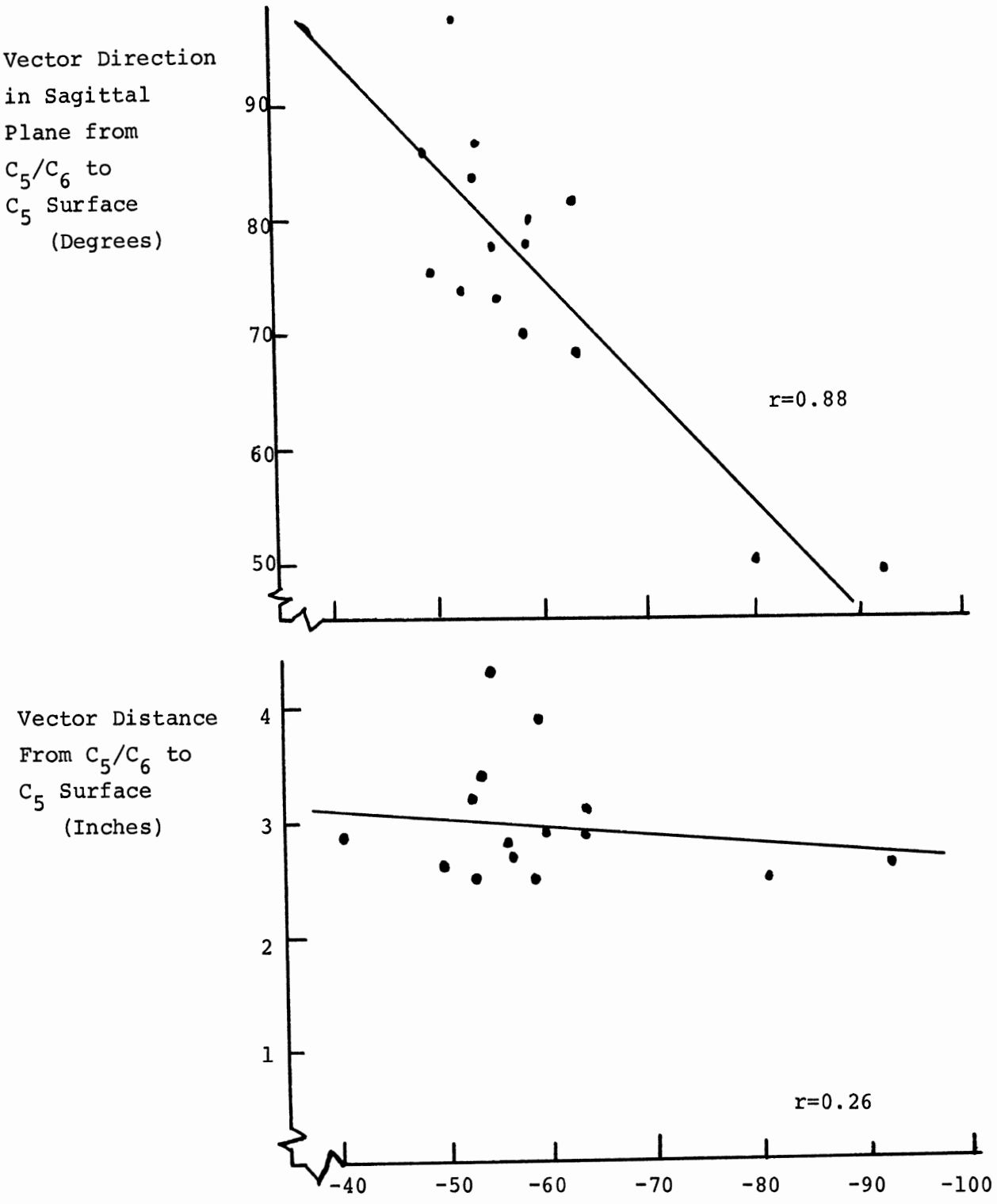

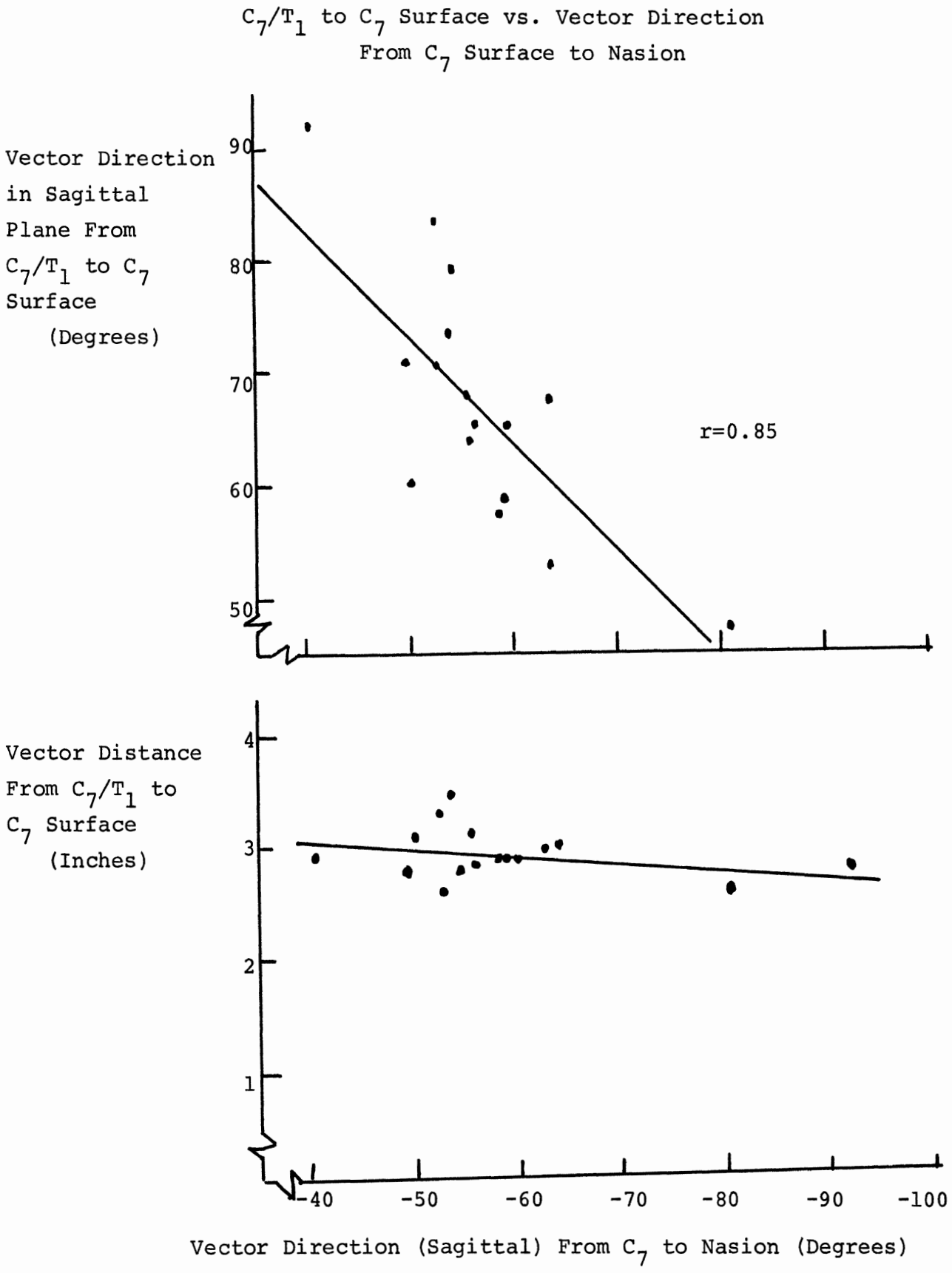
C_7/T_1 to C_7 Surface vs. Vector Direction
From C_7 Surface to Nasion
Vector Direction in Sagittal Plane From C_7/T_1 to C_7 Surface (Degrees)
90
80
70
60
50
r=0.85
Vector Distance From C_7/T_1 to C_7 Surface (Inches)
4
3
2
1
-40
-50
-60
-70
-80
-90
-100
Vector Direction (Sagittal) From C_7 to Nasion (Degrees)

C_7/T_1 to C_6/C_7 vs. Vector Direction
From C_7 Surface to Nasion

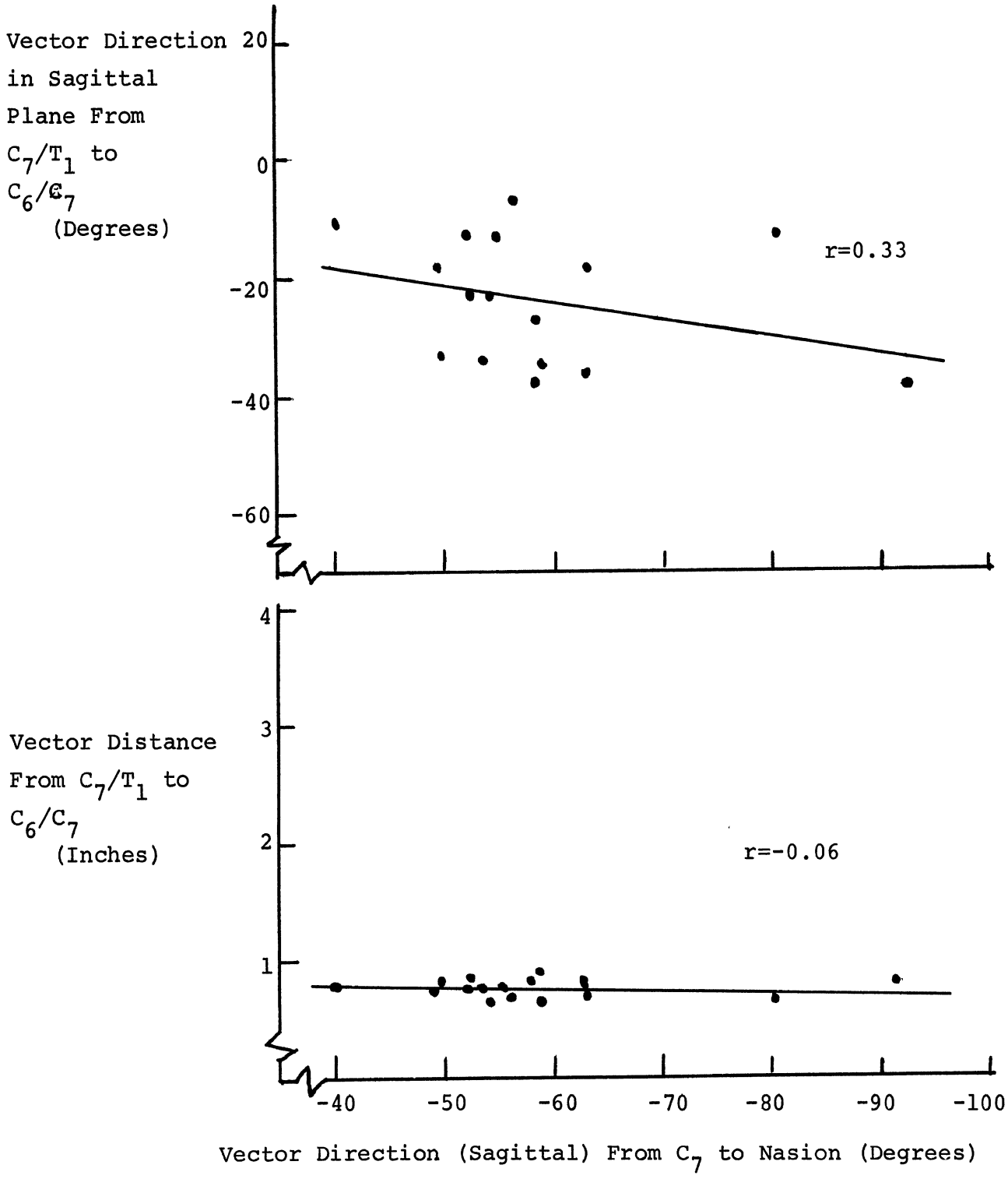

C_6/C_7 to C_5/C_6 vs. Vector Direction

From C_7 Surface to Nasion

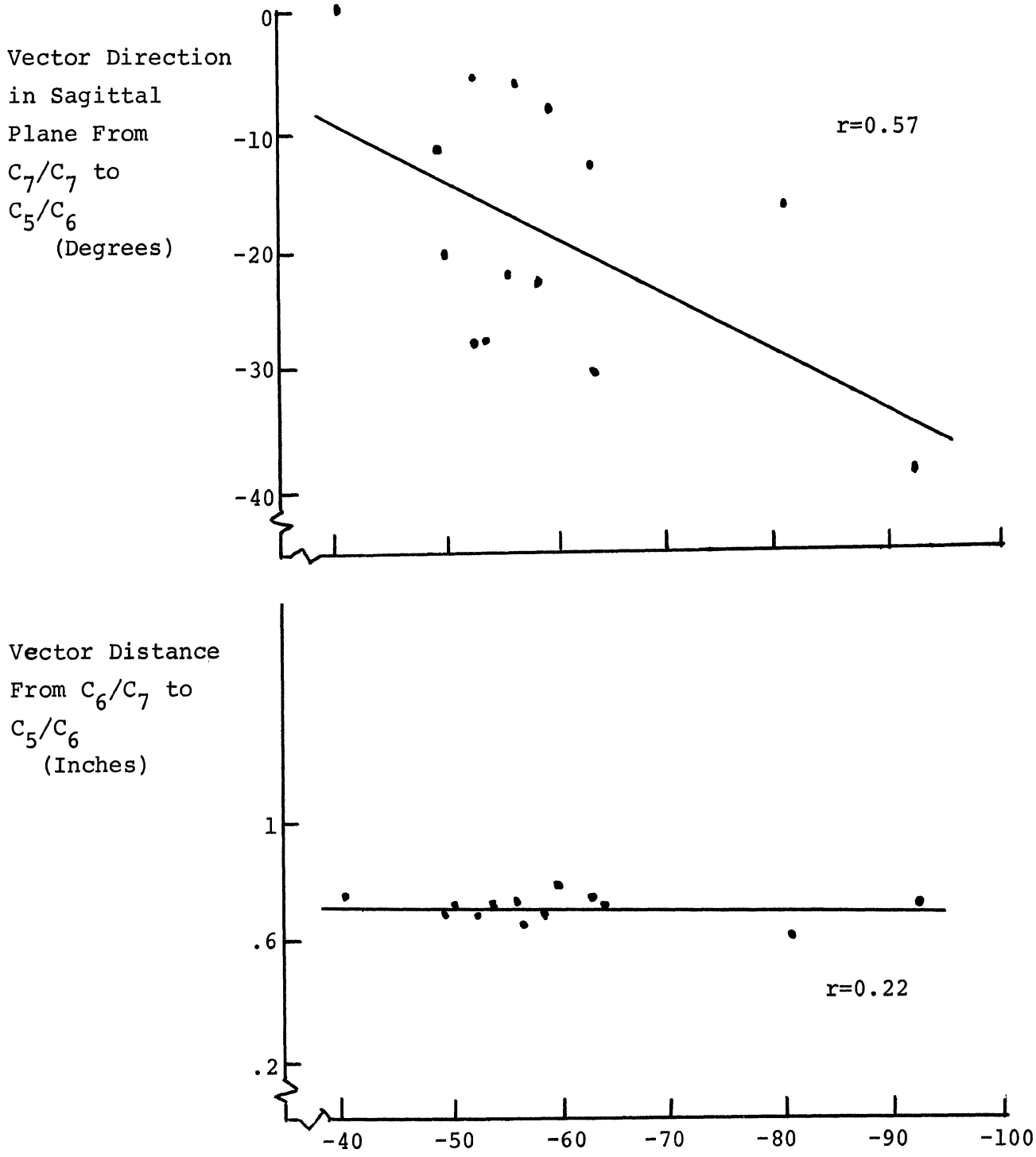

C_5/C_6 to C_4/C_5 vs. Vector Direction

From C_7 Surface to Nasion

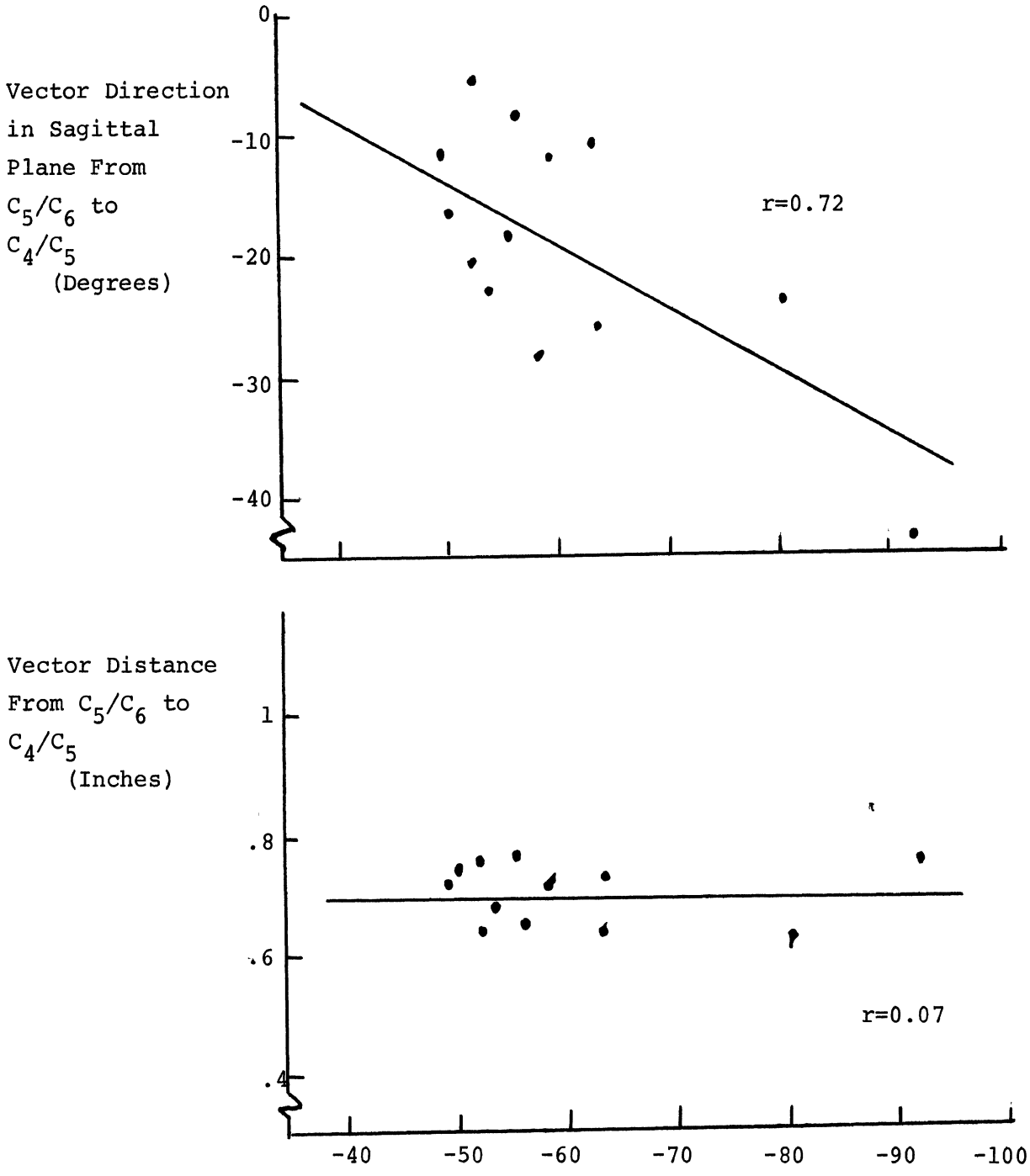

C_4/C_5 to C_3/C_4 vs. Vector Direction
From C_7 Surfact to Nasion

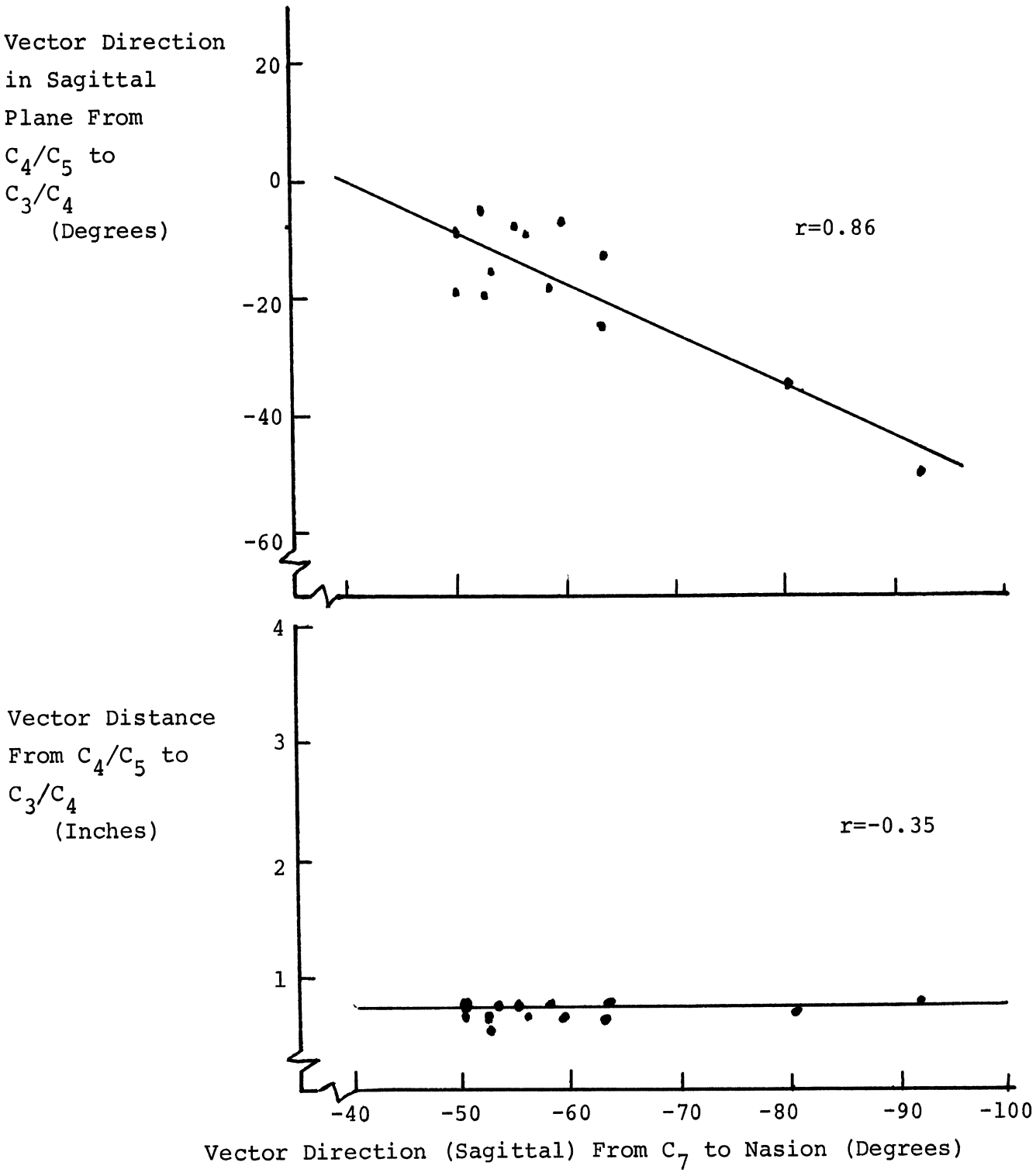

REFERENCES

1. Barter, J.T., I. Emanuel, and B. Truett. 1957 Statistical Evaluation of Joint Range Data, WADC Tech. Note 57-311, Aero Medical Research Laboratory, Wright Air Development Center, Wright-Patterson Air Force Base, Ohio. (AD-131-028).

2. Braune, W. and O. Fischer. 1889 "The Center of Gravity of the Human Body as Related to the Equipment of the German Infantry Man," Leipzig. USAAF, AMC Translation No. 379, Dayton, Ohio. (ATI-138-452, available from Defense Documentation Center).

3. Daniels, G.S. and H.T.E. Hertzberg. 1952 "Applied Anthropometry of the Hand," American Journal of Physical Anthropology n.s. 10:209-215.

4. Defebaugh, J.J. 1964 "Measurement of Head Motion," Physical Therapy 44(3):157-163.

5. Dempster, W.T. 1955 "The Anthropometry of Body Action," Annals of the New York Academy of Sciences 63(4):559-585.

6. Dempster, W.T. 1955 "Space Requirements of the Seated Operator: Geometrical, Kinematic, and Mechanical Aspects of the Body with Special Reference to the Limbs," WADC Tech. Rept. 55-159, AD-87892, Wright Air Development Center, Wright-Patterson Air Force Base, Ohio.

7. Dempster, W.T. 1956 "The Range of Motion of Cadaver Joints: The Lower Limb," The University of Michigan Medical Bulletin, Vol. 22.

8. Dempster, W.T., L.A. Shen, and J.G. Priest. 1964 "Conversion Scales for Estimating Humeral and Femoral Lengths and the Lengths of Functional Segments in the Limbs of American Caucasoid Males," Human Biology 36(3), September.

9. Drillis, R.J. 1959 "The Use of Sliding Cyclograms in the Biomechanical Analysis of Movements," Human Factors 1:1-11.

10. Dusek, E.R. 1958 "Encumbrance of Artic Clothing," Techn. Rept. EP-85-USAREC, Natick.

11. Dzendolet, E. and J.G. Rievley. 1959 Man's Ability to Apply Certain Torques While Weightless. WADC Tech. Rept. 59-94, Aero Medical Research Laboratory, Wright Air Development Center, Wright-Patterson Air Force Base, Ohio.

12. Eberhart, H.D. and V.T. Inman. 1951 "An Evaluation of Experimental Procedures Used in a Fundamental Study of Locomotion," Annals of the New York Academy of Science 51:1213-1228.

13. Emanuel, I. and J. Barter. 1957 Linear Distance Changes over Body Joints. WADC Tech. Rept. 56-364, AD-118-003, Wright Air Development Center, Wright-Patterson Air Force Base, Ohio. February.

14. Gilliland, A.R. 1921 "Norms for Amplitude of Voluntary Joint Movement," J. American Medical Association 77:1357.

15. Glanville, A.D. and G. Kreezer. 1937 "The Maximum Amplitude and Velocity of Joint Movements in Normal Male Human Adults," Human Biology 9:197-211.

16. Harless, E. 1860 "Die Statischen Momente der menschlichen Gliedmassen," Abh. d. math.-phys. Cl. d. konigl. Bayer Akad. d. Wiss. 8:69-96, 257-294.

17. Heath, B.H. and J.E.L. Carter. 1969 "A Modified Somatotype Method," Amer. J. Phys. Anthrop. 27:57-74.

18. Hewitt, D. 1928 "Range of Active Motion at the Wrist of Women," J. Bone & Joint Surgery 10:775-787.

19. Keegan, J.J. 1962 "Evaluation and Improvement of Seats," Industrial Medicine and Surgery 31:137-148.

20. Kennedy, K.W. 1964 Reach Capability of the USAF Population - Phase I. The Outer boundaries of Grasping-Reach Envelopes for Shirt-sleeved, Seated Operator. Aerospace Medical Research Laboratories, Wright-Patterson Air Force Base, Ohio Rept. AMRL-TDR-64-59 (AD608 269).

21. Nicoloff, C. 1957 Effects of Clothing on Range of Motion in the Arm and Shoulder Girdle. Tech. Rept. EP-49, U.S. Army Quartermaster Research and Engineering Center, Natick, Mass.

22. Reichel, S.M. 1966 "Moderate Auto Injuries: The Role of Reflexes in Pathogenesis and Symptomatology," Amer. Assoc. Auto. Med. November 11, Holloman Air Force Base, New Mexico.

23. Robbins, H. and V. Roberts. 1971 Anthropometrics to Support Program in Integrated Restraint Systems. Task 23. National Highway Safety Bureau, U.S. Department of Transportation. Final Report Contract FH-11-6962, July.

24. Sabanas, M. and G. Porter. 1967 "Volunteers Get Stuck for Spinal-Motion Research," Machine Design pp. 3-32, October 12.

25. Salter, N. and H.D. Darcus. 1953 "The Amplitude of Forearm and of Humeral Rotation," J. Anatomy 87:407-418.

26. Saul, E.V. and J. Jaffe. 1955 Effects of Clothing on Gross Motor Performance, Tech. Rept. EP-12, U.S. Army Quartermaster Research and Engineering Command, Natick, Mass.

27. Sinelnikoff, E. and M. Grigorowitsch. 1931 Die Beweglichkeit der Gelenke als sekundares geschlechtliches und konstitutionelles Merkmal," Zeitschrift fur Konstitutionslehre 15:679-693.

28. Smyth, C.J. (ed.) 1959 "Rheumatism and Arthritis," Annals of Internal Medicine 50:366-801.

29. Steindler, A. 1964 Kinesiology of the Human Body, Charles C Thomas, Springfield, Illinois, (second printing).

30. Taylor, C.L. and A.C. Blaschke. 1951 "A Method for Kinematic Analysis of Motion of the Shoulder, Arm and Hand Complex," Annals of the New York Academy of Sciences 51:1251-1265.

31. West, C.C. 1945 "Measurement of Joint Motion," Archives of Physical Medicine 26:414-425.

BIBLIOGRAPHY

Alexander, M. and C.E. Clauser. 1965 Anthropometry of Common Working Positions, AMRL-TR-65-73, Aerospace Medical Research Laboratories, Wright-Patterson Air Force Base, Ohio. (AD-632-241), December.

Alexander, M., J.W. Garrett, and J.C. Robinette. 1971 "Role of Anthropology in Air Force Systems," Aerospace Medicine 42(4):388-393, April.

Anthropometric Data on the USAF Flying Population. 1967 Aerospace Medical Research Laboratory, Wright-Patterson Air Force Base, Ohio. Unpublished data.

Asmussen, E. and K. Heeboll-Nielsen. 1959 "Posture, Mobility and Strength of the Back in Boys Ages 7 to 16 Years Old," Acta Orthop. Scand. 28:174.

Asmussen, E. and K. Klausen. 1962 "Form and Function of the Erect Human Spine," Clin. Orthop. 25:55-63.

Barter, J.T. 1957 Estimation of the Mass of Body Segments, WADC Tech. Rept. 57-260, Aero Medical Research Laboratory, Wright Air Development Center, Wright-Patterson Air Force Base, Ohio. AD118 222.

Barter, J.T., I. Emanuel, and B. Truett. 1957 Statistical Evaluation of Joint Range Data, WADC Tech. Note 57-311, Aero Medical Research Laboratory, Wright Air Development Center, Wright-Patterson Air Force Base, Ohio. (AD-131-028.)

Beal, M.C. and C.G. Beckwith. 1963 "Studies of Vertebral Motion: I. Cineradiographic Studies on the Halladay Spine," J.Amer. Osteopath. Assoc. 63:319-322, December.

Beal, M.C. and C.G. Beckwith. 1963 "Studies of Vertebral Motion: II. Clinical Applications," J. Amer. Osteopath. Assoc. 63:323-325, December.

Bonney, M.C., D.G. Evershed and E.A. Roberts. 1969 "SAMME-A Computer Model of Man and his Environment," Annual Meeting Ergonomus Research Soc. Bristol, England, March.

Bresler, B. and J.P. Frankel. 1950 "The Force and Movements in the Leg During Level Walking," Trans. Amer. Society of Mechanical Engineers 72:27-36.

Buck, C.A., F.B. Dameron, M.J. Dow, and H.V. Skowlund. 1959 "Study of Normal Range of Motion in the Neck Utilizing a Bubble Goniometer," Archives of Physical Medicine and Rehabilitation 40:390-392.

Chaffee, J.W. 1961 Andrometry: A Practical Application of Coordinate Anthropometry in Human Engineering. Convair, General Dynamics Corporation, Ft. Worth, Texas. Rept. FZY-012, April 18.

Chaffin, D.B. 1969 "A Computerized Biomechanical Model-Development of and Use in Studying Gross Body Actions," J. Biomechanics 2:429-441.

Chaffin, D.B. and E.J. Moulis. 1969 "An Empirical Investigation of Low Back Strains and Vertebrae Geometry," J. Biomechanics 2:89-96.

Chaffin, D.B. and W.H. Baker. 1970 "A Biomechanical Model for Analysis of Symmetrical Sagittal Plane Lifting," AIIE Transactions, Industrial Engineering Research and Development .

Churchill, E. 1961 Selection of Experimental Sample Subjects. Antioch College, Yellow Springs, Ohio. Unpublished manuscript.

Clauser, C.E., J.T. McConville, and J.W. Young. 1969 Weight, Volume, and Center of Mass of Segments of the Human Body. Aerospace Medical Research Laboratory, Wright-Patterson Air Force Base, Ohio. Rept. AMRL-TR-69-70, August.

Cobe, H.M. 1928 "Range of Active Motion at the Wrist of White Adults," J. Bone and Joint Surg. 26:763-774.

Colachis, S.C., Jr. and M.A. Strohm. 1965 "Radiographic Studies of Cervical Spine Motion in Normal Subjects: Flexion and Hyperextension," Archives of Physical Med. and Rehab. 46(11):753-760.

Cossette, J.W., H.F. Farfan, G.H. Robertson and R.V. Wells. 1971 "The Instantaneous Center of Rotation of the Third Lumbar Intervertebral Joint," J. Biomechanics 4(2):149-153, March.

Coupe, C.W. 1962 "Cervico-Dorsal Region: Lateral Projection," X-Ray Techn. 33:256-257, January.

Damon, A., H.W. Stoudt, and R.A. McFarland. 1966 The Human Body in Equipment Design. Harvard University Press, Cambridge, Massachusetts.

Dankmeijer, J. and B.J. Rethmeier. 1943 "The Lateral Movement in the Atlanto-Axial Joints and Its Clinical Significance," Acta Radiol. 24:55-66.

Darcus, H.D. 1954 "The Range and Strength of Joint Movement," in, Proceedings of the Erogonomics Society, II. Symposium on Human Factors in Equipment Design, London.

Davis, P.R. 1959 "The Posture of the Trunk During the Lifting of Weights," Brit.Med.J. 1:87-89.

Davis, P.R., J.D.G. Troup, and J.H. Burnard. 1965 "Movements of the Thoracic and Lumbar Spine when Lifting: A Chrono-Cyclophatographic Study," J. Anat. (London) 99(1):13-26.

Dempster, W.T. 1955 "The Anthropometry of Body Action," Annals of the New York Academy of Sciences 63 4):559-585.

Dempster, W.T. 1955 Space Requirements of the Seated Operator: Geometrical, Kinematic, and Mechanical Aspects of the Body with Special Reference to the Limbs, WADC Tech. Rept. 55-159, Wright Air Development Center, Wright-Patterson Air Force Base, Ohio.

Dempster, W.T. 1956 "The Range of Motion of Cadaver Joints: The Lower Limb," The University of Michigan Medical Bulletin, 22:364-379.

Dempster, W.T. 1958 "Analysis of Two-Handed Pulls Using Free-Body Diagrams," J. Applied Physiology 13:469-480.

Dempster, W.T. 1961 "Free-Body Diagrams as an Approach to the Mechanics of Human Posture and Motion," in, F.G. Evans (ed.), Biomechanical Studies of the Musculo-skeletal System, Charles C Thomas, Springfield, Ill.

Dempster, W.T. 1965 "Mechanisms of Shoulder Movement," Archives of Physical Medicine and Rehabilitation, 46:49-70, January.

Dempster, W.T., W.C. Gabel, and W.J.L. Felts. 1959 "The Anthropometry of the Manual Work Space for the Seated Subject," Amer. J. of Physical Anthropology 17:289-317, December.

Dempster, W.T., L.A. Shen, and J.G. Priest. 1964 "Conversion Scales for Estimating Humeral and Femoral Lengths and the Lengths of Functional Segments in the Limbs of American Caucasoid Males," Human Biology 36(3), 246-262, September.

Dempster, W.T. and G.R.L. Gaughran. 1967 "Properties of Body Segments Based on Size and Weight," Amer. J. of Anatomy 120:33-54.

Drillis, R.J. 1959 "The Use of Sliding Cyclograms in the Biomechanical Analysis of Movements," Human Factors 1:1-11.

Dusek, E.R. 1958 Encumberance of Artic Clothing, Tech. Rept. EP-85-USAREC, Natick, Mass.

Dyson, G.H.G. 1963 The Mechanics of Athletics. University of London Press, Ltd., London (1962).

Dzendolet, E. and J.F. Rievley. 1959 Man's Ability to Apply Certain Torques While Weightless. WADC Tech. Rept. 59-94, Aero Medical Research Laboratory, Wright Air Development Center, Wright-Patterson Air Force Base, Ohio AD220 363.

Ermenegilde, F., G. Grella, and L. Leonardi. 1964 "On the Application of the Photo-Fluorographic Method in Detection of Alterations of the Lumbo Sacral Column in Mass Survey," (Sull' Applicazione Del Metodo Schermo-Grafico Nella Ricerca Delle Alrerazioni Della Colonna Lombe-Sacrale Nelle Indagini Di Massa). Rossegna Unternazione Di Clinica E Terapia 44(21):1195-1200, November 15.

Evans, F.G. 1961 Biomechanical Studies of the Musculoskeletal System. Charles C Thomas, Springfield, Ill.

Evans, F.G. 1971 "Human Vertebral Column from the Biomechanical Viewpoint," Proceedings, VIII International Congress of Anthropological Sciences. (In press.)

Evans, F.G. 1971 "Some Basic Aspects of Biomechanics of the Spine," American Academy of Physical Medicine and Rehabilitation. Archives Phys. Med. (In press.)

Ferlic, D. 1962 "The Range of Motion of the 'Normal' Cervical Spine," Bull. Johns Hopkins Hosp. 110:59-65, February.

Fielding, J.W. 1957 "Cineroentgenography of the Normal Cervical Spine," J. Bone & Joint Surg. 39A:1280-1288, December.

Fielding, J.W. 1964 "Normal and Abnormal Motion of the Cervical Spine from the Second Cervical Vertebra to the Seventh Cervical Vertebra Based on Cineroentgenography," J. Bone & Joint Surg. 46A(8):1779-1781, December.

Fischer, O. 1906 Theoretical Fundamentals for a Mechanics of Living Bodies with Special Applications to Man as Well as to Some Processes of Motion in Machines. B. G. Teubner, Berlin. (ATI-153668, available from Defense Documentation Center.)

Fisher, B.O., Jr. 1967 Analysis of Spinal Stresses During Lifting - A Biomechanical Model. M.S. Industrial Engineering Thesis, The University of Michigan, Ann Arbor, Michigan.

Flint, M.M. 1963 "Lumbar Posture: A Study of Roentgenographic Measurement and the Influence of Flexibility and Strength," Res. Quart. 34:15-20, March.

Freedman, L. and R.R. Munro. 1966 "Abduction of the Arm in the Scapular Plane: Scapular and Glenohumeral Movements," J. Bone & Joint Surg. 48A: (8): 1503-1510.

Gregorson, G.G. and D.B. Lucas. 1967 "An In vivo Study of the Axial Rotation of the Human Thoracolumbar Spine," J. Bone & Joint Surg. 49A:247-262, March.

Hagen, D.P. 1964 "A Continuing Roentgenographic Study of Rural School Children Over a 15-Year Period," J. Amer. Osteopath. Assoc. 64:1030-1037, June.

Hagen, D.P. 1965 "A Roentgenographic Evaluation of the Lumbar Spine and Pelvis: The Lateral Projection," J. Amer. Osteopath. Assoc. 64:1030-1037, June.

Hagen, D.P. 1965 "A Continuing Roentgenographic Study of Rural School Children Over a 15-Year Period: The Lumbosacral Angle," J. Amer. Osteopath. Assoc. 64:1163-1170, July.

Hellebrandt, F.A. and E.B. Franseen. 1943 "Physiological Study of the Vertical Stance of Man," Physiol. Rev. 23:220-255, July.

Hellebrandt, F.A., E.N. Duvall, and M.L. Moore. 1949 "The Measurement of Joint Motion: Part 3," Phys. Ther. Rev. 29:302-307.

Hertzberg, H.T.E., G.S. Daniels, and E. Churchill. 1954 Anthropometry of Flying Personnel - 1950. Wright Air Development Center, Wright-Patterson Air Force Base, Ohio. Rept. WADC-TR-52-321 AD47953.

Hickey, L.F., W.E. Springer, and F.L. Cundari. 1968 A Development in Cockpit Geometry Evaluation. The Boeing Company, Seattle, Washington. Report D6-53594, November.

Hirsch, C. and A. Nochemson. 1954 "New Observations on the Mechanical Behavior of Lumbar Discs," Acta Orthopedica Scaninavica 23:254-283.

Ho, R.W.H. and R. Izbicki. 1965 "Spinal-Pelvic Adaptation in the Standing Posture," J. Amer. Orthop. Assoc. 64:941-944, May.

Hoag, J.M., et al. 1960 "Kinematic Analysis and Classification of Vertebral Motion," J. Amer. Osteopath. Assoc. 59:899-908, 982-986, July and August.

Hohl, M. and H.R. Baker. 1964 "The Atlanto-Axial Joint," J. Bone & Joint Surgery 46A(8):1739-1752, December.

Hohl, M. 1964 "Normal Motions in the Upper Portion of the Cervical Spine," J. Bone & Joint Surgery 46A(8):1777-1779, December.

Inman, V.T., J.B. Saunders and L.C. Abbott. 1944 "Observations on the Function of the Shoulder Joint," J. Bone & Joint Surgery 20:1-30.

Janair 1969 Cockpit Geometry Evaluation, Project No. 690106, Boeing Aircraft Corporation, Vol. 1, Project Description and Summary; Vol. 2, Human Data; Vol. 3, Computer Program; Vol. 4, Mathematical Model; Vol. 5, Validation.

Jones, M.D. 1960 "Cineradiographic Studies of the Normal Cervical Spine," Calif. Med. J. 93:293-296.

Karpovich, P.V., E.L. Herden, and M.M. Asa. 1960 "Electrogoniometric Study of Joints," U.S. Armed Forces Medical Journal 11:424-450.

Kilpatrick, K.E. 1970 A Model for the Design of Manned Work Stations. Dissertation. Department of Industrial Engineering, The University of Michigan, Ann Arbor.

Kottke, F.J. and M.O. Mundale. 1959 "Range of Mobility of the Cervical Spine," Arch. Phys. Med. 40:379-382, September.

Leighton, J.R. 1955 "An Instrument and Technique for Measurement of Range of Joint Motion," Arch. Phys. Med. 36:571, September.

Leighton, J.R. 1956 "Flexibility Characteristics of Males Ten to Eighteen Years of Age," Arch. Phys. Med. 37:494, August.

Leighton, J.R. 1957 "Flexibility Characteristics of Four Specialized Skill Groups of College Athletes," Arch. Phys. Med. 38:24, January.

Military Standard MS-33574. Dimensions, Basics, Cockpit, Stick Controlled, Fixed Wing Aircraft. Revised June 2, 1969.

Murrell, K.F.H. 1965 Erogonomics: Man in His Working Environment. Chapman and Hall, London.

Nachemson, A. n.d. "The Influence of Spinal Movements on the Lumbar Intradiscal Pressure and on the Tensile Stresses in the Annulus Fibrosus," Acta Orthop. Scan. 33:183-207.

Olsen, G.A. 1970 The Interaction of the Components of the Human Back. Department of Civil Engineering, School of Engineering, City College of The City University of New York, New York.

Parnell, R.W. 1958 Behavior and Physique: An Introduction to Practical and Applied Somatometry. Edward Arnold, Ltd., London.

Paul, L.W. and W.W. Moir. 1949 "Non-Pathologic Variations in Relationship of the Upper Cervical Vertebrae," Amer. J. Roentgenol. 62:519-524.

Pearson, W.M., et al. 1951 "Progressive Structural Study of School Children: Eight-Year Study of Children in Rural Areas of Adair County, Missouri," J. Amer. Osteopath. Assoc. 51:155-167, November.

Pernkoff, E. 1963 Atlas of Topographical and Applied Human Anatomy. (H. Ferner, and H. Monsen, eds.), Vol. I. Head and Neck. W.B. Saunders Co., Philadelphia.

Pizon, P. 1963 "Mensurations Anatomiques Lombo-Sacrees" [Lumbo-Sacral Anatomical Measurements], Presse Med. 71:1603-1605, June 29.

Provins, K.A. 1955 "Maximum Forces Exerted About the Elbow and Shoulder Joints on Each Side Separately and Simultaneously," J. Applied Physiol. 7:390-392.

Rosenburg, P. 1955 "R-Center Method for Analyzing Vertebral Motion by X-Rays," J. Amer. Osteopath. Assoc. 55:103-111, October.

Salter, N. 1955 "Methods of Measurement of Muscle and Joint Function," J. Bone & Joint Surg. 37-B:474-491.

Salter, N. and H.D. Darcus. 1952 "The Effect of the Degree of Elbow Flexion on the Maximum Torques Developed in Pronation and Supination of the Right Hand," J. Anatomy 86:197-202.

Schanne, F.J., Jr. 1971 A Proposed Three Dimensional Static Strength Model of Man. Dissertation. Department of Industrial Engineering, The University of Michigan, Ann Arbor. (In preparation)

Sheldon, W.H. 1954 Atlas of Men: A Guide for Samatotyping the Adult Male at All Ages. Harper Brothers, New York.

Snyder, R.G. and C.C. Snow. 1965 Anthropometry of Air Traffic Controllers. Office of Aviation Medicine, Federal Aviation Agency, Oklahoma City, AM65-26, September.

Stoudt, H.W. and R.A. McFarland. 1970 "Anthropometric Characteristics of Automobile Drivers," International Automobile Safety Conference Compendium, Society of Automotive Engineers, Inc., New York.

Sullivan, W.E. and M. Miles. 1959 "Lumbar Segment of the Vertebral Column," Anat. Rec. 133:619-636, April.

Taylor, C.L. 1954 "The Biomechanics of the Normal and of the Amputated Upper Extremity," In, Human Limbs and Their Substitutes, McGraw-Hill Company, New York.

Thieme, F.P. 1950 "Lumbar Breakdown Caused by Erect Posture in Man - With Emphasis on Spondylolishthesis and Herniated Intervertebral Discs," Anthropological Papers, Museum of Anthropology, The University of Michigan, No. 4, 1-44.

Wells, L.H. 1963 "Variation in the Human Vertebral Column, With Particular Reference to the Lumbar-Sacral Junction," S. Aft. Med. J. 37:60-64, January 19.

Wiles, P. 1935 "Movements of the Lumbar Vertebrae During Flexion and Extension," Proc. Rev. Soc. Med. 28:647.

Wilmer, H.A. and E.C. Elkins. 1957 "An Optical Goniometer for Observing Range of Motion and Joints; A Preliminary Report of a New Instrument,"Arch. Phys. Med. 28:695-705.

☆U.S.Government Printing Office: 1973 — 759-494/536